

Roles for NF κ B, PHD3 and Neural Activity in the Development of the Peripheral Nervous System

**A thesis submitted to Cardiff University for the degree of PhD
2008**

Denis J. Gallagher

**Cardiff School of Biosciences
Cardiff University**

UMI Number: U585100

All rights reserved

INFORMATION TO ALL USERS

The quality of this reproduction is dependent upon the quality of the copy submitted.

In the unlikely event that the author did not send a complete manuscript and there are missing pages, these will be noted. Also, if material had to be removed, a note will indicate the deletion.



UMI U585100

Published by ProQuest LLC 2013. Copyright in the Dissertation held by the Author.
Microform Edition © ProQuest LLC.

All rights reserved. This work is protected against
unauthorized copying under Title 17, United States Code.



ProQuest LLC
789 East Eisenhower Parkway
P.O. Box 1346
Ann Arbor, MI 48106-1346

Abstract

In the developing peripheral nervous system, neuronal survival and axonal growth are regulated to a large extent by neurotrophic factors acting via intracellular signalling cascades that are not fully understood. Here, I describe crucial roles for the nuclear factor-kappa B (NF κ B) transcription cascade and the cellular oxygen sensor proline hydroxylase domain 3 (PHD3) in the regulation of axonal growth and neuronal survival during the phase of target field innervation, and I describe a novel role for purinergic signalling in promoting neuronal survival at a later stage of development. Using sensory neurons of the nodose ganglion, I show that distinct NF κ B activation mechanisms are responsible for neurite growth promoted by ciliary neurotrophic factor (CNTF) and brain-derived neurotrophic factor (BDNF). Whereas a non-canonical NF κ B signalling pathway that requires tyrosine phosphorylation of I κ B α is crucial for CNTF-promoted growth, canonical signalling that requires serine phosphorylation of I κ B α contributes to BDNF-promoted growth. Using sympathetic neurons of the superior cervical ganglion of wild type and PHD3-deficient mice, I show that PHD3 exerts a negative regulatory effect on neuronal survival and neurite growth, implicating oxygen sensitive pathways in the regulation of sympathetic neuron development. Despite increased numbers of sympathetic neurons in PHD3-deficient mice there was decreased target innervation density and defective sympathetic function. Finally, in nodose neurons I describe roles for depolarization and purinergic signalling in promoting neuronal survival during a window of development as the neurons begin to lose their dependence on BDNF for survival.

CONTENTS

| | PAGE |
|--|-------------|
| TITLE | 1 |
| DECLARATION | 2 |
| ABSTRACT | 3 |
| CONTENTS | 4 |
| LIST OF FIGURES | 9 |
| ABBREVIATIONS | 13 |
| ACKNOWLEDGEMENTS | 16 |
| DEDICATION | 17 |
| | |
| CHAPTER 1 – INTRODUCTION | 18 |
| 1.1 Brief Overview of Neuronal Development | 19 |
| <i>1.1.1 Introduction</i> | 19 |
| <i>1.1.2 Neural Induction</i> | 19 |
| <i>1.1.3 The Neural Tube</i> | 21 |
| <i>1.1.4 Neurogenesis</i> | 25 |
| <i>1.1.5 Neuronal Migration</i> | 29 |
| <i>1.1.6 Axon Growth and PCD</i> | 31 |
| <i>1.1.7 Synaptogenesis</i> | 31 |
| 1.2 Organisation and Development of the Peripheral Nervous system ... | 34 |
| <i>1.2.1 Introduction</i> | 34 |
| <i>1.2.2 Organisation of the Somatic PNS</i> | 34 |
| <i>1.2.3 Organisation of the Autonomic Nervous System</i> | 38 |
| <i>1.2.4 Development of the Sensory and Autonomic PNS</i> | 42 |
| 1.3 Regulation of Neuronal Survival in the PNS | 43 |
| <i>1.3.1 The Neurotrophic Theory</i> | 44 |
| <i>1.3.2 Neurotrophic Requirements of Selected Peripheral Ganglia</i> | 47 |
| <i>1.3.3 NGF</i> | 49 |
| <i>1.3.4 BDNF</i> | 50 |

| | | |
|------------------|--|-----------|
| 1.3.5 | <i>NT-3</i> | 51 |
| 1.3.6 | <i>CNTF</i> | 52 |
| 1.3.7 | <i>Trk Receptors</i> | 53 |
| 1.3.8 | <i>P75^{NTR}</i> | 57 |
| 1.3.9 | <i>CNTF Receptor Complex</i> | 57 |
| 1.3.10 | <i>Neural Activity Regulates Survival</i> | 58 |
| 1.4 | Regulation of Neurite Outgrowth | 59 |
| 1.4.1 | <i>Axon Extension and Guidance</i> | 59 |
| 1.4.2 | <i>The Role of Neurotrophic Factors in Neurite Outgrowth from PNS Neurons</i> | 60 |
| 1.4.3 | <i>Intracellular Signalling Pathways Downstream of Neurotrophic Factors Regulating Neuronal Survival and Neurite Outgrowth</i> | 61 |
| 1.5 | NFκB Signalling | 63 |
| 1.5.1 | <i>The NFκB Family of Transcription Factors</i> | 63 |
| 1.5.2 | <i>Emerging Roles for NFκB in the Nervous System</i> | 64 |
| 1.5.3 | <i>NFκB Activation Mechanisms</i> | 66 |
| 1.5.4 | <i>Downstream of NFκB</i> | 69 |
| 1.6 | Hypoxia-Inducible Factor (HIF) Signalling | 70 |
| 1.6.1 | <i>Oxygen Sensing</i> | 70 |
| 1.6.2 | <i>Regulation of HIF</i> | 71 |
| 1.6.3 | <i>PHD Enzymes</i> | 73 |
| CHAPTER 2 | – Materials and Methods | 76 |
| 2.1 | Introduction | 77 |
| 2.2 | Maintenance of Wild-Type Mice | 77 |
| 2.3 | Maintenance of Transgenic Mice | 77 |
| 2.4 | Genotyping of Transgenic Mice | 78 |
| 2.4.1 | <i>Isolation of Genomic DNA</i> | 78 |
| 2.4.2 | <i>Genotyping Protocol</i> | 78 |
| 2.5 | Isolation of Mouse Embryos | 79 |
| 2.6 | Dissection of Peripheral Ganglia | 80 |

| | |
|---|-----------|
| 2.7 Preparation of Tungsten Needles..... | 81 |
| 2.8 Dissociated Neuronal Cultures..... | 81 |
| 2.8.1 <i>Preparation of Dishes.....</i> | 81 |
| 2.8.2 <i>Culture Media.....</i> | 82 |
| 2.8.3 <i>Dissociation of Ganglia.....</i> | 82 |
| 2.8.4 <i>Seeding of Neurons.....</i> | 83 |
| 2.9 Estimation of Neuronal Survival..... | 83 |
| 2.10 Quantification of Neurite Outgrowth..... | 84 |
| 2.11 Ballistic Transfection..... | 85 |
| 2.11.1 <i>Plasmid Preparation.....</i> | 85 |
| 2.11.2 <i>Preparation of Gold Microcarriers.....</i> | 85 |
| 2.11.3 <i>Ballistic Transfection.....</i> | 86 |
| 2.12 Preparation of κB Decoy DNA..... | 88 |
| 2.13 NFκB Activation Assay..... | 88 |
| 2.14 qPCR analysis of PHD3 induction after NGF withdrawal..... | 88 |
| 2.15 Western Blots..... | 89 |
| 2.16 Dissociated Cell Counts..... | 90 |
| 2.17 Adult Stereology..... | 91 |
| 2.18 Measuring Sympathetic Innervation Density..... | 92 |
| 2.19 Pupillometry..... | 92 |
| 2.20 Statistical Analyses..... | 93 |

CHAPTER 3 –NF κ B Activation Via Tyrosine Phosphorylation of I κ B- α is Crucial for CNTF-Promoted Neurite Growth from Developing Neurons.....94

| | |
|--|-----------|
| 3.1 Introduction..... | 95 |
| 3.2 SN50 Reduces Neurite Growth from Nodose Neurons..... | 97 |
| 3.3 κ B decoy DNA Reduces Neurite Growth from Nodose Neurons..... | 98 |
| 3.4 Overexpression of p50/p65 Increases Neurite Growth | 99 |

| | |
|--|------------|
| 3.5 Serine Phosphorylation of IκB-α Contributes to BDNF-Promoted Neurite Growth but is Not Required for CNTF-Promoted Growth..... | 107 |
| 3.6 Tyrosine Phosphorylation of IκB-α is Crucial for CNTF-Promoted Neurite Growth but is Not Required for BDNF-Promoted Growth..... | 108 |
| 3.7 Proteasome-Independent Mechanism for CNTF-Promoted Neurite Growth..... | 111 |
| 3.8 BDNF and CNTF Induce a Differential Pattern of IκB-α Phosphorylation..... | 112 |
| 3.9 Spleen Tyrosine Kinase (SYK) is Required for CNTF-Promoted Neurite Growth..... | 116 |
| 3.10 NFκB Reporter Activation..... | 120 |
| 3.11 Discussion..... | 122 |

CHAPTER 4 – Abnormal sympathoadrenal development in *PHD3*^{-/-} mice.....126

| | |
|---|------------|
| 4.1 Introduction..... | 127 |
| 4.2 Expression of PHD3 in sympathoadrenal tissues..... | 130 |
| 4.3 PHD3 inactivation increases survival of SCG neurons in vitro | 130 |
| 4.4 Specific survival effect of <i>PHD3</i>^{-/-} in SCG neurons..... | 131 |
| 4.5 Induction of PHD3 mRNA following withdrawal of NGF..... | 132 |
| 4.6 Reversal of survival effect in <i>PHD3</i>^{-/-};<i>HIF2</i>^{+/-} mice..... | 132 |
| 4.7 PHD3 inactivation increases NT-3 dependent survival of SCG neurons..... | 133 |
| 4.8 Enhanced NGF-promoted neurite growth from PHD3-deficient sympathetic neurons in vitro..... | 141 |

| | |
|--|------------|
| 4.9 PHD3-deficient mice have increased numbers of SCG neurons..... | 145 |
| 4.10 PHD3-deficient mice have increased numbers of cells in the adrenal medulla and carotid body..... | 146 |
| 4.11 Sympathetic innervation of target tissues..... | 150 |
| 4.12 Physiological effects on the sympathetic nervous system..... | 154 |
| 4.13 Discussion..... | 156 |

CHAPTER 5 – Neural activity regulates survival during a postnatal window in the development of sensory neurons.....158

| | |
|---|------------|
| 5.1 Introduction..... | 159 |
| 5.2 Onset of postnatal neurotrophin- independence differs between neuronal populations..... | 161 |
| 5.3 KCl-induced depolarisation increases survival of peripheral sensory neurons..... | 161 |
| 5.4 L-Type Ca²⁺ channel blockers reverse effects of KCl on sensory neuronal survival..... | 166 |
| 5.5 Extracellular ATP promotes the survival of nodose neurons..... | 169 |
| 5.6 Hypoxia reverses effect of ATP on neuronal survival..... | 169 |
| 5.7 Discussion..... | 172 |
| Bibliography..... | 176 |
| Appendix..... | 202 |

List of Figures

Figure 1 **Neural tube formation** (p23)

Figure 2 **Neural tube defects** (p24)

Figure 3 **Neurogenesis** (p27)

Figure 4 **Early embryonic CNS** (p28)

Figure 5 **Neuronal migration** (p30)

Figure 6 **Synaptic structure** (p33)

Figure 7 **Spinal nerves** (p36)

Figure 8 **Cranial nerves** (p37)

Figure 9 **Sympathetic and parasympathetic nervous systems** (p41)

Figure 10 **Trk signalling** (p56)

Figure 11 **NF κ B activation** (p68)

Figure 12 **HIF regulation** (p75)

Figure 13 **Experimental outline** (p87)

Figure 14 **Effect of SN50 on BDNF-dependent neurite growth** (p101)

Figure 15 **Effect of SN50 on CNTF-dependent neurite growth** (p102)

Figure 16 **Effect of κ B decoy DNA on BDNF-dependent neurite growth** (p103)

Figure 17 Effect of κ B decoy DNA on CNTF-dependent neurite growth (p104)

Figure 18 Effect of inhibiting NF- κ B activity on neurite arbor size (p105)

Figure19 Effect of Overexpressing NF κ B subunits on neurite growth (p106)

Figure 20 Effect of Serine I κ B- α mutant on neurite growth (p109)

Figure 21 Effect of Tyrosine I κ B- α mutant on neurite growth (p110)

Figure 22 Effects of proteasome inhibition on BDNF and CNTF-dependent neurite growth (p113)

Figure 23 No degradation of I κ B α after treatment with CNTF (p114)

Figure 24 Preferential tyrosine phosphorylation of I κ B α after treatment with CNTF (p115)

Figure 25 Effect of Syk inhibition on neurite growth (p118)

Figure 26 Effect of Syk-DN on CNTF-supported neurite growth (p119)

Figure 27 NF κ B activation by CNTF (p121)

Figure 28 PHD3 expression (p134)

Figure 29 Increased survival of SCG neurons from *PHD3*^{-/-} mice (p135)

Figure 30 Specificity of PHD3^{-/-} effect (p136)

Figure 31 PHD3 induction (p137)

Figure 32 Specificity of PHD3 induction (p138)

Figure 33 HIF dependence of the PHD3 survival effect (p139)

Figure 34 Increased NT-3-dependent survival of SCG neurons from *PHD3*^{-/-} mice (p140)

Figure 35 PHD3 inactivation and neurite outgrowth at saturating NGF concentration (p142)

Figure 36 PHD3 inactivation and neurite outgrowth at a sub-saturating NGF concentration (1) (p143)

Figure 37 PHD3 inactivation and neurite outgrowth at a sub-saturating NGF concentration (2) (p144)

Figure 38 Effect of genetic inactivation of PHD3 on the anatomy of the SCG (p147)

Figure 39 HIF2 mediates the effect of PHD3 inactivation on SCG anatomy (p148)

Figure 40 Effect of genetic inactivation of PHD3 on the anatomy of other sympatho-adrenal tissues (p149)

Figure 41 Decreased sympathetic innervation of the iris in *PHD3*^{-/-} mice (p151)

Figure 42 Decreased sympathetic innervation of the pineal gland in *PHD3*^{-/-} mice (p152)

Figure 43 Decreased sympathetic innervation of the submandibular gland in *PHD3*^{-/-} mice (p153)

Figure 44 Physiological defect in an SCG target of *PHD3*^{-/-} mice (p155)

Figure 45 Neurotrophin-independent survival increases with age (p163)

Figure 46 Depolarisation causes neurotrophin-independence in nodose neurons from P0 (p164)

Figure 47 Depolarisation causes neurotrophin-independence in DRG neurons from P5 (p165)

Figure 48 Depolarisation has no effect on SCG neurons during early postnatal life (p167)

Figure 49 L-type calcium channel inhibitors reverse the effects of KCl in nodose neurons (p168)

Figure 50 L-type calcium channel inhibitors reverse the effects of KCl in DRG neurons (p170)

Figure 51 ATP promotes survival of neonatal nodose neurons (p171)

Figure 52 Hypoxia reverses effects of ATP (p172)

List of Abbreviations

[Ca²⁺]_i - Internal Calcium Concentration
AchR- Acetylcholine receptor
ADNF – Activity-Dependent neurotrophic factor
Akt – Ak transforming/protein kinase B
ANOVA- Analysis of variance
APAF-1-Apoptotic protease activating factor
APP- Amyloid precursor protein
ATP- Adenosine tri-phosphate
BCL-2- B cell lymphoma
BDNF- Brain-derived neurotrophic factor
BMP-Bone morphogenetic protein
CaMKII- Calcium/calmodulin-dependent kinase II
CDNF – Conserved dopaminergic neurotrophic factor
CNS- Central nervous system
CNTF- Ciliary neurotrophic factor
CNTFR α - Ciliary neurotrophic factor receptor alpha
Cox-2- Cyclo-oxygenase 2
CREB-CAMP response element binding protein
CT-1- Cardiotrophin 1
DRG- Dorsal root ganglion
EPO- Erythropoetin
ERK- Extracellular signal regulated kinase
FGF- Fibroblast growth factor
GDNF- Glial derived neurotrophic factor
GFP- Green fluorescent protein
gp130- Glycoprotein 130
GPI- Glycophosphatidylinositol
HBSS- Hanks balanced salt solution
HGF- Hepatocyte growth factor
HIF- Hypoxia-inducible factor
IKK- Inhibitor kB kinase
IL-6- Interleukin 6
I κ B- Inhibitor kappa B
I κ B- Inhibitor kappa B
JAK- Janus kinase
KCl- Potassium chloride
KIF4- Kinesin family 4
LGE- Lateral ganglionic eminence
LIF- Leukaemia inhibitory factor
LIFR β - LIF receptor beta

LTP- Long term potentiation
MAPK- Mitogen activated protein kinase
MEK- Mitogen activated protein kinase kinase
MGE- Medial ganglionic eminence
MSP- Macrophage stimulatory protein
MuSK- Muscle specific kinase
N-Cam- Neural cell adhesion molecule
NEMO- Nuclear factor kappa B essential modifier
NFκB- Nuclear factor kappa B
NG- Nodose ganglion
NIK- NF kappa B inhibitory kinase
NMJ- Neuromuscular junction
NOS-II – Nitric oxide synthase II
NT-3- Neurotrophin 3
NT4/5- Neurotrophin 4/5
NT-6- Neurotrophin 6
NT-7- Neurotrophin 7
NTD- Neural tube defect
ODD- Oxygen dependent degradation domain
OSM- Oncostatin M
P2X- Purinergic 2X
p75- Low affinity neurotrophin receptor
PARP-1- Poly ADP ribose polymerase
PBS- Phosphate buffered saline
PCD- Programmed cell death
PHD- Proline hydroxylase domain
PI-3K- Phosphatidyl inositol 3 kinase
PKC- Protein kinase C
PLCγ- Phospho lipase C gamma
PNS- Peripheral nervous system
pRb- Retinoblastoma protein
Rapsyn- Receptor associated protein of the synapse
RHD- Rel homology domain
SCG- Superior cervical ganglion
SH2- Src homology 2
STAT- Signal transducer and activator of transcription
Syk- Spleen tyrosine kinase
TG- Trigeminal ganglion
TH- Tyrosine hydroxylase
TNF-α- Tumour necrosis factor alpha
Trk- Tropomyosin related kinase
VEGF- Vascular endothelial growth factor
VHL- Von-Hippel Lindau
Wnt- Wingless

Y42F- Tyrosine IκB mutant
YFP- Yellow fluorescent protein

Acknowledgements

Many thanks to Prof. Alun Davies for the excellent supervision and support over the last few years. Thanks for your sound advice and permanent good nature.

Thanks also to Dr. Humberto Gutierrez for always having the time to help with techniques or discuss experiments in a patient, enthusiastic and friendly manner.

To all members of the Davies' lab, past and present, who helped create a relaxed working environment and were always supportive inside and outside the lab. Thanks also for the entertaining lunchtime discussions covering a range of important issues from baby-throwing technique to extreme leaning.

Thanks to all my friends in Cardiff and Ireland, especially Michelle Finnegan who was always there to help during stressful times.

Thanks to my Dad, Rob, Lyn, Amy and Zoe, who it was always a pleasure to return home to.

Go raibh mile maith agaibh go leir.

To Christine and Phil

Chapter 1 – General Introduction

1.1 Brief overview of neuronal development

1.1.1 Introduction

A series of tightly regulated mechanisms have been conserved throughout evolutionary time to construct the vertebrate nervous system. Neurons are born, migrate, extend processes towards their targets and finally make an appropriate number of functional synaptic contacts with a target tissue. I will first provide a brief overview of these stages of neuronal development followed by a description of the structure and development of the peripheral nervous system (PNS). I will then describe in detail the regulation of neuronal survival and neurite outgrowth. Finally, I will introduce two families of proteins, the NF κ B transcription factor family and PHD family, whose roles in peripheral neuronal survival and / or neurite outgrowth are the main focus of this research.

1.1.2 Neural induction

The fertilised ovum undergoes multiple divisions eventually forming a bilaminar disc. The bilaminar disc contains two cell types, ectodermal and endodermal cells. Ectodermal cells migrate to form an intermediate layer called the mesoderm. The formation of the trilaminar embryo, consisting of ectoderm, endoderm and mesoderm is known as gastrulation. These three layers give rise to the adult body. The ectoderm will eventually give rise to the entire nervous system as well as the epidermis. Neural induction is the process by which ectodermal cells “decide” to become neuronal. Once ectodermal cells have been induced, they elongate and are referred to as neuroectodermal cells or neural plate cells.

A series of pioneering experiments using amphibian embryos, established that the signal which specifies induction of ectoderm is contained within an “organiser” tissue in the dorsal blastopore lip. Transplantation of “Spemann’s organiser” from the dorsal side of one embryo to the ventral side of another embryo induced the formation of a secondary neural axis ventrally. Interestingly, transplantation of “organiser” tissue (Hensen’s node in mammals) from one species can induce the formation of a neural axis in another species which indicates that the mechanisms of neural induction are highly conserved [1-3]

Hilde Mangold, who carried out the classical experiments which identified the “organiser”, died in 1924 at the age of 26 in a kitchen fire. Had she survived, she would have witnessed decades of research dedicated to identifying the molecular mechanisms of neural induction. It was not until the early 1990s that three proteins were identified within the organiser that were capable of neuralising the ectoderm ; Noggin [4-7], Follistatin [8] and Chordin [9, 10]. All three proteins are inhibitors of bone morphogenetic proteins (BMPs) [11-13] The finding that BMP4 inhibits neural fate but promotes epidermal fate led to the proposal of a default model of neural induction [14-16]. The default model of neural induction proposes that ectodermal cells tend to differentiate into neuronal cells but when BMP4 is present ectodermal cells differentiate into epidermal cells. Molecules like noggin, follistatin and chordin therefore induce neural differentiation by inhibiting the promoter of epidermal differentiation. Other BMP-inhibiting molecules have been identified such as Cerberus [17, 18], Gremlin, Dan and Drm [19-23] and Ogon/Sizzled [24, 25]. Recent findings have suggested that the simple default model described above may be too

simple to account for the complexity of neural induction. In addition to BMP signalling, Fibroblast growth factor (FGF), Wingless (Wnt), Protein kinase C (PKC) and Ca^{2+} have all been implicated in the regulation of neural induction [26]. It has become clear that the activation or repression of many genes at various times during induction regulate the formation of the neural plate.

1.1.3 The neural tube

A critical event during neuronal development is the formation of the neural tube. The neural tube gives rise to the entire adult central nervous system (CNS). The formation of the neural tube begins when the flat layer of cells making up the neural plate begins to fold and eventually fuses in the midline to form a hollow tube (Fig. 1). The fusion of the neural tube proceeds rostrally and caudally from the initial site(s) of fusion, forming a hollow cylinder with openings at both ends called the cranial and caudal neuropores. Although the cellular events leading to neural tube formation are well known [27], the molecular mechanisms are only beginning to be elucidated.

The initial neural plate re-shaping involves a process called convergent extension, during which laterally placed cells move towards the midline [28-30]. Convergent extension appears to be regulated by members of a non-canonical Wnt signalling pathway, the planar cell polarity pathway. The subsequent bending and folding of the neural plate is at least partially regulated by Sonic Hedgehog [31, 32]. The neural folds fuse in the midline and processes are extended between the neural folds whilst glycoproteins are deposited at the point of fusion [27]. Failure of the neural folds to elevate and fuse can result in a myriad of birth defects collectively referred to as

neural tube defects (NTDs). In humans the most common NTDs are anencephaly (a fatal failure of rostral neural tube closure) and myelomeningocele (failure of the vertebral neural tube fusion). To date, there have been over 80 mouse mutants generated which display NTDs, examples of which are shown in figure 2. The coordinated action of many genes and environmental signals regulate neural tube formation and expansion of this simple tube leads to the formation of the brain and spinal cord [33].

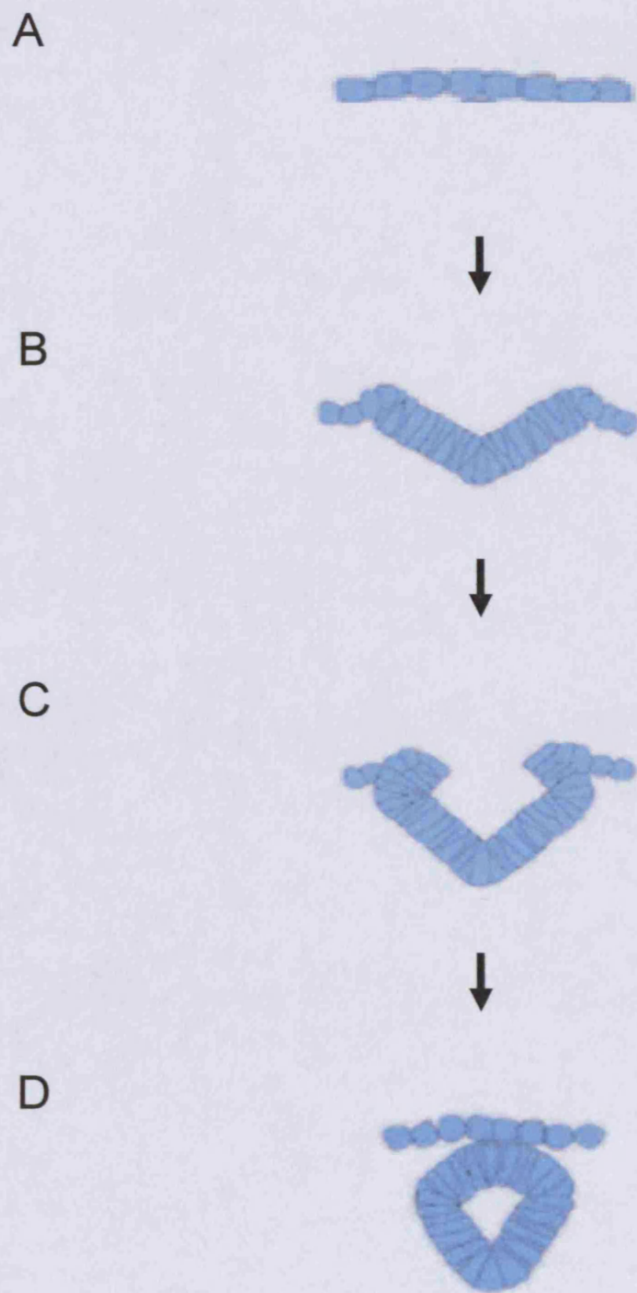


Figure 1 | **Neural tube formation.** The neural tube is formed as the flat neural plate (A) folds towards the midline (B and C). The apices of the neural folds join in the midline to form the neural tube (D).

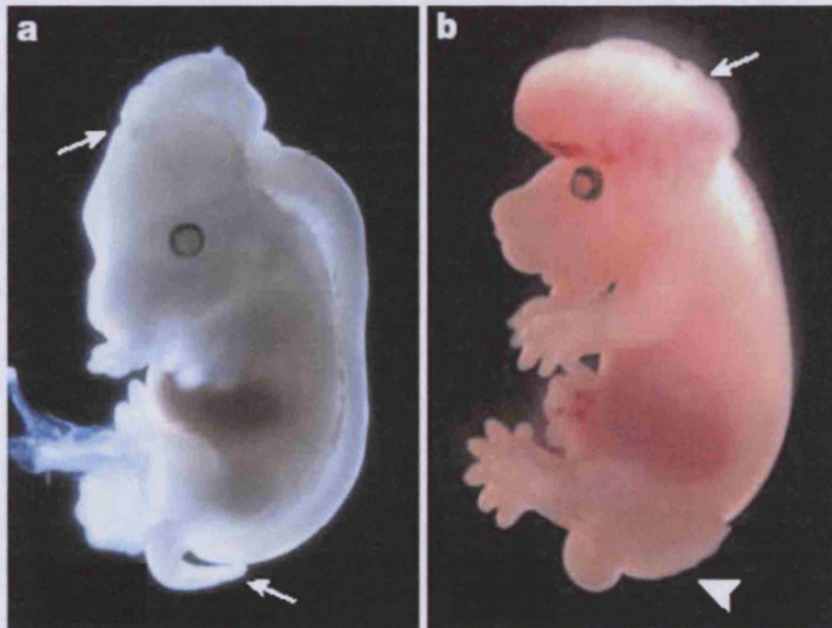


Figure 2 | **Neural tube defects.** Mouse foetuses at embryonic day (E) 15.5 illustrate the appearance of (a) craniorachischisis and (b) exencephaly and open spina bifida. In craniorachischisis, the neural tube is open from the midbrain to the lower spine (between the two thin arrows in a). In the foetus shown in b, exencephaly is restricted to the midbrain (thin arrow in b), whereas spina bifida affects the lumbosacral region (arrowhead in b).

1.1.4 Neurogenesis

The neural tube consists of bi-polar neuroepithelial cells that stretch the width of the tube from the pial surface to the ventricular surface. The nuclei of neuroepithelial cells move between the pial and ventricular surfaces in a process termed interkinetic nuclear migration [34] which is illustrated in figure 3. The position of the nuclei varies depending on the stage of the cell cycle. Nuclei move towards the pial surface during G₁ where they begin DNA synthesis (S). Once DNA synthesis is complete cells enter G₂ and the nuclei return to the ventricular surface [35-37]. At the ventricular surface the neural epithelial cell divides by mitosis (M). Daughter cells then “decide” whether to re-join the pial surface and re-enter the cell cycle or exit the cell cycle and accumulate in a region called the intermediate zone. Proliferation of cells in the early embryonic neural tube leads to the formation of swellings called the telencephalon, diencephalon, metencephalon, myelencephalon mesencephalon and rhombencephalon, the precursors of the adult forebrain, midbrain and hindbrain (Fig. 4).

Markers like [³H]-thymidine and BrdU have been used to identify the birth dates of neurons by binding to cells in S-phase [38-41]. Birth dating studies have revealed that withdrawal from the mitotic cell cycle occurs at defined times and varies between different regions of the neural tube. Neurons in the hindbrain are first to withdraw, followed by neurons in the spinal cord and ventral mesencephalon. Neocortical and cerebellar neurons withdraw from the cell cycle later in development. In general, firstborn neurons contribute to ventral brain structures and neurons born later in development form dorsal structures involved in sensory and integrative functions. The

decision to exit the cell cycle may be regulated by retinoblastoma protein (pRb) through its inhibitory effect on the E2F family of transcription factors which are essential for G₁ to S transition. Inactivation of cyclin-dependent kinases by cyclin kinase inhibitors may also be required for cell cycle withdrawal[42]. Post-mitotic (G₀) progenitor cells in the intermediate zone then begin migration and differentiation. The multitude of neuronal and glial cell types found in the adult CNS originate from a population of neuroepithelial precursors in the embryonic neural tube.

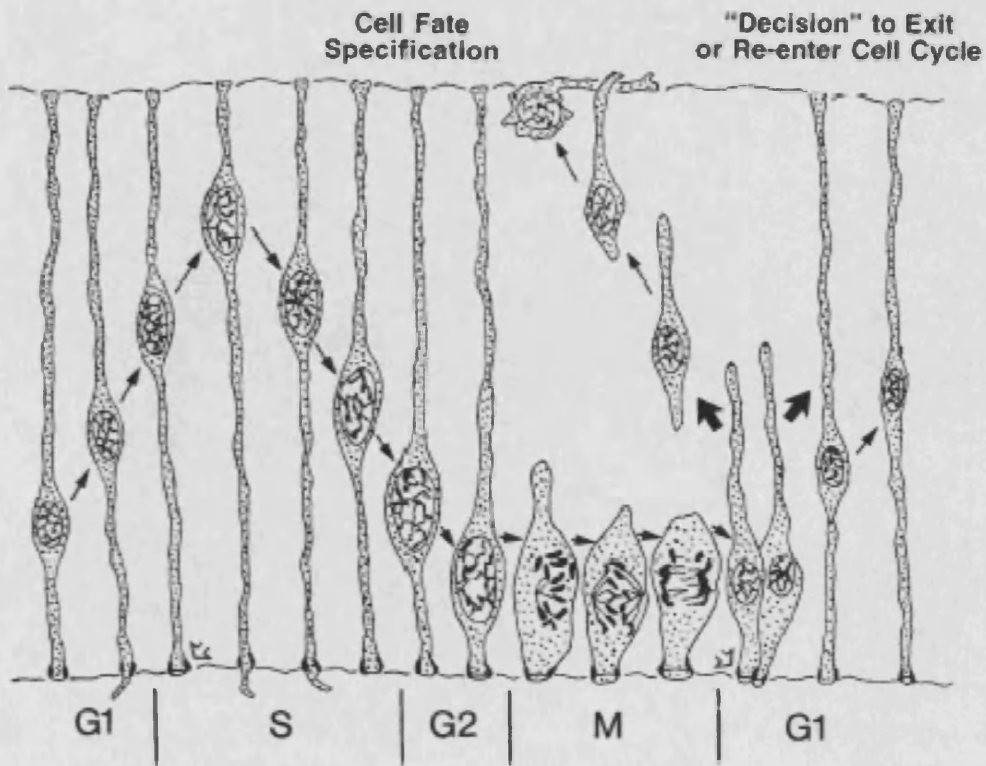


Figure 3 | **Neurogenesis.** Drawing illustrating interkinetic nuclear migration. The ventricular surface is at the bottom and the pial surface at the top of the illustration. Nuclei move towards the pial surface during G1 , where DNA synthesis (S) begins. Nuclei return to the ventricular surface at G2 where mitosis begins (M). Taken from (Hollyday 2001) based on (Sauer 1935)

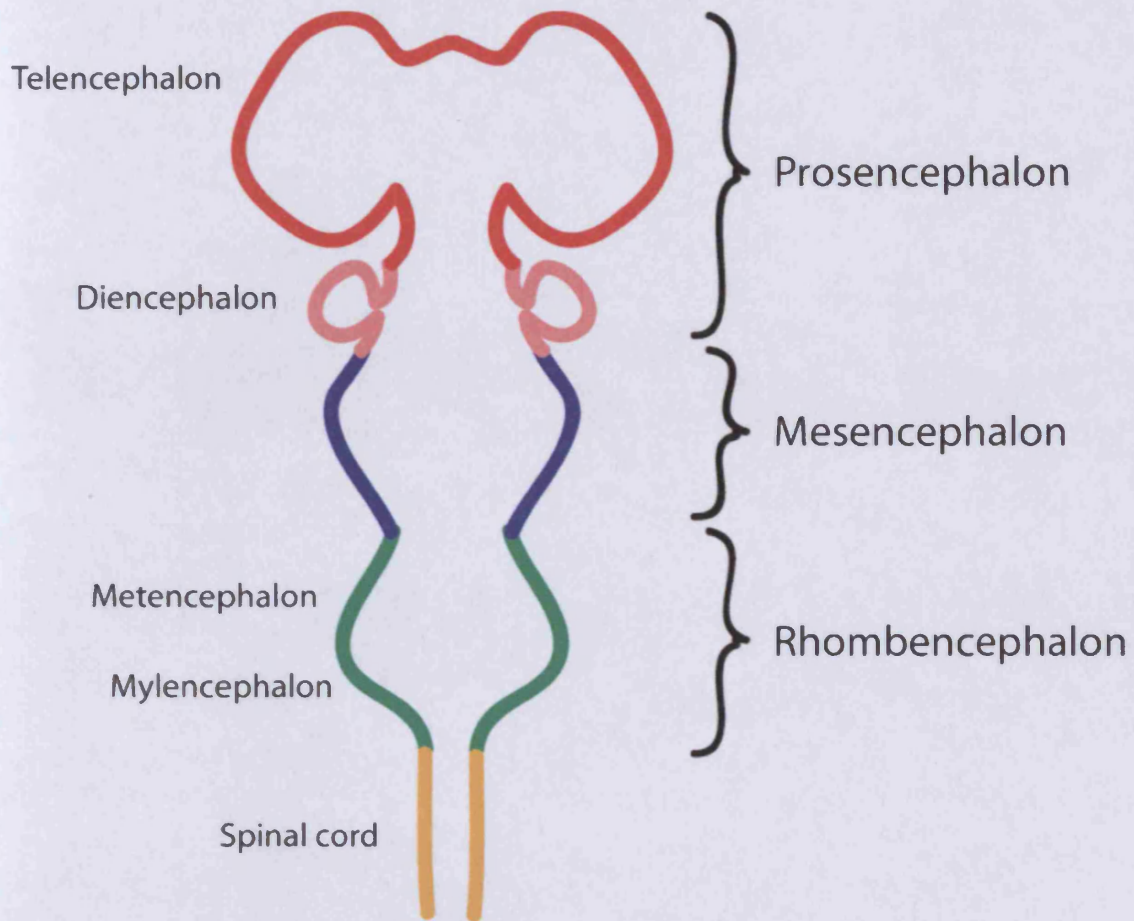


Figure 4| **Early embryonic CNS.** Illustration showing the neural tube and vesicles. Proliferation and migration of progenitor cells in the walls of the neural tube will give rise to the forebrain, midbrain, hindbrain and spinal cord.

1.1.5 Neuronal migration

Neurons are born when proliferating neuroepithelial cells withdraw from the cell cycle and accumulate in the ventricular zone. Newborn neurons must then migrate to their final destination. One type of neural progenitor in the early neural tube, the radial glial cell, retains its contacts with both the pial and ventricular surfaces. The processes of radial glial cells stretch, like the spokes of a bicycle wheel, between the pial and ventricular surfaces [43]. These long radial processes provide a scaffold for neurons migrating from the site of proliferation to their final destination (Fig. 5A-C) [44, 45]. Radial migration is the route by which the vast majority of neuronal precursors in the mammalian cortex reach their final destination [46]. In addition to the cerebral cortex, other laminated structures such as the cerebellar cortex, spinal cord, striatum and thalamus use either radial migration, or a mixture of radial and tangential migration. Tangential migratory routes have also been identified from the medial ganglionic eminence (MGE) to the neocortex and hippocampus, and from the lateral ganglionic eminence (LGE) to the olfactory bulb [47, 48].

Molecular regulation of neuronal migration requires complex co-ordination of external guidance cues and intracellular signalling mechanisms involved in cell motility [49]. Mutations affecting these pathways of neuronal migration can result in severe developmental abnormalities such as lissencephaly (Fig. 5D).

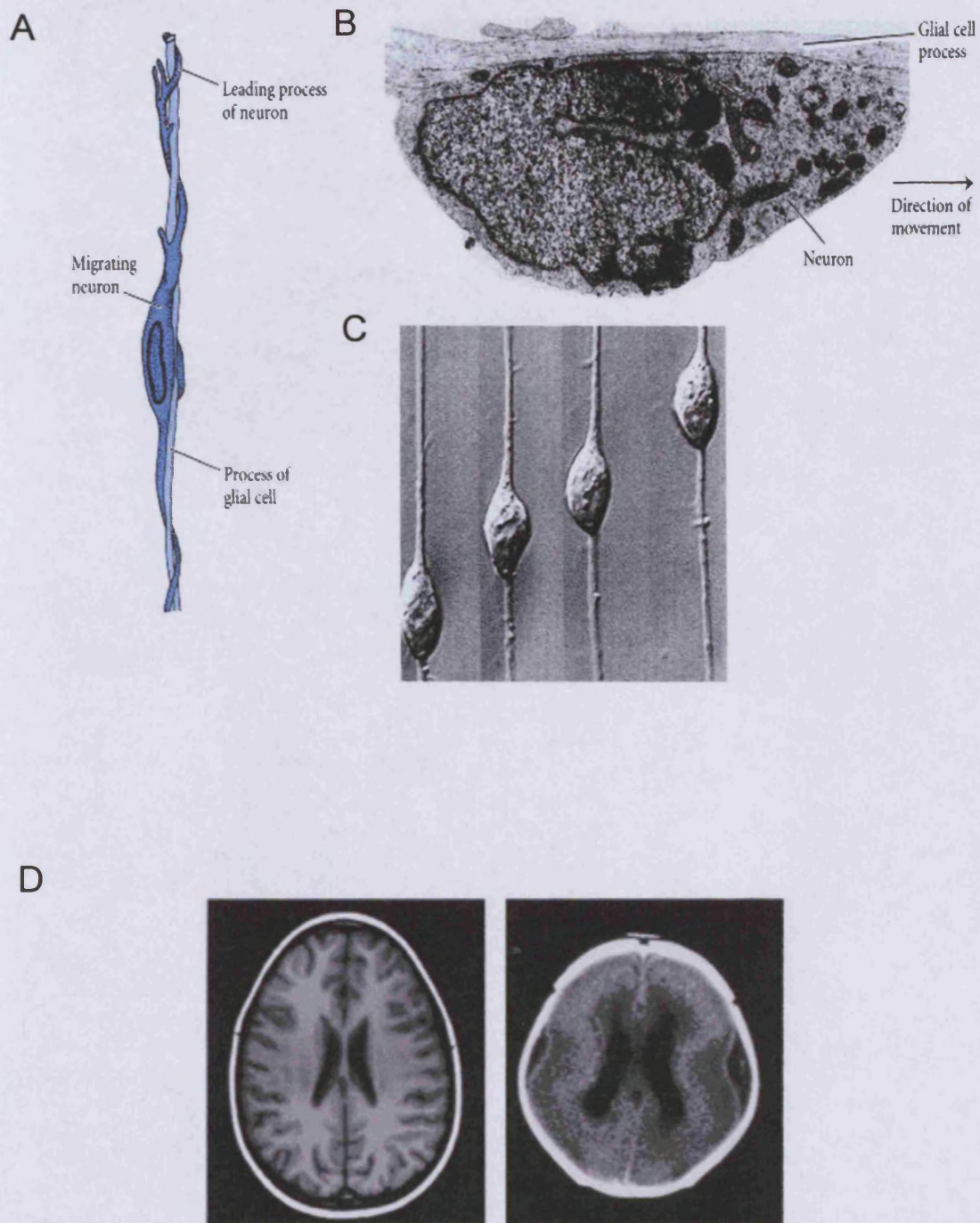


Figure 5 | **Neuronal migration.** (A) Illustration of a cortical neuron migrating on a glial cell process. (B) Electron micrograph of the region where the neuronal cell body adheres to the glial process. (C) Sequential photographs of a neuron migrating on a cerebellar glial process. Images taken from Gilbert *Developmental Biology* 6th edition. (D) MRI images comparing normal brain (left) with Lissencephaly (right).

1.1.6 Axon growth and PCD

Before, during or after migration is complete, neurons begin to extend axons which are guided towards their targets. A combination of locally acting and diffusible guidance cues and target-derived neurotrophic factors regulate the final innervation pattern in the target tissue. During the period of target innervation approximately 50% of neurons die by programmed cell death (PCD). The regulation of PCD and axon growth / guidance is discussed in detail in sections 1.3 and 1.4.

1.1.7 Synaptogenesis

Neural signalling is based on complex patterns of activity between networks of neuronal and non-neuronal cells. Waves of activity are communicated between neurons via specialised regions of apposition called synapses. Neurotransmitters are released from the presynaptic active zone, traverse the synaptic cleft and bind to receptors that are clustered in a region called the postsynaptic density. The binding of neurotransmitters to postsynaptic receptors then stimulates or inhibits electrical activity in the postsynaptic cell. The structure of a typical synapse is shown in figure 6. The formation of synapses occurs over a protracted period of embryonic and postnatal development. Synapse formation and elimination are also crucial for complex adult brain functions such as learning and memory so the cellular and molecular events involved are of broad interest to neurobiologists.

Much of our understanding of synapse formation comes from studies of the neuromuscular junction (NMJ). The clustering of nicotinic acetylcholine receptors (AChR) at the site of innervation is a crucial step in the development of the NMJ [50]. Agrin, a protein expressed at the NMJ, can induce clustering [51] and mice lacking

agrin die perinatally due to defective NMJ development [52]. The physiological role of agrin appears to be to prevent the dispersion of AChR clusters on developing muscle cells rather than inducing the initial clustered pattern [50]. Receptor associated protein of the synapse (Rapsyn) forms complexes with AChRs which are required for the formation of clusters [53]. Another postsynaptic protein, muscle specific tyrosine kinase (MuSK) has also been implicated in receptor clustering in vivo [54]. MuSK regulates synaptic formation by stabilising the postsynaptic density [55, 56]. The formation and maintenance of synapses in the CNS also requires the co-ordinated action of many cell surface adhesion molecules, secreted proteins like Wnt and FGF and neural activity [57].

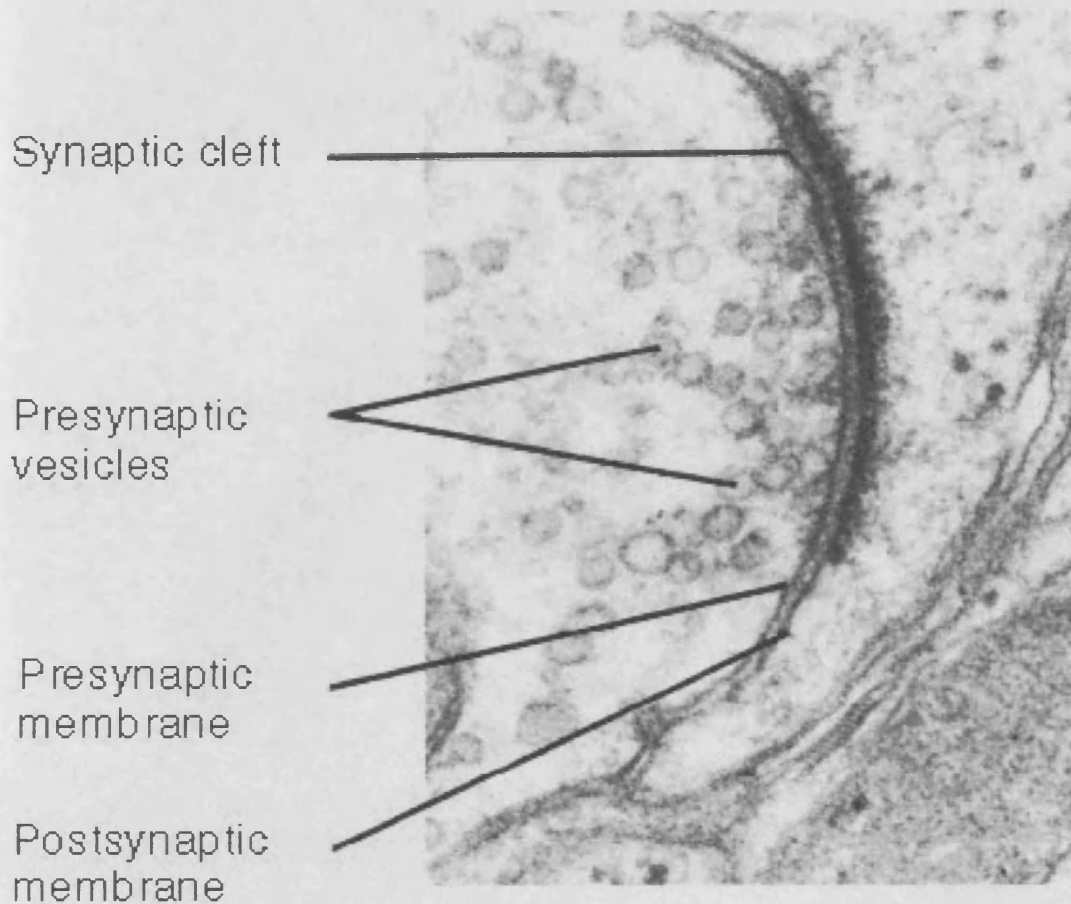


Figure 6 | **Synaptic structure.** Micrograph showing a synapse between two neurons. Neurotransmitters contained within synaptic vesicles are released from the presynaptic cell, traverse the synaptic cleft and bind to receptors on the postsynaptic membrane.

1.2 Organisation and development of the peripheral nervous system

1.2.1 Introduction

The CNS, which develops from proliferating cells in the neural tube (as described above), consists of the brain and spinal cord. The PNS provides a link between the CNS and the periphery. The PNS can be separated into somatic and autonomic subdivisions. The somatic sensory PNS consists of sensory neurons of the dorsal root and cranial sensory ganglia. The autonomic PNS consists of the sympathetic, parasympathetic and enteric systems. The work described in this thesis is centred on the roles of the NF κ B family of transcription factors and PHD3, in the regulation of neuronal survival and/or neurite growth from discrete populations of sensory and sympathetic peripheral neurons during development. A pilot study will also be presented examining the role of neural activity in the regulation of neuronal survival during the development of the same populations of peripheral neurons. In this section I will therefore describe the organisation of the PNS and then provide a brief overview of the embryonic development of the PNS.

1.2.2 Organisation of the somatic PNS

Sensory information from the skin, muscles and joints of the limbs and trunk is relayed to the spinal cord by neurons contained in the dorsal root ganglia (DRG). The DRG lie adjacent to the spinal cord and contain pseudounipolar neurons. The peripheral branch of DRG neurons forms the dorsal root of the appropriate spinal nerve for that level and the central branch synapses in the dorsal column of the spinal cord. The ventral root of each spinal nerve consists of motor axons originating in the ventral spinal cord. The organisation of a typical spinal nerve is illustrated in figure 7.

The twelve pairs of cranial nerves (Fig. 8) provide peripheral innervation to various tissues in the head and thorax. There are seven cranial sensory ganglia whose axons form part of five of the twelve cranial nerves. The trigeminal ganglion is located on cranial nerve V and its neurons innervate mechanoreceptors, thermoreceptors and nociceptors in the face. The geniculate ganglion, found on cranial nerve VII, innervates taste buds on the anterior tongue. The vestibulo-cochlear ganglion, which joins cranial nerve VIII, innervates hair cells in the inner ear. The petrosal ganglion is located on cranial nerve IX and innervates taste buds in the posterior tongue. The jugular and nodose ganglia join cranial nerve X and innervate various targets in the pharynx, thorax and abdomen. Finally, the superior glossopharyngeal ganglion, is also located on cranial nerve IX. In summary, spinal and cranial nerves link muscles, glands and other peripheral end organs with the CNS.

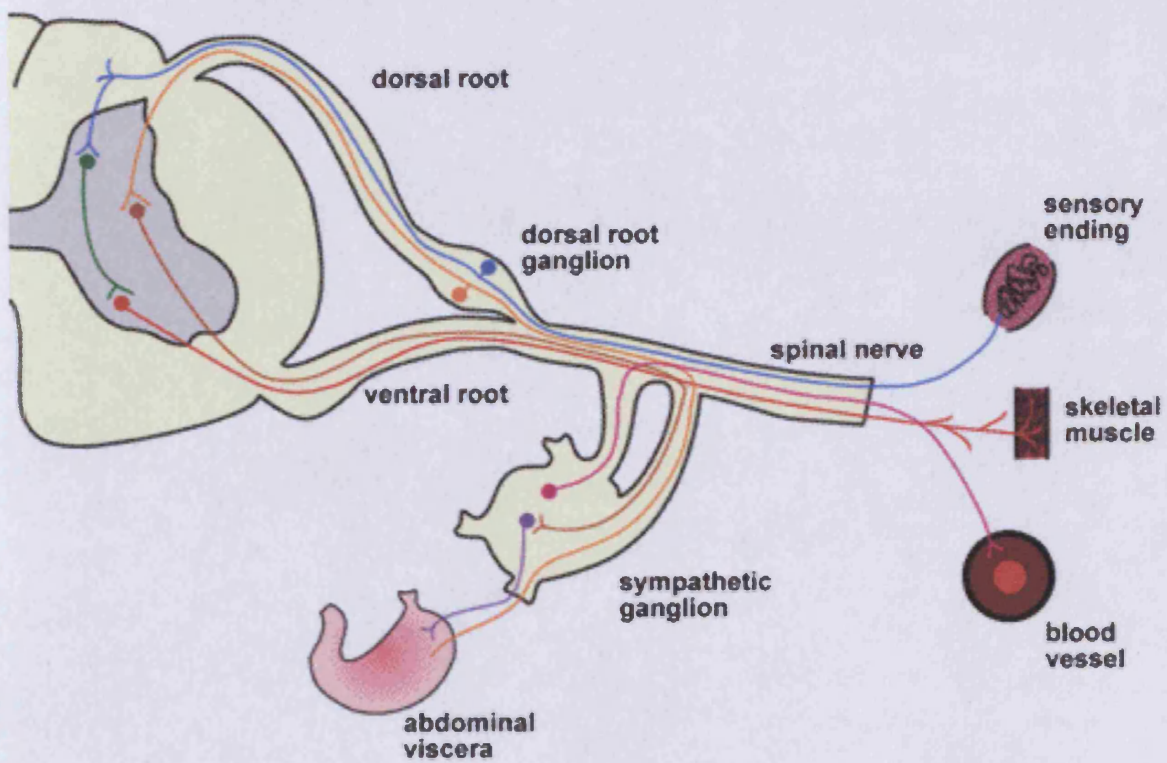


Figure 7 | **Spinal nerves.** Illustration showing the typical composition of a spinal nerve. Sensory neurons are contained in the DRG and synapse centrally in the dorsal horn of the spinal cord. Motor neurons from the ventral spinal cord form the ventral root of the spinal nerve and sympathetic ganglia in thoracolumbar spinal levels join the spinal nerve to innervate smooth muscles and glands.

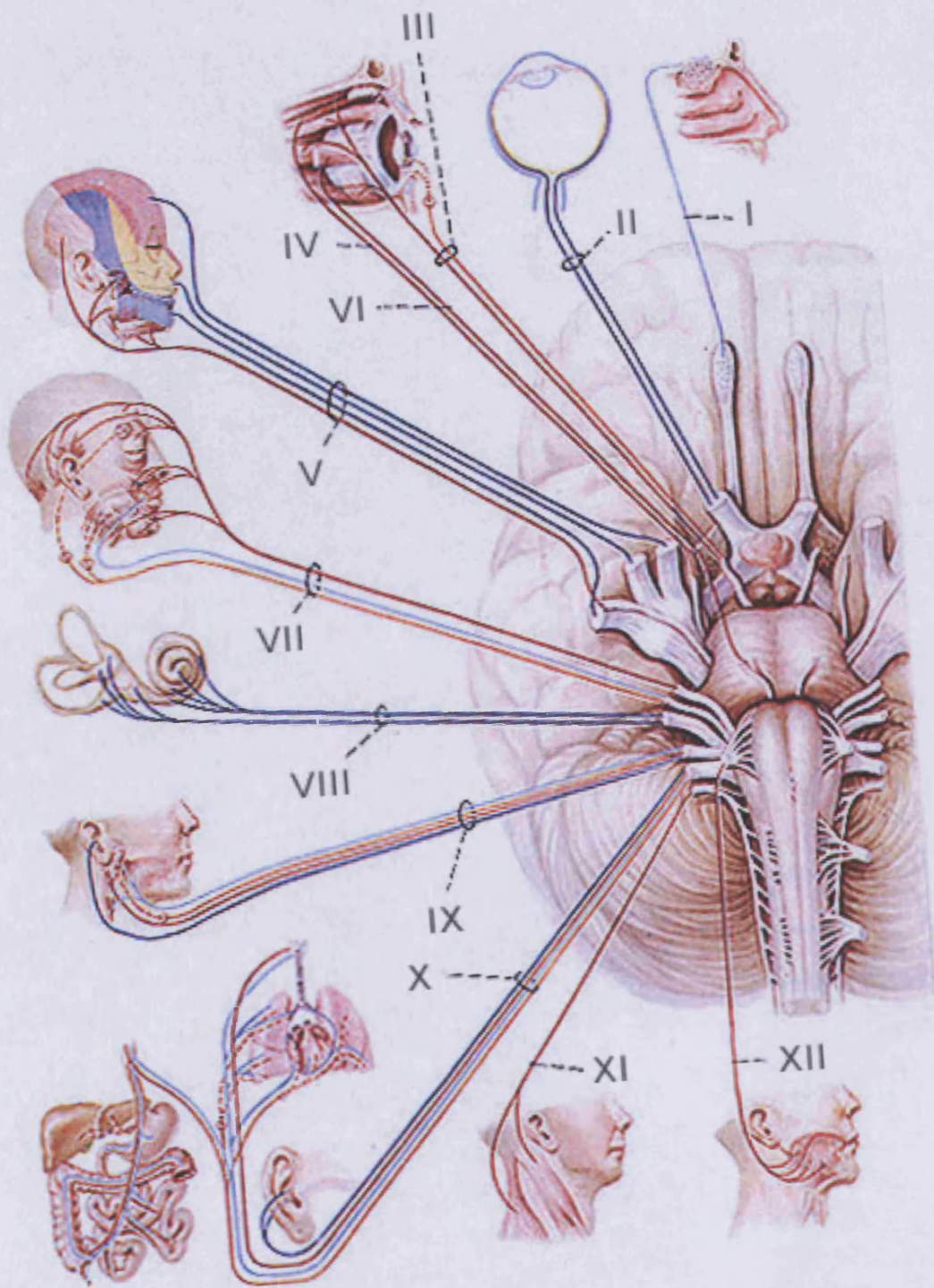


Figure 8 |Cranial nerves. Illustration showing the roots of the 12 cranial nerves and their peripheral target tissues.

1.2.3 Organisation of the autonomic nervous system

The autonomic nervous system provides visceral motor innervation to smooth muscle, heart muscle and exocrine glands. The autonomic nervous system can be separated into three subdivisions ; the sympathetic nervous system, the parasympathetic nervous system and the enteric nervous system.

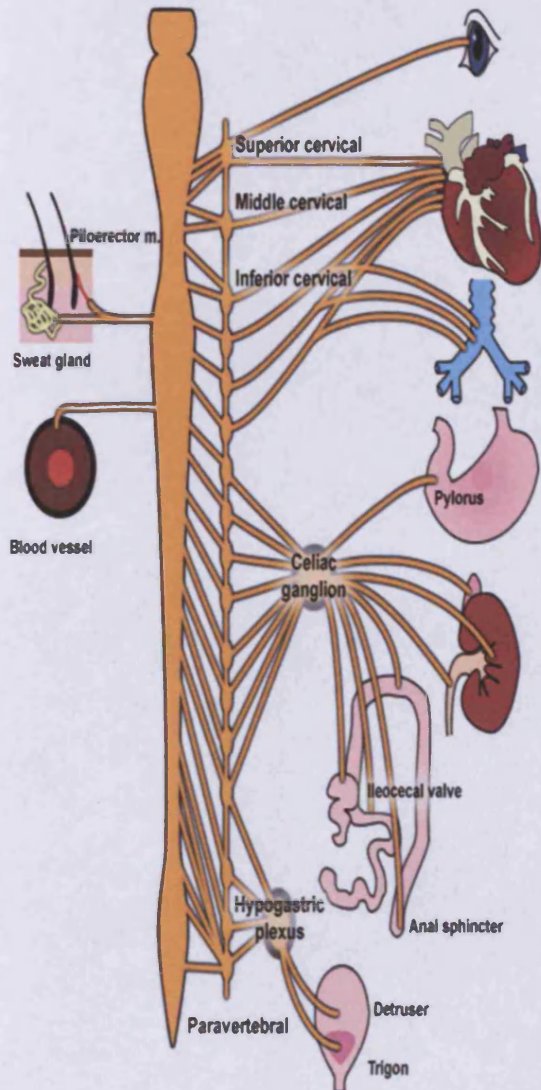
Preganglionic sympathetic neurons are found in the intermediolateral column of the spinal cord between segments T1-L2. Preganglionic sympathetic axons leave the spinal cord via the ventral root and synapse with neurons contained within sympathetic paravertebral ganglia. The paired sympathetic paravertebral ganglia are found adjacent to the spine from cervical to sacral segments. There are three cervical paravertebral ganglia: the superior cervical ganglion, the middle cervical ganglion, and the stellate ganglion. There are eleven thoracic ganglia, four lumbar ganglia, and four or five sacral ganglia. At the level of the coccyx, the two sympathetic ganglia chains join in the single ganglion impar [58]. Postganglionic axons leave the paravertebral ganglia via the gray rami communicantes to join segmental spinal nerves. Postganglionic sympathetic fibres from the superior cervical ganglion innervate the eyes, salivary glands, lacrimal glands and major blood vessels of the head and neck. Prevertebral ganglia, found in groups related to major abdominal blood vessels, including the coeliac, aorticorenal and mesenteric ganglia innervate organs of the digestive and urogenital tracts. Preganglionic neurons innervating the prevertebral ganglia are situated in the intermediolateral column but also receive afferent input from neurons located in the walls of the target organs.

Sweat glands, piloerector muscles, and blood vessels throughout the body receive sympathetic innervation from postganglionic sympathetic fibres. Sympathetic stimulation results in pupillary dilatation, increased heart rate and contractility, bronchodilation, vasoconstriction of the mesenteric circulation, and vasodilation of skeletal muscle arterioles in what is commonly referred to as the “fight or flight” response.

Preganglionic parasympathetic neurons are found in the brainstem and sacral spinal segments (S2, S3 and S4) and are often referred to as craniosacral outflow. Cranial parasympathetic neurons are found in four brainstem nuclei ; Edinger-Westphal nucleus, superior salivatory nucleus, inferior salivatory nucleus, and the dorsal vagal complex of the medulla. Axons emerging from these nuclei travel in cranial nerves III (oculomotor); VII (facial nerve); IX (glossopharyngeal nerve); and X (vagus nerve) respectively. Cranial postganglionic parasympathetic ganglia are embedded in or found close to their peripheral targets and innervate the ciliary body, lacrimal glands, salivary glands and mucous glands and provide the parasympathetic innervation to thoracic and abdominal viscera as far as the transverse colon. Sacral preganglionic parasympathetic fibres exit via the sacral ventral roots S2-S4 and corresponding sacral spinal nerves and then continue to the pelvic viscera as the pelvic nerve. The sacral preganglionic parasympathetic efferent axons of the pelvic nerve synapse with postganglionic parasympathetic neurons in the ganglia of the pelvic plexus. Postganglionic axons innervate the descending colon, rectum, urinary bladder and sexual organs.

The enteric nervous system controls the coordinated muscular contractions involved in digestion and also innervates blood vessels and glands of the gastric mucosa. The enteric nervous system has two divisions that are connected by nerve processes: the submucosal plexus (Meissner's plexus), which innervates the mucosa and regulates secretion; and the myenteric plexus (Auerbach's plexus), which innervates the circular and longitudinal smooth muscle layers and regulates motility.

Sympathetic Division



Parasympathetic Division

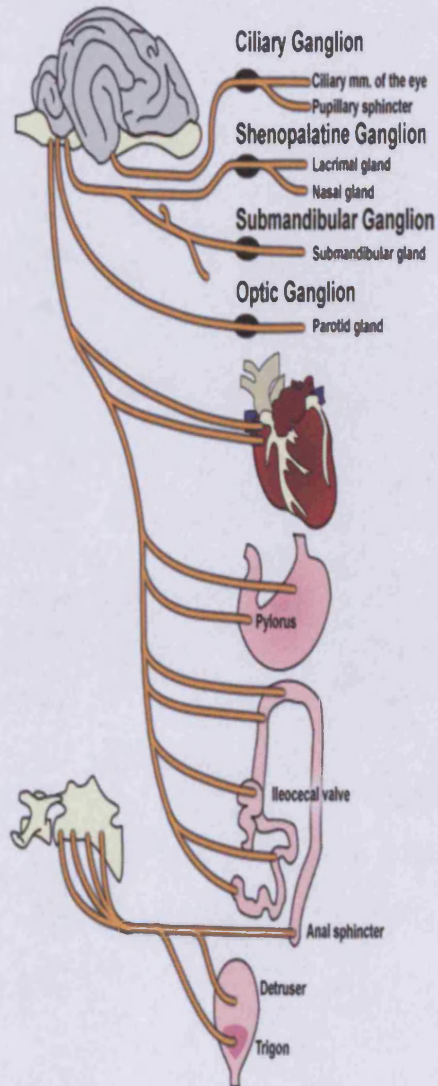


Figure 9 | **Sympathetic and parasympathetic nervous systems** Illustration showing the organisation of the sympathetic (left) and parasympathetic (right) nervous systems and some peripheral target tissues of each system.

1.2.4 Development of the sensory and autonomic PNS

Peripheral sensory neurons are derived from two sources: the neural crest and the neurogenic placodes. The neural crest is an incredibly diverse structure which originates from the neural folds after interactions between the neural plate and the presumptive epidermis [59, 60]. Migration and differentiation of neural crest cells from the dorsal neural tube gives rise to many cell types including; neurons and glia of the sensory, sympathetic, and parasympathetic nervous systems, melanocytes, facial cartilage, bone and connective tissue [61]. The fate of neural crest cells is largely dependent on the migratory route taken and the final position of the cells.

The trunk neural crest is a transitory structure whose cells begin to migrate as the neural tube closes [61]. There are two principal modes of migration utilised by trunk neural crest cells, the dorsolateral pathway and the ventral pathway. Cells that migrate along the dorsolateral pathway travel into the epidermis and become melanocytes. Cells migrating in the ventral pathway give rise to the dorsal root ganglia (DRG), sympathetic ganglia and cells of the adrenal medulla. The dorsomedial part of the trigeminal ganglion, the trigeminal mesencephalic nucleus, and the jugular ganglion are all derived from the cranial neural crest. Neurons of the parasympathetic nervous system are derived from the mesencephalic neural crest and the enteric nervous system is derived from the vagal and lumbrosacral neural crest [62]. All Schwann and satellite cells in sensory and autonomic ganglia have been shown to be neural crest derived [63]. The molecular regulation of neural crest formation and migration is incompletely understood [64]. Both BMP and FGF signalling have been implicated in neural crest induction [59, 65]. Mouse embryos in which β -catenin has been inactivated have malformed neural crest derivatives, including the DRG and various

craniofacial regions, implicating Wnt signalling in neural crest formation and differentiation [66].

Although the majority of sensory neurons are formed after migration and differentiation of neural crest cells, cranial sensory ganglia are derived from both neural crest cells and neurogenic placodes [67]. Neurogenic placodes are focal thickenings of embryonic ectoderm which are induced by signals originating in the surrounding cranial tissue. The neurogenic placodes can be divided into two groups, dorsolateral and epibranchial, based on their position in the developing cranium. The dorsolateral placodes give rise to the vestibular and ventrolateral trigeminal ganglia. The epibranchial placodes give rise to the nodose, petrosal and geniculate ganglia.

1.3 Regulation of neuronal survival in the PNS

1.3.1 Introduction

Apoptosis or programmed cell death (PCD) is crucial both during normal development and in the adult. A family of intracellular proteases known as caspases are largely responsible for the well-described biochemical and morphological changes associated with apoptosis. The intrinsic apoptotic pathway is activated by developmental cues, DNA damage and growth factor deprivation and is tightly controlled by members of the B-cell lymphoma-2 (Bcl-2) family. The extrinsic apoptotic pathway is triggered by activation of death receptors leading to caspase activation independently of Bcl-2 family members. Members of the Bcl-2 family are

typically divided into three groups ; anti-apoptotic (Bcl-2, Bcl-X_L, Bcl-W), pro-apoptotic (BAX, BAK, BOK) and BH3-only proteins (BAD, BIK, BIM, NOXA, PUMA) which regulate anti-apoptotic members of the Bcl-2 family to promote apoptosis [68]. Pro-apoptotic members like BAX can permeabilise the mitochondrial membrane leading to the release of apoptogenic molecules such as cytochrome c and DIABLO. Cytochrome c binds to apoptotic protease-activating factor-1 (APAF1) to form a protein ring known as the apoptosome that binds to and activates caspase 9 to promote apoptosis [69, 70]. Signal transduction pathways link the extracellular environment to cell death/survival machinery during development and in the adult. Neuronal apoptosis is regulated by a tightly controlled balance of survival-promoting, target-derived neurotrophic factors and death signals. For example, nerve growth factor (NGF) binding to TrkA activates numerous pro-survival pathways like PI-3 kinase, Akt and MEK/MAPK which support survival by inhibiting pro-apoptotic proteins like Bad and Forkhead and by activating other pro-survival pathways like CREB (Yuan and Yankner 2000). The following sections introduce the origins of the neurotrophic theory, describe the neurotrophic requirements of relevant PNS neurons and introduce the biology of the neurotrophic factors.

1.3.2 The neurotrophic theory

During the development of the nervous system excess neurons are generated. The surplus neurons are removed during a phase of naturally occurring cell death shortly after axons reach their targets [71-73]. This phase of apoptotic cell death is thought to remove neurons with inappropriate synaptic connections and ensures that a suitable number of neurons survive relative to the size of the target field. Neurons compete for a limited supply of neurotrophic factors. According to the neurotrophic theory,

neurons that acquire neurotrophic support survive and those that do not die by apoptosis. The neurotrophic theory was formulated following the discovery of the first neurotrophic factor, nerve growth factor (NGF). The pioneering studies of Hamburger and Levi-Montalcini in the 1940s and 1950s led to the discovery of NGF. Since the discovery of NGF evidence has mounted in support of the neurotrophic theory.

Whereas populations of sympathetic and sensory neurons that are dependent on NGF *in vitro* are eliminated by administration of anti-NGF antibodies *in vivo* during the period of target innervation, administration of NGF during this period prevents naturally occurring neuronal death in these populations [74-79]. Genetic deletion of genes encoding NGF or its receptor tyrosine kinase (TrkA) also results in decreased numbers of peripheral sensory and sympathetic neurons [80-82]. The production of NGF begins in target tissues with the arrival of the earliest axons [83], and removal of the target tissue increases programmed cell death (PCD) in the relevant peripheral ganglia [84]. The neurotrophic theory, as described above, is an over-simplification because neurons require trophic support before and after synaptogenesis from sources other than the target field [85]. Furthermore, many populations of neurons switch their dependence from one trophic factor to another depending on their stage of development [86, 87]. *In vitro* studies have shown that populations of PNS neurons survive independently of neurotrophic factors at the stage when axons begin to sprout (Davies, 1994). The duration of neurotrophic factor independence is proportional to the distance axons need to travel in order to reach their targets [88, 89].

Since the discovery of the original neurotrophic factor, NGF, much effort has been made to identify novel neurotrophins. Brain-derived neurotrophic factor (BDNF) was

the second neurotrophic factor to be purified [90]. Since then several other neurotrophic factors have been identified. The neurotrophin family of proteins has 6 members; nerve growth factor (NGF), brain-derived neurotrophic factor (BDNF) neurotrophin-3 (NT-3), neurotrophin 4/5 (NT-4/5), neurotrophin 6 (NT-6) and neurotrophin-7 (NT-7). These proteins are both structurally and functionally secreted proteins that signal through two classes of receptor; the high-affinity tyrosine kinase receptors of the Trk family (TrkA, TrkB, and TrkC) and a common lower-affinity receptor, p75. Several other families of proteins have been shown to promote the survival of various populations of neurons during particular stages of their development. These include the glial cell-derived neurotrophic factor (GDNF) family, the neurotrophic cytokines [ciliary neurotrophic factor (CNTF), leukaemia inhibitory factor (LIF), oncostatin-M (OSM), cardiotrophin-1 (CT-1) and interleukin-6 (IL-6)] and some other related factors including hepatocyte growth factor (HGF) and macrophage-stimulating protein (MSP) [86, 91-93]. The search for novel neurotrophic factors is ongoing, and as recently as July 2007, a novel neurotrophic factor for midbrain dopaminergic neurons, conserved dopamine neurotrophic factor (CDNF) was identified [94].

In addition to regulating neuronal survival during development, neurotrophins also have a role in diverse processes from cellular proliferation, differentiation and process outgrowth to synaptic plasticity [95-99]. The original research described in this thesis is focused on the role of neurotrophins in the regulation of neuronal survival and process outgrowth during the development of specific populations of peripheral sensory and sympathetic neurons. Although the individual neurotrophic requirements of PNS neurons during development have been described, the downstream signalling

events mediating neuronal survival and neurite outgrowth are only beginning to be elucidated. I will therefore briefly describe the neurotrophic requirements of the relevant peripheral ganglia, followed by an introduction to the biology of the neurotrophic factors and their receptors.

1.3.3 Neurotrophic requirements of selected peripheral ganglia

The studies described in this thesis were performed on sensory neurons of the mouse nodose ganglion (NG), trigeminal ganglion (TG) and DRG and on the sympathetic neurons of the superior cervical ganglion (SCG).

Numerous *in vitro* studies have implicated BDNF and to a lesser extent, NT-3 and NT-4 in promoting the survival of nodose neurons [89, 100-103]. Genetic inactivation of BDNF, NT-3 and NT-4 results in increased cell death in nodose neurons [104-107]. Early in the development of the NG, the survival of a small subpopulation of nodose neurons is supported *in vitro* by NGF [108]. This *in vitro* observation was substantiated by the slight decrease in the number of nodose neurons in NGF $-/-$ mice [108]. Subpopulations of nodose neurons respond to a variety of other neurotrophic factors, notably the neurotrophic cytokines, CNTF, LIF, OsM and CT-1 [109]. The *in vitro* survival of neonatal nodose neurons is supported equally well by both BDNF and neurotrophic cytokines [109].

Trigeminal neurons switch their dependence between different neurotrophic factors during development. Early trigeminal neurons are dependent on both NT-3 and BDNF for survival but by E12 the vast majority of trigeminal neurons are NGF-dependent [110]. The switch in responsiveness from NT-3 and BDNF to NGF is correlated with a switch in the expression of appropriate Trk receptor and the switch to expression of

NGF in the target tissue [83, 110-112] . The DRG contains a mixture of functionally distinct sensory neurons. Thermoceptive and nociceptive, small diameter neurons, express TrkA and are dependent on NGF for survival *in vitro*. Neonatal TrkA^{-/-} mice display a substantial reduction in the number of small diameter neurons, but not large diameter DRG neurons [80]. This observation combined with the decrease in small diameter DRG neurons in NGF^{-/-} mice suggest that thermoceptive and nociceptive DRG neurons are dependent on NGF signalling through TrkA for survival during development [80]. Large diameter, proprioceptive DRG neurons are dependent on both BDNF and NT-3 during development [86] .

The sympathetic neurons of the SCG originate from proliferating precursors in the neural crest. Throughout their development, SCG neurons respond to a variety of neurotrophic factors and *in vitro* survival of SCG neurons can be supported by a wide range of neurotrophic factors between early embryonic and early adult life. Artemin promotes sympathetic precursor proliferation and hepatocyte growth factor (HGF) promotes the differentiation of sympathetic neuroblasts into postmitotic sympathetic neurons [97, 113, 114]. SCG neurons respond to NGF at E14 and remain dependent on NGF for survival throughout the remainder of embryonic life [115]. By birth, and into early adulthood the survival of SCG neurons *in vitro* can be supported by both NGF and NT-3. The dependence of SCG neurons on NGF and / or NT-3 correlates with expression of TrkA and not TrkC during and after the period of naturally occurring cell death [116]. Late postnatal SCG neurons also respond to CNTF, LIF and HGF *in vitro* [117, 118].

Cell culture systems, described herein, were used to analyse neuronal survival and / or process outgrowth in embryonic or postnatal DRG (supported by NGF), TG

(supported by NGF), NG (supported by BDNF or CNTF), and SCG (supported by NGF or NT-3). The biology of these neurotrophic factors and their associated receptor systems is introduced in the upcoming sections.

1.3.4 NGF

NGF, the founding member of the neurotrophin family, is a highly conserved protein first isolated from mouse salivary glands [119-123]. The amino acid sequence [124] and subsequently the 3-dimensional structure of NGF [125] have been determined. The NGF gene encodes a precursor protein which is cleaved to form mature NGF which is a homodimer consisting of two 118 amino acid subunits, each containing a cysteine knot motif and two anti-parallel β strands [125-128].

NGF is expressed in many regions of the CNS including the basal forebrain and hippocampus [129]. The targets of NGF-dependent peripheral neurons also secrete NGF, including the heart, submandibular glands and whisker pads [83, 129-132]. Many other non-neuronal cells of the cardiovascular, endocrine, reproductive and immune systems express NGF but the developmental function of NGF in these systems is poorly understood [133]. The crucial role of NGF signalling in the development of certain populations of sympathetic and sensory neurons is highlighted by the severe defects in cell survival and target innervation observed in NGF $-/-$ mice [80]. In addition to well documented roles in neuronal survival, NGF also regulates terminal innervation patterns in target tissues. The significant loss of sensory neurons brought about by deletion of NGF can be prevented when NGF $-/-$ mice are crossed with Bax-deficient mice [134]. However, peripheral target innervation remains decreased in these mice, suggesting that NGF signalling regulates the extent of

terminal branching in target tissues [134]. NGF also regulates neurite growth in sympathetic neurons [135]. NGF released by the target tissue is taken up by distal processes and transported retrogradely in signalling endosomes along with TrkA, to support neuronal survival [136, 137].

1.3.5 BDNF

The identification and purification of BDNF in 1982 expanded the field of neurotrophic factor biology and generalised the role of target-derived neurotrophic factors in neuronal survival and process outgrowth during development [90]. Like NGF, BDNF is synthesized as a precursor protein that is cleaved to produce a 119aa mature protein. BDNF shares approximately 50% of its sequence with NGF, including the 6 cysteine residues involved in forming the cysteine knot structure, and also forms a homodimer to produce its biologically active species [90, 138].

BDNF is relatively highly expressed in the central nervous system with strong expression in the cortex, hippocampus and cerebellum, as well as lower expression in the striatum, olfactory bulb, midbrain, hindbrain and spinal cord [139, 140]. BDNF signalling has been implicated in almost all aspects of CNS development from proliferation to synaptic plasticity, learning and memory [141]. In the CNS, BDNF expression is upregulated during periods of neuronal activity [142]. As early as 1949, Hebb proposed that strengthening of synaptic contacts may underlie synaptic plasticity [143]. BDNF, and many other molecules, have been shown to translate neural activity into synaptic plasticity and BDNF^{-/-} mice display defects in long-term potentiation (LTP) [144, 145].

BDNF is also expressed in certain populations of peripheral sensory ganglia and in the target tissues of BDNF-dependent neurons, including the heart, skin, muscle, and lung [110, 146, 147]. BDNF promotes the survival of placode-derived trigeminal, nodose, geniculate, petrosal and vestibular neurons during development and also increases the survival of some early neural crest-derived sensory neurons such as those in the DRG [100, 148-150]. Like NGF^{-/-}, BDNF^{-/-} mice die perinatally and display significant defects in populations of sensory neurons dependent on BDNF for survival [151, 152]. BDNF is also involved in neurite outgrowth in vestibular, DRG, sympathetic and nodose neurons [153-160] of the PNS and in neurite outgrowth and maintenance of cortical and hippocampal processes [145, 161-168].

1.3.6 NT-3

NT-3 was discovered after identification of highly conserved regions of NGF and BDNF using a homology cloning approach [146, 169, 170]. Like BDNF, NT-3 shares approximately 50% identity in amino acid sequence with NGF including conservation of critical cysteine residues [171]. NT-3 is also formed from cleavage of a precursor protein into a 119 amino acid mature protein [169].

NT-3 is expressed in the CNS and in the targets of many populations of sensory neurons during development and in the adult [146, 169, 170]. *In vitro*, subpopulations of neurons from the nodose, cochlear and dorsal root ganglia as well as the proprioceptive neurons of the trigeminal mesencephalic nucleus respond to NT-3 and a transient survival response of neural crest-derived sensory neurons can also be detected [103, 110, 146, 169, 170, 172-176]. NT-3 also promotes the survival, differentiation and proliferation of sensory neuronal precursors [107, 177, 178]. NT-

3-/- mice have significantly reduced numbers of neurons in SCG, DRG, trigeminal and nodose ganglia [116, 152, 173, 175, 176, 179, 180] . Recent evidence suggests that, unlike NGF, NT-3 is not retrogradely transported from peripheral targets of sympathetic neurons but promotes the growth of some sympathetic axons along intermediate targets like blood vessels [136, 137] . Interestingly, terminal target derived NGF may reduce the sensitivity of developing neurons to NT-3 in a proposed hierarchical mechanism of neurotrophin-dependent development [137] . NT-3 also regulates terminal innervation patterns in vestibular, DRG, trigeminal and sympathetic neurons [135, 137, 154, 155, 158, 159, 181, 182] .

1.3.7 CNTF

CNTF was first identified and purified from the embryonic chick eye and supports the survival of parasympathetic ciliary ganglion neurons [183-185] . CNTF is a 20-24kDa protein bearing no similarity with known members of the neurotrophin or fibroblast growth factor gene families [186-188] . However, there are significant structural similarities, including a four helix bundle, between CNTF and other neurotrophic cytokines such as LIF, IL-6, OSM and G-CSF [189, 190] .

Highest levels of CNTF mRNA are found in postnatal peripheral nerves [191]. In the adult rat central nervous system, highest levels of CNTF mRNA are found in the optic nerve, olfactory bulb [192] and spinal cord [193]. Low but still significant levels are detectable in the brain stem, cerebellum, septum, hippocampus, striatum, midbrain, and thalamus / hypothalamus [192, 194, 195] . CNTF supports the survival of a wide variety of peripheral and central neurons *in vitro*, including neurons of the nodose, trigeminal, dorsal root and sympathetic ganglia, spinal motoneurons, hippocampal

neurons and Purkinje cells [109, 184, 196-199]. Recent evidence suggests that CNTF is only secreted from injured or damaged cells, hence there is no observable neuronal phenotype in neonatal CNTF^{-/-} mice [200]. However, a slow degeneration of adult motoneurons is observed in these mice [200]. The potential role of CNTF in regeneration has sparked a lot of interest in CNTF signalling in the regulation of neuronal survival and growth in the CNS and PNS. Some of the intracellular mediators of CNTF-promoted growth from developing sensory neurons are investigated in detail in chapter 3

1.3.8 Trk receptors

The effects of neurotrophic factors on neuronal survival and process outgrowth are mediated by intracellular signalling pathways downstream of the Trk or p75 receptors. The original Trk receptor was discovered as an oncogene product of the *trk* gene (tropomyosin-related kinase), an oncoprotein present in a human colon carcinoma [201]. The Trk proto-oncogene encodes a 140 kDa transmembrane glycoprotein with the typical structure of tyrosine protein kinase cell surface receptors including an extracellular domain which recognises NGF, a single transmembrane domain and a cytoplasmic domain with tyrosine kinase activity which activates intracellular signalling pathways [202, 203]. After the discovery of TrkA, two other related Trk genes were identified; TrkB [204, 205] and TrkC [206]. TrkB mediates the biological activity of both BDNF [207-209] and NT-4 [210-212], and TrkC is the primary receptor for NT-3 [206]. There is also some physiologically relevant, lower affinity binding between NT-3 and *trkA* and *trkB* and between NT-4/5 and *trkA* [207-210]. This small group of three kinases [213] is one of twenty subfamilies of tyrosine kinase receptors, with unique common structural features and high levels of expression in

both the CNS and PNS [214, 215]. The importance of neurotrophin signalling through Trk receptors in the developing PNS is highlighted by the observation that all peripheral neurons express Trk receptors, with the exception of parasympathetic ciliary neurons [112, 179, 204, 216-218].

Trk receptors are activated through ligand-mediated dimerisation followed by phosphorylation of several conserved cytoplasmic tyrosine residues, providing docking sites for adaptor molecules and enzymes mediating intracellular signalling pathways [98, 219-221]. Neurotrophin signalling through Trk receptors leads to the activation of many intracellular signalling molecules such as Ras, PI3-K and PLC γ [222] as illustrated in Figure 10. Neurotrophin signalling in the cell soma and nucleus is crucial for neuronal differentiation and survival [75, 223]. However, especially in the PNS, the source of neurotrophic factor may be quite a distance from the soma. These observations have prompted investigations into the mechanisms of retrograde signal transduction after ligand engagement. Ligand engagement stimulates internalization of Trk receptors through clathrin-coated pits and by macropinocytosis in cell surface ruffles [224, 225]. After internalization, neurotrophins are localized with Trk receptors in endosomes that also contain activated signaling intermediates, such as Shc and PLC- γ 1 [226]. NGF-TrkA internalisation and retrograde transport to the soma is required for transmission of the neurotrophin signal [137, 227]. Recent data describing NGF-promoted neuronal survival without NGF internalisation [228] and the lack of retrograde signalling of NT-3/TrkA in sympathetic neurons have added layers of complexity to neurotrophin signalling cascades.

In general, populations of neurons depleted in Trk^{-/-} mice overlap with those lost in the knockout mouse of the primary neurotrophin for that receptor. TrkA^{-/-} mice have decreased neuronal numbers in trigeminal, dorsal root and sympathetic ganglia [81]. TrkB^{-/-} mice lose a substantial proportion of trigeminal, nodose and DRG neurons [229], while trkC^{-/-} mice have decreased numbers of myelinated axons emerging from the dorsal root and posterior columns of the spinal cord, as well as loss of a subpopulation of DRG neurons [230].

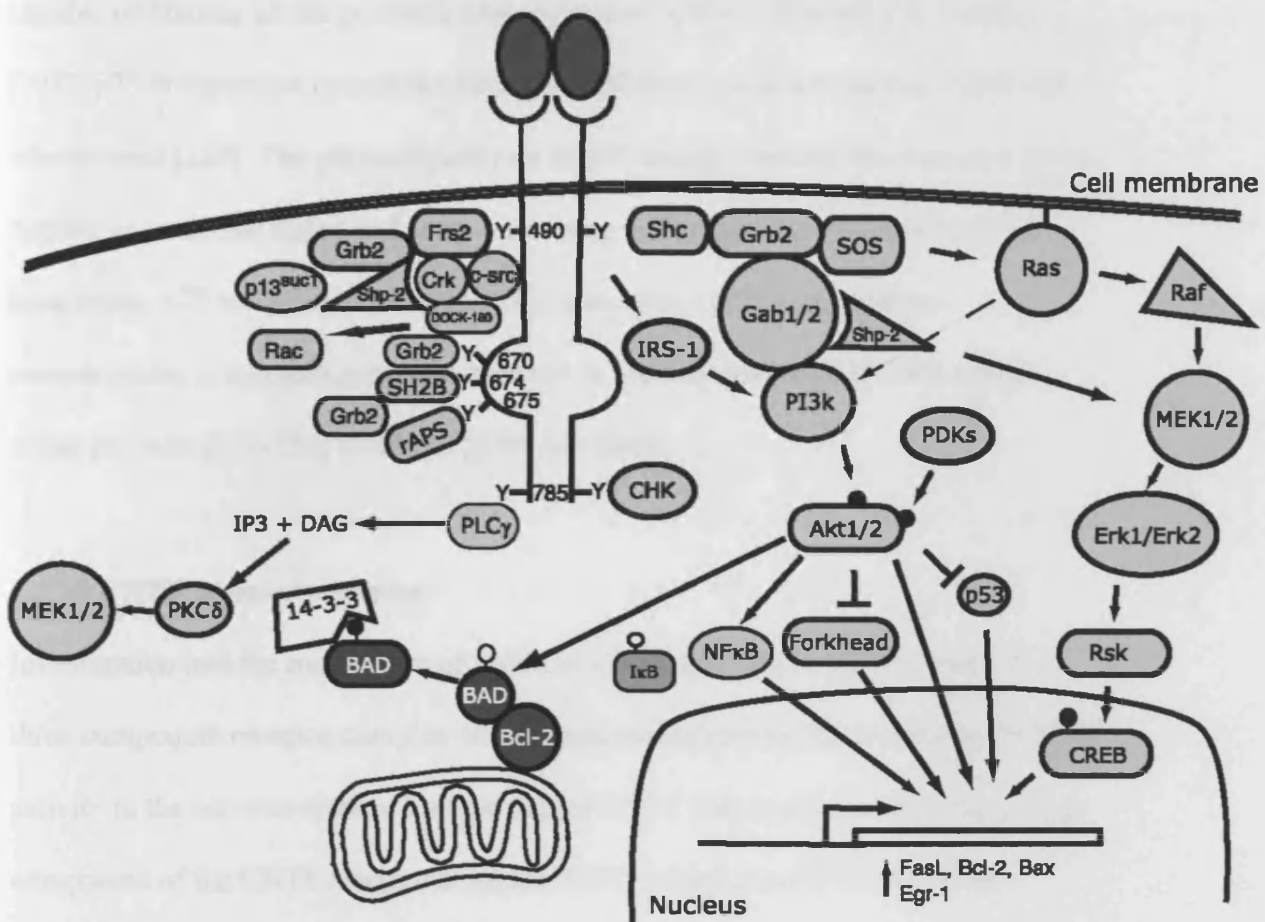


Figure 10 | **Trk signalling.** Illustration detailing some of the intracellular signalling pathways activated after ligand-mediated Trk activation which result in gene expression, increased neuronal survival and neurite outgrowth (Illustration from Huang and Reichardt (2003)).

1.3.9 P75^{NTR}

The p75 common neurotrophin receptor is a 75kDa transmembrane glycoprotein capable of binding all the neurotrophins with lower affinity than the Trk receptors [231]. p75 is expressed in both the PNS and CNS but also in non-neuronal cells and after trauma [222]. The physiological role of p75 during neuronal development is only beginning to be elucidated and some interesting and surprising observations have been made. p75 modifies the function of Trk receptors [222], can bind pro-neurotrophins in complex with a co-receptor to elicit apoptosis [232-234] and can either promote [235-237] or inhibit [238] cell death.

1.3.10 CNTF receptor complex

Investigation into the mechanism of action of CNTF has led to the discovery of a three component receptor complex whose expression explains the specificity of CNTF activity in the nervous system. Epitope tagged CNTF was used to identify the unique component of the CNTF receptor complex, CNTF receptor α (CNTFR α) [239]. CNTFR α expression was limited to neuronal cells and was expressed by all CNTF-responsive cells including sympathetic, sensory, motor and parasympathetic neurons [194, 240]. Sequence analysis revealed that CNTFR α , unlike other neurotrophic factor receptors, does not have a transmembrane domain but is attached to the cell surface via glycosyl phosphatidylinositol (GPI) linkage [240]. CNTFR α is a member of the cytokine receptor superfamily, closely related to interleukin-6 (IL-6). Subsequent analysis revealed that CNTF and CNTFR α could form a complex with two transmembrane proteins that become tyrosine phosphorylated upon ligand binding, gp130 and LIFR β [193, 241, 242]. Numerous studies have found that coexpression of all three subunits of the CNTFR complex were required to generate a

functional receptor [243-245] . Reconstitution experiments have revealed that the CNTFR complex is initially unassociated and only assembles after ligand binding [246]. CNTFR α -/- mice die perinatally, and like CNTF-/- mice exhibit a significant loss of motoneurons [247]. The phenotype of CNTFR α -/- mice is more severe than the CNTF-/- mice, correlating with relatively early expression of the receptor compared to the ligand [193, 195]. The more severe phenotype observed in CNTFR α -/- mice may also be partially explained by studies describing a role for a soluble form of the receptor as a co-factor for CNTF [243]. Experiments using a soluble form of CNTFR α revealed that it can bind to CNTF and activate cells which are not normally responsive to CNTF [243]. LIFR β -/- mice also die within hours of birth, with significant reductions in the number of facial, trigeminal hypoglossal and spinal motor neurons and a loss of astrocytes in the brainstem and spinal cord [248, 249]. In gp130-/- mice there is loss of DRG neurons and specific populations of motor neurons, that occurs between E14.5 and E18.5, suggesting that cytokines are principally involved in regulating neuronal survival during the period of naturally occurring cell death [250].

1.3.11 Neural activity regulates survival

During development, approximately half of all neurons generated die by PCD which is largely regulated by the availability of target-derived neurotrophic factors as described above [71]. However, *in vitro* survival of neurotrophin-deprived cells from both the CNS and PNS is supported by increased neural activity [251-258] . The crucial role of activity has also been shown *in vivo*, where removal or inhibition of afferent input increases neuronal PCD [259] [260]. Patterned neural activity is crucial for normal development of thalamocortical, local intracortical, and long-range

horizontal connections in the cortex [261]. The survival-promoting effects of neural activity on various neuronal populations have been studied extensively *in vitro* using increased K^+ in the culture media [262]. Elevation of K^+ leads to depolarisation of the membrane and activation of voltage gated calcium channels. K^+ -dependent neuronal survival is largely mediated by increases in intracellular calcium concentration $[Ca^{2+}]_i$ [262]. The calcium set-point hypothesis has been proposed to explain the relationship between neurotrophin-dependent survival and activity dependent survival [262, 263]. Low $[Ca^{2+}]_i$ is associated with neurotrophic factor dependence, moderate $[Ca^{2+}]_i$ is associated with neurotrophin independence and high $[Ca^{2+}]_i$ is associated with toxicity. It has been suggested that trophic factor dependence is inversely related to $[Ca^{2+}]_i$ which correlates with the observation that $[Ca^{2+}]_i$ increases with age [264]. Most studies using depolarising concentrations of K^+ to promote the survival of peripheral neurons have relied on neonatal neurons artificially aged in culture. The cell culture studies described in this thesis (chapter 5) have used peripheral sensory and sympathetic neurons dissected from mice over a range of embryonic and postnatal ages and tracked the onset of neurotrophin independence and examined the mechanisms involved in the survival promoting effects of elevated K^+ .

1.4 Regulation of neurite outgrowth

1.4.1 Axon extension and guidance

To form a functional nervous system, every neuron must make appropriate synaptic connections. The first step towards a properly wired nervous system is the extension

of an axon towards a target cells. The growing axon extends at its leading edge by means of a specialised structure called the growth cone. Important fibrillar structures including microfilamentous actin and microtubules give the growth cone its characteristic structure. The growth cone appears as a hand-like enlargement at the leading edge of the developing axon which reaches into the external environment with numerous finger-like extensions called filopodia. Microtubules extend as far as the filopodia and are polarised such that the end at which tubulin polymerises most rapidly faces the leading edge of the growth cone. Axon extension is achieved through polymerisation of actin and tubulin filaments in the growth cone which pushes the membrane forwards [265, 266] . The ability of developing axons to twist and turn their way through diverse environments and successfully reach the appropriate target, has amazed neurobiologists since Ramon Y Cajal in the 1890s. The direction of growth cone extension is determined by gradients of both locally acting and diffusible attractive or repellent cues in the external environment. Many of these attractive and/or repellent cues have been identified and include semaphorins, netrins, slits, ephrins, morphogens and associated receptor systems [267, 268] .

1.4.2 The role of neurotrophic factors in neurite outgrowth from PNS neurons

The role of neurotrophic factors in the regulation of neurite growth *in vitro*, is well established [135, 137, 155, 269-272] . The role of neurotrophic factors in neurite growth *in vivo* is less straight forward and it has been demonstrated that the initial extension of axons from peripheral ganglia occurs normally in the absence of neurotrophin/ Trk signalling [72, 273]. The major effects of neurotrophic factors on neuronal survival have impeded efforts to investigate the requirement of neurotrophic factors for axon extension and peripheral target innervation. The separation of

survival effects from effects on neurite outgrowth was achieved by crossing NGF^{-/-} and TrkA^{-/-} mice with Bax^{-/-} mice [134]. Bax deletion prevents PCD in developing peripheral neurons [274] so crossing these mice with NGF^{-/-} or TrkA^{-/-} mice provided an ideal framework for analysing the growth-promoting effects of NGF/TrkA signalling *in vitro* and *in vivo* [134]. In the absence of NGF/TrkA signalling, DRG neurons extend processes through the dorsal roots and into the dorsal horn but cutaneous peripheral axons fail to develop, establishing that neurotrophin signalling is required for peripheral target field innervation [134]. Further work has shown that peripheral axons can be induced to grow towards ectopic sources of neurotrophic factors, a process which can be reversed by application of function-blocking antibodies directed towards NGF, BDNF or NT-3 [154]. Further *in vivo* analyses have revealed that increased levels of NGF or NT-3 in the brain, pancreas, heart or skin leads to increased axonal growth in sensory and sympathetic neurons [180, 275-277]. CNTF can also promote neurite outgrowth from a variety of neuronal populations *in vitro* but its role *in vivo* is poorly understood [278].

1.4.3 Intracellular signalling pathways downstream of neurotrophic factors regulating neuronal survival and neurite outgrowth

Binding of neurotrophic factors to Trk receptors results in the phosphorylation of 10 conserved cytoplasmic tyrosine residues. Phosphorylation of these residues either further activates the receptor or promotes intracellular signalling by creating docking sites for adaptor proteins containing phosphotyrosine-binding (PTB) or src-homology-2 (SH-2) motifs [220, 279]. Phosphorylation of tyrosine residues and binding of adaptor proteins couple Trk receptors to intracellular signalling pathways including

the Ras/Erk protein kinase pathway, the PI-3 kinase / AKT pathway, phospholipase C (PLC γ) and Shc. All of these pathways have been implicated in neuronal survival and / or neurite outgrowth in various populations of neurons [220, 280]. JAK/Tyk tyrosine kinases have been shown to associate with both gp130 and LIFR β components of the CNTFR complex and become active upon dimerisation of the receptor components [280]. After activation of JAK/Tyk kinases a host of intracellular pathways are activated, many of which overlap with those activated by other cytokines and growth factors, such as PLC γ , PI3-kinase, STAT proteins, ERK1/2 and nuclear-factor κ B (NF κ B) [281, 282] to regulate survival and growth.

The signalling events downstream of neural activity that regulate neuronal survival and process outgrowth are poorly understood, but recent studies in cerebellar granular cells have demonstrated that Ca²⁺ signalling mediated by calcium calmodulin dependent protein kinase 2 (CaMKII) induces dissociation of kinesin superfamily protein 4 (KIF4) from poly (ADP-ribose) polymerase-1 (PARP-1) which supports neuronal survival [283, 284]. Studies in primary sympathetic neurons have shown that depolarisation and neurotrophic factors converge on the PI-3 kinase / AKT pathway to synergistically regulate neuronal survival [285]. Further studies on sympathetic neurons have revealed that neural activity can promote local axonal outgrowth via activation of L-type calcium channels and subsequent activation of CaMKII-MEK pathway [286].

1.5 NFκB Signalling

1.5.1 The NFκB family of transcription factors

In order to trigger specific long-term structural, morphological or functional changes, short-term events such as synaptic activity or receptor engagement must elicit differential gene expression [287-290]. This may be achieved by activation of transcription factors. NFκB was first described as a nuclear factor that, when activated by bacterial lipopolysaccharides binds to the enhancer region of the gene encoding the κ light chain of antibodies in B cells [291]. Since this original description NFκB has been shown to be expressed in a variety of tissues from drosophila to man and regulates expression of genes involved mainly in the immune response [292]. Five NFκB family members have been cloned and characterised, c-Rel, NFκB1 (p50/p105), NFκB2 (p52/p100), RelA (p65), and RelB. All members of the NFκB family contain a characteristic Rel homology domain (RHD) involved in DNA binding, dimerization and interaction with inhibitory proteins called IκB [293]. The NFκB family can be divided into two groups. One group (p105 and p100) have long C-terminal containing ankyrin repeats. P105 and p100 give rise to shorter proteins containing the RHD (p50 from p105 and p52 from p100) by limited proteolysis or arrested translation [294-297]. These proteins cannot act as activators of transcription unless they form dimers with members of the second group, which include c-Rel, p65 and RelB. In addition to the RHD these proteins contain C-terminal transcriptional activation domains. All NFκB proteins form either homo or heterodimers, NFκB being the original name for the p50-p65 heterodimer, which is the most abundant form in the nervous system. In unstimulated cells NFκB dimers are held inactive in the cytoplasm by members of a family of inhibitory proteins called IκB. IκB proteins, IκBα, IκBβ, IκBγ, IκBε and Bcl-3 contain C-terminal ankyrin repeats essential for

their interaction with NF κ B dimers. I κ B proteins inhibit NF κ B by masking several important regions of the NF κ B subunits such as the nuclear localisation sequence of p65, regions important for DNA binding of NF κ B and phosphorylation sites necessary for transcriptional activation [298]. Free NF κ B then migrates to the nucleus and binds to κ B sites with consensus sequence GGGRNNYYCC (N = any base, R = purine, and Y = pyrimidine) in the promoter or enhancer regions of target genes, and activates their transcription.

Cells of the immune system must respond rapidly to diverse stimuli from bacterial infection to UV light and the ability of NF κ B to rapidly transduce extracellular stimuli into defensive genetic responses is crucial. NF κ B-dependent gene transcription regulates the function of T cells, B cells, macrophages and monocytes [292, 299-301]. The mechanisms of NF κ B signalling are also of major interest in cancer research due to the role of this family of transcription factors in apoptosis, the cell cycle, differentiation and cell migration [302]. Constitutive NF κ B activation has been associated with almost all forms of human cancer and many other human diseases [303]. NF κ B signalling has more recently been implicated in diverse functions within the developing and adult nervous system.

1.5.2 Emerging roles for NF κ B in the nervous system

NF κ B is widely expressed throughout the nervous system [304-309] and has been implicated in plasticity, learning and memory, development and neurodegenerative disease. p65 is located distally on dendrites and basal synaptic input has been shown to stimulate retrograde transport of p65, in association with dynein/dynactin to the

nucleus [310-312]. The relationship between synaptic activity and nuclear translocation of p65 implies that NF κ B may be involved in synaptic plasticity. Indeed, inhibition of NF κ B or deletion of p65 has been shown to impair spatial memory formation in the mouse [311, 313, 314]. NF κ B signalling is also regulated during development and plays a role in proliferation and migration of early neurons [308, 315, 316]. NF κ B promotes survival and process outgrowth during development [317-321]. NF κ B promotes the survival of cortical neurons, cerebellar granule cells and sympathetic and sensory neurons [238, 308, 318, 319, 322, 323]. Conversely, NF κ B activation may lead to increased apoptosis under certain conditions, such as ischaemia and p50^{-/-} mice display increased infarct volumes [324, 325]. Inhibiting NF κ B decreases neurite growth and arborisation in the neonatal somatosensory cortex and NG [321]. Since many of the same signal transduction pathways regulating neuronal survival and process outgrowth during normal development are also implicated in neurodegeneration, numerous studies have investigated the role of NF κ B in neurodegenerative pathology. Increased NF κ B activity has been demonstrated in brain tissue from Alzheimer's and Parkinson's disease patients [326-328]. NF κ B activation promotes cell death programs in central neurons exposed to excitotoxic insults or DNA damage, as well as during exposure to dopamine, mutant huntingtin and β -amyloid peptide [327, 329-335]. Whether increased NF κ B activation has a causative role in promoting neurodegeneration or simply becomes upregulated as part of a general neuroprotective response is still in question [336].

1.5.3 NF κ B activation mechanisms

NF κ B is induced in various cell types by a range of stimuli including cytokines, bacterial cell wall components, viruses, physical or chemical stress and UV light [337, 338]. In neurons, NF κ B can also be induced by a variety signals, including tumour necrosis factor- α (TNF- α), glutamate, NGF, CNTF, activity-dependent neurotrophic factor (ADNF) and cell adhesion molecules have been identified [291, 318, 319, 339-343].

Activation of NF κ B begins with the release of NF κ B dimers from I κ B proteins (Fig. 11). In the canonical NF κ B activation pathway, this is achieved by phosphorylation of Serines 32 and 36 of I κ B α . Phosphorylated I κ B α is then recognised by the β TrCP subunit of the SCF ubiquitin ligase complex and degraded [296]. Free NF κ B translocates to the nucleus and activates the transcription of a wide range of genes. Both p105 and p100 function as I κ B-like inhibitors of NF κ B [344, 345]. Phosphorylation of p100 on at least 5 serine residues results in degradation of the C-terminus and the formation of p52/RelB active dimers [346, 347]. Processing of p105 is constitutive but processing of p100 is tightly regulated and highly inducible [348]. The NF κ B activation mediated by p100 processing, resulting in nuclear translocation of p52-containing dimers, thus is termed non-canonical NF κ B pathway [349]. Recently, an alternative mechanism of NF κ B activation has been described involving phosphorylation of I κ B α on tyrosine 42 [350]. This mechanism has been observed as a cellular response to oxidative stress and interestingly does not involve proteasomal degradation of I κ B α [350-352].

In short, NF κ B activation is brought about by phosphorylation of specific residues on I κ B which results in the dissociation or degradation of I κ B and translocation of NF κ B to the nucleus. The I κ B kinase (IKK) complex, consisting of three members IKK α , IKK β and IKK γ (also called NEMO ; NF κ B Essential Modifier) is a key activator of NF κ B due to its ability to phosphorylate I κ B [353]. IKK β is essential for NF κ B activation via the canonical pathway and cannot be replaced by IKK α [298]. IKK α phosphorylates p100 on C-terminal serine residues resulting in NF κ B activation via a non-canonical pathway [348, 354]. Less is known about phosphorylation of I κ B α on tyrosine 42, although some evidence links spleen tyrosine kinase (Syk), to tyrosine 42 phosphorylation and NF κ B activation in cells exposed to hydrogen peroxide [350]. Several MAP kinases, including NF κ B -inducing kinase (NIK), mitogen-activated protein/extracellular signal-regulated kinase (ERK) kinase kinase 1 (MEKK1), MEKK3, TGF β -activating kinase 1 (TAK1) and NF κ B activating kinase (NAK) all phosphorylate IKKs and can induce NF κ B activation under *in vitro* or overexpression conditions. Other proposed upstream kinases include Cot/Tpl-2, the novel protein kinase C (PKCs) isoforms PKC θ , ζ or λ and others [291, 298, 353, 355].

Studies presented in chapter 3 describe how different neurotrophic factors can promote neurite growth using either canonical (BDNF) or non-canonical (CNTF) NF κ B activation pathways. Given the diversity on NF κ B function, the elucidation of NF κ B activation mechanisms in response to diverse stimuli and identification of NF κ B-regulated genes is of broad interest to biologists and clinicians.

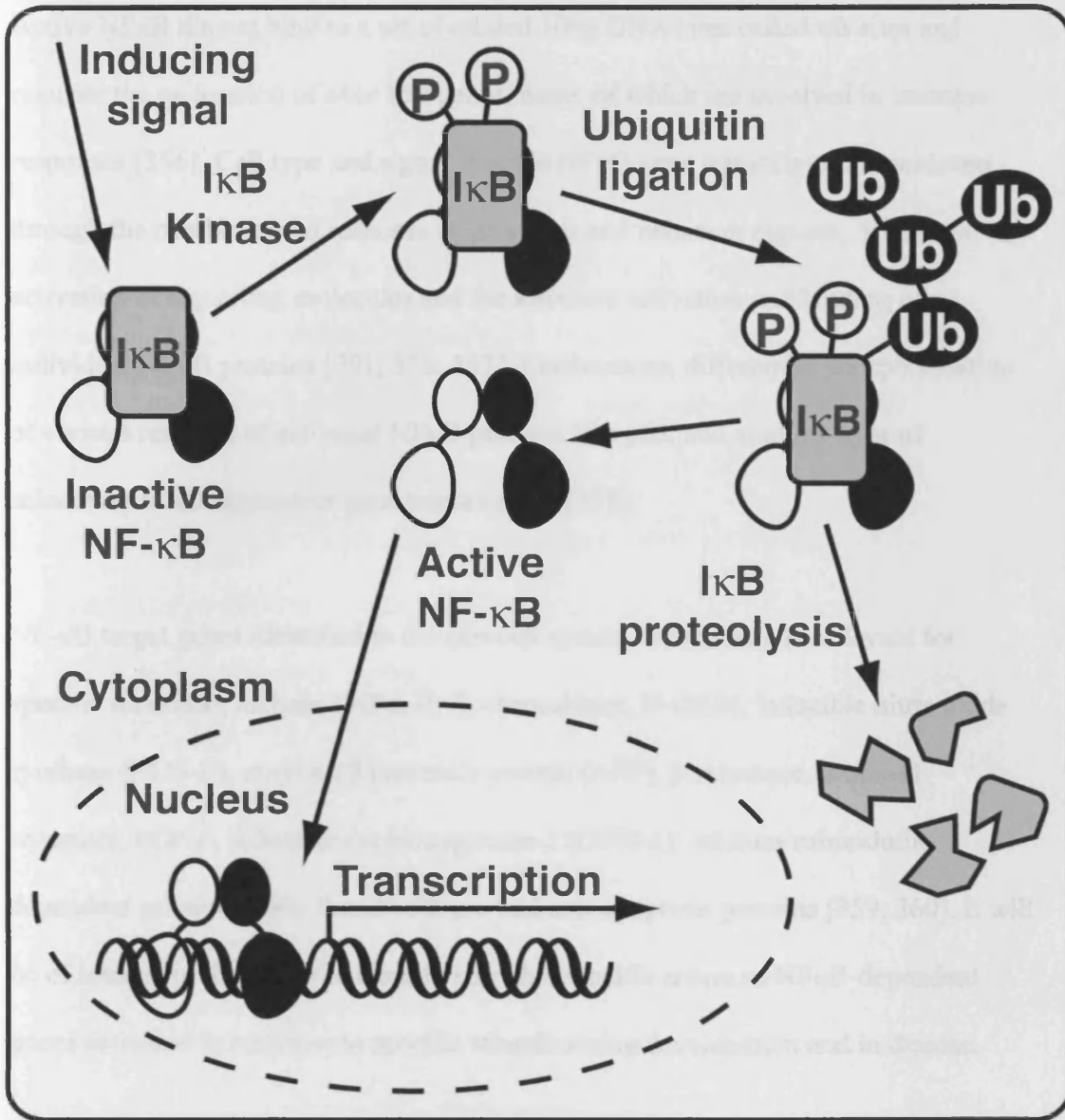


Figure 11 | **NFκB activation.** NFκB-inducing signals lead to the phosphorylation and subsequent degradation of IκB proteins. Free, or active NFκB then translocates to the nucleus where it directs the transcription of numerous genes.

1.5.4 Downstream of NFκB

Active NFκB dimers bind to a set of related 10bp DNA sites called κB sites and regulate the expression of over 150 genes, many of which are involved in immune responses [356]. Cell type and signal specific NFκB gene transcription is achieved through the combinatorial response of promoter and enhancer regions, the selective activation of signalling molecules and the selective activation and binding of individual NFκB proteins [291, 356, 357]. Furthermore, differential phosphorylation of various residues of activated NFκB proteins like p65, add another layer of selectivity to κB-dependent gene transcription [358].

NF-κB target genes identified in the nervous system, which may be relevant for specific functions, include TNFα, IL-6, chemokines, N-CAM, inducible nitric oxide synthase (NOS-II), amyloid β precursor protein (APP), β-secretase, μ-opioid receptors, BDNF, inducible cyclooxygenase-2 (COX-2), calcium/calmodulin-dependent protein kinase II and both pro and anti-apoptotic proteins [359, 360]. It will be of interest in the future to identify stimulus specific arrays of NFκB-dependent genes activated in response to specific stimuli during development and in disease.

1.6 Hypoxia-inducible factor (HIF) signalling

1.6.1 Oxygen sensing

A significant event in the evolution of life occurred approximately 2 billion years ago when atmospheric oxygen concentration began to increase dramatically [361-364].

The rise in oxygen concentration allowed a switch from anaerobic metabolism to the more efficient aerobic metabolism, and facilitated the later evolution of complex multicellular, eukaryotic organisms [365, 366]. Large multicellular animals developed systems of oxygen uptake (lungs) and distribution to all tissues (cardiovascular). Since oxygen deficit causes irreversible damage to cells and excess oxygen produces reactive oxygen species that can also damage cells, an oxygen sensing system that maintains oxygen tension within a narrow physiological range is crucial for survival.

The primary site of oxygen sensing is the carotid body, which lies at the bifurcation of the common carotid artery and senses the partial pressure of oxygen in the mammalian bloodstream. Small decreases in oxygen tension activate neurons in the carotid body which send signals to the brain resulting in increased ventilatory and cardiac rates and thus increased tissue oxygenation [367]. Erythropoietin-producing cells of the liver and kidney also respond to low oxygen by stimulating increased production of red blood cells which also increases tissue oxygenation.

Recently, oxygen sensing has been shown to be a general, adaptive property of all nucleated cells by the identification of families of transcription factors that respond to hypoxia [367-369]. One such family of highly conserved transcription factors, the hypoxia-inducible factors (HIFs), regulate the expression of many genes involved in adaptive physiological responses to hypoxia, such as, angiogenesis, erythropoiesis,

vasodilation, glycolysis and cell survival [369-371] . HIF proteins and their regulation are discussed in more detail in sections 1.6.2 and 1.6.3.

Mean tissue oxygen levels in vivo are as low as 3% and the hypoxia-specific marker EF5 has recently been used to identify hypoxic (considerably less than 1% oxygen) regions within the normally developing rat embryo at E11 [372, 373] . These areas include the otic vesicle, optic cup, first branchial arch, somites, and interestingly the neural tube in both the midbrain and hindbrain [373]. When neural crest stem cells are cultured at low oxygen levels, there is a marked increase in survival , proliferation and multilineage differentiation [374]. Increased survival , proliferation and dopaminergic differentiation of CNS stem cells is also observed when cultured at low oxygen levels [375]. It is likely that there are critical periods during which an embryo must be exposed to a hypoxic environment in order for normal development to proceed [373]. Some of the mechanisms by which hypoxic environments may influence gene transcription during development are introduced in the following sections.

1.6.2 Regulation of HIF

HIF comprises heterodimers of two subunits, HIF α and HIF β , of the Per-Arnt-Sim (PAS) family of basic helix-loop-helix proteins [376, 377] . Under hypoxic conditions, HIFs are active and bind to consensus binding motifs in hypoxia-responsive genes [376]. Three HIF α subunits have been identified so far ; HIF1 α , HIF2 α and HIF3 α , all of which bind to the ubiquitously expressed HIF-1 β subunit [378, 379]. Under normoxic conditions, HIF α subunits are rapidly degraded, whereas

the HIF β subunit is unaffected by oxygen tension [380]. HIF1 α is ubiquitously expressed and is the major regulator of hypoxia-induced gene transcription, HIF2 α shows more tissue restricted expression patterns and HIF3 α expression is not well characterised and encodes at least one splice variant that inhibits HIF [381-383]. HIF1 and HIF2 contain dedicated DNA dimerisation domains as well as two transactivation domains [384]. HIF1 and HIF2 activate the transcription of many overlapping genes but also activate unique, specific downstream genes in response to hypoxia [385-387]. Previous studies of HIF proteins have revealed an essential role during development of the neural tube and the vasculature [368, 388-391]. Interestingly, the phenotype of HIF1 $^{-/-}$ mice is very similar to that observed in embryos which are denied a low oxygen environment ; defective neural tube closure, reduction in the number of somites and malformation of the neural folds [373]. Genetic inactivation of either HIF1 or HIF2 is lethal, but results in different phenotypes, indicating specific, non-redundant roles for HIF proteins during development [389, 390, 392-394]. However, the mechanisms regulating HIF activation during hypoxia or normoxia remained unknown. The first vital clue came from studies of a rare inherited form of cancer called von-Hippel-Lindau (VHL) disease. Individuals with VHL disease are susceptible to highly vascularised tumours in the CNS, renal carcinoma and pheochromocytoma [395]. Individuals with VHL disease are VHL heterozygotes carrying one wild-type allele and one defective allele [396]. Highly vascularised tumours begin to develop when the remaining wild-type allele is inactivated in susceptible cells [395]. Tumour cells removed from VHL patients were highly vascularised, with overproduction of vascular endothelial growth factor (VEGF) and erythropoietin (EPO) [395, 397]. The observed over production of VEGF and EPO, normally observed during hypoxia lead to the hypothesis that the VHL gene product,

pVHL might be involved in oxygen sensing [398]. Subsequent studies revealed that hypoxia inducible genes were negatively regulated by pVHL and that HIF α was not degraded in VHL $^{-/-}$ tumor cells due to binding of pVHL to an oxygen-dependent degradation domain (ODD) on HIF α which targets it for proteasomal degradation [399-402]. Mutational and peptide mass spectrophotometric analysis revealed that the interaction between the ODD of HIF α with pVHL required hydroxylation of proline 564 of HIF α [403]. Mutation of EGL-9 in *C. elegans* leads to an increase in HIF α levels under normoxic conditions and EGL-9 was also shown to hydroxylate proline 564 of HIF *in vitro* [404]. Sequence homology identified three human orthologues of EGL-9, the HIF proline hydroxylase domain containing proteins (PHDs), which can act as cellular oxygen sensors by hydroxylating HIF α [404].

1.6.3 PHD enzymes

Three specific residues in the ODD of HIF are subject to hydroxylation by PHD enzymes. In humans, hydroxylation of prolines 564 and 402 promotes proteasomal degradation, whereas hydroxylation of asparagine804 inactivates the HIF complex by preventing the binding of the transcriptional co-activator p300 [405]. These residues are conserved in HIF1 α and HIF2 α and are crucial for cellular oxygen sensing [405]. PHD-dependent regulation of HIF during normoxia and hypoxia is illustrated in figure 12. To date, members of the 2-oxoglutarate (2-OG)-dependent dioxygenase superfamily have been shown to perform this crucial post-translational modification of HIF. There are three PHD enzymes, PHD1-3, which are dependent on iron and dioxygen [405]. PHD enzymes use one oxygen atom to hydroxylate a proline residue on HIF α and the other in the decarboxylation of 2-OG to yield succinate and carbon dioxide [406]. PHD homologues have been identified in *C. elegans*, *Drosophila*

Melanogaster, mouse, rat and human [368, 404, 407-409]. Although widely expressed, PHD enzymes have distinct patterns of tissue expression [408, 410]. PHD2 is the most widely expressed, PHD1 expression is highest in the testis and PHD3 expression is highest in the heart and placenta [368, 411, 412]. In addition to distinct patterns of subcellular location and tissue expression, there are differential functions of the PHD enzymes in regulation of HIFs. PHD2 preferentially regulates HIF1 α over HIF2 α , whereas PHD3 had a greater influence on HIF2 α [413].

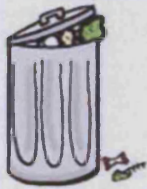
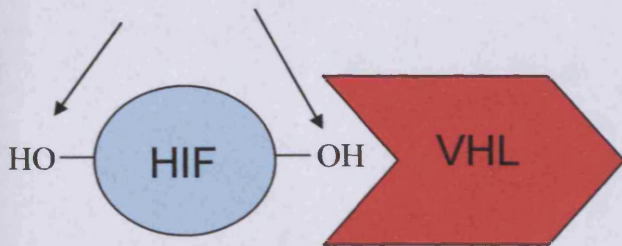
Numerous recent studies have linked oxygen sensing pathways to neuronal PCD [368, 373, 414-418]. Interestingly, numerous reports have shown that HIF signalling can be influenced by stimuli other than hypoxia, including, growth factors like EGF and HGF, oncogenes and cytokines like TNF α [405]. The expression of PHD3 is induced following withdrawal of NGF from sympathetic neurons and promotes apoptosis [417, 418]. These observations taken together with studies showing a requirement for hypoxic microenvironments during development [373] suggest that oxygen sensitive PHD enzymes may play a role in the developing PNS. I have investigated this possibility by analysing the survival and growth of sympathetic and sensory neurons dissected from mice deficient for the PHD enzymes (Chapter 4).



O_2



Prolyl Hydroxylase Domain (PHD) enzymes



Low O_2



Prolyl Hydroxylase Domain (PHD) en



Transcription

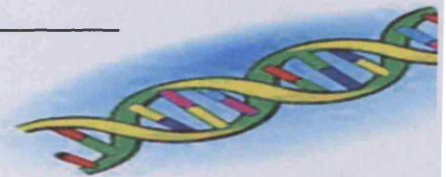


Figure 12 | **HIF regulation.** Cartoon illustrating the regulation of HIF signalling by PHD enzymes. During normoxia (left), PHD enzymes hydroxylate the ODD of HIF α which targets HIF for proteasomal degradation. PHD enzymes are oxygen dependent, so during hypoxia (right) there is no hydroxylation of HIF α and it is free to direct the transcription of hypoxia responsive genes.

Chapter 2

Materials and Methods

2.1 Introduction

The research described in this thesis uses a variety of *in vitro* and *in vivo* protocols to analyse neuronal survival and process outgrowth in wild-type and various transgenic animals. The *in vitro* protocols developed in this lab are well established, widely used and serve as a powerful tool for investigating the mechanisms of neuronal survival and neurite outgrowth (overview of experimental design shown in Fig. 13). In certain cases, *in vitro* observations were substantiated by using *in vivo* quantification of neuronal number and target field innervation density.

2.2 Maintenance of wild-type mice

Embryonic and postnatal wild-type mice were obtained from timed matings of CD1 mice. Adult CD1 mice were fed with rodent global diet pellets (Harlan) and given water *ad libidum*.

2.3 Maintenance of transgenic mice

Wild-type, *PHD3*^{-/-}, *PHD1*^{-/-}, *PHD2*^{+/-}, *PHD3*^{-/-}; *HIF-1 α* ^{+/-}, *PHD3*^{-/-}; *HIF-2 α* ^{+/-} and *HIF-2 α* ^{+/-} mice on a mixed Swiss/ 129SvEv genetic background were kindly provided by Dr. Peter Ratcliffe (University of Oxford) and Dr. Peter Carmeliet (Centre for Transgene Technology and Gene Therapy (CTG), K. U. Leuven) and fed with rodent global diet pills and given water *ad libidum*. Wild-type, heterozygous and homozygous animals were obtained from overnight matings of heterozygous mice and offspring were genotyped as described in section 2.3. Breeding was confirmed by the presence of a vaginal plug and the period of gestation was considered to be embryonic day (E) 0.5.

2.4 Genotyping of transgenic mice

2.4.1 Isolation of genomic DNA

For routine colony maintenance and rapid genotyping of neonatal tissue required for *in vitro* or *in vivo* analysis, a Maxwell™ 16 Blood Purification Kit (Promega) was used in combination with a Maxwell™ 16 Instrument and carried out according to the manufacturer's instructions.

2.4.2 Genotyping protocol

To determine the genotype at the PHD1 locus, two PCR reactions were required for each animal. The wild type PHD1 allele was amplified using forward (5'- AGT CCC TCT GGT TCT AGA GTG GGG -3') and reverse (5'- TCT CAG CAT CTC ATC ACT CCC CTG -3') PHD1-WT primers. The recombinant PHD1 null allele was detected using forward (5'- TTG CAT CGC ATT GTC TGA GTA GGT GT -3') and reverse (5'- TCT CAG CAT CTC ATC ACT CCC CTG -3') PHD1-null primers.

To determine the genotype at the PHD2 locus, the wild type PHD2 allele was amplified using forward (5'- ACC TAT GAT CTC AGC ATT TGG GAG -3') and reverse (5'- AAA TTC TAA TCG TAG CTG ATG TGA GC-3') PHD2-WT primers.

The recombinant PHD2 allele was detected using forward (5'- TCA GGA CAG TGA AGC CTA GAA ACT CT -3') and reverse (5'- ACC TAT GAT CTC AGC ATT TGG GAG -3') PHD2-recombinant primers. Similarly, the genotype at the PHD3 locus was detected using forward (5'- CGA GAT GCC TCT GGG ACA CAT CAT -3') and reverse (5'- GGA CCG CTC CTT GAC ATA GTA TTT -3') PHD3-WT primers and the recombinant PHD3-null allele was detected using forward (5'- CGA CGG GCG TTC CTT GCG CAG -3') and reverse (5'- CGG ATC GAT CCC CTC AGA AGA AC -3') PHD3-null primers.

All reactions were assembled in 0.2 ml PCR tubes containing 1 µl each of forward and reverse primers, 12.5 µl of 2 x BioTaq buffer (BioLine), 1 µl Taq DNA polymerase and 8.5 µl of PCR-grade dH₂O to give a final volume of 23.5 µl. 2 x BioTaq buffer contained 200 µl of 10 x Taq buffer (BioLine), 80 µl of 50mM magnesium chloride, 16 µl of 100mM dNTP mixture and 704 µl of dH₂O. Samples were amplified using a PTC-100 programmable thermal controller (details of PCR cycle conditions are shown in the appendix). PCR products were then run on a 1.5% agarose gel with ethidium bromide (0.5mg/ml) against a 1Kb DNA ladder with the following expected band sizes PHD1 wild-type allele 900bp, PHD1-null allele 590bp, PHD2 wild-type allele 350bp, PHD2-null allele 400bp, PHD3 wild-type allele 357bp and PHD3-null allele 590bp.

2.5 Isolation of mouse embryos

Pregnant CD1 females were killed at the required stage of gestation by exposure to a rising concentration of CO₂, followed by cervical dislocation in line with the regulations of the Home Office Animals (Scientific Procedures) Act, ASPA, 1986. Death was confirmed by pedal reflex. Embryos were isolated by laparotomy as follows; scissors that had been sterilised in 70% ethanol were used to make a small incision across the front of the abdomen. The skin lying above and below the incision was then pulled manually in opposing directions, exposing the underlying abdominal muscles. A pair of toothed forceps was used to hold the anterior abdominal muscle whilst making an incision using scissors, allowing air to enter the peritoneal cavity. The incision was then extended across the abdominal muscles without the hazard of cutting the intestines and contaminating the dissection with gut bacteria [419]. Each

gravid uterine horn was removed from the abdomen using toothed forceps cutting tissue free with a pair of scissors, and transferring to a 50ml Falcon tube (Greiner) containing sterile L-15 medium (Gibco, Invitrogen). Embryos were then transferred to a 90mm Petri dish (Greiner) containing L-15 medium where one continuous incision was made along the anti-mesometrial border of each uterine horn, exposing the embryos enclosed within their membranes [419]. Embryos were detached from their uterine horns using a pair of scissors and finally removed from the chorion and amnios using watchmaker's forceps and transferred to a fresh 90mm Petri dish containing L-15 medium [419].

2.6 Dissection of peripheral ganglia

The nodose ganglion, superior cervical ganglion, trigeminal ganglion and dorsal root ganglion were removed from embryonic or postnatal pups as follows, using standard sterile technique, in a laminar flow hood. Embryos (E16) and pups (P0-P5) were killed by decapitation with a pair of sharp scissors. Mouse pups older than P5 were killed using a rising concentration of CO₂ in line with ASPA (1986). The top of the skull and underlying forebrain was removed and the head was cut in half along the sagittal plane. The jugular foramen was opened up by deflection of the occipital bone using watchmaker's forceps, revealing the nodose and superior cervical ganglia at the mouth of the foramen. The nodose ganglion was identifiable due to its spherical appearance and prominent vagus nerve attached to its distal aspect [419]. The SCG is a more elongated structure lying above the carotid artery, attached caudally to the sympathetic chain [419]. The trigeminal ganglion was dissected from neonatal mice by removing the top of the skull and forebrain in a plane above the eyes and whisker pads. Trigeminal ganglia were found bilaterally on the base of the skull and identified

by their elongated appearance. In order to isolate the dorsal root ganglion, thoracolumbar vertebral columns of embryonic and neonatal mice were removed and cut in the midline. The dorsal root ganglia were identified by their characteristic appearance and by following the posterior root of the spinal nerve. All ganglia were then cleaned of adherent tissue using tungsten needles as described in section 2.6.

2.7 Preparation of tungsten needles

The tips of two 3cm lengths of 0.5mm tungsten wire were bent into a 90° angle, placed in 1M KOH and a 3-12 V AC current passed through the solution. A second electrode was placed in the solution which resulted in the gradual etching away of the tungsten tip forming a sharp, tapered end. The tip may be placed vertically in the KOH solution to form an extra sharp point. The sharpened tungsten needles are then held in chuck-grip platinum wire holders during the dissection. Tungsten needles were sterilised using ethanol and a Bunsen burner flame before and after each use.

2.8 Dissociated neuronal cultures

2.8.1 Preparation of dishes

Neurons were cultured on a laminin/poly-ornithine substratum. Dishes were prepared by adding 2ml poly-DL-ornithine (Sigma) / borate solution to 35mm tissue culture dishes (Greiner) and left overnight at room temperature. The poly-ornithine solution was aspirated after 24 hours and the dishes were washed three times with sterile distilled water before being allowed to air dry in a laminar flow hood. 50-100µl of a 20mg.ml⁻¹ solution of laminin (Sigma) in Hank's Balance Salt Solution (HBSS) (Gibco, Invitrogen) was added to the centre of each dish. The dishes with laminin

solution were then placed in an incubator at 37°C for 2 hours. After dissection and dissociation, neurons were plated onto the prepared dishes having washed and removed the laminin.

2.8.2 Culture media

A 10x concentrated Ham's Modified F-14 (JRH Biosciences) stock solution was prepared and stored at -30°C. 1x F14 media was prepared as follows; 500mg of sodium hydrogen carbonate was added to 250mls of distilled water. 25 mls of this solution was removed and replaced with 25mls of 10x stock F-14 solution containing streptomycin (Sigma) and penicillin (Sigma). The 1X F-14 solution was then supplemented with 2.5ml 200mM glutamine (Gibco, Invitrogen) (2mM final) and 5.5ml of an Albumax I solution containing Albumax I (Gibco, Invitrogen), progesterone, putrescine, L-thyroxine, sodium selenite and tri-iodothyronine (all Sigma). The supplemented F-14 medium was then filter sterilised using a 0.2µm Acrocip filter unit (Pall Corporation) and stored at 4°C for up to a month (Davies book chapter).

2.8.3 Dissociation of ganglia

After dissection and removal of adherent tissue using tungsten needles, ganglia were added to 950µl HBSS (Gibco, Invitrogen) containing 50µl of 1% trypsin (Worthington). The trypsin-HBSS mixture was then incubated at 37°C for a period of time suitable for that developmental stage. Embryonic neurons were incubated with trypsin for 15-18 minutes and postnatal neurons were incubated with trypsin for 20-25 minutes. The trypsin-HBSS mixture was then aspirated and the ganglia were washed twice with 10ml of F-12 (Gibco, Invitrogen) with 10% heat inactivated horse serum

(HIHS), to inactivate any residual trypsin [419]. Ganglia were then gently triturated using a fire-polished siliconised glass pipette to provide a dissociated cell suspension [419].

2.8.4 Seeding of neurons

Neurons were seeded in laminin-coated 35mm dishes. A cell suspension was made by visualising 10 μ l of dissociated neurons using an Nikon Diaphot inverted phase-contrast microscope to estimate the volume of suspension needed to seed 100-200 neurons per 12mm² grid in order to study neurite growth or neuronal survival. The volume of cell suspension required to seed the total number of dishes in the experiment was transferred to a 50ml Falcon tube containing the total volume of F-14 required. The cell suspension was kept uniform by mixing end over end, while 1ml was added to each 35mm dish. At the time of plating, or shortly afterwards in the case of transfected neurons, neurotrophic factors (NGF, BDNF, CNTF, NT-3) or pharmacological inhibitors (SN50, Piceatannol, ALLN, MG132, nifedipine, verapamil, KN-62) were added to the culture media at the concentrations indicated in figure legends.

2.9 Estimation of neuronal survival

To quantify the percentage neuronal survival, a standard graticule for examining each culture dish was constructed from the base of a 900mm plastic Petri dish, where a scalpel blade was used to inscribe a 12 x 12mm² grid consisting of 2mm squares [419]. Cells were counted 3-4hrs after plating by mounting the graticule on an inverted phase-contrast Nikon Diaphot microscope. Each dish was then placed over the graticule and the number of neurons present in the 12mm² grid was then counted.

Neurons which had not attached to the substratum were ignored. The number of phase-bright neurons in all dishes was counted at 24hr intervals until necessary. The number of phase-bright neurons at 24hrs ,48hrs or 72hrs was then expressed as a percentage of the initial cell count.

For estimating the survival of transfected neurons, cultures were transfected with a YFP-plasmid along with a plasmid of interest, using the gene gun (Helios, described in section...) and the number of YFP-labelled neurons was counted 12 hours after plating and again at 24 hours. The number of labelled neurons surviving at 24 hours was expressed as a percentage of the initial number of labelled neurons. The area counted was defined by the area in which gold particles could be seen to be embedded in the bottom of the culture dish.

2.10 Quantification of neurite outgrowth

Transfected, YFP-labelled neurons were visualized and digitally acquired using an Axioplan Zeiss laser scanning confocal microscope. For experiments in which the neurons were not transfected, viable neurons were stained with Calcein-AM dye (Invitrogen) and digitally acquired as described above. Neurons were incubated at 37°C for 15-20 minutes with Calcein-AM prior to digital acquisition. For every condition studied, between 40 and 70 neurons were captured, and neuritic arbors were traced using LSM510 software. These traces were used to ascertain total neurite length and number of branch points. Sholl analysis was also carried out on these traces. For this, concentric, digitally generated rings, 30 μm apart were centered on the cell soma, and the number of neurites intersecting each ring was counted [420].

2.11 Ballistic Transfection

2.11.1 Plasmid preparation

Competent, *E. coli* H107 cells was transferred from -70°C and thawed on ice. To 100µl of these, 5-20ng of plasmid DNA was added in a volume of 1-5µl and incubated on ice for 30mins. Competent *E. coli* were heat shocked at 42°C for 30secs and returned to ice for 2min before adding 800µl LB and shaking at 37°C for 45mins. 100µl of transformation reaction was subsequently spread onto selective LB/agar plates and incubated overnight. A single colony was selected and added to 100ml LB media and incubated overnight at 37 °C in a shaking incubator. The LB containing plasmid DNA was then centrifuged for 10 minutes at 6000rpm. Plasmid DNA was isolated from the resulting bacterial pellet using a plasmid midi kit (Qiagen) according to the manufacturer's protocol. The concentration of plasmid DNA was then measured using the nanodrop spectrophotometer system.

2.11.2 Preparation of gold microcarriers for ballistic transfection

Ballistic transfection was carried out by shooting gold microcarriers coated with plasmid DNA and YFP into dissociated neurons. To prepare the microcarriers, 20 mg of 1.6 µm gold particles (Biorad) were suspended in 100µl of 50 mM spermidine (Sigma) and 2µg of pYFP (Clontech) together with 10µg pIκBa super-repressor or Y42F mutants, constructs expressing NFκB subunits p50, p65 or both p50 plus p65, Syk-DN or pCDNA control plasmid. The gold particles were precipitated with 100 µl of 2M CaCl₂, washed three times with 100% ethanol, resuspended in 1.2 ml of 100%

ethanol plus 0.01 mg/ml polyvinylpyrrolidone and loaded into Teflon tubing. The gold particles were then thoroughly dried and stored at 4°C for up to 30 days.

2.11.3 Ballistic transfection

Gold microcarriers coated with plasmid DNA and YFP were shot into dissociated neurons using a hand-held gene gun (Helios Gene-gun, BioRad Hercules, CA USA). Between 1,000 and 3,000 neurons were plated in a 50 µl droplet of defined medium in the centre of a 35 mm diameter tissue culture dish that had been pre-coated with polyornithine (Sigma) and laminin (Sigma). Neurons were incubated at 37.5°C in a humidified 3.5% CO₂ incubator for 2 hours to allow the cells to attach, and the medium was removed from the dish just prior to transfection. The coated gold particles were shot into the cultured neurons with the gun pressurized at 200 psi. A 70 µm nylon mesh screen was placed between the gun and the culture to protect the cells from the shock wave. After transfection, 2mls of F-14 containing the appropriate neurotrophic factor were added and cells returned to the incubator at 37°C overnight.

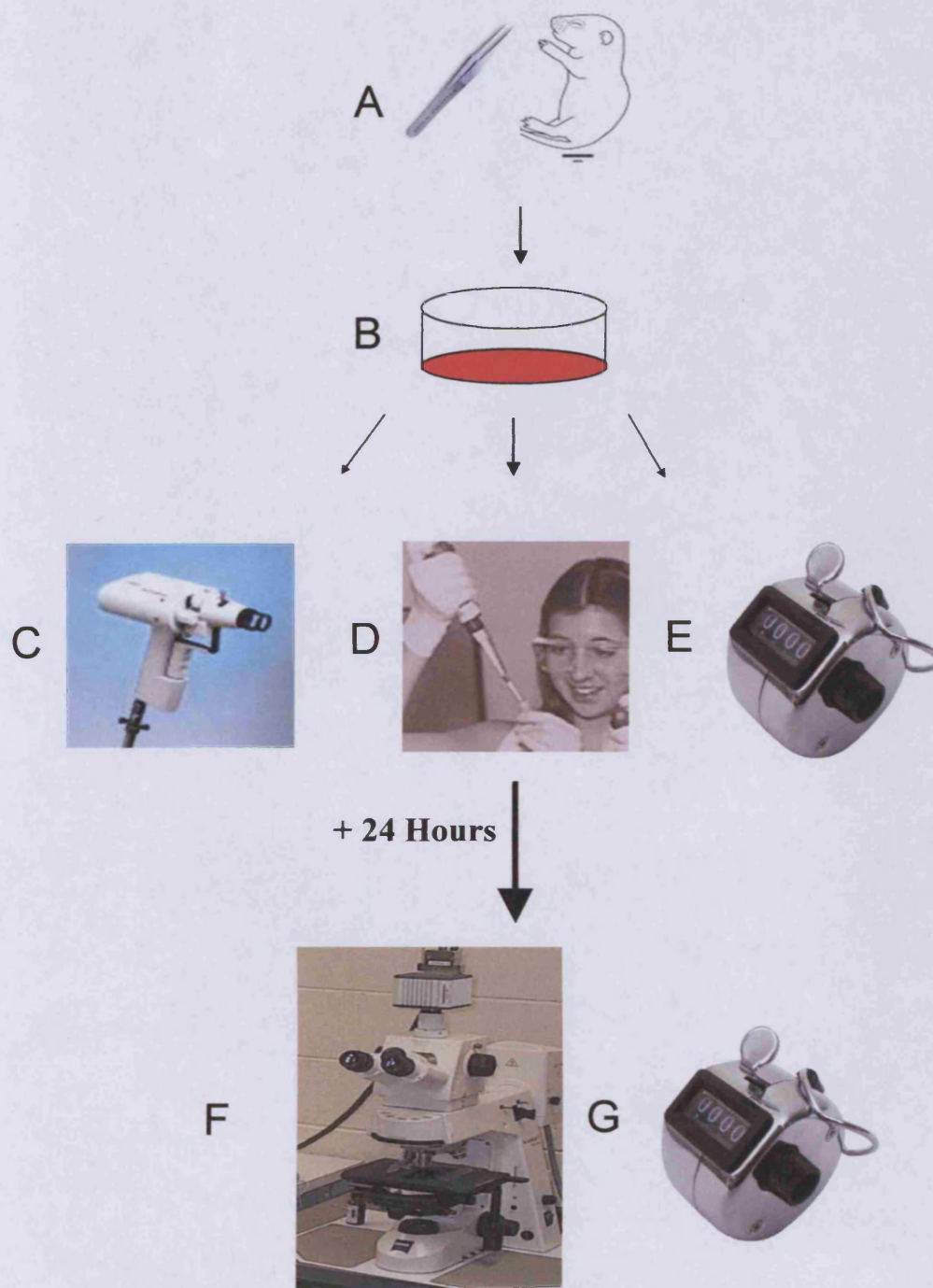


Figure 13 | **Experimental outline.** Flowchart describing the basic experimental design. Ganglia from wild-type and transgenic mice are dissected (A) and plated in defined media (B). Neurons may be transfected with a plasmid using the gene gun (C) or pharmacological agents added along with neurotrophic factors (D). Quantification of neuronal survival requires an initial count 3 hours after plating (E). Cells are then incubated overnight and may be digitally acquired and analysed for neurite growth (F) or a second count is performed and percentage neuronal survival estimated (G). 87

2.12 Preparation of κ B decoy DNA

Double-stranded κ B Decoy DNA was prepared by annealing complementary single stranded oligonucleotides of the following sequences: 5'-GAGGGGACTTTCCCT-3' and 5'-AGGGAAAGTCCCCTC-3'. Control DNA with a scrambled sequence was prepared by annealing the following sequences: 5'-GATGCGTCTGTGCGCA-3' and 5'-TGCGACAGACGCACT-3'. Double-stranded DNA solutions were prepared at a concentration of 50 mmol/l and ethanol precipitated onto the gold microcarriers along with pYFP and used to transfect neonatal nodose neurons.

2.13 NF κ B activation assay

To estimate the relative level of NF κ B activation in cultured neurons under different experimental conditions, the neurons were transfected with a plasmid expressing GFP under the control of an NF κ B promoter. Neurons were imaged with a Zeiss Axioplan laser scanning confocal microscope. The mean fluorescence intensity for each soma was obtained after 24 hours in culture using LSM510 software, based on the standard 255 intensity level scale after subtraction of background intensity. 40-60 neurons were imaged for each experimental condition. Levels of NF κ B activation were measured in this way after treatment of nodose neurons with 50ng CNTF, after treatment of CNTF-supported neurons with piceatannol (10 μ M), or after transfection of CNTF-supported neurons with Syk dominant negative or I κ B α tyrosine mutant Y42F.

2.14 qPCR analysis of PHD3 induction after NGF withdrawal

Dissociated SCG, DRG and TG neurons from wild-type P0 mouse pups were cultured overnight in 10 ng/ ml NGF as described above. Neurons were then washed with defined culture medium and grown either in the presence or absence of NGF for 10 h

(timepoint at which PHD3 mRNA induction is maximal in the SCG; (Lipscomb 1999) before harvesting the cells for RNA. Total RNA was isolated with the RNeasy Mini extraction kit (Qiagen, Hilden, Germany). The RNA was reverse transcribed for 1 hr at 37°C with StrataScript reverse transcriptase (Stratagene) in a 40 µl reaction containing the manufacturer's buffer supplemented with 5 mM dNTPs (Stratagene) and 10 µM random hexamers (Amersham). 3 µl aliquots of the reverse transcription reactions were amplified in a 25 µl reaction volume using the Brilliant QPCR core reagent kit (Stratagene). Each reaction mixture consisted of 1xPCR buffer, 3 mM MgCl₂, 300 pmol primers, 0.4 mM dNTPs, 1 unit of Taq, 1x reference dye and 1 unit of SYBR green (Molecular Probes). The forward and reverse primers for PHD3 cDNA were 5'-CTATGGGAAGAGCAAAGC -3' and 5'-AGAGCAGATGATGTGGAA - 3', respectively. The PCR was performed with the Mx3000P (Stratagene) for 45 cycles of 95 °C for 30 s, 52 °C (for PHD3) or 51 °C (for GAPDH) for 1 min, 72 °C for 30 s. A melting curve was obtained to confirm that the SYBR green signal corresponded to a unique and specific amplicon. Standard curves were generated for every real-time PCR run by using serial three-fold dilutions of a reverse transcribed RNA extract from an E13 whole mouse embryo. All values obtained were normalized to GAPDH mRNA. The forward and reverse primers for GAPDH cDNA were 5'-TCCCACTCTTCCACCTTC-3' and 5'-CTGTAGCCGTATTCATTGTC- 3', respectively. qPCR was performed three times, as described above, on ganglia obtained from three separate litters.

2.15 Western blots

Neurons were plated at high density in poly-ornithine/laminin coated 96-well plates (5,000 neurons per well) in defined medium. Four hours after plating, 50 ng/ml

CNTF or 10ng/ml BDNF was added to the wells for the indicated times. The medium was removed and the cells were lysed in RIPA buffer (50mM Tris pH7.4, 150mM NaCl, 10% Glycerol, 1% Triton X-100, 1mM EDTA and 100µg/ml PMSF) and the cell extract was incubated on ice for 1h. Insoluble debris was removed by centrifugation at 10,000 x g for 10 min at 4°C. Equal amounts of each sample were transferred to PVDF membranes using the Bio-Rad trans-blot system. Membranes were blocked for 1 h in 5% dried milk in PBS with 0.1% Tween-20. Following this, membranes were incubated with antibodies for phospho Syk (Cell signalling technology ; 1:1000), serine phosphorylated IκBα (Cell signalling technology ; 1:1000), tyrosine phosphorylated IκBα (Cell signalling technology ; 1:1000) or β-III tubulin (Promega ; 1:1000) diluted in 1% dried milk in 1xPBS with 0.1% Tween-20. The appropriate peroxidase-linked secondary antibody (Amersham) was used to detect each primary antibody on the blots and staining was visualised using ECL-plus (Amersham). Densitometry was carried out using Adobe photoshop to determine the levels of phosphorylated forms of IκBα or Syk after treatment with either BDNF or CNTF.

2.16 Dissociated cell counts

Superior cervical ganglia were carefully dissected from neonatal wild-type, PHD1^{-/-}, PHD2^{+/-}, PHD3^{-/-}, PHD3^{-/-};HIF1^{+/-} and PHD3^{-/-} ;HIF2^{+/-} mice. Ganglia were then dissociated in trypsin as described above and a 1ml single cell suspension was obtained. Triplicate counts were made of the total number of phase bright, viable neurons per SCG using a Neubauer haemocytometer for each genotype. This process

was repeated at least three times using SCG obtained from at least three separate litters.

2.17 Adult stereology

As part of a collaborative project investigating the neuronal phenotype of PHD3^{-/-} mice, the total number of tyrosine hydroxylase (TH)-positive cells in SCG, carotid body and adrenal medulla were counted in wild-type and PHD3^{-/-} mice using standard stereological analysis. Adult stereology was carried out by Alberto Pascual (University of Sevilla, Spain). Briefly, the SCG, adrenal medulla and carotid body from adult mice were fixed in formalin overnight then transferred into PBS containing 30 % sucrose. 20 μm sections were blocked for 1 h at room temperature with 10 % FCS and 1 mg/ml BSA containing 0.1 % tritonX-100 in PBS, then incubated for 16 h at 4 °C with a rabbit anti-TH polyclonal antibody (Pel-Freez; diluted 1:1000 in blocking solution). The sections were washed four times in PBS-triton before being incubated with goat anti-rabbit secondary antibody (Envision+, Dako). Stereological estimation of the number of TH-positive cells was performed on sections spaced 80 μm (SCG and adrenal medulla) or 40 μm (carotid body) throughout the organ. The number of cells was estimated by systematic random sampling using a 106954 μm^3 optical dissector [421], excluding cells in the superficial planes of sections. The volume of each organ was estimated according to Cavalieri's principle [422]. Stereological measurements were performed using the C.A.S.T. Grid System (Olympus) with a coefficient of error < 0.09.

2.18 Measuring sympathetic innervation density

To assess the density of sympathetic innervation, the eyes, submandibular and pineal glands from adult (or P5 for the pineal glands) wild-type and *PHD3*^{-/-} mice were fixed in 4% paraformaldehyde for 24 h and were cryoprotected in 30% sucrose before being frozen. 15 µm serial sections were cut through the tissue which were then mounted onto poly-lysine-coated slides (BDH), blocked with 10% normal goat serum containing 0.1% tritonX-100 in 10 mM PBS for 1 h at room temperature, and then incubated for 18 hr at 4°C with a rabbit anti-TH polyclonal antibody (Chemicon) diluted 1:200 in PBS with 1% normal goat serum (Sigma). The sections were washed three times in PBS before being incubated with goat anti-rabbit secondary antibody (Alexa-Fluor, Invitrogen, 1:500) for 2 hours. In the case of the iris and submandibular glands, four random images were taken from each section using an Axioplan Zeiss laser scanning confocal microscope. One image from the smaller pineal gland was taken per section. The images were then traced using Adobe Photoshop 7 and the total area and the area containing TH-positive fibres were estimated by automated pixel counts. The ratio of TH-positive area to total area was then calculated as a percentage.

2.19 Pupillometry

As part of a collaborative project examining the physiological effects of *PHD3* inactivation on the sympathetic nervous system, Dr. Joseph de Bono (University of Oxford) measured pupillary reflexes in *PHD3*^{-/-} mice. Briefly, adult wild-type and *PHD3*^{-/-} mice were dark-adapted for 1 h. Subsequently, animals were removed from their home cage, immobilised by scruffing and pupil reactions were monitored (at 0 lux followed by 150 lux of bright white light) using a commercial CCD camcorder (DCR-HC17E, Sony, Tokyo, Japan) attached to a dissecting microscope (Olympus,

Tokyo, Japan) under infrared LED illumination (λ_{max} of 850nm). Pupil areas were estimated by manually fitting an ellipse to digitalised video still images using Windows Movie Maker (Microsoft, Redmond, WA) and Adobe Photoshop (San Jose, CA) software.

2.20 Statistical analyses

Data are presented as means \pm SEM, and statistical significance was determined by student's T-test or, if there were more than two sets of data to compare, the one-way analysis of variance (ANOVA) with Fisher's post hoc test was used. The level of significance accepted was $P < 0.05$. For neurite growth analysis, between 40 and 70 neurons were sampled per condition and each experiment was repeated at least three times. All other studies presented were performed on litter mate-controls and were repeated using at least three* separate litters and the error calculated using the average values obtained from each repeat.

* In cases where more than three repeats were performed, the number of repeats is indicated in the parentheses (see figures).

Chapter 3

**NF κ B Activation via Tyrosine Phosphorylation of I κ B- α is Crucial
for CNTF-promoted neurite growth from developing neurons**

3.1 Introduction

Nuclear factor-kappa B (NF- κ B) is a ubiquitously expressed transcription factor system that consists of homodimers or heterodimers of five structurally related proteins: p65, RelB, c-Rel, p50 and p52, of which the p50/p65 heterodimer is the most abundant and widely expressed [298]. NF- κ B is held in an inactive form in the cytosol by interaction with a member of the I κ B family of inhibitory proteins: I κ B α , I κ B β , I κ B ϵ , I κ B γ , Bcl-3, p100 and p105, of which I κ B α is the predominantly expressed inhibitor. In the canonical NF- κ B signalling pathway, NF- κ B is activated by phosphorylation of I κ B α on serine residues 32 and 36 by an I κ B kinase complex. This leads to ubiquitination and proteasome-mediated degradation of I κ B α and translocation of liberated NF- κ B to the nucleus where it binds to consensus κ B sequences in the promoter and enhancer regions of responsive genes [298]. NF- κ B can also be activated by several alternative mechanisms including one in which I κ B α is phosphorylated on tyrosine 42, which results in its dissociation from NF- κ B without proteasome-mediated degradation [350, 423-425].

Classically, NF- κ B has been shown to regulate the expression of genes involved in innate and adaptive immune responses, stress responses, cell survival and cell proliferation [426]. In the nervous system, NF- κ B is activated by a variety of neurotrophic factors, cytokines and neurotransmitters, and can promote neuronal survival or bring about neuronal death [427]. NF- κ B signalling also regulates synaptic function, plays a role learning and memory and participates in peripheral nerve myelination [313, 428-430]. Most recently, the ability of the neurotrophins nerve growth factor (NGF) and brain-derived neurotrophic factor (BDNF) to promote



neurite growth has been shown to be partially dependent on NF- κ B signalling [291, 321, 431].

Because neurotrophins and other families of neurotrophic factors exert qualitatively and quantitatively different effects on neurite growth from various kinds of neurons, we asked to what extent NF- κ B signalling is involved in regulating neurite growth in response to different kinds of neurotrophic factors. For these studies I chose the sensory neurons of the nodose ganglion of newborn mice because the survival of the great majority of these neurons is supported equally well by two different neurotrophic factors, the neurotrophin BDNF and the cytokine ciliary neurotrophic factor (CNTF), both of which promote neurite growth [102, 109]. Moreover, these neurotrophic factors utilize different receptor systems that engage downstream signalling networks in different ways. BDNF binds to the TrkB receptor tyrosine kinase and the common neurotrophin receptor p75^{NTR}, and CNTF binds to a receptor complex consisting of gp130, LIFR β and CNTFR α [220, 280]. I find that NF- κ B signalling contributes to the neurite growth-promoting effects of BDNF and is essential for CNTF-promoted neurite growth, but plays no role in mediating the survival-promoting effects of either of these factors in the postnatal period. Whereas the contribution of NF- κ B signalling to BDNF-promoted neurite growth occurs via the canonical pathway, the requirement of NF- κ B signalling for CNTF-promoted growth occurs via a non-canonical NF- κ B signalling pathway.

Results

3.2 SN50 reduces neurite growth from nodose neurons

Translocation of NF- κ B (p65/p50 dimers) from the cytoplasm to the nucleus is an essential step in its regulation of gene transcription. SN50 is a cell membrane permeable inhibitor of NF- κ B nuclear translocation that blocks NF- κ B-dependent transcription by blocking the nuclear localisation sequence of p50 [432]. To test and contrast the effect of SN50 on neurite growth promoted by neurotrophins and cytokines, dissociated cultures of P0 nodose ganglion neurons were treated with either SN50 or an inactive control peptide (SM) 3 hours after plating. The culture medium was supplemented with either BDNF or CNTF 3 hours after plating, and neuronal survival and the size and complexity of neurite arbors was quantified 24 hours after plating. In BDNF supplemented cultures, SN50 but not the control peptide, significantly inhibited neurite growth. Total neurite length (Fig. 14B) and the total number of branch points (Fig. 14C) were reduced by about half by SN50, and branching with distance from the cell body was reduced by about half at each 30 μ m interval (Fig. 14A). The typical appearances of SN50-treated and control peptide-treated neurons grown with BDNF are illustrated in Figure 18. SN50 did not significantly reduce the number of neurons surviving with BDNF (Fig. 14D).

In CNTF supplemented cultures, SN50 but not the control peptide virtually eliminated neurite growth as quantified by Sholl analysis, total neurite length and number of branch points (Figs. 15A, 15B and 15C). Despite the dramatic effect on neurite growth, the cell bodies of the SN50-treated neurons retained a normal appearance (Fig. 18) and continued to survive just as well as control peptide-treated neurons in the presence of CNTF, with around 80% of the neurons surviving at this time (Fig.

15D) as evidenced by staining with the vital dye calcein. In contrast, over half of the neurons grown without neurotrophic factors were dead by 24 hours (data not shown). BDNF and CNTF promoted the survival of similar numbers of nodose neurons (Figs. 14D and 14H), and because there was no additional survival in the presence of both factors (data not shown) it appears that BDNF and CNTF promote the *in vitro* survival of the same major subset of nodose neurons at this stage of development.

These results demonstrate that blocking nuclear translocation of NF- κ B in nodose neurons markedly affects neurite growth without affecting survival. The virtual elimination of neurite growth from neurons grown with CNTF suggests that NF- κ B signalling is crucial for CNTF-promoted neurite growth, whereas the significant reduction in neurite growth from neurons grown with BDNF suggests that NF- κ B signalling makes an important contribution to BDNF-promoted neurite growth.

3.3 κ B decoy DNA reduces neurite growth from nodose neurons

To further investigate the importance of NF- κ B in neurotrophic factor-promoted neurite growth, the consequences of inhibiting another key step in NF- κ B signalling, the binding of activated NF- κ B to DNA were studied. This was blocked by transfecting neurons with double stranded DNA oligonucleotides containing the κ B consensus binding sequence found in the promoters and enhancers of NF- κ B target genes. This κ B decoy DNA has been successfully used *in vitro* and *in vivo* to inhibit NF- κ B transcriptional activity by sequestering transcriptionally active NF- κ B complexes [321, 433, 434]. P0 nodose ganglion neurons were transfected with either the κ B decoy DNA or a control oligonucleotide of scrambled sequence 3 hours after

plating. The culture medium was supplemented with either BDNF or CNTF immediately after transfection and neuronal survival and the size and complexity of neurite arbors was quantified 24 hours after plating.

In BDNF-supplemented cultures, the κ B decoy DNA but not the control oligonucleotide caused a significant reduction in neurite growth. In these cultures, total neurite length, number of branch points and branching with distance of the cell body were reduced by just under 50% (Figs. 16A, 16B and 16C). κ B decoy DNA did not affect the number of neurons surviving with BDNF (Fig. 16D). In CNTF supplemented cultures, the κ B decoy DNA but not the control oligonucleotide caused a marked, three-fold reduction in neurite length (Fig. 17B) and branching (fig. 17C) and a marked reduction in neurite growth as quantified by Sholl analysis (Fig. 17A). As with SN50, κ B decoy DNA had no detrimental effect on the survival of CNTF-supplemented neurons (Fig. 17D). The typical appearances of CNTF-treated and BDNF-treated neurons transfected with κ B decoy DNA are illustrated in Figure 18.

These results show that blocking NF- κ B-dependent transcription reduces neurite growth from newborn nodose ganglion neurons supported by CNTF or BDNF without significantly affecting survival. As with blocking nuclear translocation of NF- κ B, blocking NF- κ B-dependent transcription has a much greater effect on CNTF-promoted neurite growth than BDNF-promoted neurite growth.

3.4 Overexpression of p50/p65 increases neurite growth

To further characterize the role of NF κ B signalling in neurite growth, P0 nodose neurons were transfected with plasmids expressing NF κ B subunits p50, p65, p50 plus

p65 or control pcDNA and neurite growth was measured after 24 hours in culture with BDNF or CNTF. Figure 6 shows that cotransfection of nodose neurons supported by BDNF with p50/p65 significantly increased neurite growth (Fig. 19A), length (Fig. 19B) and branching (Fig. 19C) without effecting neuronal survival (data not shown) compared to control transfected neurons. Figure 19 also shows that expression of either p50 or p65 alone had no effect on neurite growth. Similarly, for neurons supported by CNTF, cotransfection with p50/p65 significantly increased growth (Fig. 19D), length (Fig. 19E) and branching (Fig. 19F) compared to control transfected neurons. Again, expression of either p50 or p65 alone had no effect on neurite growth in neurons supported by CNTF (not shown). These data support the above observations implicating NF κ B in the positive regulation of neurite growth. These data also suggest that the NF κ B p50/p65 heterodimer regulates the growth of nodose neurons supported by either BDNF or CNTF.

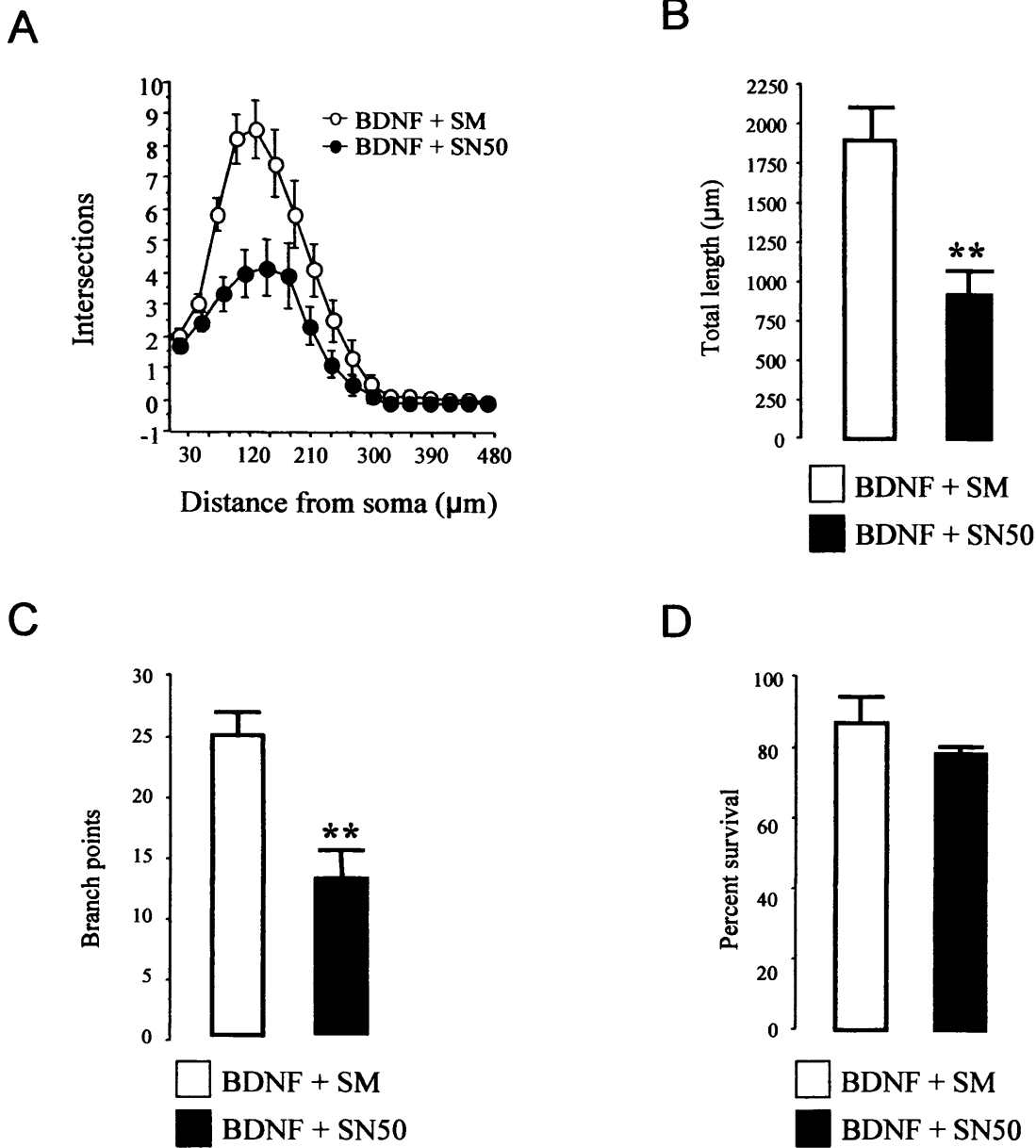


Figure 14 | Effect of SN50 on BDNF-dependent neurite growth. P0 nodose neurons were treated with either SN50 (10 μM) or the inactive peptide SM (10 μM) together with BDNF (10 ng/ml) 3 hours after plating. The neurons were fluorescently labelled with Calcein-AM dye and images were digitally acquired for analysis of neurite growth and morphology 24 hours after plating. Sholl analysis (A), total neurite length (B) and number of branch points (C) in the neurite arbors of 50-90 neurons in each condition from a typical experiment are shown (means \pm standard errors). Very similar data were obtained in three independent experiments. The percentage survival of neurons after 24 hours incubation in these conditions is shown in D. Statistical comparisons are with respect to SM-treated neurons (* $p < 0.05$, ** $p < 0.01$).

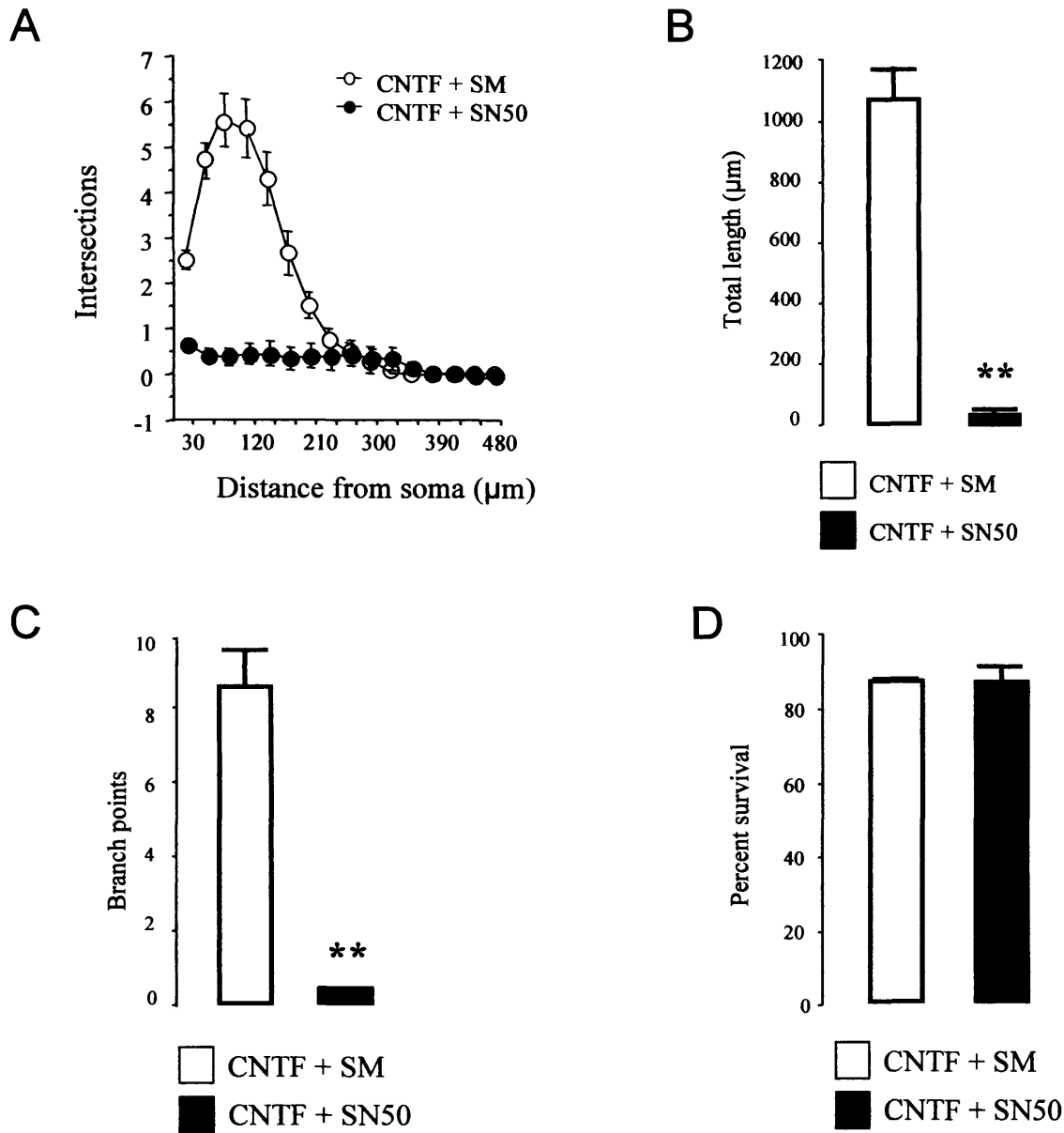


Figure 15 | Effect of SN50 on CNTF-dependent neurite growth. P0 nodose neurons were treated with either SN50 (10μM) or the inactive peptide SM (10μM) together with CNTF (10 ng/ml) 3 hours after plating. The neurons were fluorescently labelled with Calcein-AM dye and images were digitally acquired for analysis of neurite growth and morphology 24 hours after plating. Sholl analysis (A), total neurite length (B) and number of branch points (C) in the neurite arbors of 50-90 neurons in each condition from a typical experiment are shown (means ± standard errors). Very similar data were obtained in three independent experiments. The percentage survival of neurons after 24 hours incubation in these conditions is shown in D. Statistical comparisons are with respect to SM-treated neurons (* p<0.05, **p<0.001).

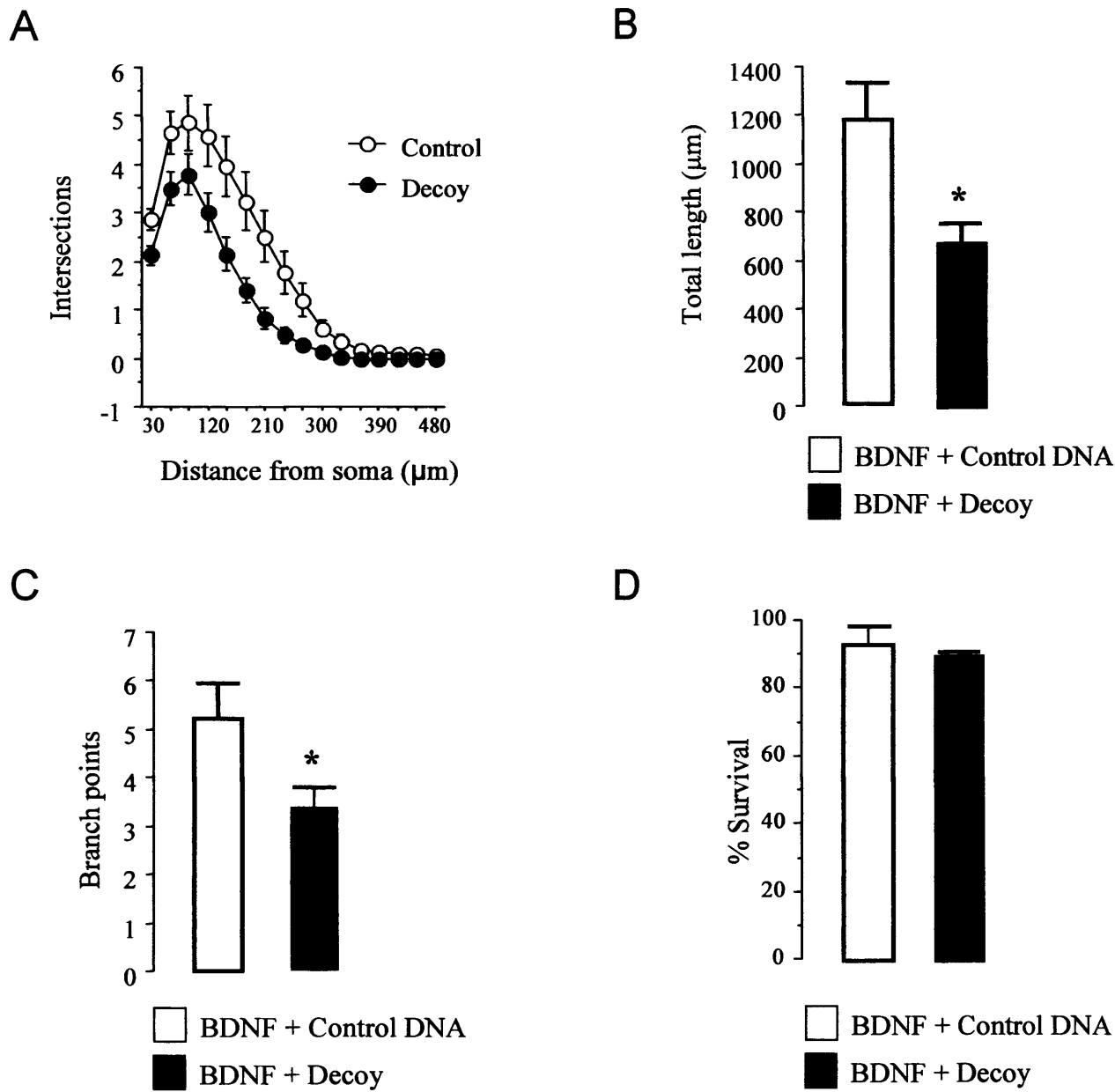


Figure 16 | Effect of κ B decoy DNA on BDNF-dependent neurite growth. P0 nodose neurons were transfected 3 hours after plating with a YFP expression plasmid together with either κ B decoy DNA oligonucleotide or a scrambled control DNA oligonucleotide and were incubated with BDNF (10 ng/ml) until 24 hours after plating when images of labelled neurons were digitally acquired for analysis of neurite growth and morphology. Sholl analysis (A), total neurite length (B) and number of branch points (C) in the neurite arbors of 50-90 neurons in each condition are shown (means \pm standard errors) from a typical experiment (very similar data were obtained in three independent experiments). The percentage survival of neurons after 24 hours incubation in these conditions as shown in D. Statistical comparisons are with respect to control-transfected neurons (* $p < 0.05$).

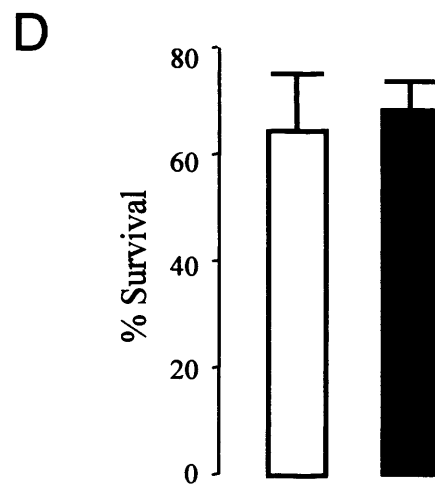
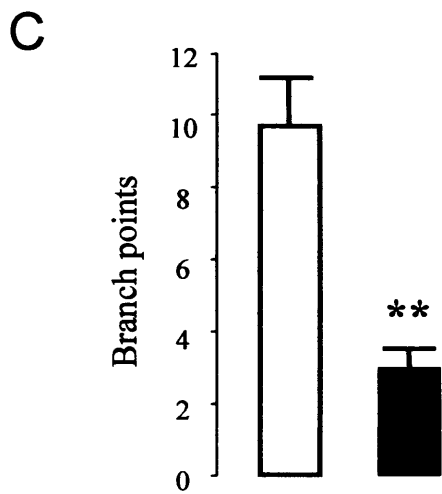
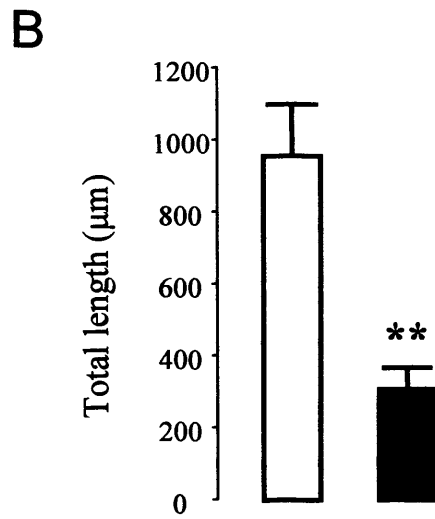
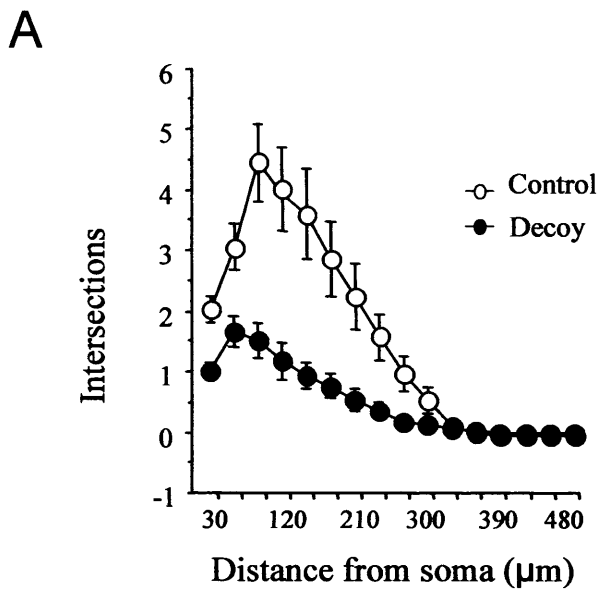


Figure 17 | Effect of κB decoy DNA CNTF-dependent neurite growth. P0 nodose neurons were transfected 3 hours after plating with a YFP expression plasmid together with either κB decoy DNA oligonucleotide or a scrambled control DNA oligonucleotide and were incubated with CNTF (50 ng/ml) until 24 hours after plating when images of labelled neurons were digitally acquired for analysis of neurite growth and morphology. Sholl analysis (A), total neurite length (B) and number of branch points (C) in the neurite arbors of 50-90 neurons in each condition are shown (means \pm standard errors) from a typical experiment (very similar data were obtained in three independent experiments). The percentage survival of neurons after 24 hours incubation in these conditions as shown in D. Statistical comparisons are with respect to control-transfected neurons (* $p < 0.05$, ** $p < 0.001$).

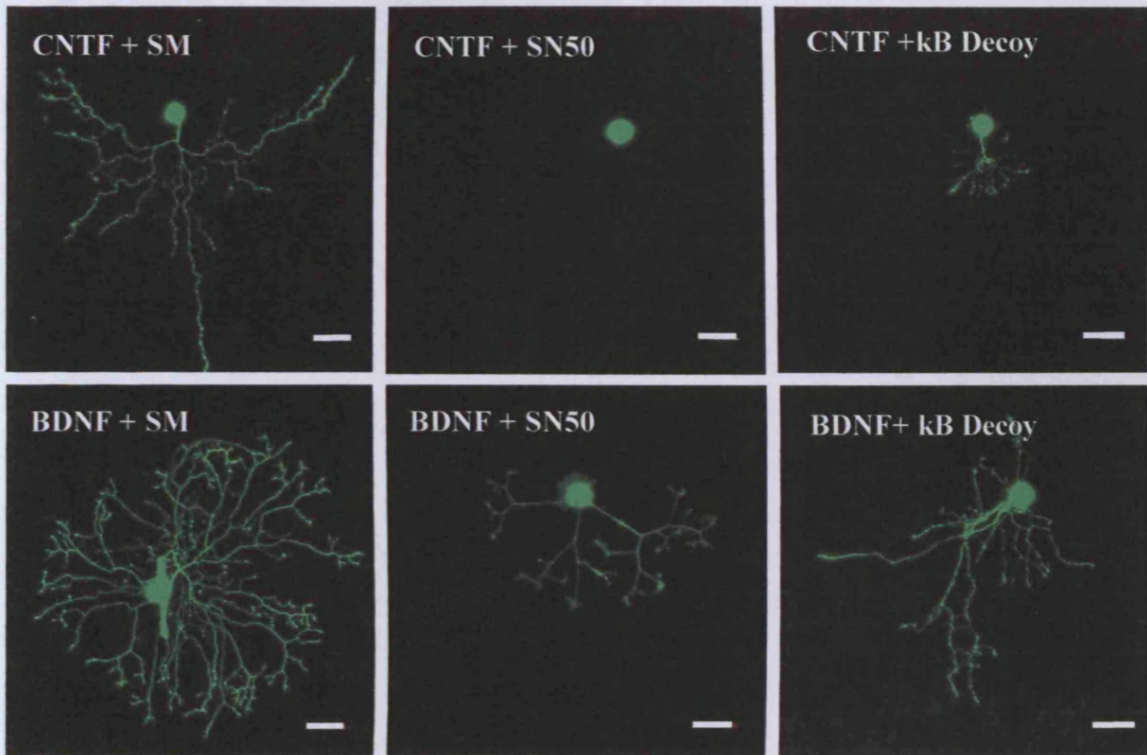


Figure 18 | **Effect of inhibiting NF- κ B activity on neurite arbor size.** Photomicrographs of typical P0 nodose neurons incubated for 24 hours with either CNTF or BDNF together with either SN50 or SM control peptide and labelled with calcein-AM (4 panels on left) or transfected with a YFP plasmid and κ B decoy DNA (2 panels on right). Scale bar = 30 μ m.

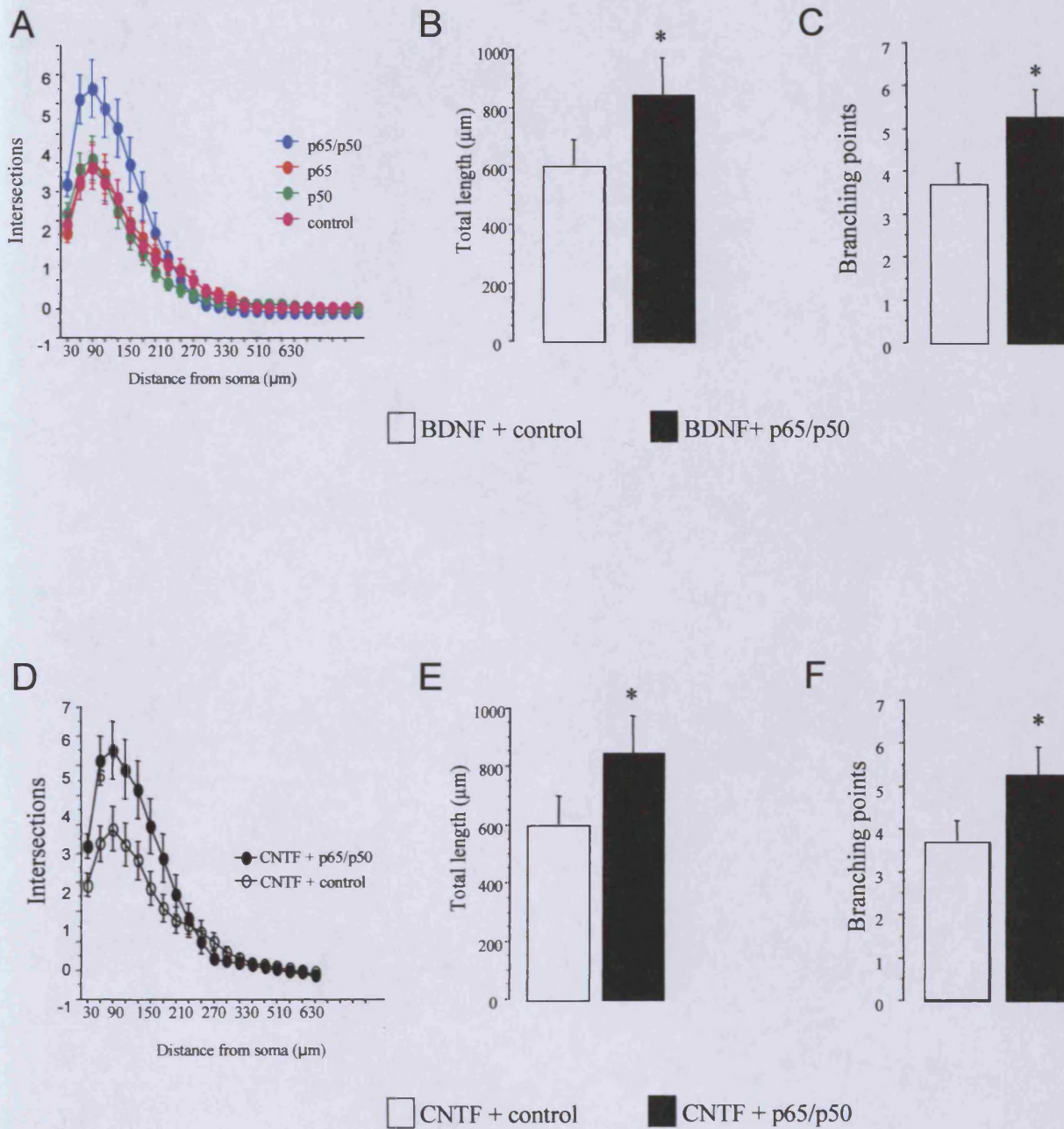


Figure 19 | Effect of Overexpressing NFκB subunits on neurite growth. P0 nodose neurons were transfected 3 hours after plating with a YFP expression plasmid together with p65, p50 or p65 plus p50 and cultured with BDNF(10ng/ml) or CNTF (50ng/ml). Sholl analysis (A,D), total neurite length (B,E) and number of branch points (C,F) in the neurite arbors of 50-90 neurons in each condition are shown (means ± standard errors) from a typical experiment (very similar data were obtained in three independent experiments). The percentage survival of neurons after 24 hours incubation in these conditions as shown in D. Statistical comparisons are with respect to control-transfected neurons (* p<0.05).

3.5 Serine phosphorylation of I κ B- α contributes to BDNF-promoted neurite growth but is not required for CNTF-promoted growth

It has been previously shown that inhibiting the canonical NF- κ B activation pathway in neonatal nodose ganglion neurons supported in culture with BDNF by transfecting these neurons with a plasmid expressing a super-repressor form of I κ B- α results in reduced neurite growth [321]. This mutant form of I κ B- α associates normally with NF- κ B but has serine to alanine mutations at residues 32 and 36 that specifically prevent phosphorylation of I κ B- α by the IKK complex and subsequent proteasome-mediated degradation, thereby preventing release and translocation of NF- κ B to the nucleus [291, 435, 436]. Confirming previous findings, expression of the 32/36-SS/AA I κ B- α mutant in nodose grown under the same conditions with BDNF in the medium caused clear and significant reductions in neurite length, number of branch points and branching with distance from the cell body (Figs. 20A, 20B and 20C). Surprisingly, when nodose neurons were supported by CNTF, transfecting them with this 32/36-SS/AA I κ B- α mutant did not affect neurite arbor size and complexity (Figs. 20E-G). There were no significant differences in neurite length and branching between neurons expressing the 32/36-SS/AA I κ B- α mutant and control transfected neurons grown with CNTF (Figs. 20E-G). Expression of the 32/36-SS/AA I κ B- α mutant did not significantly affect the number of neurons surviving in the presence of either CNTF or BDNF (Figs. 20D and 20H).

3.6 Tyrosine phosphorylation of I κ B- α is crucial for CNTF-promoted neurite growth but is not required for BDNF-promoted growth

Because NF- κ B activation and NF- κ B-dependent transcription are required for CNTF-promoted neurite growth (Figs.14-19) the potential role of an alternative mechanism of NF- κ B activation for CNTF-promoted neurite growth was investigated. NF- κ B activation by tyrosine phosphorylation of I κ B- α has recently been implicated in NGF-promoted survival and differentiation of PC12 cells [291, 437, 438]. Newborn nodose neurons were transfected with a plasmid expressing a Y42F I κ B- α mutant that effectively and specifically blocks NF- κ B activation by tyrosine phosphorylation of I κ B- α [424]. The Y42F I κ B- α mutant had no significant effect on the size and complexity of neurite arbors growing from nodose neurons supported by BDNF (Figs. 21A, 21B and 21C). In marked contrast, the neurite arbors of neurons expressing this Y42F I κ B- α mutant were 4-fold shorter (Fig.21F) and had four-fold fewer branch points (Fig. 21G) and showed very clear reductions in branching with distance from the cell body (Fig. 21E) compared with control-transfected neurons in the presence of CNTF. Like the 32/36-SS/FF I κ B- α mutant, the Y42F I κ B- α mutant had no significant effect on the survival of newborn nodose neurons grown with either BDNF (Fig. 21D) or CNTF (Fig. 21H).

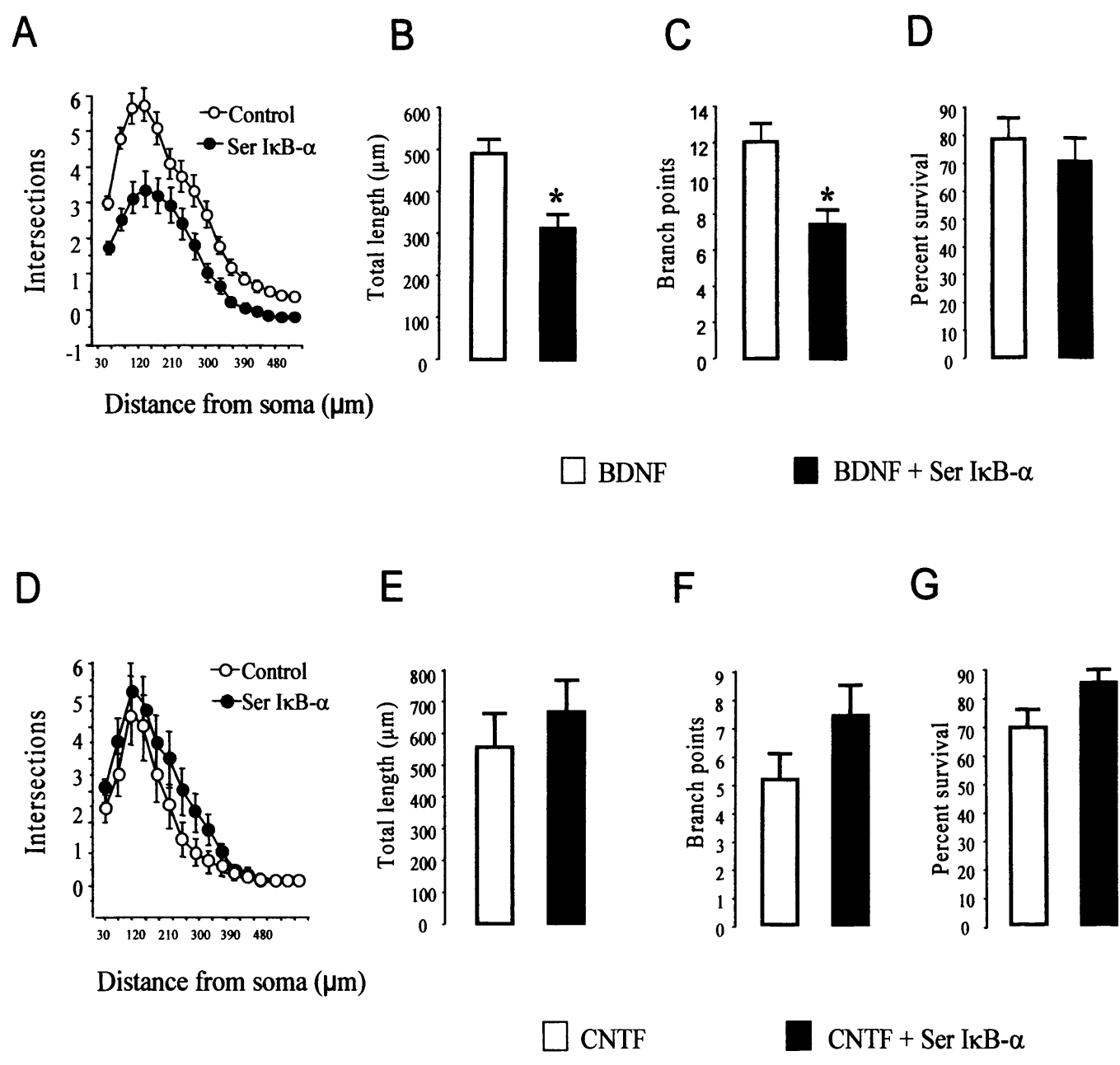


Figure 20 | Effect of Serine I $\kappa\text{B-}\alpha$ mutant on neurite growth. P0 nodose neurons were transfected 3 hours after plating with a YFP expression plasmid together with Ser I κB mutant and were incubated with BDNF (10 ng/ml) or CNTF (50ng/ml) until 24 hours after plating. Sholl analysis (A,D), total neurite length (B,E) and number of branch points (C,F) in the neurite arbors of 50-90 neurons in each condition are shown (means \pm standard errors) from a typical experiment (very similar data were obtained in three independent experiments). The percentage survival of neurons after 24 hours incubation in these conditions as shown in D and G. Statistical comparisons are with respect to control-transfected neurons (* $p < 0.05$).

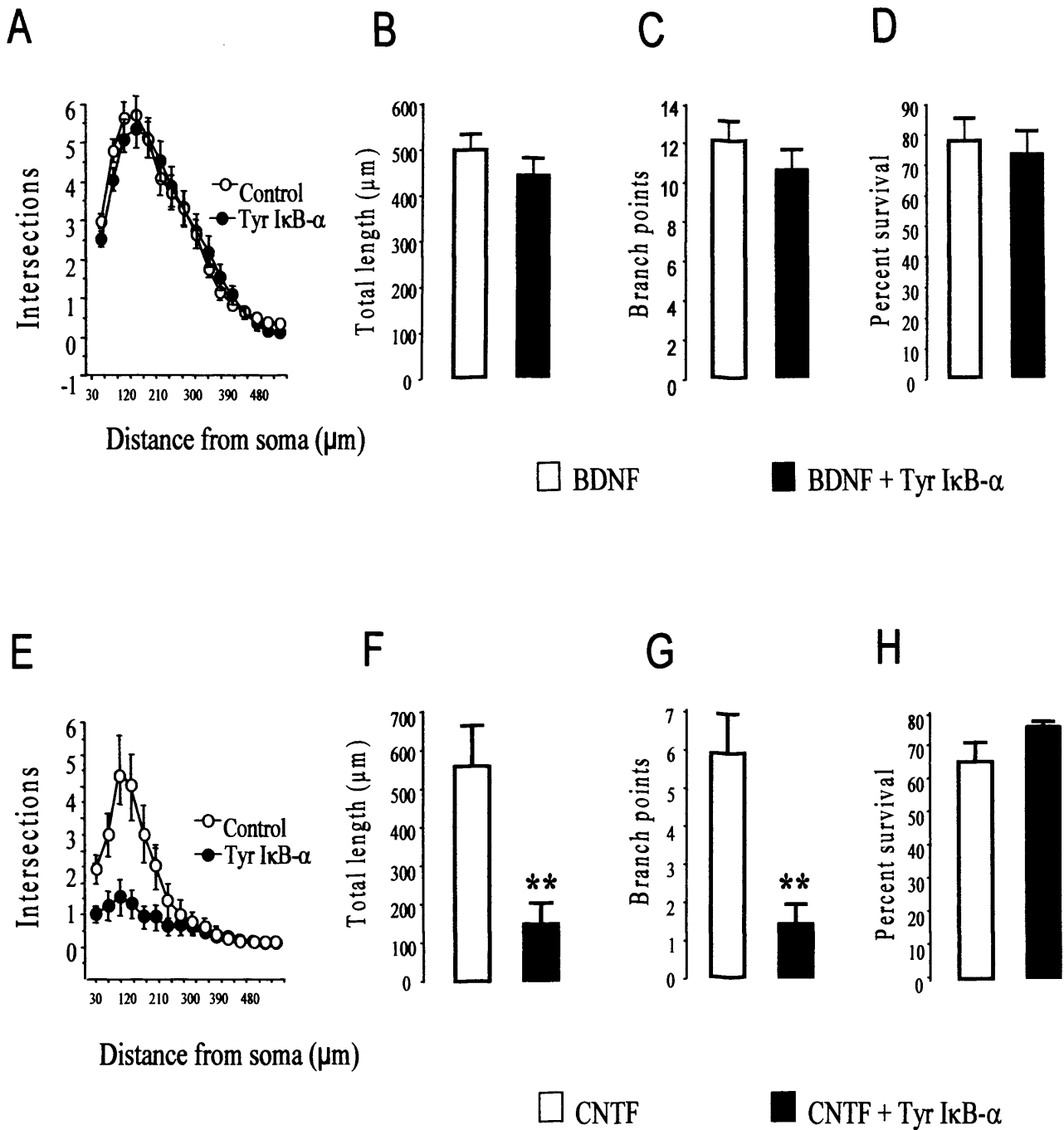


Figure 21 | Effect of Tyrosine IκB-α mutant on neurite growth. P0 nodose neurons were transfected 3 hours after plating with a YFP expression plasmid together with Tyr IκB mutant and were incubated with BDNF (10 ng/ml) or CNTF (50ng/ml) until 24 hours after plating. Sholl analysis (A,D), total neurite length (B,E) and number of branch points (C,F) in the neurite arbors of 50-90 neurons in each condition are shown (means ± standard errors) from a typical experiment (very similar data were obtained in three independent experiments). The percentage survival of neurons after 24 hours incubation in these conditions as shown in D and G. Statistical comparisons are with respect to control-transfected neurons (* p<0.05, **p<0.01).

3.7 Proteasome-independent mechanism for CNTF promoted neurite growth

Phosphorylation of I κ B- α on serine residues leads to ubiquitination and proteasomal degradation. It has been reported that the proteasome inhibitor N-acetyl-Leu-Leu-norleucinal (ALLN) causes a highly significant decrease in neurite arbor size of newborn nodose neurons grown with BDNF [321]. Interestingly, addition of ALLN to CNTF-stimulated nodose neurons did not affect neurite growth and branching, implying a proteasome-independent mechanism for CNTF-promoted neurite growth (Figs. 22A-C). In addition, treatment of CNTF-supported neurons with another proteasome inhibitor, MG132 had no effect on neurite growth, length or branching (Figs. 22D-F). Representative images illustrating the inhibition of BDNF-dependent neurite growth elicited by MG132 is shown Figs 22G and 22H. Whereas in the canonical NF κ B activation pathway phosphorylation of I κ B- α on serine residues 32 and 36 leads to proteasome-mediated degradation, phosphorylation of I κ B- α on tyrosine 42 leads to dissociation of NF κ B from I κ B- α without degradation of I κ B- α [350]. In agreement with this, no detectable degradation of I κ B- α upon treatment of nodose neurons with CNTF was observed (Fig. 23A,B).

These results show that the contribution of NF- κ B signalling to neurite growth and branching from neurons grown with BDNF and CNTF occurs by fundamentally different mechanisms within the NF- κ B signalling network. Whereas the canonical NF- κ B signalling pathway contributes to neurite growth from neurons supported with BDNF, NF- κ B activation by an alternative mechanism involving tyrosine phosphorylation of I κ B- α is critically required for neurite growth from the same neurons when they are supported with CNTF.

3.8 BDNF and CNTF induce a differential pattern of I κ B- α phosphorylation

To determine if BDNF and CNTF change the phosphorylation pattern of I κ B- α , Western blots of proteins extracted from nodose neurons treated with these factors were probed with antibodies that specifically recognise phosphoserine I κ B- α and phosphotyrosine I κ B- α . P0 nodose neurons were plated in neurotrophic factor free medium for 3 hours and treated with either CNTF or BDNF for 5, 15 and 30 minutes before protein extraction and Western blotting. To avoid changes in the overall level of I κ B- α confounding the results because of potential differences in proteasomal degradation, the proteasome inhibitor ALLN was added to all cultures 3.5 hours after plating. Figure 24 shows that BDNF and CNTF each promoted transient increases in the levels of both phosphorylated forms of I κ B- α . However, in three independent experiments, BDNF was consistently more effective than CNTF in increasing the level of phosphoserine I κ B- α and CNTF was consistently more effective than BDNF increasing the level of phosphotyrosine I κ B- α . The peak of these preferential increases in phospho-serine I κ B- α with BDNF and phosphotyrosine I κ B- α with CNTF was consistently between 60 and 80% above the basal levels of these phosphoproteins in unstimulated neurons, whereas the transient rises in the reciprocal phosphoprotein species reached no more than 30% above basal levels. These findings demonstrate that BDNF and CNTF promote preferential increases in phosphoserine I κ B- α and phosphotyrosine I κ B- α , respectively.

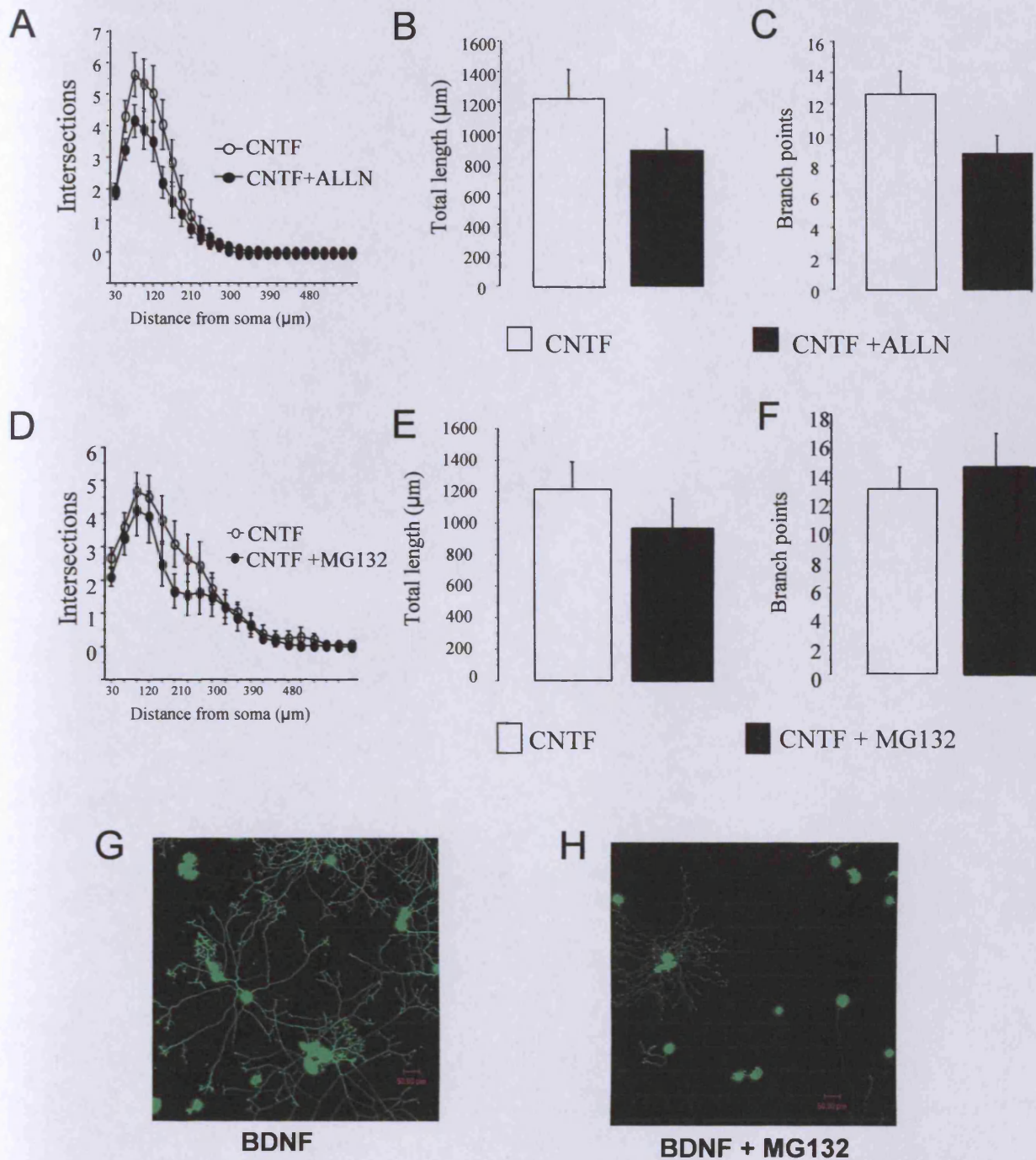


Figure 22 | Effects of proteasome inhibition on BDNF and CNTF-dependent neurite growth. P0 nodose neurons were cultured for 24 hours in the presence of either BDNF (10ng/ml) or CNTF (50ng/ml) and proteasome inhibitors ALLN (4μM) or MG132 (20nM) and neurite growth was analysed. (A-C) Effects of ALLN on CNTF-dependent growth. (D-F) Effects of MG132 on CNTF-dependent neurite growth. Both inhibitors ALLN and MG132 strongly reduced BDNF-dependent neurite growth. Representative images of the effects of MG132 on BDNF-supported growth are shown in G and H.

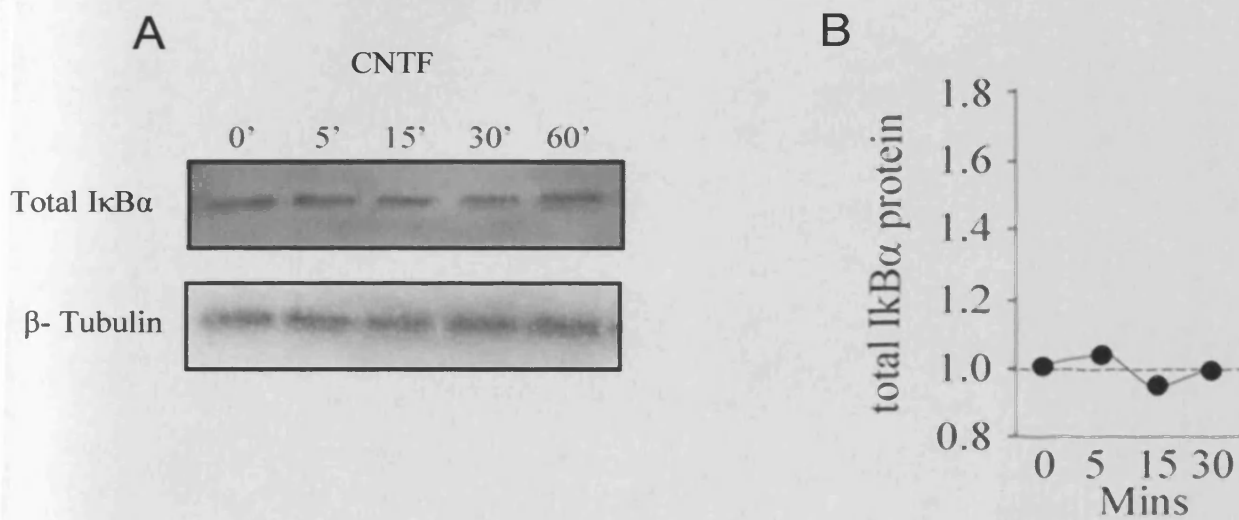


Figure 23 | **No degradation of I κ B α after treatment with CNTF.** P0 nodose neurons were incubated, for the period of time indicated on the X-axis (B), with CNTF (50ng/ml) after which cells were lysed and total protein collected. Western blots and densitometry were then used to detect the levels total I κ B α . (A) Western blot showing no effect of CNTF on I κ B α . (B) Densitometry showing no effect of CNTF on I κ B α .

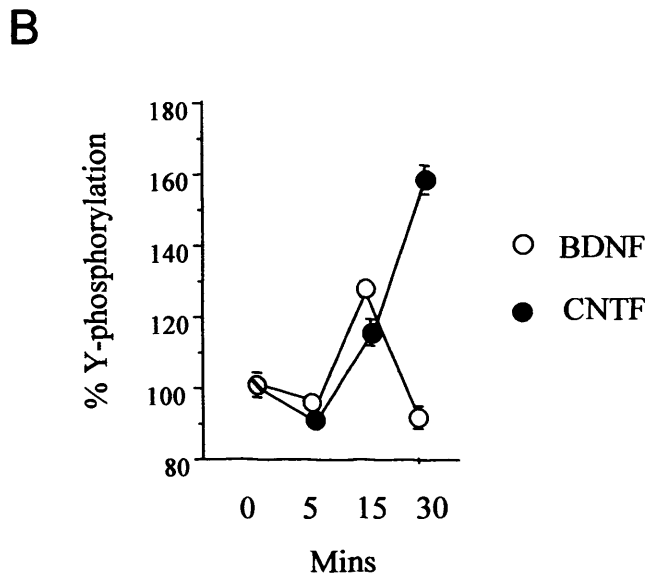
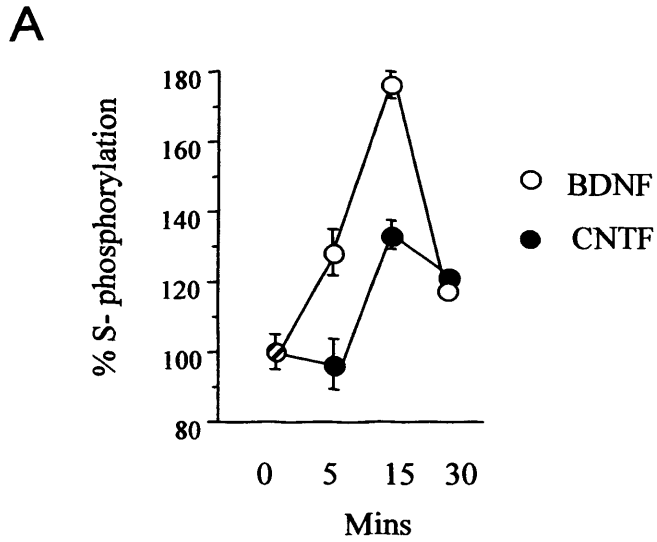


Figure 24 | Preferential tyrosine phosphorylation of IκBα after treatment with CNTF. P0 nodose neurons were incubated, for the period of time indicated on the X-axis, with either BDNF (10ng/ml) or CNTF (50ng/ml) after which cells were lysed and total protein collected. Western blots and densitometry were then used to detect the levels of serine and tyrosine-phosphorylated forms of IκBα. (A) Preferential increase in serine-phosphorylated IκBα upon treatment with BDNF. (B) Preferential increase in tyrosine-phosphorylated IκBα upon treatment with CNTF.

3.9 Spleen tyrosine kinase (SYK) is required for CNTF-promoted neurite growth

In contrast to the extensive literature on NF- κ B activation by the canonical pathway involving serine phosphorylation of I κ B by the IKK complex, much less is known about NF- κ B activation by tyrosine phosphorylation of I κ B. However, SYK protein-tyrosine kinase has recently been shown to phosphorylate I κ B- α on tyr42 following treatment of human myeloid KBM-5 cells with hydrogen peroxide [350]. To test the potential involvement of SYK in CNTF-promoted neurite growth, P0 nodose neurons were either treated with piceatannol, a potent selective SYK inhibitor [439], 3 hours after plating or transfected with a SYK dominant negative mutant construct. The culture medium was also supplemented with CNTF or BDNF at this time and the size and complexity of neurite arbors was quantified 24 hours after plating.

Figure 25 shows that the neurite arbors of CNTF-supplemented neurons treated with piceatannol were greatly reduced in size compared with untreated control cultures (Figs. 25E, 25F and 25G). In contrast, piceatannol had no significant effect on the size and complexity of the neurites of neurons grown with BDNF (Figs. 25A, 25B and 25C). Like the Y42F I κ B- α mutant, piceatannol did not affect the number of neurons surviving with either CNTF or BDNF (Figs. 25D and 25H). These results show that piceatannol selectively inhibits CNTF-promoted neurite growth, suggesting that SYK-dependent tyrosine phosphorylation of I κ B- α is a key step in the neurite growth response of neurons to CNTF but not BDNF. To further investigate the effect of Syk inactivation on neurite outgrowth, DN-Syk (a truncated form of Syk that contains only tandem SH2 domains with no catalytic domain that interrupts endogenous active Syk kinase) was expressed in nodose neurons supported by CNTF, and neurite outgrowth, length and branching were measured. DN-Syk expression caused a marked decrease

in neurite length (Fig. 26A) and the number of branch points (Fig. 26B). These data implicate Syk as an intracellular mediator of neurite growth downstream of CNTF receptor activation. Indeed, exposure of newborn nodose neurons to CNTF causes a marked increase in Syk phosphorylation within 5 minutes (Fig 26C). Treatment of the same neurons with BDNF has no effect on the level of Syk phosphorylation (Fig 26D). The timecourse of Syk-phosphorylation (Fig. 26C) and tyrosine phosphorylation of I κ B- α (Fig. 24), combined with the significant reduction in NF κ B reporter activation following Syk inhibition (Fig. 27B) strongly suggest that Syk signals upstream of NF κ B in the regulation of CNTF-dependent neurite growth.

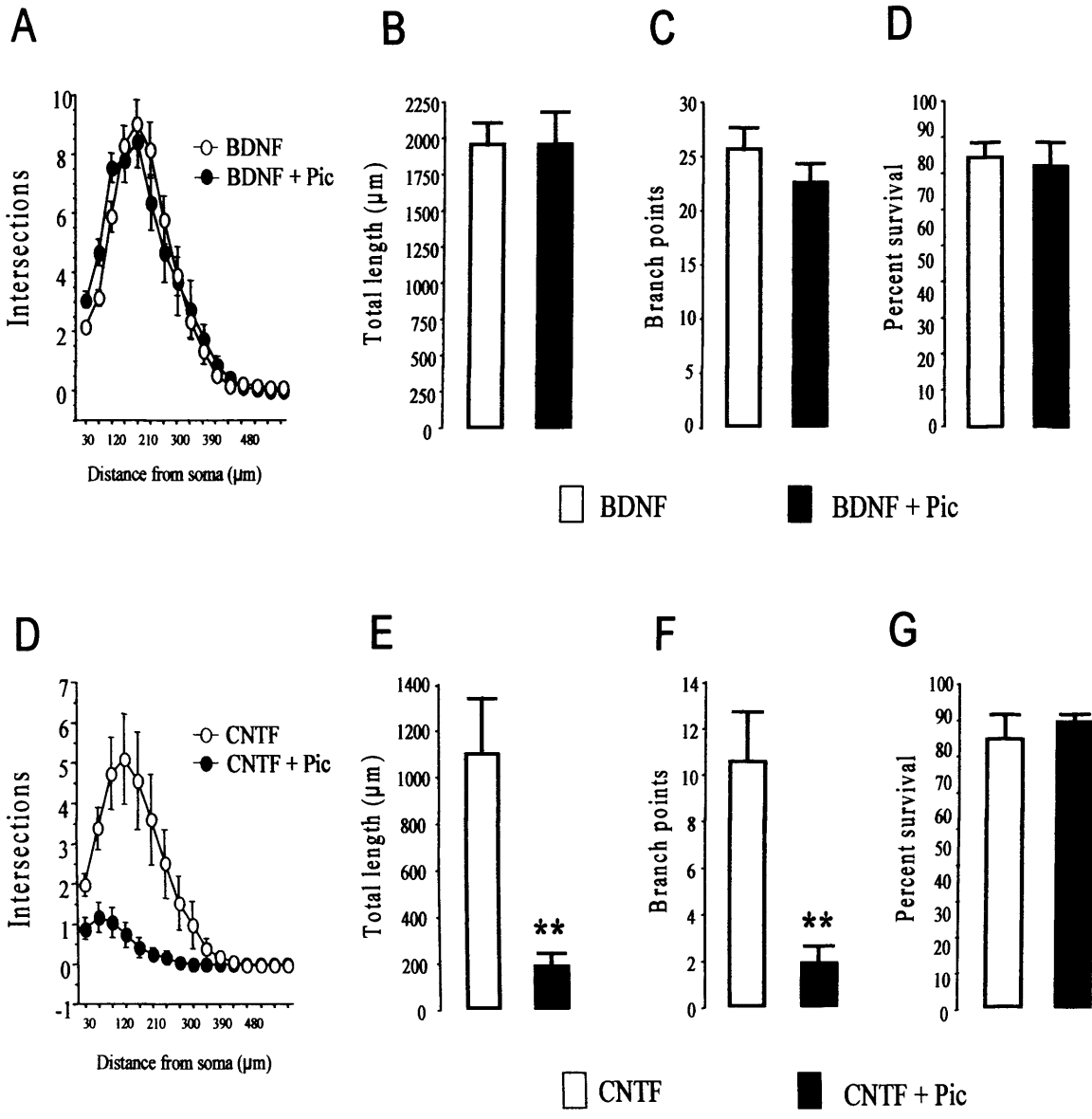


Figure 25 | Effect of Syk inhibition on neurite growth. P0 nodose neurons were incubated with BDNF (10 ng/ml) or CNTF (50ng/ml) and 10 μM piceatannol. Sholl analysis (A,D), total neurite length (B,E) and number of branch points (C,F) in the neurite arbors of 50-90 neurons in each condition are shown (means \pm standard errors) from a typical experiment (very similar data were obtained in three independent experiments). The percentage survival of neurons after 24 hours incubation in these conditions as shown in D and G. Statistical comparisons are with respect to control. (* $p < 0.05$, ** $p < 0.01$).

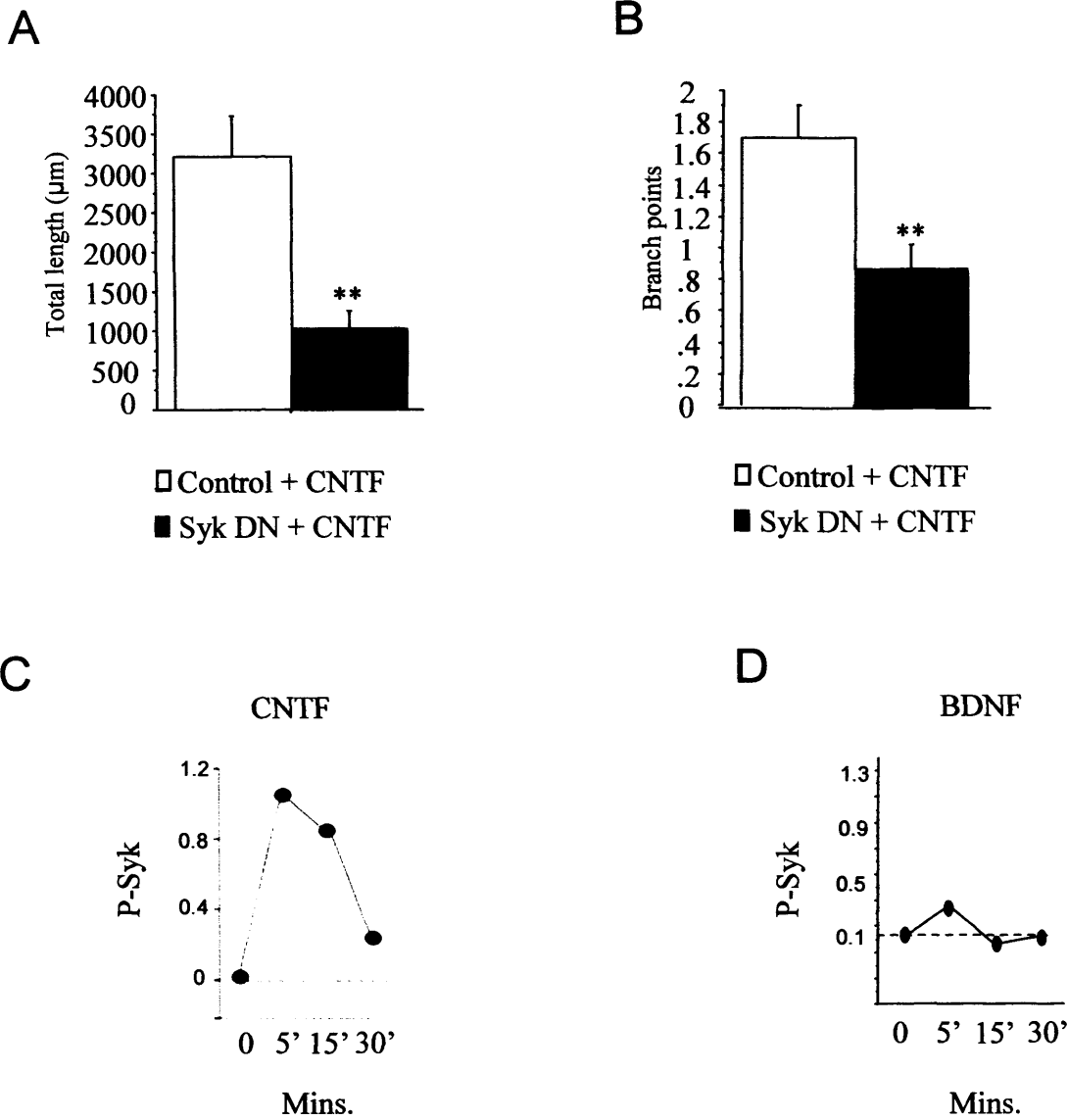


Figure 26 |Effect of Syk-DN on CNTF-supported neurite growth. P0 nodose neurons were transfected with Syk-DN and incubated with CNTF (50ng/ml) overnight. Total neurite length (A) and number of branch points (B) in the neurite arbors of 50-90 neurons in each condition are shown (means \pm standard errors) from a typical experiment. (C) Western blot densitometry using anti-phospho Syk antibodies showing increased Syk activation in nodose neurons treated with CNTF. (D) No significant activation of Syk after treatment with BDNF. Statistical comparisons are with respect to control-transfected neurons (** $p < 0.01$).

3.10 NF κ B reporter activation

Taken together, the above data suggest that NF κ B signalling is crucial for CNTF-mediated neurite growth. To determine if NF- κ B transcriptional activity is influenced by CNTF, newborn nodose neurons were transfected with a reporter construct in which GFP is under the control of an NF- κ B promoter. Transfected neurons were positively identified by co-transfection with an RFP expression plasmid. Neurons were shot 3 hours after plating with gold particles coated with both these plasmids together with either the tyrosine I κ B- α plasmid or treated with Syk inhibitor and were incubated for a further 24 hours with CNTF. CNTF treatment promoted a two-fold increase in reporter signal compared with untreated controls and this rise was completely blocked in neurons transfected with the Y42F I κ B- α plasmid and in neurons treated with the potent selective SYK inhibitor (Fig. 27). Previous work has shown that the level of NF κ B activation at P0 is not increased when neurons are treated with BDNF [321].

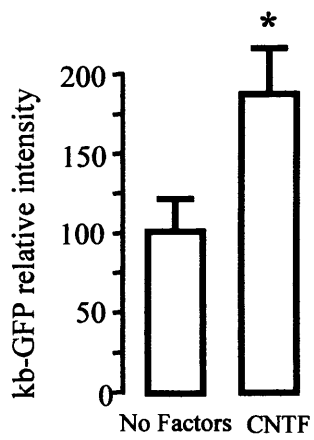
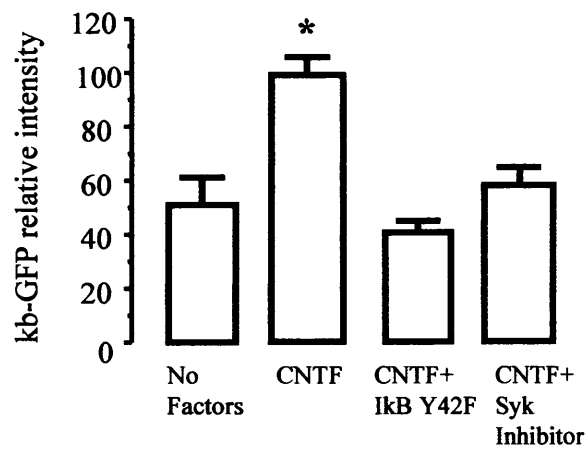
A**B**

Figure 27 | NFκB activation by CNTF. P0 nodose neurons were transfected with an NFκB construct and incubated for 24 hours with CNTF. (A) Increased NFκB activation after CNTF treatment. (B) CNTF-dependent increases in NFκB activation are reversed in neurons expressing Y42F or neurons treated with piceatannol. Statistical comparisons are with respect to control-transfected neurons (* p<0.05)

3.11 Discussion

I have studied the relative importance of NF- κ B signalling in the neurite growth-promoting effects of BDNF and CNTF on developing sensory neurons and delineated the selective involvement of different NF- κ B activation mechanisms in the response of neurons to these neurotrophic factors. General inhibition of NF- κ B signalling in newborn nodose neurons by either blocking nuclear translocation of NF- κ B with SN50 or inhibiting NF- κ B dependent transcription with decoy κ B DNA reduced neurite arbor size and complexity from BDNF-stimulated neurons by half, but almost eliminated neurite growth from CNTF-stimulated neurons. These results show that NF- κ B signalling significantly contributes to BDNF-promoted neurite growth, but is crucial for CNTF-promoted neurite growth. While NF- κ B signalling is known to play a participatory role in the neurite growth-promoting effects of the neurotrophins NGF and BDNF [321, 431], the essential role of NF- κ B signalling in CNTF-promoted growth is a striking, novel finding. Although CNTF is known to activate signalling pathways implicated in regulating neurite growth such as MEK/ERK and PI3-K/Akt [440, 441], there have been no studies of the involvement of these or other signalling pathways in mediating the neurite growth promoting effects of CNTF and related neurotrophic cytokines in primary neurons. These results therefore provide an important insight into the intracellular signalling mechanisms that are crucial for the neurite growth-promoting actions of CNTF and possibly related cytokines.

Investigation and comparison of the involvement of NF- κ B signalling in the neurite growth-promoting effects of BDNF and CNTF was facilitated in our experimental paradigm because these factors each support the survival of the majority of postnatal nodose neurons in culture and because inhibiting NF- κ B signalling has no

detectable effect on the number of neurons that survive with either factor. Previous work has established a neuroprotective role for NF- κ B for a variety of CNS neurons [308, 339, 442-446] and NF- κ B signalling has been shown to contribute to the survival response of embryonic sympathetic and sensory to NGF [238, 318] and adult DRG neurons to TNF- α [447]. Although it has been reported that blocking NF- κ B activation reduces the number of fetal nodose neurons that survive in culture with CNTF [319], our extensive investigation in which NF- κ B activation has been blocked by a variety of complementary approaches and cell survival has been followed with vital dye staining contradicts this general conclusion. In CNTF supplemented cultures the cell bodies of neurons in which NF- κ B signalling is blocked retain a normal appearance, even though these neurons are virtually devoid of processes. Importantly, staining with the vital dye calcein-AM showed no significant loss in the viability of these neurons in the presence of CNTF up to 72 hours *in vitro*. These findings therefore clearly demonstrate that NF- κ B signalling is crucial for the growth of neurites from developing nodose neurons stimulated with CNTF, but is not required for the survival of these neurons with CNTF.

One of the most striking findings of this study is that different NF- κ B activation mechanisms are exclusively required for the neurite growth-promoting effects of BDNF and CNTF, respectively. Specifically blocking NF- κ B activation by serine phosphorylation of I κ B- α using a 32/36-SS/AA I κ B- α mutant selectively reduced BDNF-promoted neurite growth but had no effect on CNTF-promoted neurite growth. Specifically blocking NF- κ B activation by tyrosine phosphorylation of I κ B- α using a Y42F I κ B- α mutant selectively inhibited CNTF-promoted neurite growth whilst having no effect on BDNF-promoted neurite growth. Phosphorylation of I κ B- α on serine residues 32 and 36 leads to ubiquitination and proteasome-mediated

degradation of I κ B α and translocation of the liberated NF- κ B to the nucleus [298]. The importance of this particular NF- κ B activation mechanism for BDNF-promoted neurite growth is reinforced by the observation that the proteasome inhibitor ALLN reduces significantly the size of neurite arbors growing from nodose neurons cultured with BDNF [321]. ALLN does not, however, affect neurite arbor size when these neurons are cultured with CNTF, reinforcing the idea that serine phosphorylation and subsequent proteasome-mediated degradation of I κ B- α is not required for CNTF-promoted neurite growth. Furthermore, the demonstration that inhibition of the SYK protein-tyrosine kinase or expression of dominant-negative SYK, whose substrates include I κ B- α [350], selectively blocks CNTF-promoted neurite growth, provides corroborating evidence for the importance of tyrosine phosphorylation of I κ B- α and implicates SYK in the neurite growth-promoting effects of CNTF but not BDNF. This is the first described role for Syk in primary neurons and it will be interesting in the future to investigate whether Syk activation regulates neurite growth in other populations of neurons.

BDNF and CNTF promote preferential transient increases in the levels of phosphoserine I κ B- α and phosphotyrosine I κ B- α , respectively. These changes in the phosphorylation pattern of I κ B- α provide the most parsimonious explanation for the selective role of serine and tyrosine phosphorylation of I κ B- α in the neurite growth-promoting effects of BDNF and CNTF, respectively. For each factor, the preferential transient rise in the corresponding phosphorylated I κ B- α species may result in differential recruitment of NF- κ B activity above a critical threshold that initiates transcriptional changes that promote neurite growth. This threshold need not be the same for each factor as a diversity of signalling pathways may cooperate with NF- κ B

to regulate neurite growth in each case. In addition to the preferential quantitative changes in the I κ B- α phosphorylation pattern brought about by BDNF and CNTF, it is possible that these factors may also promote qualitative differences in NF- κ B signalling downstream of I κ B- α , such as different patterns of p65 phosphorylation [448], which might help explain differences in the relative importance of NF- κ B in mediating the effects of these factors on neurite growth. Indeed, preliminary data (Nuria Gavalda- unpublished observation) suggest that the phosphorylation pattern of activated p65 differs between BDNF and CNTF – treated nodose neurons.

While presenting considerable technical challenges for biochemical studies, research on primary neurons is a very powerful approach for elucidating growth factor physiology and signalling in the appropriate cellular and developmental context. These studies of newborn nodose neurons have demonstrated an essential role for NF- κ B signalling in CNTF-promoted neurite growth and revealed strikingly clear differences in the mechanism of NF- κ B activation mediating the effects of this cytokine and BDNF. Future progress on unravelling how BDNF and CNTF influence NF- κ B signalling in distinctive ways, and how this in turn has such marked effects on neurite growth in sensory and other neurons will be important for understanding the novel role for NF- κ B in regulating neuronal morphology during development.

Chapter 4

Abnormal sympathoadrenal development in *PHD3*^{-/-} mice

4.1 Introduction

In response to low oxygen tensions, organisms mount a wide-ranging adaptive response involving many cellular and systemic processes. Activation of hypoxia-inducible factor (HIF) plays a central role in this process, inducing transcriptional targets that enhance oxygen delivery, better adapt cells to hypoxia or modulate cell proliferation/ survival pathways . Hypoxia may, in different circumstances, either promote or protect cells from apoptosis, and HIF itself contributes to these processes both indirectly, through the defence of cellular energy supplies, or directly, via transcriptional changes in pro-apoptotic or pro-survival genes. However, to generate the anatomical and physiological integrity required for oxygen homeostasis in the intact organism, these adaptive responses to hypoxia must also be accurately interfaced with the developmental control of growth.

Though the nature of these connections remains poorly understood, it is of interest that the cellular oxygen sensor PHD3 (otherwise termed EGLN3 or HPH1), one of three Fe (II)-dependent dioxygenases now known to negatively regulate HIF by prolyl hydroxylation of HIF- α subunits (HIF-1 α and HIF-2 α), has been previously identified as a gene involved in developmental apoptosis of neurons [417, 449, 450]. Over 50 % of neurons produced during development die through apoptosis before adulthood [71] . This process is largely regulated by neurotrophic factors that are secreted in limited amounts by target tissues such that only those neurons making appropriate connections survive. During the investigation of these phenomena, PHD3 mRNA was identified as a neuronal transcript that is induced by withdrawal of NGF [417]. Further studies have demonstrated that ectopic expression of PHD3 in primary sympathetic neurons from the developing superior cervical ganglion and in the

adrenal medullary tumour cell line PC12, resulted in apoptosis even in the presence of saturating quantities of NGF [417, 449]. This action was not reproduced by a catalytically inactive PHD3 mutant [449], whereas hypoxia was able to suppress apoptosis in sympathetic neurons [451]. Knock-down of PHD3 by siRNA in PC12 cells prevented apoptosis even in the absence of NGF [417, 449]. Taken together, these observations in cultured cells indicate that oxygen sensitive catalytic activity of PHD3 has a role in the regulation of neuronal apoptosis, raising important questions about the extent of PHD3-dependent neuronal apoptosis *in vivo* and its role in the intact animal.

To better understand the physiological function(s) of the oxygen-sensitive prolyl hydroxylases that regulate HIF, I have investigated the neuronal phenotype of mice in which three PHD (Prolyl Hydroxylase Domain) genes have been inactivated. Although *PHD2*^{-/-} animals suffered embryonic lethality with placental and other developmental defects, *PHD1*^{-/-} and *PHD3*^{-/-} mice are viable as adults permitting more detailed analysis of the function of these molecules *in vivo*.

Therefore the developmental and physiological effects of inactivation of *PHD3*^{-/-} on neuronal apoptosis were investigated. I show that PHD3-dependent modulation of NGF-dependent survival is a lineage-specific property affecting sympatho-adrenal neurones. Inter-crossing with animals heterozygous for HIF-1 α or HIF-2 α inactivation implicated HIF-2 α , but not HIF-1 α , in this process. Effects of PHD3 appeared to extend beyond simple survival decisions. Neurones from *PHD3*^{-/-}, but not *PHD2*^{+/-} or *PHD1*^{-/-}, mice manifest increased neurite growth as well as enhanced survival, and *PHD3*^{-/-} mice manifest hyperplasia of sympatho-adrenal tissues including sympathetic ganglia, the carotid body and the adrenal medulla.

However, despite hyperplasia, the sympatho-adrenal system was dysfunctional in affected animals, with reduced innervation of target organs and dysregulated sympathetic responses including reduced iridial reflexes after exposure to dark. The findings demonstrate a key role for PHD3 in regulating the anatomical integrity of the sympatho-adrenal system, exemplifying how hypoxia and growth regulatory pathways may be interfaced for developmental control.

4.2 Expression of PHD3 in sympathoadrenal tissues

PHD enzymes have distinct patterns of expression [412] and are differentially regulated in different cell types [413]. As a first step towards elucidating a role for PHD3 in neuronal development, the expression of PHD3 was analysed using an antibody directed towards PHD3 in wild type mice. PHD3 was highly expressed in tissues of the sympathoadrenal lineage including the SCG (Fig. 28A), Carotid Body (Fig. 28D) and the adrenal medulla (Fig. 28E). PHD3 expression was low in other NGF dependent neuronal populations such as the dorsal root (DRG , Fig. 28B) and trigeminal ganglion neurons TG (Fig. 28C) suggesting a specific role for PHD3 in sympathoadrenal tissues.

4.3 PHD3 inactivation increases survival of SCG neurons in vitro

PHD3 expression in PC12 cells and primary neurons from the SCG leads to apoptotic cell death [417, 418, 449, 450] . To analyse the neuronal phenotype of *PHD3*^{-/-} mice in more detail, post-mitotic neurons from the SCG of newborn (P0) animals were cultured in the presence of a range of NGF concentrations. Viable neuronal counts were performed 3 hours after plating and again at 24 hours and % neuronal survival was calculated for each concentration of NGF. At non-saturating concentrations of NGF, the survival of neurons from *PHD3*^{-/-} mice was consistently enhanced compared to that of neurons from wild-type mice (Fig. 29A). Interestingly, loss of PHD3 did not confer a survival advantage at very low NGF concentrations, suggesting that although PHD3 promotes apoptosis of these neurones, it is not absolutely required for this process. In contrast with *PHD3*^{-/-} animals, there were no significant differences in survival between neurons from *PHD1*^{-/-} or *PHD2*^{+/-} and

wild-type mice (Figure 29B and 29C; note we were unable to use *PHD2*^{-/-} mice due to embryonic lethality between E12.5 and E14.5). These data provide strong evidence that inactivation of PHD3, but not PHD1 or PHD2, leads to increased survival of sympathetic neurons.

4.4 Specific survival effect of PHD3^{-/-} in SCG neurons

NGF signalling through TrkA regulates the survival of many populations of neurons in the PNS and CNS. Expression of TrkA is required for retrograde transport of target-derived NGF [452-455] and deletion of TrkA or NGF in mice, causes extensive loss of sensory neurons of the TG and DRG [80, 81]. Since SCG, TG and DRG neurons express TrkA during development [179, 216] I investigated whether PHD3-modulated apoptosis also takes place in other NGF responsive neuronal populations. Neurons from the SCG, DRG and TG of newborn (P0) *PHD3*^{-/-} mice were cultured in the presence of a range of NGF concentrations. Viable neuronal counts were performed 3 hours after plating and again at 24 hours and the percentage neuronal survival was calculated at each concentration of NGF. In contrast with sympathetic neurones, PHD3-deficient sensory neurons from the DRG and TG showed no difference in survival at any NGF concentration tested (Figure 30B,C). These findings indicate that PHD3-dependent neuronal survival is not a general property of NGF-sensitive neurons but a specific property of sympathetic neurons.

4.5 Induction of PHD3 mRNA following withdrawal of NGF

Knockdown of PHD3 in vitro prevents apoptosis in PC12 cells even in the absence of NGF [418]. Interestingly, PHD3 mRNA is strongly induced after NGF withdrawal [417]. It was therefore considered whether a differential up regulation of PHD3 might underlie the neuronal specificity of PHD3-dependent survival. Dissociated SCG, DRG and TG neurons from wild-type P0 mouse pups were cultured overnight in 10 ng/ml NGF. Neurons were then washed thoroughly with defined culture medium and grown either in the presence or absence of NGF for 10 hours (timepoint at which PHD3 mRNA induction is maximal in the SCG; [418]) before harvesting the cells for RNA. Using quantitative RT-PCR, we found that withdrawal of NGF in explanted neurons significantly increased PHD3 mRNA levels in the SCG (Fig. 31), but not in the DRG (Fig. 32A) or TG (Fig. 32B) suggesting that PHD3-dependent neuronal survival might be the result of cell-specific responsiveness of PHD3 mRNA to NGF withdrawal.

4.6 Reversal of survival effect in PHD3^{-/-};HIF2^{+/-} mice

HIF activity is negatively regulated by modifications induced by the PHD enzymes on the HIF- α subunit (reviewed Fandrey et al. 2006). Recent investigation into the relative contribution of the three PHD enzymes to proline hydroxylation of HIF-1 and HIF-2 α subunits has revealed a relative preference for PHD3 towards HIF-2 α [413]. In order to investigate the downstream signalling mechanism which leads to increased survival of SCG neurons in PHD3^{-/-} mice, PHD3^{-/-} mice were crossed with HIF-1^{+/-} and HIF-2^{+/-} mice. Heterozygous HIF mice were used due to embryonic lethality in the corresponding homozygous knockout mouse. SCG from PHD3^{-/-}, PHD3^{-/-};HIF-

1^{+/-} and PHD3^{-/-};HIF-2^{+/-} mice were cultured in the presence of a range of NGF concentrations. Viable neuronal counts were performed 3 hours after plating and again at 24 hours and percentage neuronal survival was calculated at each concentration of NGF. In accordance with published data which describes a preference of PHD3 for HIF-2 α , inactivation of one allele of HIF-2 α significantly reduced survival of PHD3^{-/-} SCG neurons (Fig. 33B). In contrast, inactivation of one allele of HIF-1 α had no effect on the survival of PHD3^{-/-} SCG neurons at any concentration of NGF tested (Fig. 33A).

4.7 PHD3 inactivation increases NT-3 dependent survival of SCG neurons

NGF promotes neuronal survival by binding to and activating the receptor tyrosine kinase TrkA. Because neurotrophin-3 (NT-3) is also capable of promoting the survival of neonatal SCG neurons in culture by a TrkA-dependent mechanism, I investigated whether deletion of PHD3 affects the survival response of SCG neurons to this neurotrophin. Again, SCG from PHD3 mice were cultured in the presence of a range of NT-3 concentrations and percentage neuronal survival was measured at each concentration. As with NGF, PHD3-deficient SCG neurons showed increased survival in response to NT-3 compared with neurons from wild type littermates (Fig. 34).

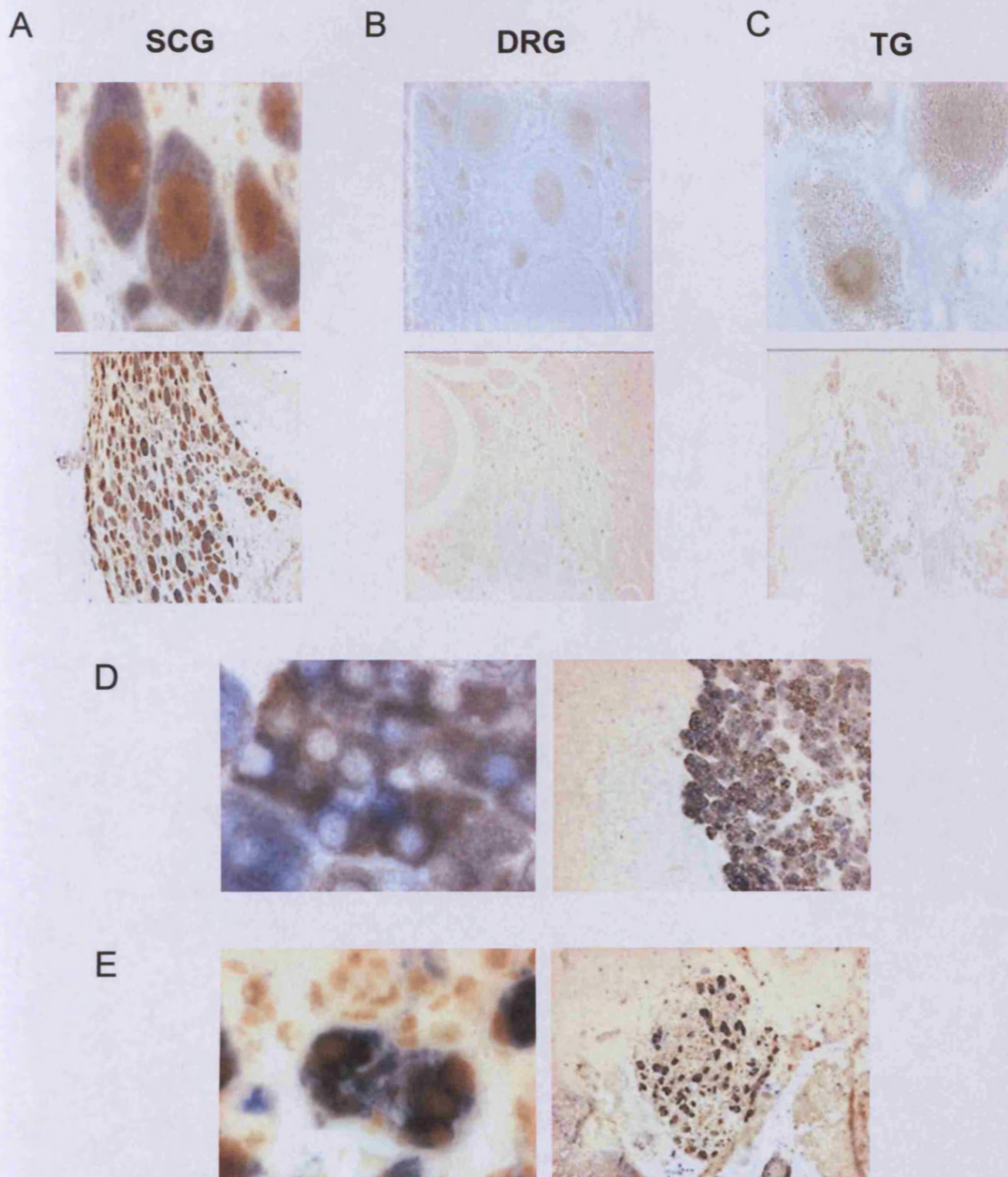


Figure 28 **PHD3 expression.** Immunohistochemistry showing strong staining of PHD3 in the SCG (A), adrenal medulla (D) and Carotid body (E) with relatively weak staining in sensory neurons of the DRG (B) and TG (C).

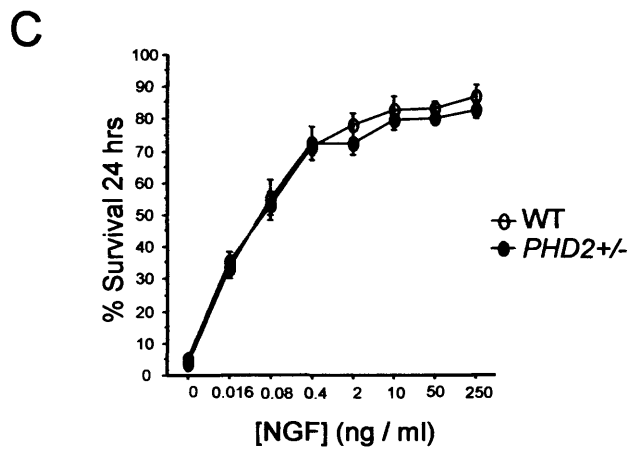
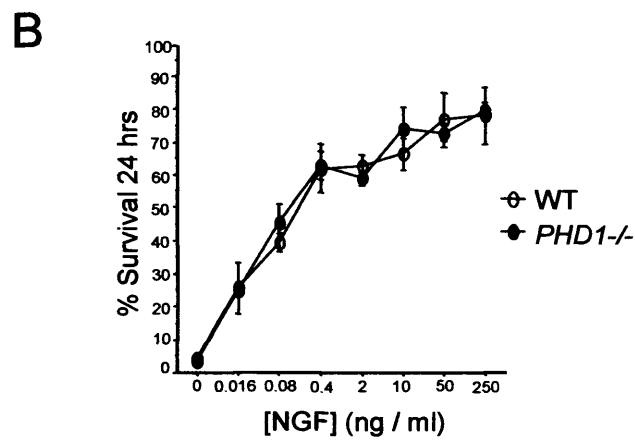
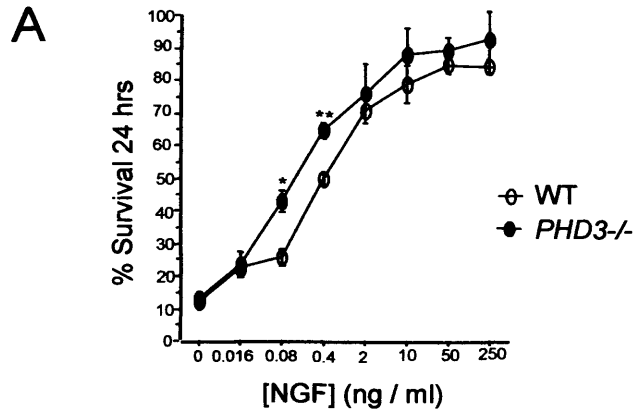


Figure 29 |Increased survival of SCG neurons from *PHD3*^{-/-} mice. P0 SCG neurons were incubated for 24 hours in the presence of a range of NGF concentrations. The percentage neuronal survival at each concentration was estimated and a dose-response curve constructed. (A) Dose response curve showing increased survival in SCG neurons from *PHD3*^{-/-} mice. No difference in survival of SCG neurons cultured from *PHD1*^{-/-} (B) or *PHD2*^{+/-} (C) mice. Statistical comparisons are with respect to wild-type controls. Data from 3 independent repeats shown (* $p < 0.05$, ** $p < 0.01$).

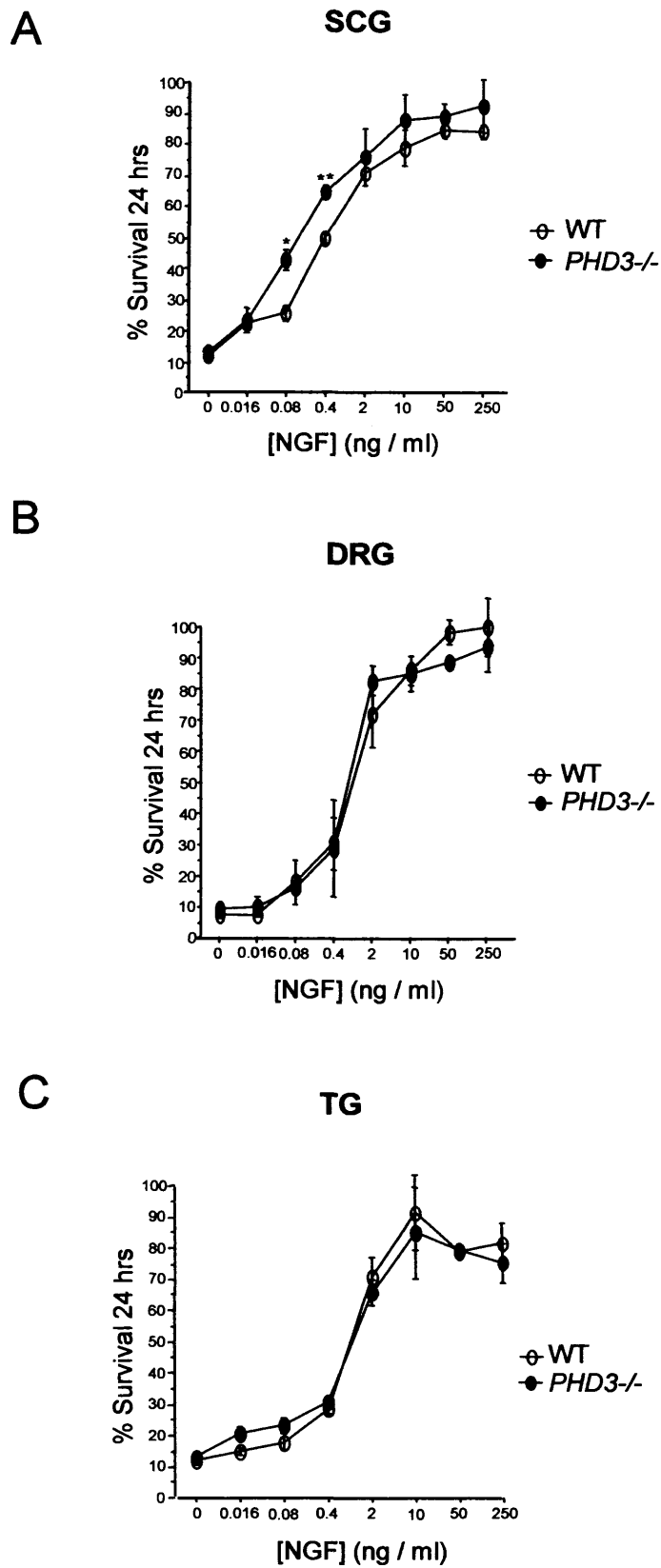


Figure 30 | **Specificity of PHD3^{-/-} effect.** PHD3 inactivation increases survival of SCG neurons (A) but has no effect on sensory neurons from the DRG (B) or TG (C).

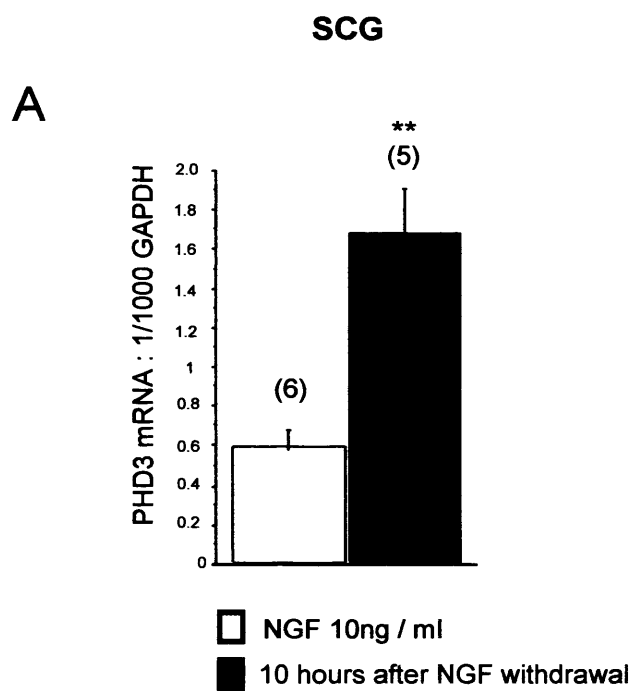


Figure 31 | **PHD3 induction.** Neonatal SCG neurons were incubated overnight with NGF (10ng/ml) after which NGF was withdrawn and total RNA isolated. (A) Induction of PHD3 mRNA expression 10 hours after NGF withdrawal from SCG neurons. Statistical comparisons are with respect to NGF control (** $p < 0.01$).

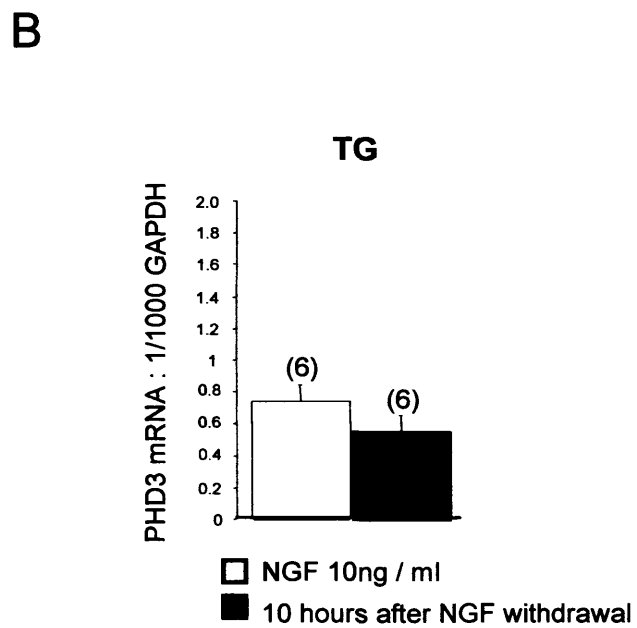
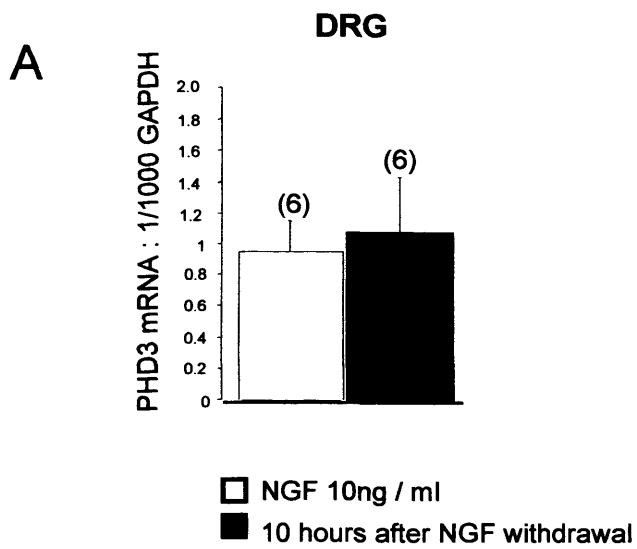
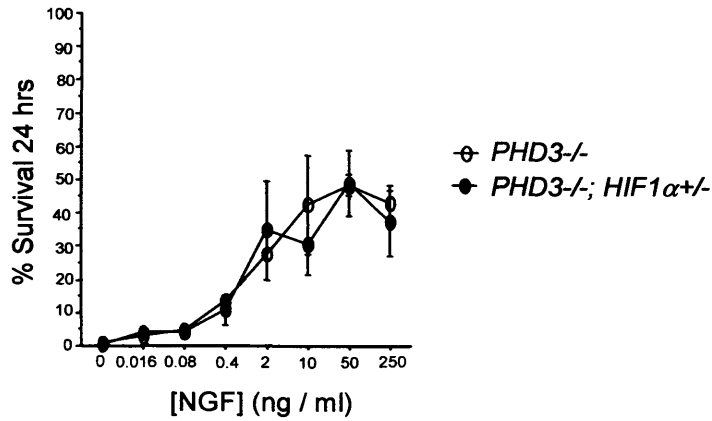


Figure 32 | Specificity of PHD3 induction. Neonatal DRG and TG neurons were incubated overnight with NGF (10ng/ml) after which NGF was withdrawn and total RNA isolated. No Induction of PHD3 mRNA expression 10 hours after NGF withdrawal from DRG (A) or TG (B) neurons.

A



B

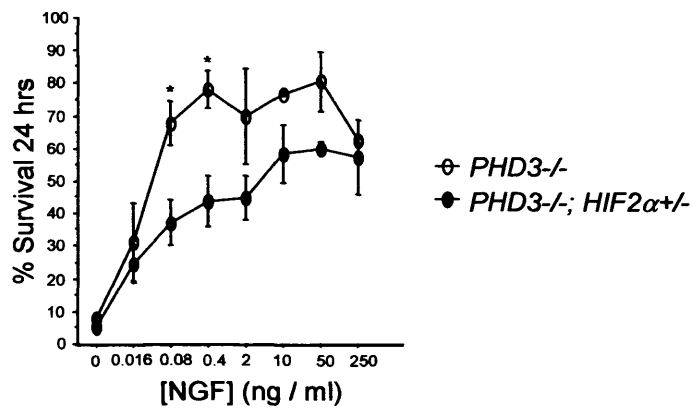


Figure 33 | **HIF dependence of the PHD3 survival effect.** NGF-dose response curves from neonatal SCG neurons showing: (A) no difference in survival of neurons derived from *PHD3*^{-/-}; *HIF-1*^{+/-} versus *PHD3*^{-/-} mice and (B) reduced survival of neurons derived from *PHD3*^{-/-}; *HIF-2*^{+/-} versus *PHD3*^{-/-} mice. Statistical comparisons are with respect to *PHD3*^{-/-} (* p<0.05).

A

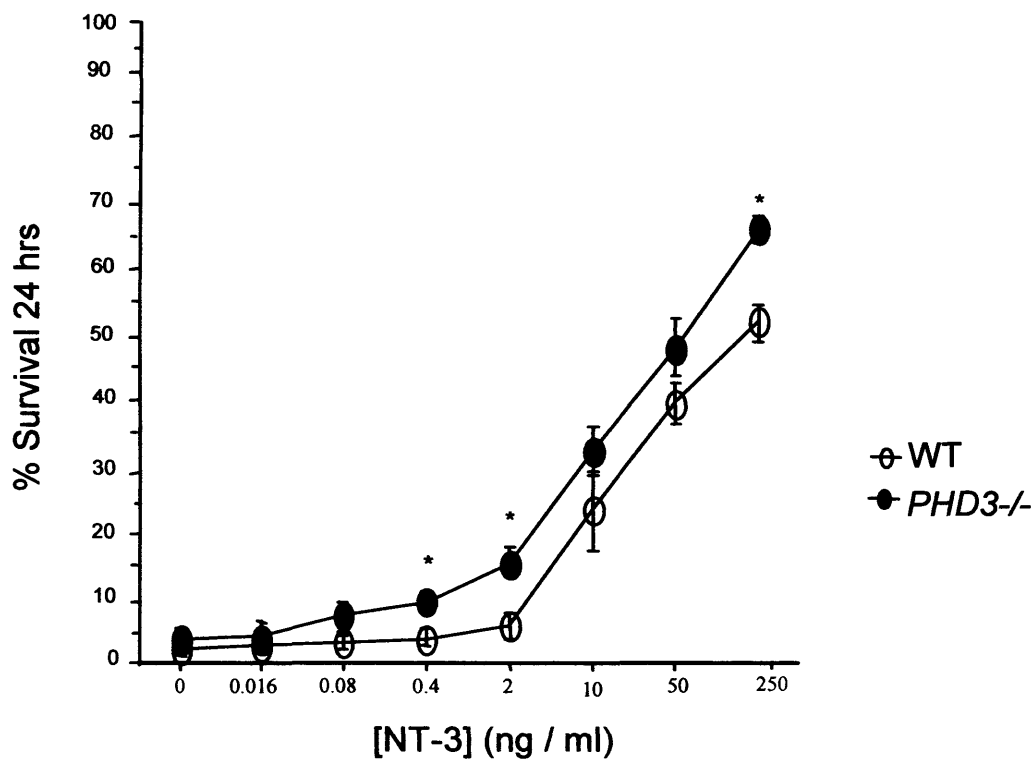
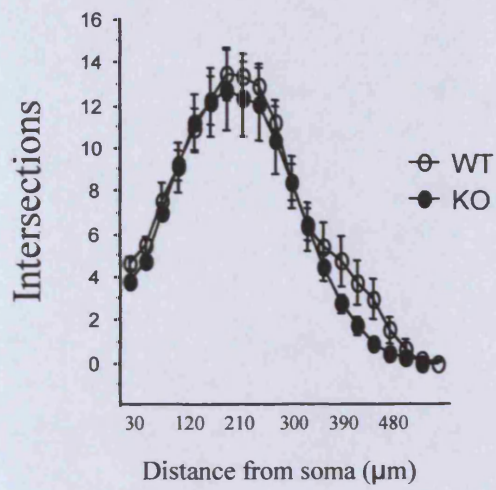


Figure 34 | Increased NT-3-dependent survival of SCG neurons from *PHD3*^{-/-} mice. P0 SCG neurons were incubated for 24 hours in the presence of a range of NT-3 concentrations. The percentage neuronal survival at each concentration was estimated and a dose-response curve constructed. (A) Dose response curve showing increased survival in SCG neurons from *PHD3*^{-/-} mice supported by NT-3. Data from 3 independent repeats shown (* p<0.05).

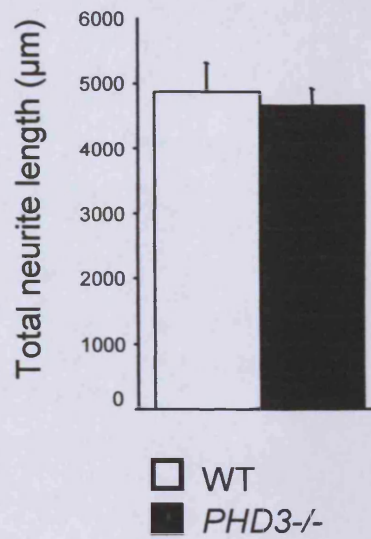
4.8 Enhanced NGF-promoted neurite growth from PHD3-deficient sympathetic neurons in vitro

In addition to supporting the survival of developing sympathetic neurons, NGF also promotes the growth of neurites from these neurons in culture. For this reason I investigated whether deletion of PHD3 affects neurite arbor size and complexity. Low density cultures of SCG neurons from P0 *PHD3*^{-/-} and wild type mice were grown with different concentrations of NGF and neurite arbor size and complexity were quantified using Sholl analysis 24 hours after plating. At subsaturating concentrations of NGF (Figs. 36 and 37), but not at saturating levels (Fig. 35), the neurite arbors of PHD3-deficient neurons were significantly longer than those of wild type neurons. Sholl analysis, which provides a spatial representation of neurite branching with distance from the cell body, revealed that the neurite arbors of PHD3-deficient neurons were larger and more branched than those of wild type mice in the presence of subsaturating levels of NGF. The typical appearance of the neurite arbors of PHD3-deficient and wild type SCG neurons grown at each concentration of NGF used are illustrated in Figures 35B-37B. These findings suggest that PHD3-deficient SCG neurons are more sensitive to the neurite growth-promoting, and survival-promoting effects of NGF.

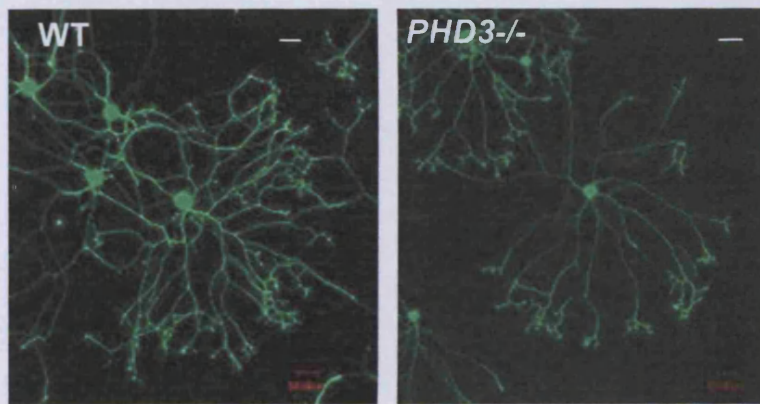
A



B



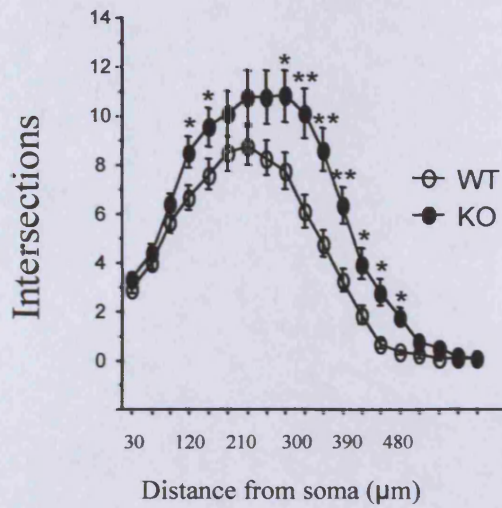
C



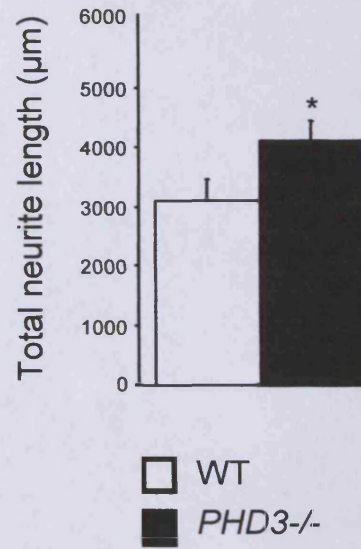
[NGF] 10 ng / ml

Figure 35 | PHD3 inactivation and neurite outgrowth at saturating NGF concentration. P0 SCG neurons from wild-type and *PHD3*^{-/-} mice were incubated for 24 hours in NGF (10ng/ml) after which neurite growth was analysed. (A) Sholl analysis and (B) neurite length analysis revealed no significant differences in process outgrowth between wild-type and *PHD3*^{-/-} SCG. (C) Photomicrographs showing the typical appearances of wild-type and *PHD3*^{-/-} neurons cultured with NGF (10 ng/ml)

A



B



C

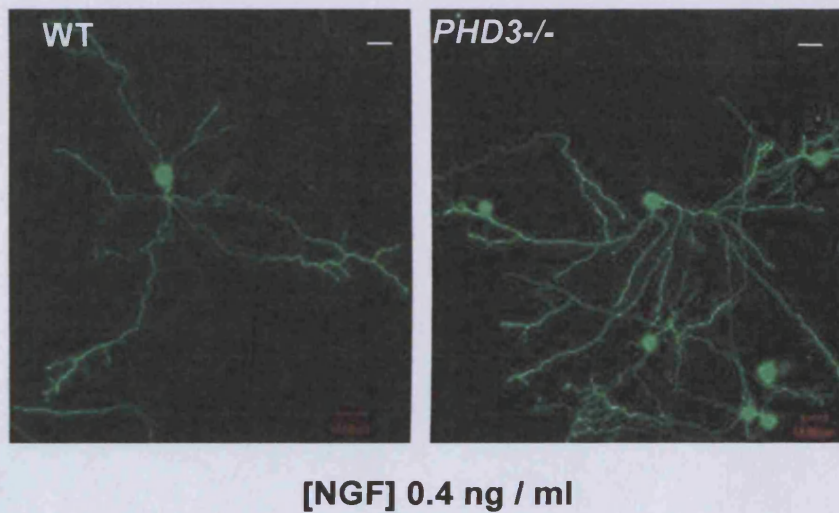
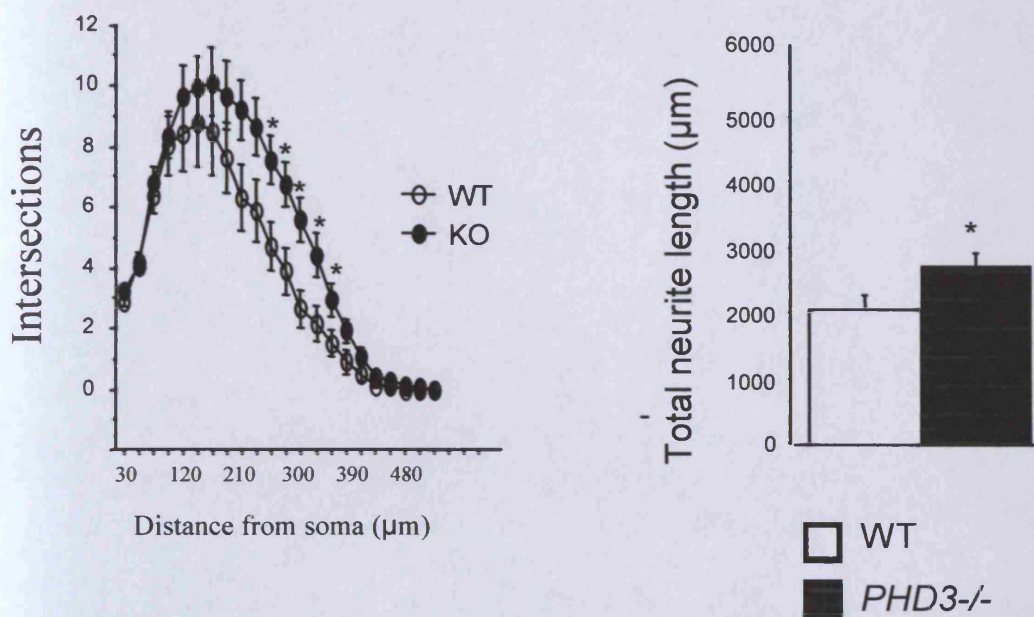
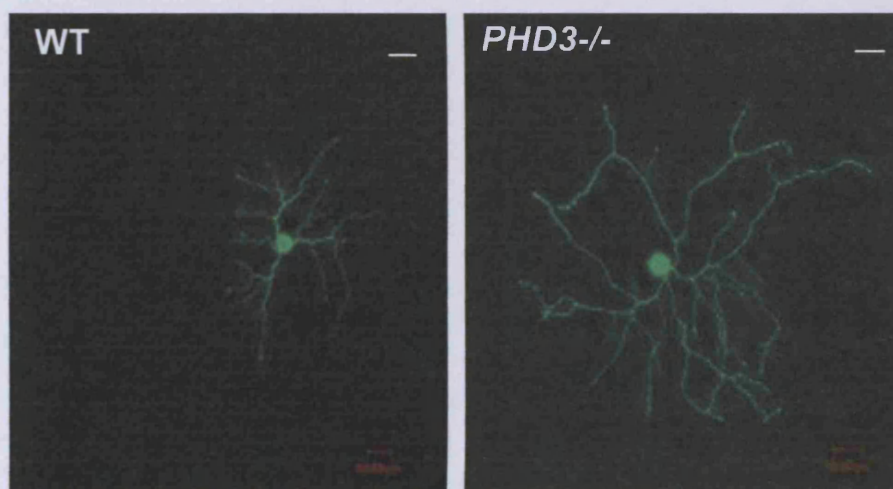


Figure 36 | PHD3 inactivation and neurite outgrowth at a sub-saturating NGF concentration (1). P0 SCG neurons from wild-type and *PHD3*^{-/-} mice were incubated for 24 hours in NGF (0.4ng/ml) and caspase inhibitors after which neurite growth was analysed. (A) Sholl analysis and (B) neurite length analysis revealed a significant increase in process outgrowth in *PHD3*^{-/-} SCG. (C) Photomicrographs showing the typical appearances of wild-type and *PHD3*^{-/-} neurons cultured with NGF (10 ng/ml). Statistical comparisons are with respect to wild-type controls and between 40-70 neurons were analysed per genotype. (* $p < 0.05$, ** $p < 0.01$).

B



C



[NGF] 0.08 ng / ml

Figure 37 | **PHD3 inactivation and neurite outgrowth at a sub-saturating NGF concentration (2).** P0 SCG neurons from wild-type and *PHD3*^{-/-} mice were incubated for 24 hours in NGF (0.08ng/ml) and caspase inhibitors after which neurite growth was analysed. (A) Sholl analysis and (B) neurite length analysis revealed a significant increase in process outgrowth in *PHD3*^{-/-} SCG. (C) Photomicrographs showing the typical appearances of wild-type and *PHD3*^{-/-} neurons cultured with NGF (10 ng/ml). Statistical comparisons are with respect to wild-type controls and between 40-70 neurons were analysed per genotype. (* $p < 0.05$, ** $p < 0.01$).

4.9 PHD3-deficient mice have increased numbers of SCG neurons

To ascertain the developmental and physiological relevance of the *in vitro* observations, the total number of neurons in the SCG of wild type and *PHD3*^{-/-} mice were compared. The neuronal complement of the SCG of newborn animals was estimated by counting the number of neurons in trypsin-dissociated cell suspensions obtained from carefully dissected ganglia. Neurons were recognized and distinguished from non-neuronal cells by their characteristic large, phase-bright, spherical cell bodies under phase contrast optics. SCG dissected from *PHD3*^{-/-} newborn mice appeared larger than those of wild type littermates (Fig. 38A) and contained significantly more neurons (Fig. 38B). Likewise, stereological measurements carried out on serially sectioned SCG in 3 to 6 month old mice revealed that the SCG was larger and contained significantly more neurons in *PHD3*^{-/-} mice compared with age-matched wild type animals (Fig. 38C and D). As expected, the number of the neurons in the SCG of wild type adults was lower than that in newborns as a result of ongoing programmed cell death in the immediate postnatal period. However, the number of neurons in the SCG of *PHD3*^{-/-} remained substantially unchanged between birth and adulthood, suggesting that programmed cell death during at least the postnatal period was largely curtailed in these mice. In contrast to the effect of *PHD3* deletion on SCG neuron number, there were no significant differences between the numbers of neurons in the SCG of either *PHD1*^{-/-} (Fig. 38E) or *PHD2*^{+/-} (Fig. 38F) neonates compared with wild type littermates. Interestingly, in keeping with *in vitro* survival data (Fig. 29), there was a significant reduction in total viable neurons in neonatal *PHD3*^{-/-};*HIF-2α*^{+/-} compared to *PHD3*^{-/-} mice (Fig. 39A). This reduction was not observed in total counts from *PHD3*^{-/-};*HIF-1α*^{+/-} SCG (Fig. 39B). Taken together with our *in vitro* survival data, these *in vivo* observations suggest that the selective

increase in SCG neurons in *PHD3*^{-/-} mice results from reduced cell loss during the phase of programmed cell death in the perinatal period as a consequence of the enhanced sensitivity of PHD3-deficient neurons to NGF.

4.10 PHD3-deficient mice have increased numbers of cells in the adrenal medulla and carotid body

The discovery that *PHD3*^{-/-} mice have significantly more sympathetic neurons than wild type mice prompted an examination cell number elsewhere in the sympathoadrenal system. Stereological analysis of adult mice (3 - 6 months) revealed significantly more TH-positive cells in both the adrenal medulla and the carotid body (Figure 40). These data suggest that PHD3 specifically regulates the development of the sympatho-adrenal axis.

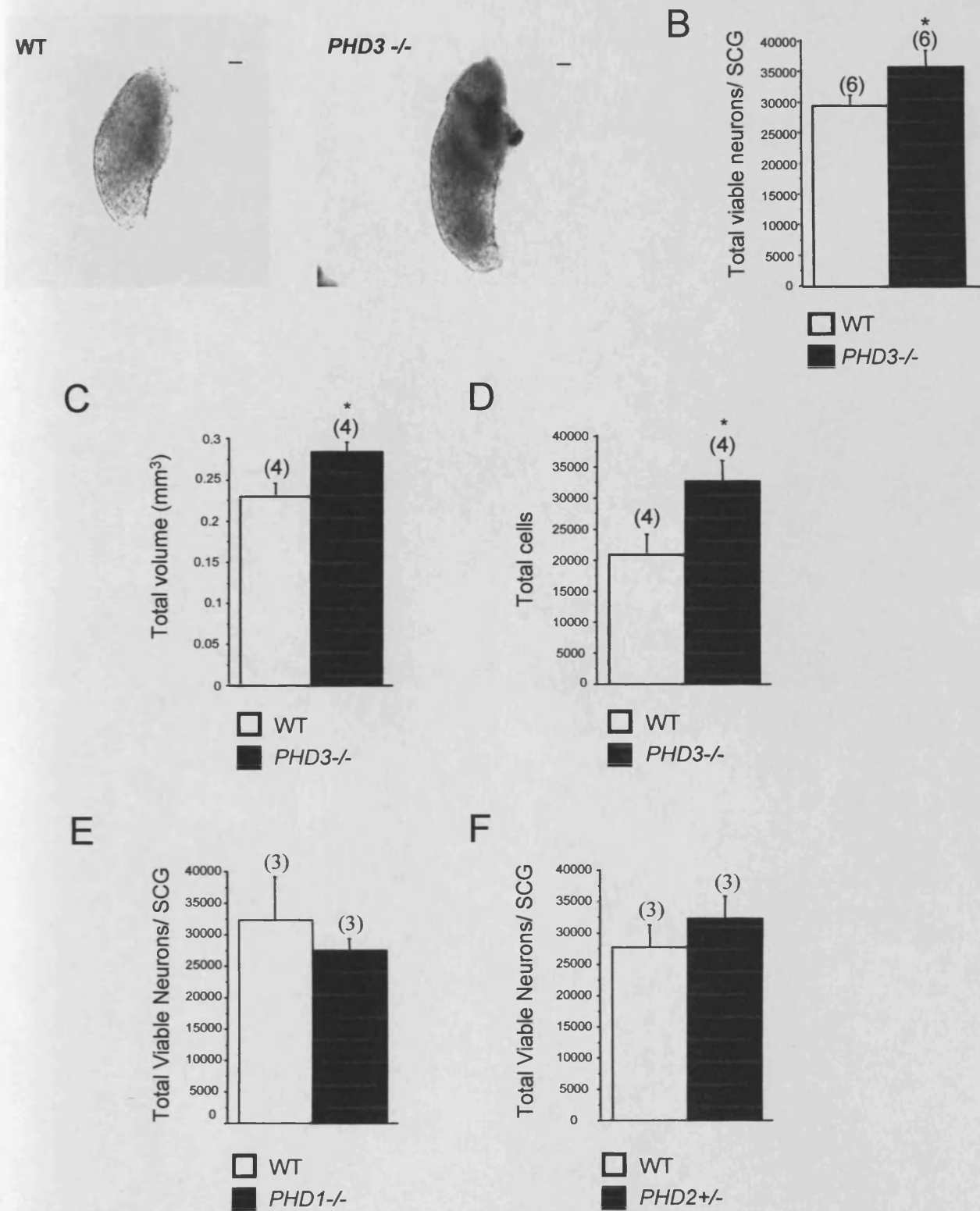
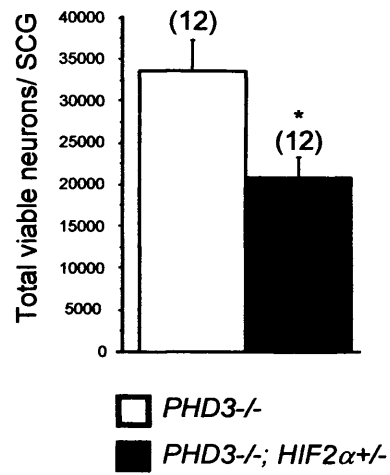


Figure 38 | Effect of genetic inactivation of PHD3 on the anatomy of the SCG. (A) Bright field images of wild-type and *PHD3*^{-/-} neonatal SCG; black bar represents 100 μm. (B) Neuronal complement of neonatal SCGs in wild-type and *PHD3*^{-/-} mice; counts are of viable trypsin-dissociated neurons. (C,D) Stereological analysis of TH-positive neurons showing increased volume and cell numbers in the SCG from adult *PHD3*^{-/-} mice. (E,F) No difference in total number of neurons in the SCG of *PHD1*^{-/-} or *PHD2*^{+/-} mice. Statistical comparisons are with respect to wild-type controls and values shown are averages from (n) separate mice as indicated in the parentheses. (* P < 0.05)

A



B

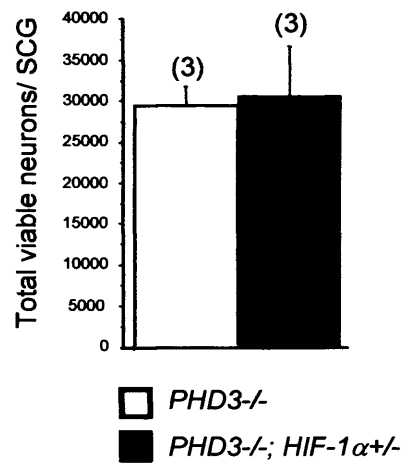


Figure 39 | **HIF2 mediates the effect of PHD3 inactivation on SCG anatomy.** Comparison of neuronal complement of neonatal SCGs in mice of the indicated genotypes. HIF-2 α heterozygosity (A), but not HIF-1 α heterozygosity (B), is associated with reduced neuronal complement. Statistical comparisons are with respect to wild-type controls and values shown are averages from (n) separate mice as indicated in the parentheses. (* $P < 0.05$)

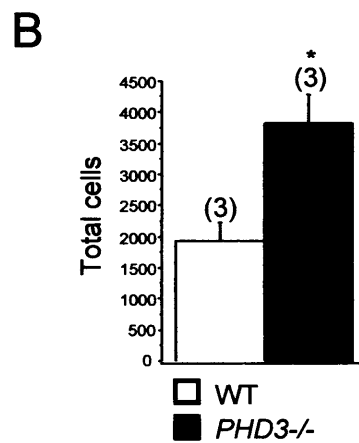
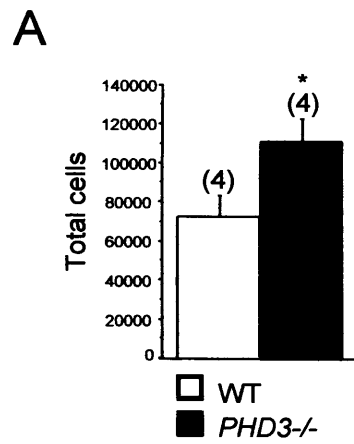


Figure 40 |Effect of genetic inactivation of PHD3 on the anatomy of other sympatho-adrenal tissues. Adult stereological analysis displaying increased number of cells in the adrenal medulla (A) and carotid body (B). Statistical comparisons are with respect to wild-type controls and values shown are averages from (n) separate mice as indicated in the parentheses. (* $P < 0.05$)

4.11 Sympathetic innervation of target tissues

Given that inactivation of PHD3 *in vivo* results in increased numbers of SCG neurons surviving to adulthood and that NGF is more effective in promoting neurite growth from cultured PHD3-deficient SCG neurons, I asked whether sympathetic innervation density is altered in PHD3^{-/-} mice. The SCG innervates several anatomically discrete structures, including the iris, submandibular gland and pineal gland, whose innervation density can be relatively easily estimated by quantifying the area occupied by tyrosine hydroxylase (TH)-positive nerve fibres in tissue sections. Surprisingly, this analysis revealed significantly less TH-positive fibres in the iris (Fig 41), pineal gland (42) and submandibular gland (43) of *PHD3*^{-/-} mice compared with wild type animals.

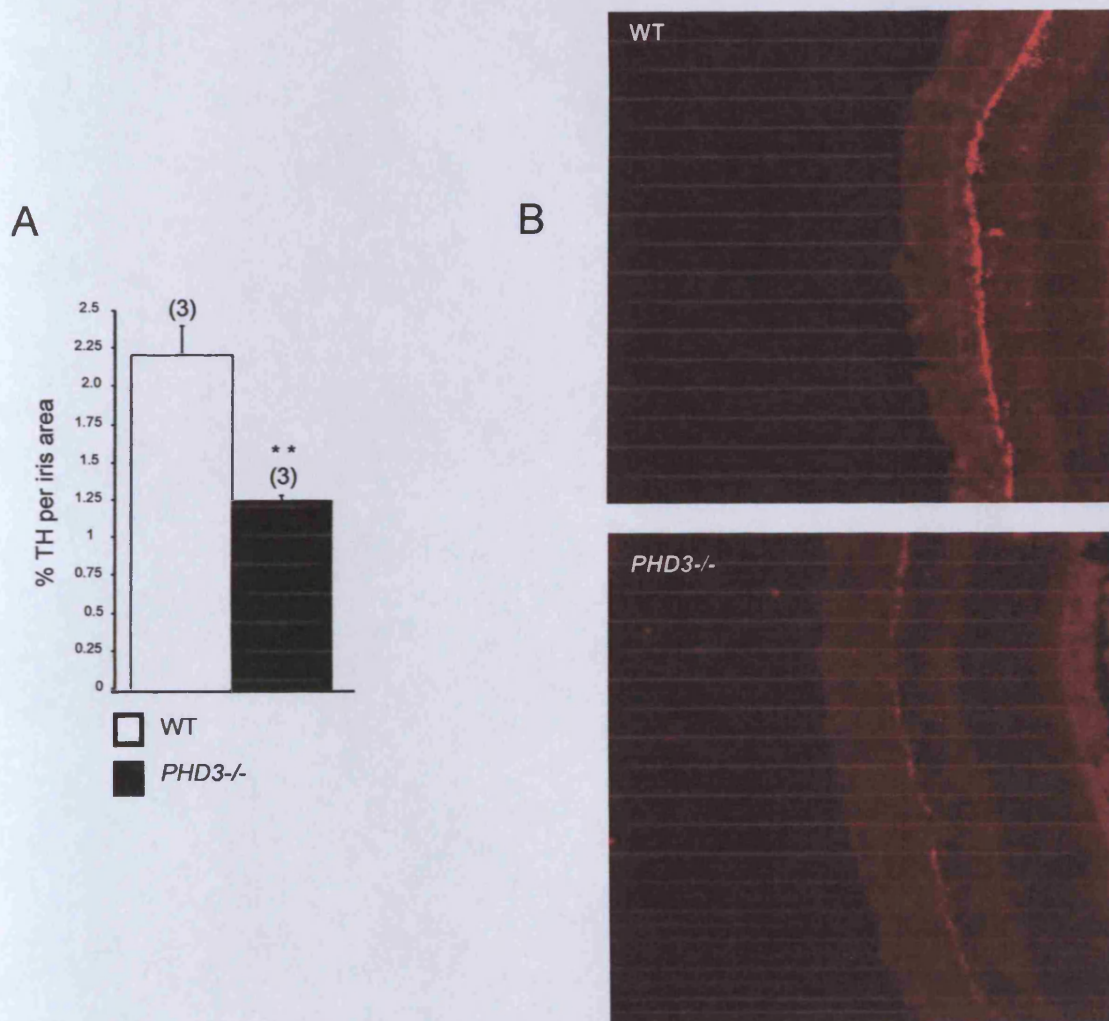
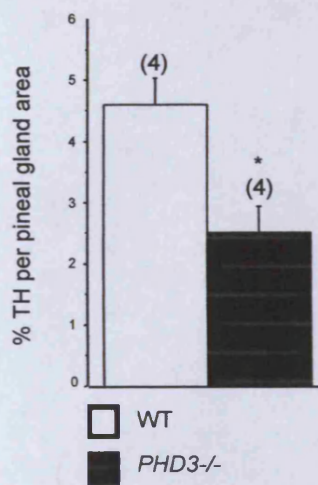


Figure 41 | Decreased sympathetic innervation of the iris in PHD3^{-/-} mice. (A) Comparison of sympathetic innervation density of the iris from adult wild type and PHD3^{-/-} mice. (B) Representative images showing immunohistochemical detection of TH in the iris of wild type and PHD3^{-/-} mice. Statistical comparisons are with respect to wild-type controls and values shown are averages from (n) separate mice as indicated in the parentheses. (** P < 0.01)

A



B

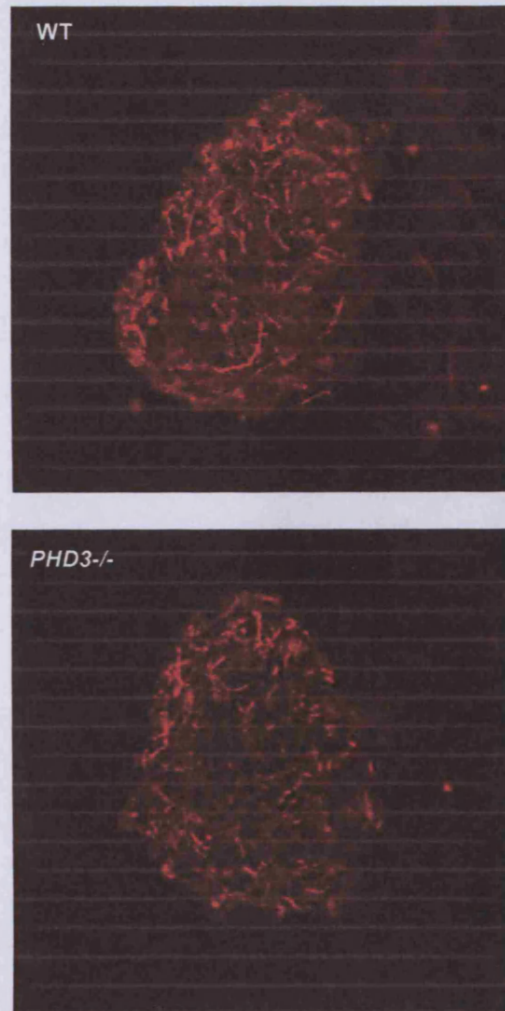
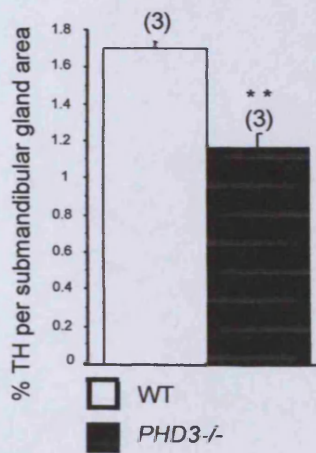


Figure 42 | **Decreased sympathetic innervation of the pineal gland in PHD3-/- mice.** (A) Comparison of sympathetic innervation density of the pineal gland from adult wild type and PHD3-/- mice. (B) Representative images showing immunohistochemical detection of TH in the iris of wild type and PHD3-/- mice. Statistical comparisons are with respect to wild-type controls and values shown are averages from (n) separate mice as indicated in the parentheses. (* $P < 0.05$)

A



B

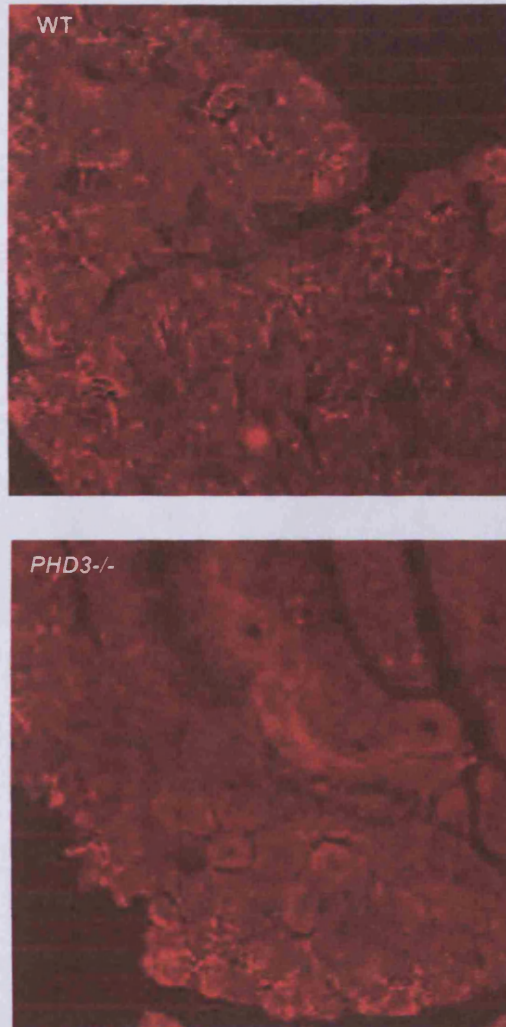


Figure 43 | **Decreased sympathetic innervation of the submandibular gland in PHD3-/- mice.** (A) Comparison of sympathetic innervation density of the iris from adult wild type and PHD3-/- mice. (B) Representative images showing immunohistochemical detection of TH in the iris of wild type and PHD3-/- mice. Statistical comparisons are with respect to wild-type controls and values shown are averages from (n) separate mice as indicated in the parentheses. (** P < 0.01)

4.12 Physiological effects on the sympathetic nervous system

We next sought to assess the integrity of a physiological response that is dependent on the sympathetic nervous system. Because of the reduced sympathetic innervation of the iris in *PHD3*^{-/-} mice (Figure 44), we tested light-to-dark pupillary responses.

Postganglionic oculosympathetic fibers from the SCG travel with the long ciliary nerves to innervate the dilator pupillae muscle. Activation of the sympathetic nervous system leads to dilation of the pupil following relaxation of the dilator pupillae. While no differences in pupil diameter were seen under normal lighting conditions (150 lux; Figure 44A), pupil diameter was significantly decreased in the dark-adapted eye from *PHD3*^{-/-} mice (0 lux; Figure 44B). This implies decreased tone in the sympathetically innervated dilator pupillae muscle fibres of *PHD3*^{-/-} mice.

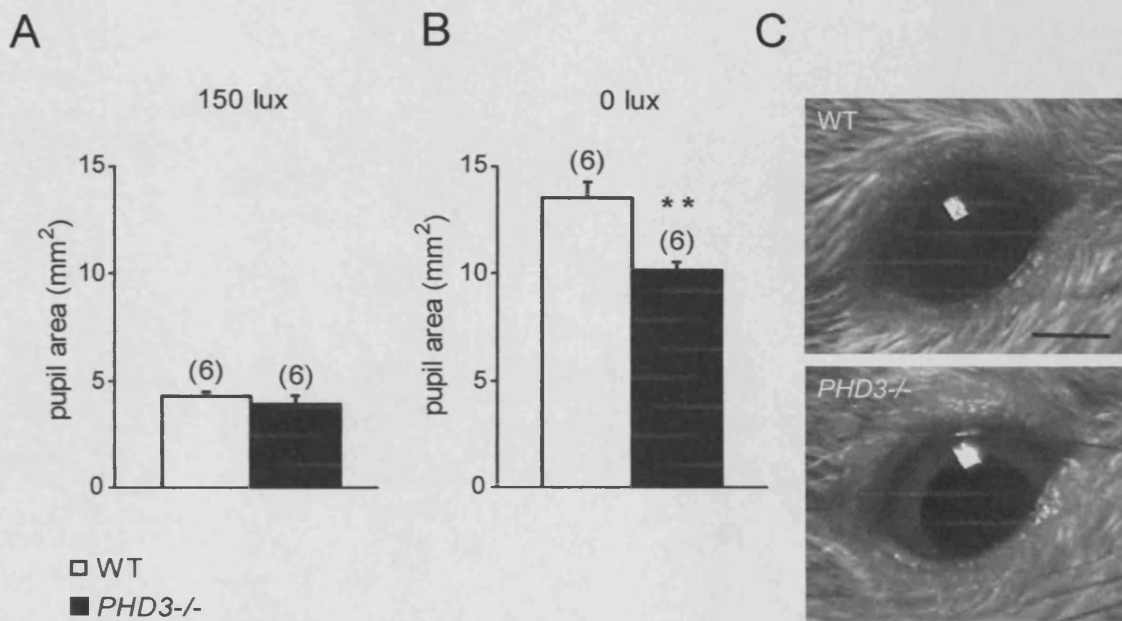


Figure 44 | **Physiological defect in an SCG target of *PHD3*^{-/-} mice.** Measurements of total pupil area in normal light, 150 lux (A) and in darkness, 0 lux (B). Representative images showing dark adapted eyes from wild-type and *PHD3*^{-/-} mice. Statistical comparisons are with respect to wild-type controls and values shown are averages from (n) separate mice as indicated in the parentheses. (** $P < 0.01$)

4.13 Discussion

My findings show that the HIF prolyl hydroxylase PHD3 has an important role in regulating the development of the sympatho-adrenal system and that its ablation has substantial adverse physiological consequences that extend into adult life.

Significantly more neurons were observed in the SCG of newborn PHD3^{-/-} mice compared with wild type littermates, and this elevated number of SCG neurons is maintained to adulthood. The apparent failure of the neuronal complement of the SCG to decrease in PHD3^{-/-} postnatally when naturally occurring programmed cell death ordinarily matches the number of sympathetic neurons to the requirements of their targets suggests that the elevated number of neurons in the SCG of PHD3⁻ deficient mice is due to reduced cell death. It is well established that survival of SCG neurons during this period of development is critically dependent on the supply of NGF from their targets. The demonstration that the NGF survival dose response of PHD3-deficient SCG neurons in culture is shifted to lower NGF concentrations provides a plausible explanation for the enhanced survival of SCG neurons in PHD3⁻ mice. The supply of target-derived NGF is able to support the survival of more of the innervating neurons in PHD3⁻ mice because these neurons require less NGF to survive. Interestingly, the effect of PHD3 deletion on NGF responsiveness is restricted to neurons of the sympathetic lineage in the peripheral nervous system as neural crest-derived, NGF-dependent sensory neurons from PHD3⁻ mice responded normally to NGF *in vitro*.

As well as enhancing the sensitivity of SCG neurons to the survival-promoting effects of NGF, deletion of PHD3 also makes these neurons more responsive to the neurite growth-promoting effects of NGF in culture. Because target-derived NGF is

not only required for sympathetic neuron survival during development *in vivo* but is also responsible for the terminal growth and branching of sympathetic axons in their targets, I expected to find increased sympathetic innervation density in PHD3^{-/-} mice. Surprisingly, the opposite was observed in several SCG target tissues in these animals. One possible explanation for this apparent paradox is that the increased number of sympathetic neurons innervating target tissues results in elevated uptake and removal of NGF from these tissues by retrograde axonal transport, resulting in lower ambient levels of NGF in the targets. Whereas retrograde transport of NGF in signaling endosomes to the cell bodies of sympathetic neurons is required for survival, the extent of axonal growth and branching in target tissues is governed by the ambient level of NGF in these tissues. Mice overexpressing NGF also have increased survival of sympathetic neurons with increased process outgrowth but as in PHD3^{-/-} mice described above, display significant decreases in target innervation [277]. The surprising decrease in sympathetic innervation was substantiated by the observation of reduced pupillary dilation in dark-adapted mice which is dependent on sympathetic tone. This result also demonstrates how slight effects on neuronal survival during development can have profound anatomical and physiological outcomes in the adult.

In conclusion, our findings reveal an important and unsuspected role for PHD3 in the developing sympatho-adrenal system. It is an intriguing possibility that this connection between hypoxia pathways and the developing sympatho-adrenal system might be a means by which changes in oxygen tension could influence key aspects of anatomical and physiological maturation of this system. Whether this provides a paradigm for environmental influences affecting development will be of interest in the future.

Chapter 5

**Neural activity regulates survival during a postnatal window in the
development of sensory neurons**

5.1 Introduction

During the phase of naturally occurring cell death, developing neurons are reliant on target-derived neurotrophic factors. Neurons become dependent on neurotrophic factors around the time when their developing axons begin to innervate their target tissues [72]. The duration of neurotrophin independence and axonal growth rate are proportional to the distance between the developing neuron and its target, suggesting that there is an intrinsic clock that switches neurons from neurotrophin independence to dependence at the right time [72]. However, during the first few weeks of postnatal life, the expression of TrkA and TrkB on dorsal root and nodose ganglia, respectively, decreases. There is a gradual decline in TrkA expression in DRG neurons from over 80% of cells expressing TrkA at E15 to less than 50% by P21 [456]. More strikingly, only 10-20% of neonatal nodose neurons express TrkB and there is no detectable TrkB expression in adult nodose neurons [457]. Although there is some controversy surrounding the expression or lack of expression of TrkB in adult nodose neurons, there is no evidence to suggest that BDNF signalling through TrkB promotes survival in the adult.

It has been widely reported that neural activity is an important regulator of neuronal survival both *in vivo* [259, 260, 361, 458] and *in vitro* [253, 255-257]. Neural activity has been shown to increase the survival of populations of CNS and PNS neurons, which raises the possibility that a secondary mechanism such as neural activity may serve as a synergistic or alternative survival cue (Mennerick and Zorumski 2000) during or after the period of neurotrophin-dependent survival. The calcium set-point hypothesis has been proposed to explain the relationship between neurotrophin-dependent survival and activity dependent survival [262, 459]. Low intracellular free

calcium concentration $[Ca^{2+}]_i$ is associated with neurotrophic factor dependence, moderate $[Ca^{2+}]_i$ is associated with neurotrophin independence and high $[Ca^{2+}]_i$ is associated with toxicity. It has been suggested that trophic factor dependence is inversely related to $[Ca^{2+}]_i$ which correlates with the observation that $[Ca^{2+}]_i$ increases with age [264]. Most studies, however, have used peripheral neurons artificially aged in culture to examine the effects of neural activity on $[Ca^{2+}]_i$ and neurotrophin independence.

In this section I will present the results of experiments that explore the switch from neurotrophin-dependence to independence, using neurons isolated from mice at various embryonic and postnatal stages. These results show that the timing of the switch differs between neuronal populations and suggest that this switch may be regulated by the onset of neuronal activity.

5.2 Onset of postnatal neurotrophin- independence differs between neuronal populations

The survival of embryonic and neonatal neurons from the nodose, DRG and SCG is, like many other neural populations, dependent on neurotrophic factors. In contrast, adult neurons from the same populations survive in the absence of neurotrophic support *in vitro*. Since embryonic timing of neurotrophin dependence/independence varies between neuronal populations [72] I investigated the timing of postnatal neurotrophin-independence in several populations of neurons *in vitro*. Dissociated cultures were set up from nodose, DRG and SCG over a range of ages from embryonic day 16 (E16) to postnatal day 10 (P10) and percent survival in the absence of neurotrophic support was estimated. The typical percentage survival of peripheral neurons cultured with the appropriate neurotrophic factor lies within the range 65-85% (not shown). In neurons cultured in the absence of neurotrophic support, a comparable level of survival is not reached after the first 10 days of postnatal life in sympathetic neurons (Fig 44). Nodose neurons become neurotrophin independent between P0 and P5, whereas DRG neurons become independent between P5 and P10 (Fig 44). These results suggest that the onset of neurotrophin-independence *in vitro* varies between populations of PNS neurons. Notably, SCG neurons remained dependent on neurotrophin support up to 10 days after birth. SCG neurons are known to depend on neurotrophic support for as long as 40 days after birth [118] .

5.3 KCl-induced depolarisation increases survival of peripheral sensory neurons

Peripheral neurons are dependent on neurotrophic factors around the time when they start innervating their targets. Neural activity has also been shown to increase the survival of many populations of neurons in both the CNS and PNS [460] . In order to

investigate whether activity might influence neuronal survival at different developmental stages, percent survival in cultures with depolarising concentrations of K^+ (40 mM) was estimated for nodose, dorsal root and superior cervical ganglia. Neurons were cultured from ganglia obtained over a range of developmental ages from E16-P10 in the absence of neurotrophic support. The survival of nodose neurons cultured in the presence of depolarising concentrations of KCl alone was comparable to the percentage survival of nodose neurons supported by neurotrophic factors (Fig. 46). This effect was most dramatic in the immediate postnatal period, with 80% of P0 neurons surviving in the presence of KCl alone (Fig. 46B) compared to 30-40% survival in untreated cultures. The difference between both culture conditions disappeared by P10 (Fig. 46D) when these neurons become fully independent of neurotrophic factors. Similarly, an increase in neuronal survival was observed during a developmental window in sensory neurons of the DRG (Fig. 47). The age at which KCl-supported survival reached a level comparable to that of neurotrophin-supported cultures, was between P5-P10 (Fig. 47). In contrast to sensory neurons, depolarising concentrations of KCl did not affect the survival of SCG neurons at any age tested (Fig. 48). These results suggest that embryonic sensory neurons are dependent on neurotrophins during early postnatal stages, but become entirely independent by P10. Furthermore, there is a developmental window during which depolarizing concentrations of K^+ can increase the survival of sensory neurons cultured in the absence of neurotrophic factors and that the postnatal age at which this stimulation can modify survival differs between neuronal populations.

A

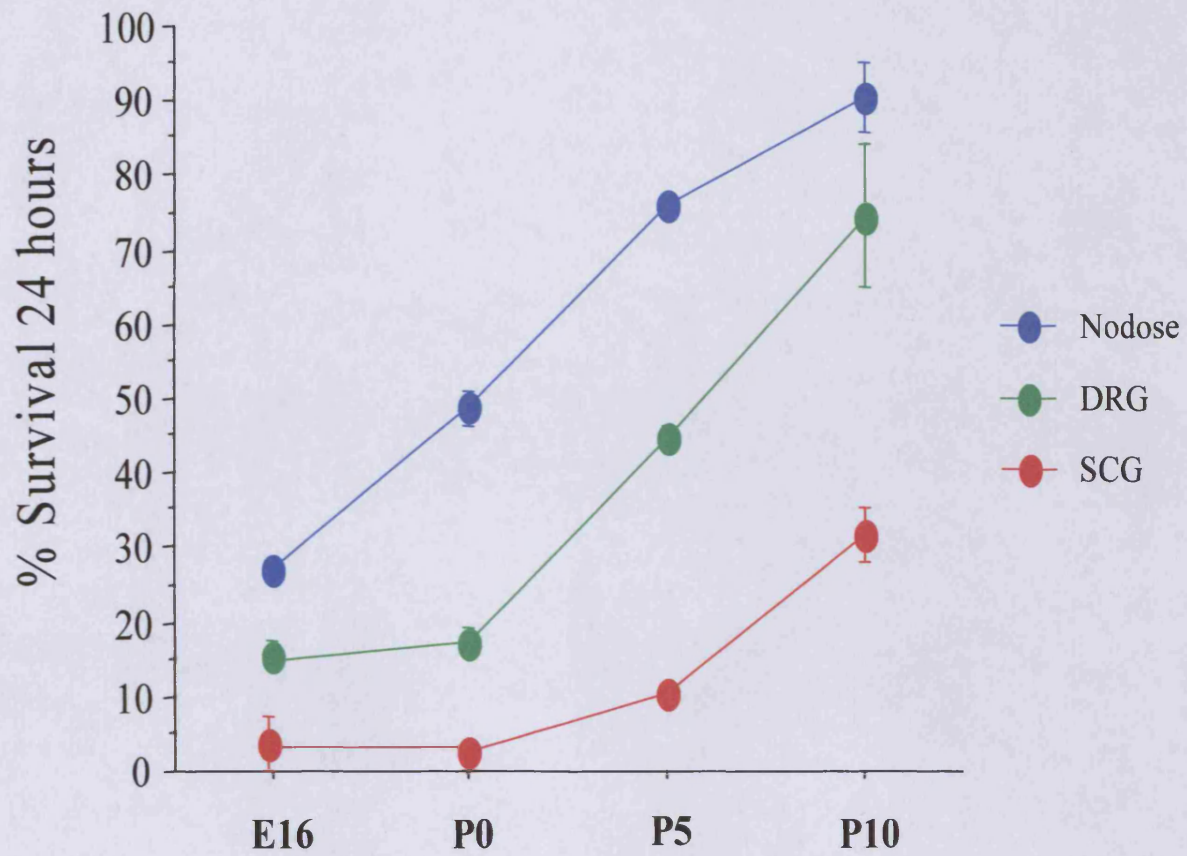


Figure 45 | **Neurotrophin-independent survival increases with age.** Neurons from the nodose, dorsal root and superior cervical ganglia (at ages indicated) were incubated without neurotrophic support in defined medium for 24 hours after which the percentage neuronal survival was calculated. (A) Neurons from both the nodose and dorsal root ganglia become neurotrophin-independent postnatally, whereas SCG neurons remain dependent on NGF for survival.

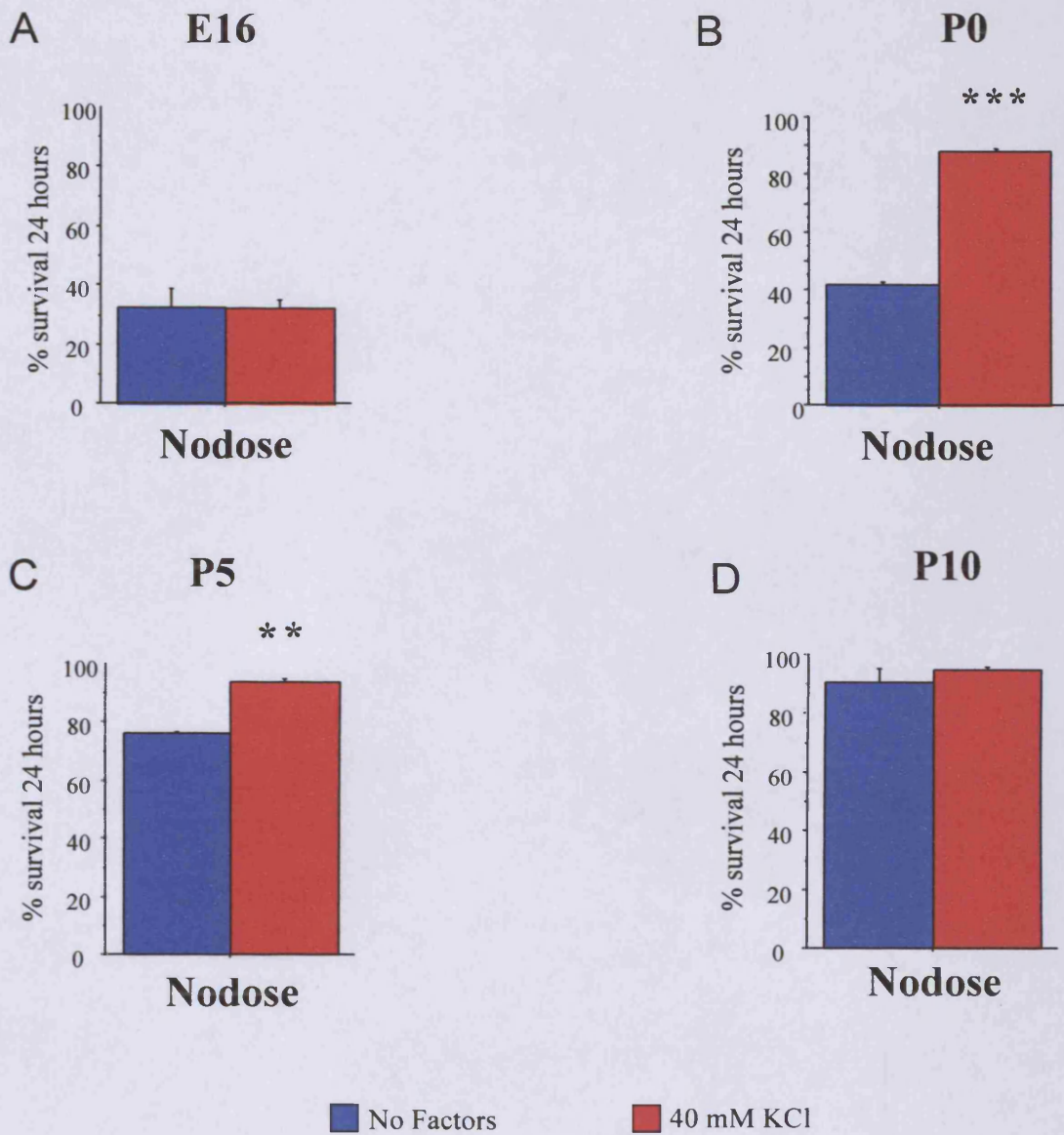


Figure 46 | Depolarisation causes neurotrophin-independence in nodose neurons from P0. Neurons from the nodose ganglion (at ages indicated) were incubated without neurotrophic support in defined medium for 24 hours in the presence or absence of KCl (40mM) after which the percentage neuronal survival was calculated. Statistical comparison is with respect to the “no factors” condition and values shown are the average survival values obtained from three independent repeats (** P < 0.01 , *** P < 0.005)

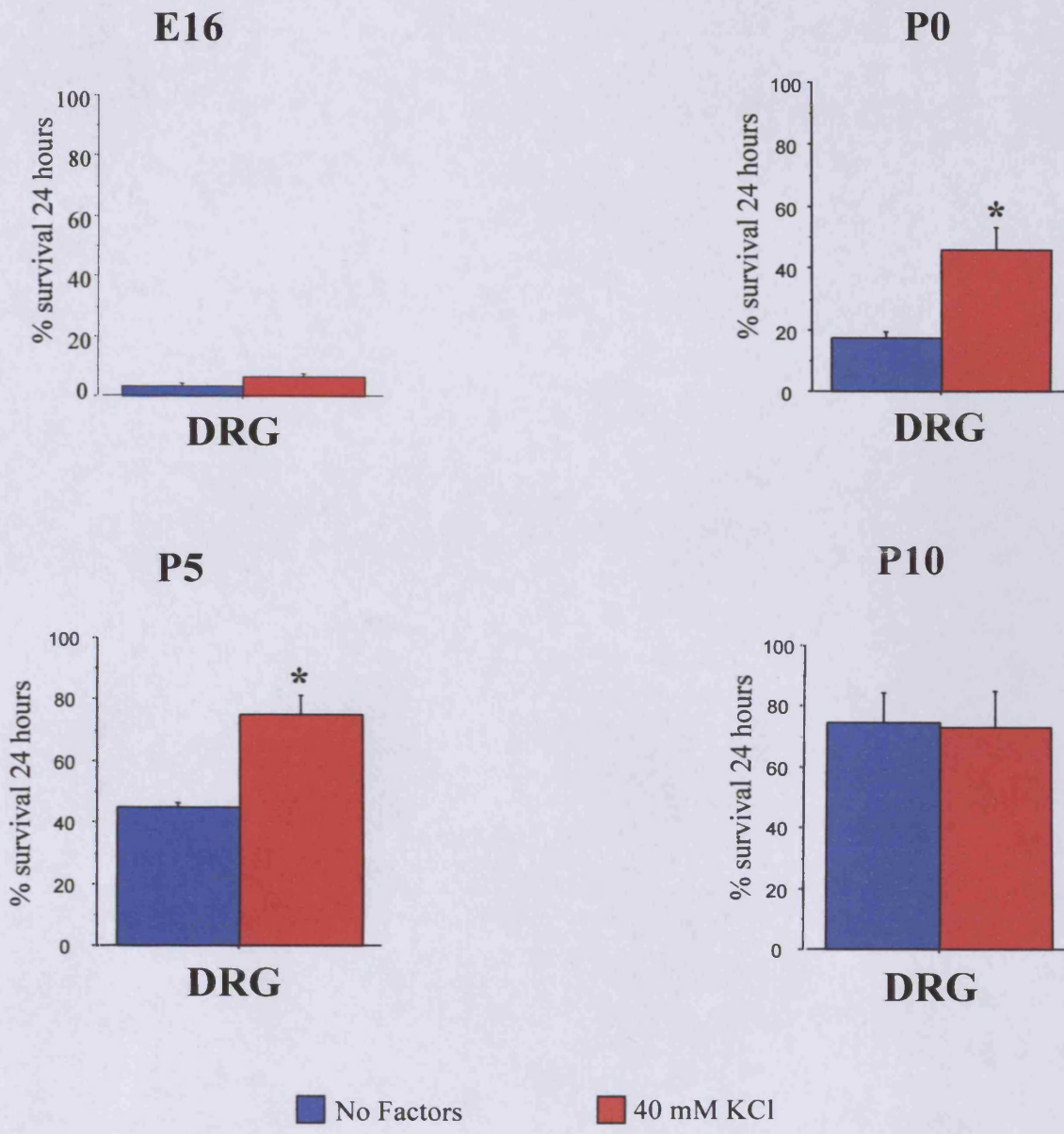


Figure 47 | **Depolarisation causes neurotrophin-independence in DRG neurons from P5.** Neurons from the DRG (at ages indicated) were incubated without neurotrophic support in defined medium for 24 hours in the presence or absence of KCl (40mM) after which the percentage neuronal survival was calculated. Statistical comparison is with respect to the “no factors” condition and values shown are the average survival values obtained from three independent repeats (** P < 0.01 , *** P < 0.005)

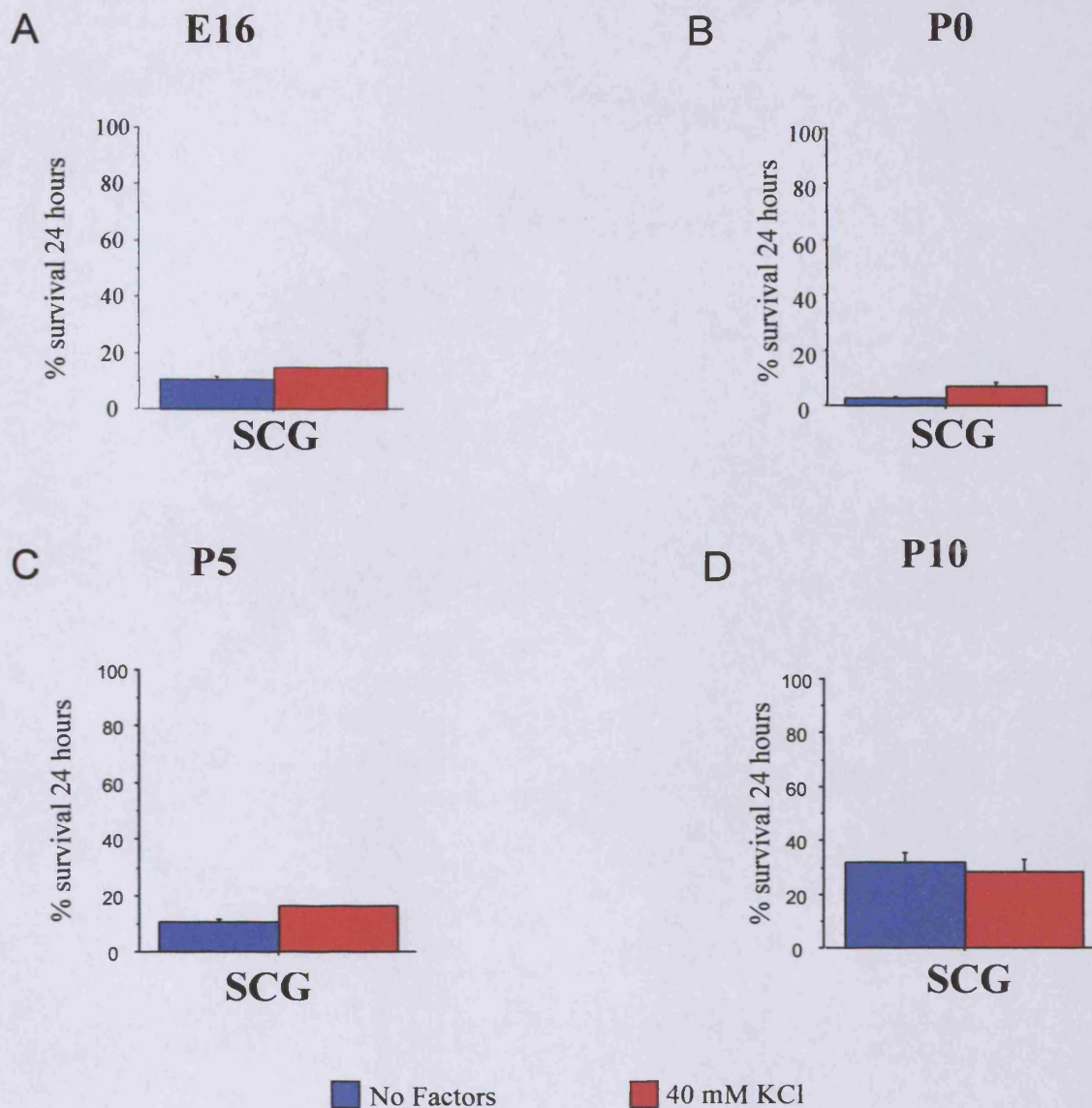


Figure 48 | **Depolarisation has no effect on SCG neurons during early postnatal life.** Neurons from the SCG (at ages indicated) were incubated without neurotrophic support in defined medium for 24 hours in the presence or absence of KCl (40mM) after which the percentage neuronal survival was calculated. Statistical comparison is with respect to the “no factors” condition and values shown are the average survival values obtained from three independent repeats.

5.4 L-Type Ca^{2+} channel blockers reverse effects of KCl on sensory neuronal survival

Depolarisation of neurons by elevation of extracellular K^+ has been shown to increase neuronal survival of central and peripheral neurons in vitro [460]. The reported survival promoting effects of elevated K^+ in peripheral neurons seem to be largely mediated by calcium influx through L-Type, voltage-gated calcium channels [460, 461]. To confirm that the increased survival in sensory neurons (Figs 46 and 47) treated with 40 mM K^+ is mediated by L-type calcium channels, we tested the effects of L-type calcium channel blockers verapamil and nifedipine. Neurons from postnatal nodose and dorsal root ganglia were cultured in defined media with and without elevated K^+ and with elevated K^+ plus either verapamil or nifedipine. Both verapamil and nifedipine reversed the increase in neuronal survival brought about by elevated extracellular K^+ (Figs. 49 and 50). The developmental window during which L-type calcium channel blockers effected survival is the same as that during which elevated K^+ influences neuronal survival for both nodose and DRG neurons (Figs. 49 and 50). These results suggest that increases in intracellular calcium concentration or neural activity, may be sufficient to promote neuronal survival in the absence of neurotrophic support during a window of postnatal development in sensory neurons.

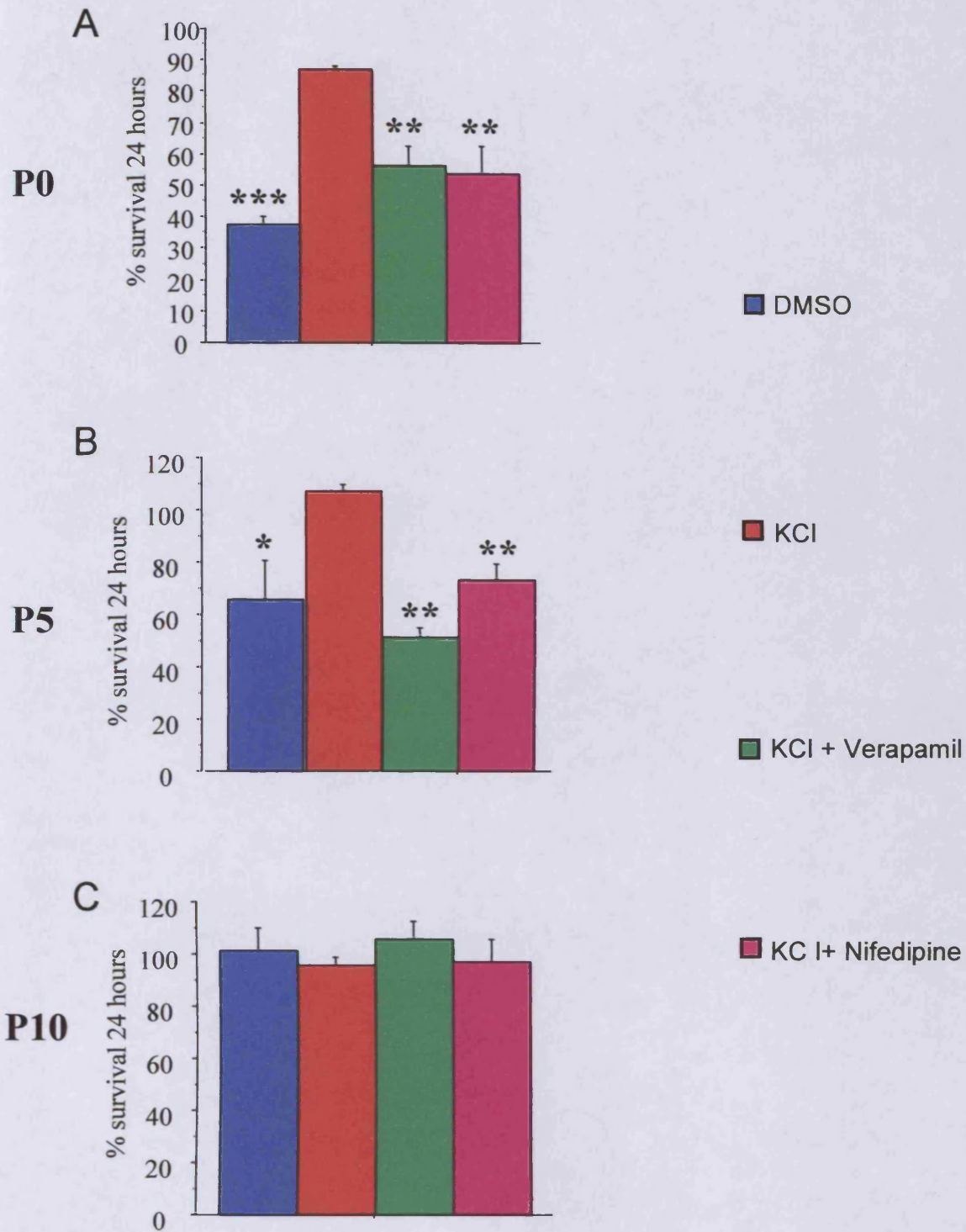


Figure 49 |L-type calcium channel inhibitors reverse the effects of KCl in nodose neurons. Neurons from the SCG (at ages indicated) were incubated without neurotrophic support in defined medium for 24 hours in the presence or absence of KCl (40mM) with verapamil (10 μ M) or nifedipine (10 μ M) after which the percentage neuronal survival was calculated. Statistical comparison is with respect to the “KCl” condition and values shown are the average survival values obtained from three independent repeats. (* $p < 0.05$, ** $p < 0.01$ *** $p < 0.001$)

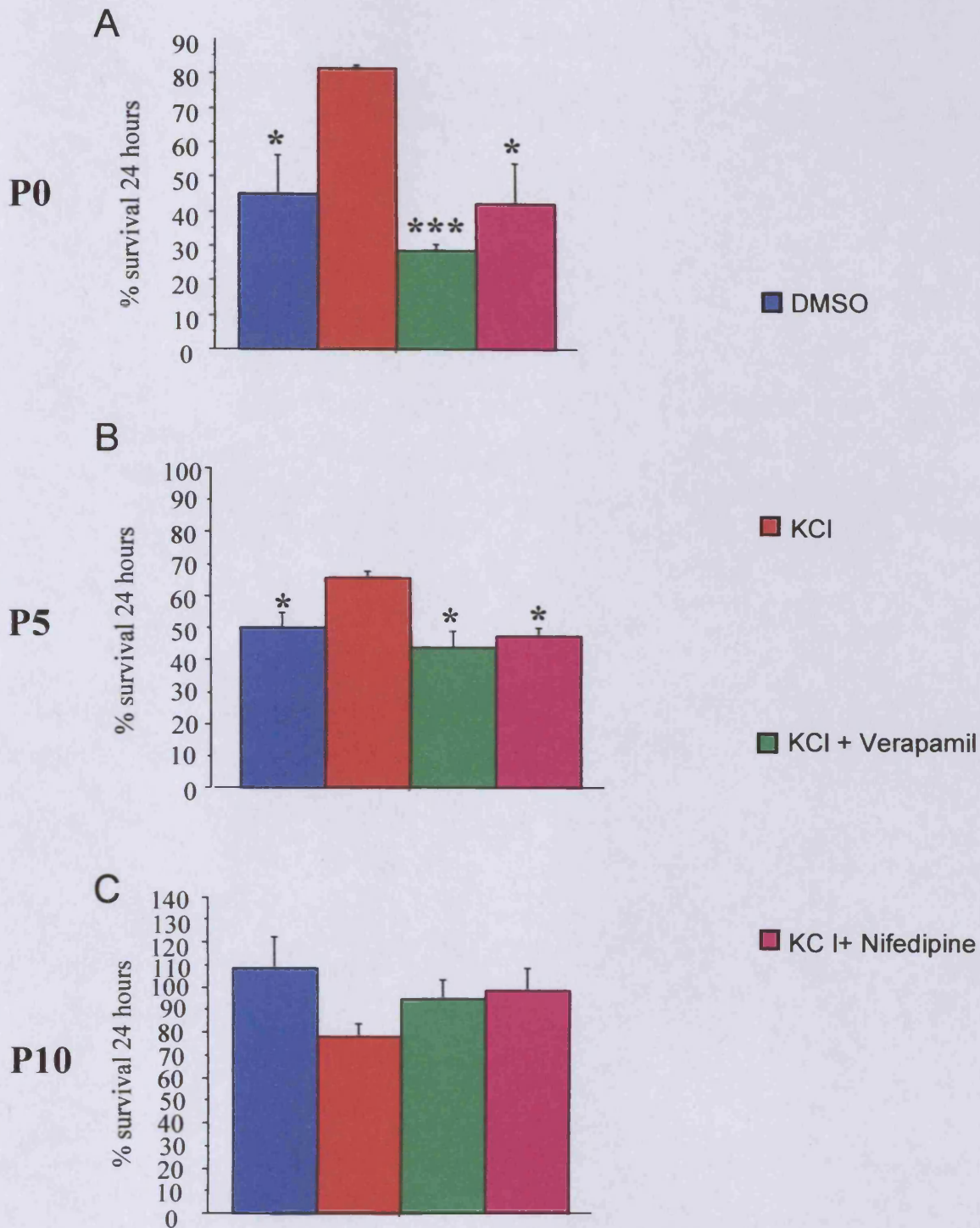


Figure 50 |L-type calcium channel inhibitors reverse the effects of KCl in DRG neurons. Neurons from the SCG (at ages indicated) were incubated without neurotrophic support in defined medium for 24 hours in the presence or absence of KCl (40mM) with verapamil (10 μ M) or nifedipine (10 μ M) after which the percentage neuronal survival was calculated. Statistical comparison is with respect to the "KCl" condition and values shown are the average survival values obtained from three independent repeats. (* $p < 0.05$, *** $p < 0.001$)

5.5 Extracellular ATP promotes the survival of nodose neurons

ATP binds to P2X receptors, ATP-gated ion channels which generate inward currents caused by Na^+ and Ca^{2+} influx, causing membrane depolarisation and facilitation of voltage-gated calcium entry. There are seven P2X receptor subunits (P2X₁-P2X₇) of which P2X₂ and P2X₃ seem to play the major role in mediating the primary sensory effects of ATP [462, 463]. P2X₂ and P2X₃ are highly expressed in nodose neurons [464] and the addition of extracellular ATP leads to depolarisation of the majority of nodose neurons [463]. Nodose neurons from E16-P10 were cultured without neurotrophic factors in the presence or absence of extracellular ATP and neuronal survival was estimated. During the same developmental window during which elevated K^+ effects survival, extracellular ATP caused a significant increase in the survival of nodose neurons (Fig 51). These results further implicate depolarisation in the regulation of survival of postnatal sensory neurons.

5.6 Hypoxia reverses effect of ATP on neuronal survival

ATP induces a sustained inward current in HEK cells expressing the homomeric P2X₂ receptor under normoxic conditions, which is significantly reduced in hypoxia [465]. In order to investigate the effects of hypoxia on ATP-induced neuronal survival, neonatal nodose neurons were incubated overnight at 1% O_2 , in the presence or absence of ATP. In contrast to the marked effect on survival described above, extracellular ATP had no effect on neuronal survival under hypoxic conditions (Fig. 52). This observation suggests that the survival-promoting effects of ATP may be mediated by binding to the highly expressed P2X₂ receptor on nodose neurons.

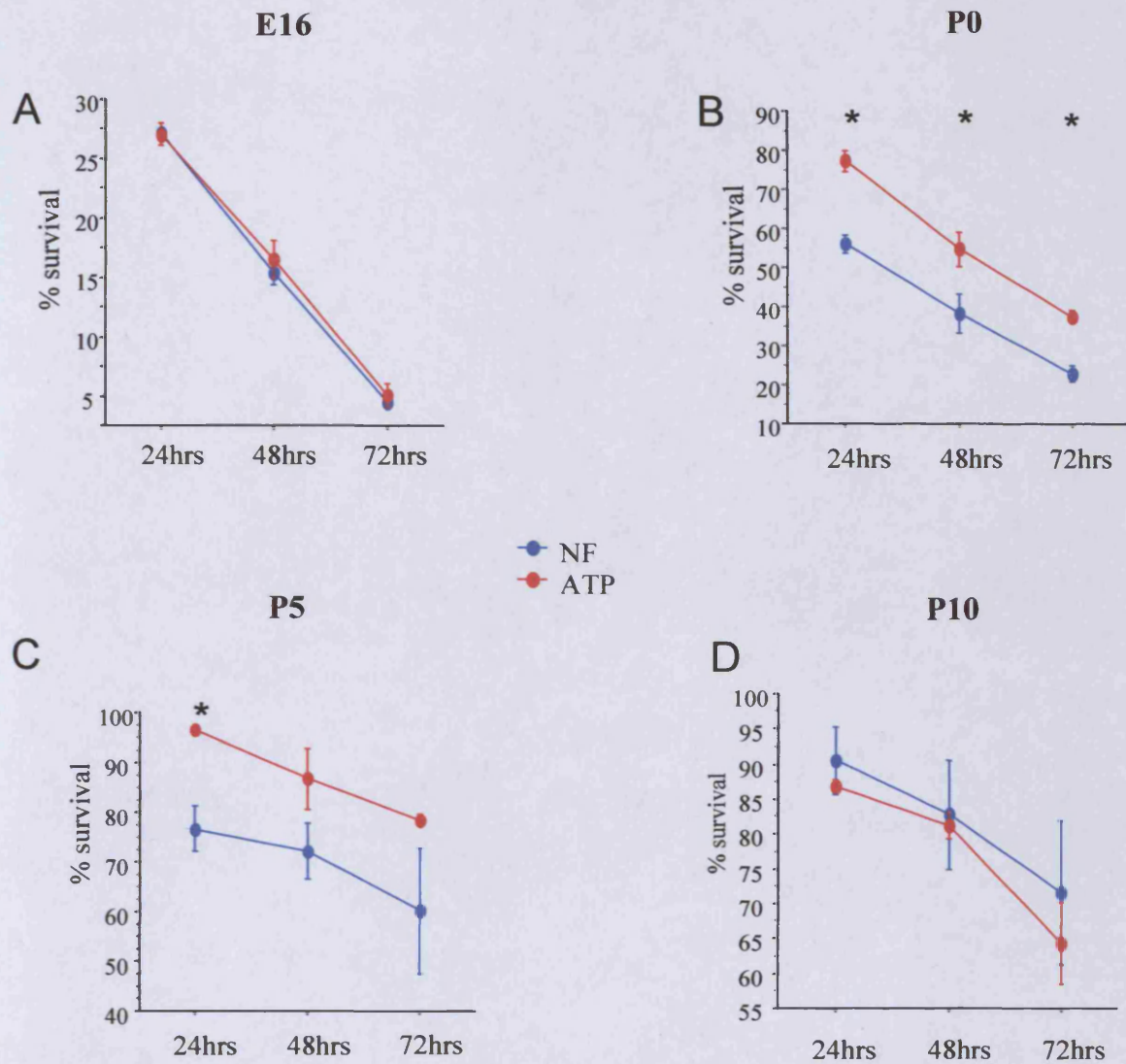
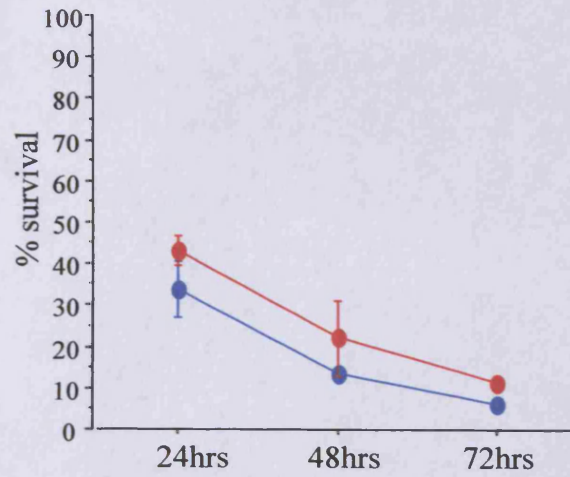


Figure 51 | ATP promotes survival of neonatal nodose neurons. Neurons from the nodose ganglion (at ages indicated) were incubated in the absence of neurotrophic factors, with or without ATP (10 μ M) and percentage neuronal survival was estimated every 24 hours up to 72 hours. ATP increases survival during a window of postnatal development in nodose neurons. Statistical comparisons are with respect to the no factors (NF) condition and values shown are the average survival values obtained from three independent repeats. (* $p < 0.05$)

A

● NF
● ATP

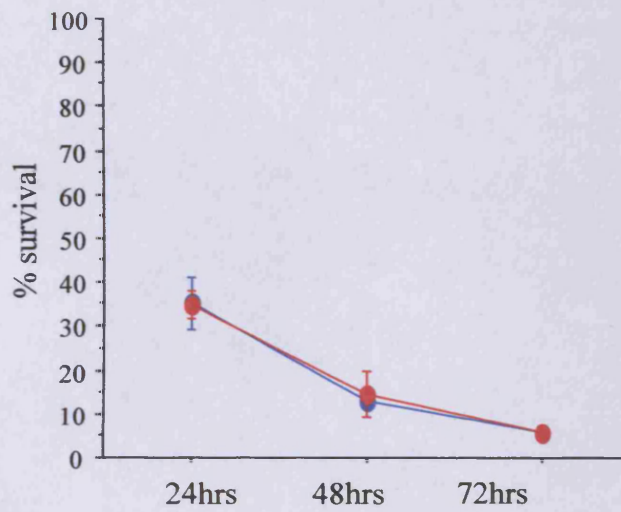
B

Figure 52 | **Hypoxia reverses effects of ATP.** Neurons from the nodose ganglion (at ages indicated) were incubated at 1% O₂ in the absence of neurotrophic factors, with or without ATP (10µM) and percentage neuronal survival was estimated every 24 hours up to 72 hours. ATP had no effect on neuronal survival when under hypoxic conditions. NF = No factors.

5.7 Discussion

Embryonic sensory neurons cultured before target field innervation begins are independent of neurotrophic support [89, 466, 467]. The survival of these early neurons is regulated by intracellular calcium [258]. Soon after this period of neurotrophin independence, sensory neurons become dependent on target-derived neurotrophic factors. According to the calcium set-point hypothesis [262], there are four postulated steady-state levels of $[Ca^{2+}]_i$ that effect neuronal survival. (1) A very low range of $[Ca^{2+}]_i$ results in cell death that cannot be reversed by addition of neurotrophic factors. (2) The $[Ca^{2+}]_i$ of neurons at rest during the period of PCD which renders neurons dependent on neurotrophic factors for survival. (3) A range of $[Ca^{2+}]_i$ slightly elevated above resting levels which promotes neuronal survival in the absence of neurotrophic factors. (4) Substantially elevated $[Ca^{2+}]_i$ which causes cell death. Studies *in vitro* describe how neurons, aged in culture, regain their independence from neurotrophins which correlates with an increase in $[Ca^{2+}]_i$ [262, 459, 468]. Further studies using DRG neurons of various developmental ages, not culture ages, confirm that older neurons become neurotrophin independent and that trophic factor dependence is inversely related to $[Ca^{2+}]_i$ since $[Ca^{2+}]_i$ increases as the neurons become independent of NGF [264]. Furthermore, mature, neurotrophin independent DRG neurons revert to neurotrophin-dependence if moved to low calcium media [468]. Here I have described how various populations of sensory neurons attain neurotrophin independence *in vitro* at different stages of postnatal development. Nodose neurons become independent of neurotrophic support between P0-P5, DRG neurons become independent between P5-P10 and sympathetic neurons did not reach independence at all within the tested range of developmental stages. During the postnatal period prior to the onset of neurotrophin independence, neuronal

survival was increased by chronic K^+ -induced depolarisation. It will be of interest to confirm that the relatively early onset of neurotrophin independence in nodose neurons correlates with an earlier rise in $[Ca^{2+}]_i$. Interestingly, the decreased dependence of nodose neurons on neurotrophic factors *in vitro* correlates with an early decrease in TrkB expression compared to a slightly later decrease in TrkA expression on DRG neurons [456, 457]. In contrast, SCG neurons remain dependent on neurotrophic support and continue to express TrkA into adulthood [469]. SCG neurons do not reach independence *in vitro* until mice are 12 weeks old and neuronal survival at this stage is unaffected by anti-NGF antibodies or TrkA inhibition [470]. It is plausible that both the cumulative effects of $[Ca^{2+}]_i$ and the availability or level of expression of neurotrophic factors and their receptors determine neurotrophin independence. Nodose neurons survive in the absence of neurotrophic support between P5 and P10 *in vitro* but stereological analyses revealed a 50% reduction in cell number in nodose ganglia during a postnatal period when the neurons are independent of neurotrophic factors between P5 and P14. Differential levels of activity may contribute to the 50% decrease in number of nodose neurons between days 1 and 14 of postnatal life, where less active neurons are eliminated [471].

As neurons are in the process of becoming neurotrophin independent (P0-P5 for nodose neurons, P5-P10 for DRG neurons), their survival is increased to maximal levels by chronic K^+ mediated depolarisation. Influx of calcium through L-type voltage-gated calcium channels, resulted in neurotrophin independence at postnatal stages of development during which neurons are normally dependent on neurotrophins for survival. Embryonic neurons from all ganglia tested were found to be fully reliant on neurotrophins. SCG neurons aged in culture for 3 weeks have been

shown to become independent of neurotrophic support and display a gradual increase in $[Ca^{2+}]_i$ from 93nM in young neurons to 241nM in 3 week old neurons [459]. Interestingly, depolarisation of young neurons with K^+ has been shown to promote an increase in $[Ca^{2+}]_i$ to 240nM, leading to neurotrophin independence [459]. My observations suggest that various populations of neurons may reach a threshold level of $[Ca^{2+}]_i$ at different stages during postnatal development due to differential levels of neural activity. It would be of interest to compare $[Ca^{2+}]_i$ of nodose, DRG and SCG neurons at different stages of postnatal development. The early onset of neurotrophin independence in nodose neurons would predict that optimal $[Ca^{2+}]_i$ is reached sooner during postnatal development in this population compared to DRG or SCG neurons. Further work is also required to determine whether the subpopulation of nodose neurons that survive in the absence of neurotrophic factors or elevated K^+ between P0-P5, do so because of comparatively higher $[Ca^{2+}]_i$. Extracellular ATP, a physiological agonist of P2X receptors on nodose neurons, promoted a significant increase in neuronal survival between P0-P5. Differential levels of activity between nodose neurons during this period of development may determine which neurons become independent and which die by PCD. Interestingly, the increase in survival promoted by ATP was reversed when neurons were grown under hypoxic conditions. It is possible that hypoxic conditions *in utero* could dampen the effects of neural activity on survival and increase dependence on neurotrophic factors.

It is well established that the survival of embryonic peripheral neurons is dependent on target derived neurotrophic factors. Deafferentation studies, studies in which ganglionic transmission has been blocked and many *in vitro* analyses have elucidated a role for activity in the regulation of survival during the development of numerous

populations of peripheral and central neurons [472]. My results suggest that the survival requirements of different populations of sensory neurons switch from neurotrophins to neural activity at different stages postnatally. My observation that the survival of nodose neurons can be increased by addition of ATP, suggests that the role of neural activity may be physiologically relevant during the early postnatal development of sensory neurons. Further work will be required to determine which of the P2 receptor subtypes mediates the observed effects of ATP on neuronal survival. Patch-clamp studies have revealed almost complete loss of ATP-induced inward current in P2X₂/P2X₃ double knockout mice [463]. It would therefore be of considerable interest to compare neuronal survival of WT and P2X₂/P2X₃ double knockout mice , in the absence and presence of ATP, during postnatal development.

Bibliography

1. Kintner, C.R. and J. Dodd, *Hensen's node induces neural tissue in Xenopus ectoderm. Implications for the action of the organizer in neural induction.* Development, 1991. **113**(4): p. 1495-505.
2. Blum, M., et al., *Gastrulation in the mouse: the role of the homeobox gene gooseoid.* Cell, 1992. **69**(7): p. 1097-106.
3. Hatta, K. and Y. Takahashi, *Secondary axis induction by heterospecific organizers in zebrafish.* Dev Dyn, 1996. **205**(2): p. 183-95.
4. Smith, W.C. and R.M. Harland, *Expression cloning of noggin, a new dorsalizing factor localized to the Spemann organizer in Xenopus embryos.* Cell, 1992. **70**(5): p. 829-40.
5. Lamb, T.M., et al., *Neural induction by the secreted polypeptide noggin.* Science, 1993. **262**(5134): p. 713-8.
6. Smith, W.C., et al., *Secreted noggin protein mimics the Spemann organizer in dorsalizing Xenopus mesoderm.* Nature, 1993. **361**(6412): p. 547-9.
7. Furthauer, M., B. Thisse, and C. Thisse, *Three different noggin genes antagonize the activity of bone morphogenetic proteins in the zebrafish embryo.* Dev Biol, 1999. **214**(1): p. 181-96.
8. Hemmati-Brivanlou, A., O.G. Kelly, and D.A. Melton, *Follistatin, an antagonist of activin, is expressed in the Spemann organizer and displays direct neuralizing activity.* Cell, 1994. **77**(2): p. 283-95.
9. Sasai, Y., et al., *Xenopus chordin: a novel dorsalizing factor activated by organizer-specific homeobox genes.* Cell, 1994. **79**(5): p. 779-90.
10. Sasai, Y., et al., *Regulation of neural induction by the Chd and Bmp-4 antagonistic patterning signals in Xenopus.* Nature, 1995. **376**(6538): p. 333-6.
11. Piccolo, S., et al., *Dorsoventral patterning in Xenopus: inhibition of ventral signals by direct binding of chordin to BMP-4.* Cell, 1996. **86**(4): p. 589-98.
12. Zimmerman, L.B., J.M. De Jesus-Escobar, and R.M. Harland, *The Spemann organizer signal noggin binds and inactivates bone morphogenetic protein 4.* Cell, 1996. **86**(4): p. 599-606.
13. Fainsod, A., et al., *The dorsalizing and neural inducing gene follistatin is an antagonist of BMP-4.* Mech Dev, 1997. **63**(1): p. 39-50.
14. Hawley, S.H., et al., *Disruption of BMP signals in embryonic Xenopus ectoderm leads to direct neural induction.* Genes Dev, 1995. **9**(23): p. 2923-35.
15. Wilson, P.A. and A. Hemmati-Brivanlou, *Vertebrate neural induction: inducers, inhibitors, and a new synthesis.* Neuron, 1997. **18**(5): p. 699-710.
16. Hemmati-Brivanlou, A. and D. Melton, *Vertebrate neural induction.* Annu Rev Neurosci, 1997. **20**: p. 43-60.
17. Bouwmeester, T., et al., *Cerberus is a head-inducing secreted factor expressed in the anterior endoderm of Spemann's organizer.* Nature, 1996. **382**(6592): p. 595-601.
18. Belo, J.A., et al., *Cerberus-like is a secreted factor with neutralizing activity expressed in the anterior primitive endoderm of the mouse gastrula.* Mech Dev, 1997. **68**(1-2): p. 45-57.

19. Hsu, D.R., et al., *The Xenopus dorsalizing factor Gremlin identifies a novel family of secreted proteins that antagonize BMP activities*. *Mol Cell*, 1998. **1**(5): p. 673-83.
20. Pearce, J.J., G. Penny, and J. Rossant, *A mouse cerberus/Dan-related gene family*. *Dev Biol*, 1999. **209**(1): p. 98-110.
21. Dionne, M.S., W.C. Skarnes, and R.M. Harland, *Mutation and analysis of Dan, the founding member of the Dan family of transforming growth factor beta antagonists*. *Mol Cell Biol*, 2001. **21**(2): p. 636-43.
22. Eimon, P.M. and R.M. Harland, *Xenopus Dan, a member of the Dan gene family of BMP antagonists, is expressed in derivatives of the cranial and trunk neural crest*. *Mech Dev*, 2001. **107**(1-2): p. 187-9.
23. Khokha, M.K., et al., *Gremlin is the BMP antagonist required for maintenance of Shh and Fgf signals during limb patterning*. *Nat Genet*, 2003. **34**(3): p. 303-7.
24. Wagner, D.S. and M.C. Mullins, *Modulation of BMP activity in dorsal-ventral pattern formation by the chordin and ogon antagonists*. *Dev Biol*, 2002. **245**(1): p. 109-23.
25. Yabe, T., et al., *Ogon/Secreted Frizzled functions as a negative feedback regulator of Bmp signaling*. *Development*, 2003. **130**(12): p. 2705-16.
26. Stern, C.D., *Neural induction: old problem, new findings, yet more questions*. *Development*, 2005. **132**(9): p. 2007-21.
27. Sadler, T.W., *Embryology of neural tube development*. *Am J Med Genet C Semin Med Genet*, 2005. **135**(1): p. 2-8.
28. Schoenwolf, G.C. and I.S. Alvarez, *Roles of neuroepithelial cell rearrangement and division in shaping of the avian neural plate*. *Development*, 1989. **106**(3): p. 427-39.
29. Keller, R., et al., *Planar induction of convergence and extension of the neural plate by the organizer of Xenopus*. *Dev Dyn*, 1992. **193**(3): p. 218-34.
30. Keller, R., et al., *Mechanisms of convergence and extension by cell intercalation*. *Philos Trans R Soc Lond B Biol Sci*, 2000. **355**(1399): p. 897-922.
31. Smith, J.L. and G.C. Schoenwolf, *Notochordal induction of cell wedging in the chick neural plate and its role in neural tube formation*. *J Exp Zool*, 1989. **250**(1): p. 49-62.
32. Jessell, T.M. and J.R. Sanes, *Development. The decade of the developing brain*. *Curr Opin Neurobiol*, 2000. **10**(5): p. 599-611.
33. Copp, A.J., N.D. Greene, and J.N. Murdoch, *The genetic basis of mammalian neurulation*. *Nat Rev Genet*, 2003. **4**(10): p. 784-93.
34. Chenn, A. and S.K. McConnell, *Cleavage orientation and the asymmetric inheritance of Notch1 immunoreactivity in mammalian neurogenesis*. *Cell*, 1995. **82**(4): p. 631-41.
35. Langman, J., R.L. Guerrant, and B.G. Freeman, *Behavior of neuro-epithelial cells during closure of the neural tube*. *J Comp Neurol*, 1966. **127**(3): p. 399-411.
36. Nagele, R.G. and H.Y. Lee, *Ultrastructural changes in cells associated with interkinetic nuclear migration in the developing chick neuroepithelium*. *J Exp Zool*, 1979. **210**(1): p. 89-106.
37. Hayes, N.L. and R.S. Nowakowski, *Exploiting the dynamics of S-phase tracers in developing brain: interkinetic nuclear migration for cells entering versus leaving the S-phase*. *Dev Neurosci*, 2000. **22**(1-2): p. 44-55.

38. Sauer, M.E. and B.E. Walker, *Radioautographic study of interkinetic nuclear migration in the neural tube*. Proc Soc Exp Biol Med, 1959. **101**(3): p. 557-60.
39. Fujita, S., *Kinetics of cellular proliferation*. Exp Cell Res, 1962. **28**: p. 52-60.
40. Fujita, H. and S. Fujita, [*Electron Microscopic Studies on the Histogenesis of Nerve Cells and Neuroglia in the Domestic Fowl. Ii. on Neuroglia.*]. Kaibogaku Zasshi, 1963. **38**: p. 95-108.
41. Miller, M.W. and R.S. Nowakowski, *Use of bromodeoxyuridine-immunohistochemistry to examine the proliferation, migration and time of origin of cells in the central nervous system*. Brain Res, 1988. **457**(1): p. 44-52.
42. Hollyday, M., *Neurogenesis in the vertebrate neural tube*. Int J Dev Neurosci, 2001. **19**(2): p. 161-73.
43. Bentivoglio, M. and P. Mazzarello, *The history of radial glia*. Brain Res Bull, 1999. **49**(5): p. 305-15.
44. Rakic, P., *Mode of cell migration to the superficial layers of fetal monkey neocortex*. J Comp Neurol, 1972. **145**(1): p. 61-83.
45. Rakic, P., *Developmental and evolutionary adaptations of cortical radial glia*. Cereb Cortex, 2003. **13**(6): p. 541-9.
46. Hatten, M.E., *Central nervous system neuronal migration*. Annu Rev Neurosci, 1999. **22**: p. 511-39.
47. Kriegstein, A.R. and S.C. Noctor, *Patterns of neuronal migration in the embryonic cortex*. Trends Neurosci, 2004. **27**(7): p. 392-9.
48. Marin, O. and J.L. Rubenstein, *A long, remarkable journey: tangential migration in the telencephalon*. Nat Rev Neurosci, 2001. **2**(11): p. 780-90.
49. Ayala, R., T. Shu, and L.H. Tsai, *Trekking across the brain: the journey of neuronal migration*. Cell, 2007. **128**(1): p. 29-43.
50. Witzemann, V., *Development of the neuromuscular junction*. Cell Tissue Res, 2006. **326**(2): p. 263-71.
51. Gesemann, M., A.J. Denzer, and M.A. Ruegg, *Acetylcholine receptor-aggregating activity of agrin isoforms and mapping of the active site*. J Cell Biol, 1995. **128**(4): p. 625-36.
52. Gautam, M., et al., *Defective neuromuscular synaptogenesis in agrin-deficient mutant mice*. Cell, 1996. **85**(4): p. 525-35.
53. Gautam, M., et al., *Failure of postsynaptic specialization to develop at neuromuscular junctions of rapsyn-deficient mice*. Nature, 1995. **377**(6546): p. 232-6.
54. DeChiara, T.M., et al., *The receptor tyrosine kinase MuSK is required for neuromuscular junction formation in vivo*. Cell, 1996. **85**(4): p. 501-12.
55. Kong, X.C., P. Barzaghi, and M.A. Ruegg, *Inhibition of synapse assembly in mammalian muscle in vivo by RNA interference*. EMBO Rep, 2004. **5**(2): p. 183-8.
56. Hesser, B.A., O. Henschel, and V. Witzemann, *Synapse disassembly and formation of new synapses in postnatal muscle upon conditional inactivation of MuSK*. Mol Cell Neurosci, 2006. **31**(3): p. 470-80.
57. Waites, C.L., A.M. Craig, and C.C. Garner, *Mechanisms of vertebrate synaptogenesis*. Annu Rev Neurosci, 2005. **28**: p. 251-74.
58. Shields, R.W., Jr., *Functional anatomy of the autonomic nervous system*. J Clin Neurophysiol, 1993. **10**(1): p. 2-13.

59. Selleck, M.A. and M. Bronner-Fraser, *Origins of the avian neural crest: the role of neural plate-epidermal interactions*. *Development*, 1995. **121**(2): p. 525-38.
60. Mancilla, A. and R. Mayor, *Neural crest formation in *Xenopus laevis*: mechanisms of *Xslug* induction*. *Dev Biol*, 1996. **177**(2): p. 580-9.
61. Gilbert, D.J., *Developmental Biology*. 6 ed: Sinauer Associates Inc.
62. Le Douarin, N.M., et al., *Neural crest cell plasticity and its limits*. *Development*, 2004. **131**(19): p. 4637-50.
63. D'Amico-Martel, A. and D.M. Noden, *Contributions of placodal and neural crest cells to avian cranial peripheral ganglia*. *Am J Anat*, 1983. **166**(4): p. 445-68.
64. LaBonne, C. and M. Bronner-Fraser, *Molecular mechanisms of neural crest formation*. *Annu Rev Cell Dev Biol*, 1999. **15**: p. 81-112.
65. LaBonne, C. and M. Bronner-Fraser, *Neural crest induction in *Xenopus*: evidence for a two-signal model*. *Development*, 1998. **125**(13): p. 2403-14.
66. Brault, V., et al., *Inactivation of the beta-catenin gene by *Wnt1-Cre*-mediated deletion results in dramatic brain malformation and failure of craniofacial development*. *Development*, 2001. **128**(8): p. 1253-64.
67. Ayer-Le Lievre, C.S. and N.M. Le Douarin, *The early development of cranial sensory ganglia and the potentialities of their component cells studied in quail-chick chimeras*. *Dev Biol*, 1982. **94**(2): p. 291-310.
68. Youle, R.J. and A. Strasser, *The BCL-2 protein family: opposing activities that mediate cell death*. *Nat Rev Mol Cell Biol*, 2008. **9**(1): p. 47-59.
69. Wang, X., *The expanding role of mitochondria in apoptosis*. *Genes Dev*, 2001. **15**(22): p. 2922-33.
70. Shi, Y., *Mechanical aspects of apoptosome assembly*. *Curr Opin Cell Biol*, 2006. **18**(6): p. 677-84.
71. Oppenheim, R.W., *Cell death during development of the nervous system*. *Annu Rev Neurosci*, 1991. **14**: p. 453-501.
72. Davies, A.M., *The role of neurotrophins during successive stages of sensory neuron development*. *Prog Growth Factor Res*, 1994. **5**(3): p. 263-89.
73. Burek, M.J. and R.W. Oppenheim, *Programmed cell death in the developing nervous system*. *Brain Pathol*, 1996. **6**(4): p. 427-46.
74. Levi-Montalcini, R. and P.U. Angeletti, *Nerve growth factor*. *Physiol Rev*, 1968. **48**(3): p. 534-69.
75. Levi-Montalcini, R., *The nerve growth factor 35 years later*. *Science*, 1987. **237**(4819): p. 1154-62.
76. Johnson, E.M., Jr. and H.K. Yip, *Central nervous system and peripheral nerve growth factor provide trophic support critical to mature sensory neuronal survival*. *Nature*, 1985. **314**(6013): p. 751-2.
77. Yip, H.K., et al., *The effects of nerve growth factor and its antiserum on the postnatal development and survival after injury of sensory neurons in rat dorsal root ganglia*. *J Neurosci*, 1984. **4**(12): p. 2986-92.
78. Pearson, J., E.M. Johnson, and L. Brandeis, *Effects of antibodies to nerve growth factor on intrauterine development of derivatives of cranial neural crest and placode in the guinea pig*. *Dev Biol*, 1983. **96**(1): p. 32-6.
79. Henderson, C.E., M. Huchet, and J.P. Changeux, *Neurite-promoting activities for embryonic spinal neurons and their developmental changes in the chick*. *Dev Biol*, 1984. **104**(2): p. 336-47.

80. Crowley, C., et al., *Mice lacking nerve growth factor display perinatal loss of sensory and sympathetic neurons yet develop basal forebrain cholinergic neurons*. Cell, 1994. **76**(6): p. 1001-11.
81. Smeyne, R.J., et al., *Severe sensory and sympathetic neuropathies in mice carrying a disrupted Trk/NGF receptor gene*. Nature, 1994. **368**(6468): p. 246-9.
82. Henderson, T.A., et al., *Fetal NGF augmentation preserves excess trigeminal ganglion cells and interrupts whisker-related pattern formation*. J Neurosci, 1994. **14**(5 Pt 2): p. 3389-403.
83. Davies, A.M., et al., *Timing and site of nerve growth factor synthesis in developing skin in relation to innervation and expression of the receptor*. Nature, 1987. **326**(6111): p. 353-8.
84. Caldero, J., et al., *Peripheral target regulation of the development and survival of spinal sensory and motor neurons in the chick embryo*. J Neurosci, 1998. **18**(1): p. 356-70.
85. Davies, A.M., *Regulation of neuronal survival and death by extracellular signals during development*. Embo J, 2003. **22**(11): p. 2537-45.
86. Davies, A.M., *Neurotrophic factors. Switching neurotrophin dependence*. Curr Biol, 1994. **4**(3): p. 273-6.
87. Davies, A.M., *Neurotrophin switching: where does it stand?* Curr Opin Neurobiol, 1997. **7**(1): p. 110-8.
88. Davies, A.M., *Intrinsic differences in the growth rate of early nerve fibres related to target distance*. Nature, 1989. **337**(6207): p. 553-5.
89. Vogel, K.S. and A.M. Davies, *The duration of neurotrophic factor independence in early sensory neurons is matched to the time course of target field innervation*. Neuron, 1991. **7**(5): p. 819-30.
90. Barde, Y.A., D. Edgar, and H. Thoenen, *Purification of a new neurotrophic factor from mammalian brain*. Embo J, 1982. **1**(5): p. 549-53.
91. Lewin, G.R. and Y.A. Barde, *Physiology of the neurotrophins*. Annu Rev Neurosci, 1996. **19**: p. 289-317.
92. Maina, F. and R. Klein, *Hepatocyte growth factor, a versatile signal for developing neurons*. Nat Neurosci, 1999. **2**(3): p. 213-7.
93. Airaksinen, M.S. and M. Saarma, *The GDNF family: signalling, biological functions and therapeutic value*. Nat Rev Neurosci, 2002. **3**(5): p. 383-94.
94. Lindholm, P., et al., *Novel neurotrophic factor CDNF protects and rescues midbrain dopamine neurons in vivo*. Nature, 2007. **448**(7149): p. 73-7.
95. Davies, A.M., *Neurotrophins: neurotrophic modulation of neurite growth*. Curr Biol, 2000. **10**(5): p. R198-200.
96. Thoenen, H., *Neurotrophins and activity-dependent plasticity*. Prog Brain Res, 2000. **128**: p. 183-91.
97. Maina, F., et al., *Multiple roles for hepatocyte growth factor in sympathetic neuron development*. Neuron, 1998. **20**(5): p. 835-46.
98. Bibel, M. and Y.A. Barde, *Neurotrophins: key regulators of cell fate and cell shape in the vertebrate nervous system*. Genes Dev, 2000. **14**(23): p. 2919-37.
99. English, A.W., *Cytokines, growth factors and sprouting at the neuromuscular junction*. J Neurocytol, 2003. **32**(5-8): p. 943-60.
100. Lindsay, R.M., et al., *Differences and similarities in the neurotrophic growth factor requirements of sensory neurons derived from neural crest and neural placode*. J Cell Sci Suppl, 1985. **3**: p. 115-29.

101. Davies, A.M., H. Thoenen, and Y.A. Barde, *The response of chick sensory neurons to brain-derived neurotrophic factor*. J Neurosci, 1986. **6**(7): p. 1897-904.
102. Davies, A.M., et al., *Neurotrophin-4/5 is a mammalian-specific survival factor for distinct populations of sensory neurons*. J Neurosci, 1993. **13**(11): p. 4961-7.
103. Buj-Bello, A., L.G. Pinon, and A.M. Davies, *The survival of NGF-dependent but not BDNF-dependent cranial sensory neurons is promoted by several different neurotrophins early in their development*. Development, 1994. **120**(6): p. 1573-80.
104. Conover, J.C., et al., *Neuronal deficits, not involving motor neurons, in mice lacking BDNF and/or NT4*. Nature, 1995. **375**(6528): p. 235-8.
105. Liu, X., et al., *Sensory but not motor neuron deficits in mice lacking NT4 and BDNF*. Nature, 1995. **375**(6528): p. 238-41.
106. Erickson, J.T., et al., *Mice lacking brain-derived neurotrophic factor exhibit visceral sensory neuron losses distinct from mice lacking NT4 and display a severe developmental deficit in control of breathing*. J Neurosci, 1996. **16**(17): p. 5361-71.
107. ElShamy, W.M. and P. Ernfors, *Brain-derived neurotrophic factor, neurotrophin-3, and neurotrophin-4 complement and cooperate with each other sequentially during visceral neuron development*. J Neurosci, 1997. **17**(22): p. 8667-75.
108. Forgie, A., et al., *In vivo survival requirement of a subset of nodose ganglion neurons for nerve growth factor*. Eur J Neurosci, 2000. **12**(2): p. 670-6.
109. Horton, A.R., et al., *Cytokines promote the survival of mouse cranial sensory neurones at different developmental stages*. Eur J Neurosci, 1998. **10**(2): p. 673-9.
110. Buchman, V.L. and A.M. Davies, *Different neurotrophins are expressed and act in a developmental sequence to promote the survival of embryonic sensory neurons*. Development, 1993. **118**(3): p. 989-1001.
111. Wyatt, S. and A.M. Davies, *Regulation of expression of mRNAs encoding the nerve growth factor receptors p75 and trkA in developing sensory neurons*. Development, 1993. **119**(3): p. 635-48.
112. Ninkina, N., et al., *Expression and function of TrkB variants in developing sensory neurons*. Embo J, 1996. **15**(23): p. 6385-93.
113. Andres, R., et al., *Multiple effects of artemin on sympathetic neurone generation, survival and growth*. Development, 2001. **128**(19): p. 3685-95.
114. Baloh, R.H., et al., *Artemin, a novel member of the GDNF ligand family, supports peripheral and central neurons and signals through the GFRalpha3-RET receptor complex*. Neuron, 1998. **21**(6): p. 1291-302.
115. Wyatt, S. and A.M. Davies, *Regulation of nerve growth factor receptor gene expression in sympathetic neurons during development*. J Cell Biol, 1995. **130**(6): p. 1435-46.
116. Wyatt, S., et al., *Sympathetic neuron survival and TrkA expression in NT3-deficient mouse embryos*. Embo J, 1997. **16**(11): p. 3115-23.
117. Kotzbauer, P.T., et al., *Postnatal development of survival responsiveness in rat sympathetic neurons to leukemia inhibitory factor and ciliary neurotrophic factor*. Neuron, 1994. **12**(4): p. 763-73.

118. Thompson, J., et al., *HGF promotes survival and growth of maturing sympathetic neurons by PI-3 kinase- and MAP kinase-dependent mechanisms*. Mol Cell Neurosci, 2004. **27**(4): p. 441-52.
119. Cohen, S., *Purification and metabolic effects of a nerve growth-promoting protein from snake venom*. J Biol Chem, 1959. **234**(5): p. 1129-37.
120. Cohen, S., *Purification of a Nerve-Growth Promoting Protein from the Mouse Salivary Gland and Its Neuro-Cytotoxic Antiserum*. Proc Natl Acad Sci U S A, 1960. **45**(3): p. 302-11.
121. Ullrich, A., et al., *Human beta-nerve growth factor gene sequence highly homologous to that of mouse*. Nature, 1983. **303**(5920): p. 821-5.
122. Mcier, R., et al., *Molecular cloning of bovine and chick nerve growth factor (NGF): delineation of conserved and unconserved domains and their relationship to the biological activity and antigenicity of NGF*. Embo J, 1986. **5**(7): p. 1489-93.
123. Ebendal, T., D. Larhammar, and H. Persson, *Structure and expression of the chicken beta nerve growth factor gene*. Embo J, 1986. **5**(7): p. 1483-7.
124. Angeletti, R.H. and R.A. Bradshaw, *Nerve growth factor from mouse submaxillary gland: amino acid sequence*. Proc Natl Acad Sci U S A, 1971. **68**(10): p. 2417-20.
125. McDonald, N.Q., et al., *New protein fold revealed by a 2.3-A resolution crystal structure of nerve growth factor*. Nature, 1991. **354**(6352): p. 411-4.
126. Berger, E.A. and E.M. Shooter, *Evidence for pro-beta-nerve growth factor, a biosynthetic precursor to beta-nerve growth factor*. Proc Natl Acad Sci U S A, 1977. **74**(9): p. 3647-51.
127. Scott, J., et al., *Isolation and nucleotide sequence of a cDNA encoding the precursor of mouse nerve growth factor*. Nature, 1983. **302**(5908): p. 538-40.
128. Edwards, R.H., et al., *Processing of the native nerve growth factor precursor to form biologically active nerve growth factor*. J Biol Chem, 1988. **263**(14): p. 6810-5.
129. Korsching, S., et al., *Levels of nerve growth factor and its mRNA in the central nervous system of the rat correlate with cholinergic innervation*. Embo J, 1985. **4**(6): p. 1389-93.
130. Korsching, S. and H. Thoenen, *Nerve growth factor in sympathetic ganglia and corresponding target organs of the rat: correlation with density of sympathetic innervation*. Proc Natl Acad Sci U S A, 1983. **80**(11): p. 3513-6.
131. Heumann, R., et al., *Relationship between levels of nerve growth factor (NGF) and its messenger RNA in sympathetic ganglia and peripheral target tissues*. Embo J, 1984. **3**(13): p. 3183-9.
132. Shelton, D.L. and L.F. Reichardt, *Expression of the beta-nerve growth factor gene correlates with the density of sympathetic innervation in effector organs*. Proc Natl Acad Sci U S A, 1984. **81**(24): p. 7951-5.
133. Tessarollo, L., *Pleiotropic functions of neurotrophins in development*. Cytokine Growth Factor Rev, 1998. **9**(2): p. 125-37.
134. Patel, T.D., et al., *Development of sensory neurons in the absence of NGF/TrkA signaling in vivo*. Neuron, 2000. **25**(2): p. 345-57.
135. Glebova, N.O. and D.D. Ginty, *Heterogeneous requirement of NGF for sympathetic target innervation in vivo*. J Neurosci, 2004. **24**(3): p. 743-51.
136. Ye, H., et al., *Evidence in support of signaling endosome-based retrograde survival of sympathetic neurons*. Neuron, 2003. **39**(1): p. 57-68.

137. Kuruvilla, R., et al., *A neurotrophin signaling cascade coordinates sympathetic neuron development through differential control of TrkA trafficking and retrograde signaling*. Cell, 2004. **118**(2): p. 243-55.
138. Radziejewski, C., et al., *Dimeric structure and conformational stability of brain-derived neurotrophic factor and neurotrophin-3*. Biochemistry, 1992. **31**(18): p. 4431-6.
139. Leibrock, J., et al., *Molecular cloning and expression of brain-derived neurotrophic factor*. Nature, 1989. **341**(6238): p. 149-52.
140. Hofer, M., et al., *Regional distribution of brain-derived neurotrophic factor mRNA in the adult mouse brain*. Embo J, 1990. **9**(8): p. 2459-64.
141. Tapia-Arancibia, L., et al., *Physiology of BDNF: focus on hypothalamic function*. Front Neuroendocrinol, 2004. **25**(2): p. 77-107.
142. Lindholm, D., et al., *Activity-dependent and hormonal regulation of neurotrophin mRNA levels in the brain--implications for neuronal plasticity*. J Neurobiol, 1994. **25**(11): p. 1362-72.
143. Hebb, C.O. and H. Konzett, *The effect of certain analgesic drugs on synaptic transmission as observed in the perfused superior cervical ganglion of the cat*. Q J Exp Physiol Cogn Med Sci, 1949. **35**(3): p. 213-7.
144. Korte, M., et al., *Hippocampal long-term potentiation is impaired in mice lacking brain-derived neurotrophic factor*. Proc Natl Acad Sci U S A, 1995. **92**(19): p. 8856-60.
145. McAllister, A.K., L.C. Katz, and D.C. Lo, *Opposing roles for endogenous BDNF and NT-3 in regulating cortical dendritic growth*. Neuron, 1997. **18**(5): p. 767-78.
146. Maisonpierre, P.C., et al., *NT-3, BDNF, and NGF in the developing rat nervous system: parallel as well as reciprocal patterns of expression*. Neuron, 1990. **5**(4): p. 501-9.
147. Schecterson, L.C. and M. Bothwell, *Novel roles for neurotrophins are suggested by BDNF and NT-3 mRNA expression in developing neurons*. Neuron, 1992. **9**(3): p. 449-63.
148. Davies, A.M., H. Thoenen, and Y.A. Barde, *Different factors from the central nervous system and periphery regulate the survival of sensory neurones*. Nature, 1986. **319**(6053): p. 497-9.
149. Barde, Y.A., et al., *Brain derived neurotrophic factor*. Prog Brain Res, 1987. **71**: p. 185-9.
150. Hofer, M.M. and Y.A. Barde, *Brain-derived neurotrophic factor prevents neuronal death in vivo*. Nature, 1988. **331**(6153): p. 261-2.
151. Jones, K.R., et al., *Targeted disruption of the BDNF gene perturbs brain and sensory neuron development but not motor neuron development*. Cell, 1994. **76**(6): p. 989-99.
152. Erfors, P., K.F. Lee, and R. Jaenisch, *Mice lacking brain-derived neurotrophic factor develop with sensory deficits*. Nature, 1994. **368**(6467): p. 147-50.
153. Wiklund, P. and P.A. Ekstrom, *Axonal outgrowth from adult mouse nodose ganglia in vitro is stimulated by neurotrophin-4 in a Trk receptor and mitogen-activated protein kinase-dependent way*. J Neurobiol, 2000. **45**(3): p. 142-51.
154. Tucker, K.L., M. Meyer, and Y.A. Barde, *Neurotrophins are required for nerve growth during development*. Nat Neurosci, 2001. **4**(1): p. 29-37.

155. Lentz, S.I., et al., *Neurotrophins support the development of diverse sensory axon morphologies*. J Neurosci, 1999. **19**(3): p. 1038-48.
156. Kohn, J., et al., *Functionally antagonistic interactions between the TrkA and p75 neurotrophin receptors regulate sympathetic neuron growth and target innervation*. J Neurosci, 1999. **19**(13): p. 5393-408.
157. Paves, H. and M. Saarma, *Neurotrophins as in vitro growth cone guidance molecules for embryonic sensory neurons*. Cell Tissue Res, 1997. **290**(2): p. 285-97.
158. Postigo, A., et al., *Distinct requirements for TrkB and TrkC signaling in target innervation by sensory neurons*. Genes Dev, 2002. **16**(5): p. 633-45.
159. Schimmang, T., et al., *Developing inner ear sensory neurons require TrkB and TrkC receptors for innervation of their peripheral targets*. Development, 1995. **121**(10): p. 3381-91.
160. Fritzsche, B., et al., *The role of neurotrophic factors in regulating the development of inner ear innervation*. Trends Neurosci, 1997. **20**(4): p. 159-64.
161. Wirth, M.J., et al., *Accelerated dendritic development of rat cortical pyramidal cells and interneurons after biolistic transfection with BDNF and NT4/5*. Development, 2003. **130**(23): p. 5827-38.
162. Kohara, K., et al., *Inhibitory but not excitatory cortical neurons require presynaptic brain-derived neurotrophic factor for dendritic development, as revealed by chimera cell culture*. J Neurosci, 2003. **23**(14): p. 6123-31.
163. Jin, X., et al., *Brain-derived neurotrophic factor mediates activity-dependent dendritic growth in nonpyramidal neocortical interneurons in developing organotypic cultures*. J Neurosci, 2003. **23**(13): p. 5662-73.
164. Sang, Q. and S.S. Tan, *Contact-associated neurite outgrowth and branching of immature cortical interneurons*. Cereb Cortex, 2003. **13**(6): p. 677-83.
165. Horch, H.W. and L.C. Katz, *BDNF release from single cells elicits local dendritic growth in nearby neurons*. Nat Neurosci, 2002. **5**(11): p. 1177-84.
166. Horch, H.W., et al., *Destabilization of cortical dendrites and spines by BDNF*. Neuron, 1999. **23**(2): p. 353-64.
167. Labelle, C. and N. Leclerc, *Exogenous BDNF, NT-3 and NT-4 differentially regulate neurite outgrowth in cultured hippocampal neurons*. Brain Res Dev Brain Res, 2000. **123**(1): p. 1-11.
168. Xu, B., et al., *The role of brain-derived neurotrophic factor receptors in the mature hippocampus: modulation of long-term potentiation through a presynaptic mechanism involving TrkB*. J Neurosci, 2000. **20**(18): p. 6888-97.
169. Hohn, A., et al., *Identification and characterization of a novel member of the nerve growth factor/brain-derived neurotrophic factor family*. Nature, 1990. **344**(6264): p. 339-41.
170. Rosenthal, A., et al., *Primary structure and biological activity of a novel human neurotrophic factor*. Neuron, 1990. **4**(5): p. 767-73.
171. Glass, D.J. and G.D. Yancopoulos, *The neurotrophins and their receptors*. Trends Cell Biol, 1993. **3**(8): p. 262-8.
172. Ernfors, P., et al., *Molecular cloning and neurotrophic activities of a protein with structural similarities to nerve growth factor: developmental and topographical expression in the brain*. Proc Natl Acad Sci U S A, 1990. **87**(14): p. 5454-8.
173. Farinas, I., et al., *Severe sensory and sympathetic deficits in mice lacking neurotrophin-3*. Nature, 1994. **369**(6482): p. 658-61.

174. Ockel, M., et al., *Roles of neurotrophin-3 during early development of the peripheral nervous system*. Philos Trans R Soc Lond B Biol Sci, 1996. **351**(1338): p. 383-7.
175. Wilkinson, G.A., et al., *Neurotrophin-3 is a survival factor in vivo for early mouse trigeminal neurons*. J Neurosci, 1996. **16**(23): p. 7661-9.
176. Farinas, I., et al., *Lack of neurotrophin-3 results in death of spinal sensory neurons and premature differentiation of their precursors*. Neuron, 1996. **17**(6): p. 1065-78.
177. Kalcheim, C., C. Carmeli, and A. Rosenthal, *Neurotrophin 3 is a mitogen for cultured neural crest cells*. Proc Natl Acad Sci U S A, 1992. **89**(5): p. 1661-5.
178. Pinco, O., et al., *Neurotrophin-3 affects proliferation and differentiation of distinct neural crest cells and is present in the early neural tube of avian embryos*. J Neurobiol, 1993. **24**(12): p. 1626-41.
179. Tessarollo, L., et al., *trkC, a receptor for neurotrophin-3, is widely expressed in the developing nervous system and in non-neuronal tissues*. Development, 1993. **118**(2): p. 463-75.
180. ElShamy, W.M. and P. Ernfors, *A local action of neurotrophin-3 prevents the death of proliferating sensory neuron precursor cells*. Neuron, 1996. **16**(5): p. 963-72.
181. Rice, F.L., et al., *Differential dependency of unmyelinated and A delta epidermal and upper dermal innervation on neurotrophins, trk receptors, and p75LNGFR*. Dev Biol, 1998. **198**(1): p. 57-81.
182. Belliveau, D.J., et al., *NGF and neurotrophin-3 both activate TrkA on sympathetic neurons but differentially regulate survival and neuritegenesis*. J Cell Biol, 1997. **136**(2): p. 375-88.
183. Adler, R., et al., *Cholinergic neuronotrophic factors: intraocular distribution of trophic activity for ciliary neurons*. Science, 1979. **204**(4400): p. 1434-6.
184. Barbin, G., M. Manthorpe, and S. Varon, *Purification of the chick eye ciliary neuronotrophic factor*. J Neurochem, 1984. **43**(5): p. 1468-78.
185. Unsicker, K., G. Stahnke, and T.H. Muller, *Survival, morphology, and catecholamine storage of chromaffin cells in serum-free culture: evidence for a survival and differentiation promoting activity in medium conditioned by purified chromaffin cells*. Neurochem Res, 1987. **12**(11): p. 995-1003.
186. Masiakowski, P., et al., *Recombinant Human and Rat Ciliary Neurotrophic Factors*. Journal of Neurochemistry, 1991. **57**(3): p. 1003-1012.
187. Lam, A., et al., *Sequence and Structural Organization of the Human Gene Encoding Ciliary Neurotrophic Factor*. Gene, 1991. **102**(2): p. 271-276.
188. Negro, A., et al., *Cloning and Expression of Human Ciliary Neurotrophic Factor*. European Journal of Biochemistry, 1991. **201**(1): p. 289-294.
189. Bazan, J.F., *Neurotrophic Cytokines in the Hematopoietic Fold*. Neuron, 1991. **7**(2): p. 197-208.
190. Taga, T. and T. Kishimoto, *Cytokine Receptors and Signal Transduction*. Faseb Journal, 1992. **6**(15): p. 3387-3396.
191. Williams, L.R., et al., *High Ciliary Neurotrophic Specific Activity in Rat Peripheral-Nerve*. International Journal of Developmental Neuroscience, 1984. **2**(2): p. 177-180.
192. Stockli, K.A., et al., *Regional Distribution, Developmental-Changes, and Cellular-Localization of Cntf Messenger-Rna and Protein in the Rat-Brain*. Journal of Cell Biology, 1991. **115**(2): p. 447-459.

193. Ip, N.Y., et al., *The Alpha Component of the Cntf Receptor Is Required for Signaling and Defines Potential Cntf Targets in the Adult and during Development*. *Neuron*, 1993. **10**(1): p. 89-102.
194. Ip, N.Y., et al., *Cntf and Lif Act on Neuronal and Hematopoietic-Cells Via Shared Signal Transducing Component-Gp130 and Lifr-Beta*. *Journal of Cellular Biochemistry*, 1993: p. 64-64.
195. Sendtner, M., et al., *Ciliary Neurotrophic Factor*. *Journal of Neurobiology*, 1994. **25**(11): p. 1436-1453.
196. Ernsberger, U., M. Sendtner, and H. Rohrer, *Proliferation and Differentiation of Embryonic Chick Sympathetic Neurons - Effects of Ciliary Neurotrophic Factor*. *Neuron*, 1989. **2**(3): p. 1275-1284.
197. Arakawa, Y., M. Sendtner, and H. Thoenen, *Survival Effect of Ciliary Neurotrophic Factor (Cntf) on Chick Embryonic Motoneurons in Culture - Comparison with Other Neurotrophic Factors and Cytokines*. *Journal of Neuroscience*, 1990. **10**(11): p. 3507-3515.
198. Ip, N.Y., et al., *Ciliary Neurotrophic Factor Enhances Neuronal Survival in Embryonic Rat Hippocampal Cultures*. *Journal of Neuroscience*, 1991. **11**(10): p. 3124-3134.
199. Larkfors, L., R.M. Lindsay, and R.F. Alderson, *Ciliary Neurotrophic Factor Enhances the Survival of Purkinje Cells in-Vitro*. *European Journal of Neuroscience*, 1994. **6**(6): p. 1015-1025.
200. Masu, Y., et al., *Disruption of the Cntf Gene Results in Motor-Neuron Degeneration*. *Nature*, 1993. **365**(6441): p. 27-32.
201. Martin-Zanca, D., S.H. Hughes, and M. Barbacid, *A human oncogene formed by the fusion of truncated tropomyosin and protein tyrosine kinase sequences*. *Nature*, 1986. **319**(6056): p. 743-8.
202. Martin-Zanca, D., et al., *Molecular and biochemical characterization of the human trk proto-oncogene*. *Mol Cell Biol*, 1989. **9**(1): p. 24-33.
203. Barbacid, M., *The Trk family of neurotrophin receptors*. *J Neurobiol*, 1994. **25**(11): p. 1386-403.
204. Klein, R., et al., *trkB, a novel tyrosine protein kinase receptor expressed during mouse neural development*. *Embo J*, 1989. **8**(12): p. 3701-9.
205. Klein, R., et al., *Expression of the tyrosine kinase receptor gene trkB is confined to the murine embryonic and adult nervous system*. *Development*, 1990. **109**(4): p. 845-50.
206. Lamballe, F., R. Klein, and M. Barbacid, *trkC, a new member of the trk family of tyrosine protein kinases, is a receptor for neurotrophin-3*. *Cell*, 1991. **66**(5): p. 967-79.
207. Klein, R., et al., *The trkB tyrosine protein kinase is a receptor for brain-derived neurotrophic factor and neurotrophin-3*. *Cell*, 1991. **66**(2): p. 395-403.
208. Soppet, D., et al., *The neurotrophic factors brain-derived neurotrophic factor and neurotrophin-3 are ligands for the trkB tyrosine kinase receptor*. *Cell*, 1991. **65**(5): p. 895-903.
209. Squinto, S.P., et al., *trkB encodes a functional receptor for brain-derived neurotrophic factor and neurotrophin-3 but not nerve growth factor*. *Cell*, 1991. **65**(5): p. 885-93.
210. Berkemeier, L.R., et al., *Neurotrophin-5: a novel neurotrophic factor that activates trk and trkB*. *Neuron*, 1991. **7**(5): p. 857-66.

211. Klein, R., et al., *The trkB tyrosine protein kinase is a receptor for neurotrophin-4*. *Neuron*, 1992. **8**(5): p. 947-56.
212. Ip, N.Y., et al., *Mammalian neurotrophin-4: structure, chromosomal localization, tissue distribution, and receptor specificity*. *Proc Natl Acad Sci U S A*, 1992. **89**(7): p. 3060-4.
213. Benito-Gutierrez, E., et al., *The single AmphiTrk receptor highlights increased complexity of neurotrophin signalling in vertebrates and suggests an early role in developing sensory neuroepidermal cells*. *Development*, 2005. **132**(9): p. 2191-202.
214. Robinson, D.R., Y.M. Wu, and S.F. Lin, *The protein tyrosine kinase family of the human genome*. *Oncogene*, 2000. **19**(49): p. 5548-57.
215. Schneider, R. and M. Schweiger, *A novel modular mosaic of cell adhesion motifs in the extracellular domains of the neurogenic trk and trkB tyrosine kinase receptors*. *Oncogene*, 1991. **6**(10): p. 1807-11.
216. Martin-Zanca, D., M. Barbacid, and L.F. Parada, *Expression of the trk proto-oncogene is restricted to the sensory cranial and spinal ganglia of neural crest origin in mouse development*. *Genes Dev*, 1990. **4**(5): p. 683-94.
217. Carroll, S.L., et al., *Dorsal root ganglion neurons expressing trk are selectively sensitive to NGF deprivation in utero*. *Neuron*, 1992. **9**(4): p. 779-88.
218. Lamballe, F., R.J. Smeyne, and M. Barbacid, *Developmental expression of trkC, the neurotrophin-3 receptor, in the mammalian nervous system*. *J Neurosci*, 1994. **14**(1): p. 14-28.
219. Stephens, R.M., et al., *Trk receptors use redundant signal transduction pathways involving SHC and PLC-gamma 1 to mediate NGF responses*. *Neuron*, 1994. **12**(3): p. 691-705.
220. Huang, E.J. and L.F. Reichardt, *Neurotrophins: roles in neuronal development and function*. *Annu Rev Neurosci*, 2001. **24**: p. 677-736.
221. Inagaki, N., H. Thoenen, and D. Lindholm, *TrkA tyrosine residues involved in NGF-induced neurite outgrowth of PC12 cells*. *Eur J Neurosci*, 1995. **7**(6): p. 1125-33.
222. Roux, P.P. and P.A. Barker, *Neurotrophin signaling through the p75 neurotrophin receptor*. *Prog Neurobiol*, 2002. **67**(3): p. 203-33.
223. Shooter, E.M., *Early days of the nerve growth factor proteins*. *Annu Rev Neurosci*, 2001. **24**: p. 601-29.
224. Beattie, E.C., et al., *NGF signals through TrkA to increase clathrin at the plasma membrane and enhance clathrin-mediated membrane trafficking*. *J Neurosci*, 2000. **20**(19): p. 7325-33.
225. Shao, Y., et al., *Pincher, a pinocytic chaperone for nerve growth factor/TrkA signaling endosomes*. *J Cell Biol*, 2002. **157**(4): p. 679-91.
226. Howe, C.L., et al., *NGF signaling from clathrin-coated vesicles: evidence that signaling endosomes serve as a platform for the Ras-MAPK pathway*. *Neuron*, 2001. **32**(5): p. 801-14.
227. Riccio, A., et al., *Mediation by a CREB family transcription factor of NGF-dependent survival of sympathetic neurons*. *Science*, 1999. **286**(5448): p. 2358-61.
228. MacIannis, B.L. and R.B. Campenot, *Retrograde support of neuronal survival without retrograde transport of nerve growth factor*. *Science*, 2002. **295**(5559): p. 1536-9.

229. Klein, R., et al., *Targeted disruption of the trkB neurotrophin receptor gene results in nervous system lesions and neonatal death*. Cell, 1993. 75(1): p. 113-22.
230. Klein, R., et al., *Disruption of the neurotrophin-3 receptor gene trkC eliminates muscle afferents and results in abnormal movements*. Nature, 1994. 368(6468): p. 249-51.
231. Arevalo, J.C. and S.H. Wu, *Neurotrophin signaling: many exciting surprises!* Cell Mol Life Sci, 2006. 63(13): p. 1523-37.
232. Lee, R., et al., *Regulation of cell survival by secreted proneurotrophins*. Science, 2001. 294(5548): p. 1945-8.
233. Nykjaer, A., et al., *Sortilin is essential for proNGF-induced neuronal cell death*. Nature, 2004. 427(6977): p. 843-8.
234. Teng, H.K., et al., *ProBDNF induces neuronal apoptosis via activation of a receptor complex of p75NTR and sortilin*. J Neurosci, 2005. 25(22): p. 5455-63.
235. Rabizadeh, S., et al., *Induction of apoptosis by the low-affinity NGF receptor*. Science, 1993. 261(5119): p. 345-8.
236. Barrett, G.L. and P.F. Bartlett, *The p75 nerve growth factor receptor mediates survival or death depending on the stage of sensory neuron development*. Proc Natl Acad Sci U S A, 1994. 91(14): p. 6501-5.
237. Frade, J.M. and Y.A. Barde, *Nerve growth factor: two receptors, multiple functions*. Bioessays, 1998. 20(2): p. 137-45.
238. Hamanoue, M., et al., *p75-mediated NF-kappaB activation enhances the survival response of developing sensory neurons to nerve growth factor*. Mol Cell Neurosci, 1999. 14(1): p. 28-40.
239. Squinto, S.P., et al., *Identification of functional receptors for ciliary neurotrophic factor on neuronal cell lines and primary neurons*. Neuron, 1990. 5(6): p. 757-66.
240. Davis, S., et al., *The receptor for ciliary neurotrophic factor*. Science, 1991. 253(5015): p. 59-63.
241. Stahl, N., et al., *Cross-linking identifies leukemia inhibitory factor-binding protein as a ciliary neurotrophic factor receptor component*. J Biol Chem, 1993. 268(11): p. 7628-31.
242. Gearing, D.P., et al., *Proliferative responses and binding properties of hematopoietic cells transfected with low-affinity receptors for leukemia inhibitory factor, oncostatin M, and ciliary neurotrophic factor*. Proc Natl Acad Sci U S A, 1994. 91(3): p. 1119-23.
243. Davis, S., et al., *Released form of CNTF receptor alpha component as a soluble mediator of CNTF responses*. Science, 1993. 259(5102): p. 1736-9.
244. Baumann, H., et al., *Reconstitution of the response to leukemia inhibitory factor, oncostatin M, and ciliary neurotrophic factor in hepatoma cells*. J Biol Chem, 1993. 268(12): p. 8414-7.
245. Gearing, D.P., et al., *Leukemia inhibitory factor receptor is structurally related to the IL-6 signal transducer, gp130*. Embo J, 1991. 10(10): p. 2839-48.
246. Davis, S., et al., *LIFR beta and gp130 as heterodimerizing signal transducers of the tripartite CNTF receptor*. Science, 1993. 260(5115): p. 1805-8.
247. DeChiara, T.M., et al., *Mice lacking the CNTF receptor, unlike mice lacking CNTF, exhibit profound motor neuron deficits at birth*. Cell, 1995. 83(2): p. 313-22.

248. Li, M., M. Sendtner, and A. Smith, *Essential function of LIF receptor in motor neurons*. *Nature*, 1995. **378**(6558): p. 724-7.
249. Ware, C.B., et al., *Targeted disruption of the low-affinity leukemia inhibitory factor receptor gene causes placental, skeletal, neural and metabolic defects and results in perinatal death*. *Development*, 1995. **121**(5): p. 1283-99.
250. Nakashima, K., et al., *Developmental requirement of gp130 signaling in neuronal survival and astrocyte differentiation*. *J Neurosci*, 1999. **19**(13): p. 5429-34.
251. Scott, B.S., *The effect of elevated potassium on the time course of neuron survival in cultures of dissociated dorsal root ganglia*. *J Cell Physiol*, 1977. **91**(2): p. 305-16.
252. Bennett, M.R. and K. Lai, *Cell death during development of the topographical distributions of cutaneous sensory neurons in amphibian ganglia*. *Dev Biol*, 1981. **85**(1): p. 224-6.
253. Lipton, S.A., *Blockade of electrical activity promotes the death of mammalian retinal ganglion cells in culture*. *Proc Natl Acad Sci U S A*, 1986. **83**(24): p. 9774-8.
254. Gallo, V., et al., *The role of depolarization in the survival and differentiation of cerebellar granule cells in culture*. *J Neurosci*, 1987. **7**(7): p. 2203-13.
255. Brenneman, D.E., et al., *N-methyl-D-aspartate receptors influence neuronal survival in developing spinal cord cultures*. *Brain Res Dev Brain Res*, 1990. **51**(1): p. 63-8.
256. Baker, R.E., J.M. Ruijter, and D. Bingmann, *Effect of chronic exposure to high magnesium on neuron survival in long-term neocortical explants of neonatal rats in vitro*. *Int J Dev Neurosci*, 1991. **9**(6): p. 597-606.
257. Ling, D.S., R.E. Petroski, and H.M. Geller, *Both survival and development of spontaneously active rat hypothalamic neurons in dissociated culture are dependent on membrane depolarization*. *Brain Res Dev Brain Res*, 1991. **59**(1): p. 99-103.
258. Larmet, Y., A.C. Dolphin, and A.M. Davies, *Intracellular calcium regulates the survival of early sensory neurons before they become dependent on neurotrophic factors*. *Neuron*, 1992. **9**(3): p. 563-74.
259. Furber, S., R.W. Oppenheim, and D. Prevet, *Naturally-occurring neuron death in the ciliary ganglion of the chick embryo following removal of preganglionic input: evidence for the role of afferents in ganglion cell survival*. *J Neurosci*, 1987. **7**(6): p. 1816-32.
260. Pasic, T.R. and E.W. Rubel, *Rapid changes in cochlear nucleus cell size following blockade of auditory nerve electrical activity in gerbils*. *J Comp Neurol*, 1989. **283**(4): p. 474-80.
261. Sur, M., A. Angelucci, and J. Sharma, *Rewiring cortex: the role of patterned activity in development and plasticity of neocortical circuits*. *J Neurobiol*, 1999. **41**(1): p. 33-43.
262. Johnson, E.M., Jr., T. Koike, and J. Franklin, *A "calcium set-point hypothesis" of neuronal dependence on neurotrophic factor*. *Exp Neurol*, 1992. **115**(1): p. 163-6.
263. Koike, T. and S. Tanaka, *Evidence that nerve growth factor dependence of sympathetic neurons for survival in vitro may be determined by levels of cytoplasmic free Ca²⁺*. *Proc Natl Acad Sci U S A*, 1991. **88**(9): p. 3892-6.

264. Eichler, M.E., J.M. Dubinsky, and K.M. Rich, *Relationship of intracellular calcium to dependence on nerve growth factor in dorsal root ganglion neurons in cell culture*. J Neurochem, 1992. **58**(1): p. 263-9.
265. Welch, M.D., et al., *Actin dynamics in vivo*. Curr Opin Cell Biol, 1997. **9**(1): p. 54-61.
266. Meyer, G. and E.L. Feldman, *Signaling mechanisms that regulate actin-based motility processes in the nervous system*. J Neurochem, 2002. **83**(3): p. 490-503.
267. Grunwald, I.C. and R. Klein, *Axon guidance: receptor complexes and signaling mechanisms*. Curr Opin Neurobiol, 2002. **12**(3): p. 250-9.
268. Charron, F. and M. Tessier-Lavigne, *Novel brain wiring functions for classical morphogens: a role as graded positional cues in axon guidance*. Development, 2005. **132**(10): p. 2251-62.
269. Campenot, R.B., *Development of sympathetic neurons in compartmentalized cultures. II Local control of neurite growth by nerve growth factor*. Dev Biol, 1982. **93**(1): p. 1-12.
270. Gundersen, R.W. and J.N. Barrett, *Neuronal chemotaxis: chick dorsal-root axons turn toward high concentrations of nerve growth factor*. Science, 1979. **206**(4422): p. 1079-80.
271. Song, H.J., G.L. Ming, and M.M. Poo, *cAMP-induced switching in turning direction of nerve growth cones*. Nature, 1997. **388**(6639): p. 275-9.
272. McAllister, A.K., *Subplate neurons: a missing link among neurotrophins, activity, and ocular dominance plasticity?* Proc Natl Acad Sci U S A, 1999. **96**(24): p. 13600-2.
273. Davies, A.M., A.G. Lumsden, and H. Rohrer, *Neural crest-derived proprioceptive neurons express nerve growth factor receptors but are not supported by nerve growth factor in culture*. Neuroscience, 1987. **20**(1): p. 37-46.
274. Deckwerth, T.L., et al., *BAX is required for neuronal death after trophic factor deprivation and during development*. Neuron, 1996. **17**(3): p. 401-11.
275. Albers, K.M., D.E. Wright, and B.M. Davis, *Overexpression of nerve growth factor in epidermis of transgenic mice causes hypertrophy of the peripheral nervous system*. J Neurosci, 1994. **14**(3 Pt 2): p. 1422-32.
276. Albers, K.M., et al., *Cutaneous overexpression of NT-3 increases sensory and sympathetic neuron number and enhances touch dome and hair follicle innervation*. J Cell Biol, 1996. **134**(2): p. 487-97.
277. Hoyle, G.W., et al., *Expression of NGF in sympathetic neurons leads to excessive axon outgrowth from ganglia but decreased terminal innervation within tissues*. Neuron, 1993. **10**(6): p. 1019-34.
278. Richardson, P.M., *Ciliary neurotrophic factor: a review*. Pharmacol Ther, 1994. **63**(2): p. 187-98.
279. Pawson, T. and P. Nash, *Protein-protein interactions define specificity in signal transduction*. Genes Dev, 2000. **14**(9): p. 1027-47.
280. Stahl, N. and G.D. Yancopoulos, *The tripartite CNTF receptor complex: activation and signaling involves components shared with other cytokines*. J Neurobiol, 1994. **25**(11): p. 1454-66.
281. Bonni, A., et al., *Characterization of a pathway for ciliary neurotrophic factor signaling to the nucleus*. Science, 1993. **262**(5139): p. 1575-9.
282. Boulton, T.G., N. Stahl, and G.D. Yancopoulos, *Ciliary neurotrophic factor/leukemia inhibitory factor/interleukin 6/oncostatin M family of*

- cytokines induces tyrosine phosphorylation of a common set of proteins overlapping those induced by other cytokines and growth factors.* J Biol Chem, 1994. **269**(15): p. 11648-55.
283. Homburg, S., et al., *A fast signal-induced activation of Poly(ADP-ribose) polymerase: a novel downstream target of phospholipase c.* J Cell Biol, 2000. **150**(2): p. 293-307.
284. Midorikawa, R., Y. Takei, and N. Hirokawa, *KIF4 motor regulates activity-dependent neuronal survival by suppressing PARP-1 enzymatic activity.* Cell, 2006. **125**(2): p. 371-83.
285. Vaillant, A.R., et al., *Depolarization and neurotrophins converge on the phosphatidylinositol 3-kinase-Akt pathway to synergistically regulate neuronal survival.* Journal of Cell Biology, 1999. **146**(5): p. 955-966.
286. Singh, K.K. and F.D. Miller, *Activity regulates positive and negative neurotrophin-derived signals to determine axon competition.* Neuron, 2005. **45**(6): p. 837-45.
287. Nguyen, P.V., T. Abel, and E.R. Kandel, *Requirement of a critical period of transcription for induction of a late phase of LTP.* Science, 1994. **265**(5175): p. 1104-7.
288. Kang, H. and E.M. Schuman, *A requirement for local protein synthesis in neurotrophin-induced hippocampal synaptic plasticity.* Science, 1996. **273**(5280): p. 1402-6.
289. Frey, U. and R.G. Morris, *Synaptic tagging and long-term potentiation.* Nature, 1997. **385**(6616): p. 533-6.
290. Martin, K.C., et al., *Synapse-specific, long-term facilitation of aplysia sensory to motor synapses: a function for local protein synthesis in memory storage.* Cell, 1997. **91**(7): p. 927-38.
291. Sen, R. and D. Baltimore, *Inducibility of kappa immunoglobulin enhancer-binding protein *Nf-kappa B* by a posttranslational mechanism.* Cell, 1986. **47**(6): p. 921-8.
292. Baeuerle, P.A. and T. Henkel, *Function and activation of *NF-kappa B* in the immune system.* Annu Rev Immunol, 1994. **12**: p. 141-79.
293. Baldwin, A.S., Jr., *The *NF-kappa B* and *I kappa B* proteins: new discoveries and insights.* Annu Rev Immunol, 1996. **14**: p. 649-83.
294. Lin, L. and S. Ghosh, *A glycine-rich region in *NF-kappaB p105* functions as a processing signal for the generation of the *p50* subunit.* Mol Cell Biol, 1996. **16**(5): p. 2248-54.
295. Orian, A., et al., *Structural motifs involved in ubiquitin-mediated processing of the *NF-kappaB* precursor *p105*: roles of the glycine-rich region and a downstream ubiquitination domain.* Mol Cell Biol, 1999. **19**(5): p. 3664-73.
296. Karin, M. and Y. Ben-Neriah, *Phosphorylation meets ubiquitination: the control of *NF-[kappa]B* activity.* Annu Rev Immunol, 2000. **18**: p. 621-63.
297. Lee, R. and T. Collins, *Nuclear factor-kappaB and cell survival: IAPs call for support.* Circ Res, 2001. **88**(3): p. 262-4.
298. Hayden, M.S. and S. Ghosh, *Signaling to *NF-kappaB*.* Genes Dev, 2004. **18**(18): p. 2195-224.
299. Bours, V., et al., *Lymphocyte activation and the family of *NF-kappa B* transcription factor complexes.* Curr Top Microbiol Immunol, 1992. **182**: p. 411-20.

300. Grilli, M., J.J. Chiu, and M.J. Lenardo, *NF-kappa B and Rel: participants in a multifunctional transcriptional regulatory system*. *Int Rev Cytol*, 1993. **143**: p. 1-62.
301. Muller, J.M., H.W. Ziegler-Heitbrock, and P.A. Baeuerle, *Nuclear factor kappa B, a mediator of lipopolysaccharide effects*. *Immunobiology*, 1993. **187**(3-5): p. 233-56.
302. Baldwin, A.S., *Control of oncogenesis and cancer therapy resistance by the transcription factor NF-kappaB*. *J Clin Invest*, 2001. **107**(3): p. 241-6.
303. Pande, V. and M.J. Ramos, *NF-kappaB in human disease: current inhibitors and prospects for de novo structure based design of inhibitors*. *Curr Med Chem*, 2005. **12**(3): p. 357-74.
304. Korner, M., et al., *A brain-specific transcription activator*. *Neuron*, 1989. **3**(5): p. 563-72.
305. Kaltschmidt, C., B. Kaltschmidt, and P.A. Baeuerle, *Brain synapses contain inducible forms of the transcription factor NF-kappa B*. *Mech Dev*, 1993. **43**(2-3): p. 135-47.
306. Kaltschmidt, C., et al., *Constitutive NF-kappa B activity in neurons*. *Mol Cell Biol*, 1994. **14**(6): p. 3981-92.
307. O'Neill, L.A. and C. Kaltschmidt, *NF-kappa B: a crucial transcription factor for glial and neuronal cell function*. *Trends Neurosci*, 1997. **20**(6): p. 252-8.
308. Bhakar, A.L., et al., *Constitutive nuclear factor-kappa B activity is required for central neuron survival*. *J Neurosci*, 2002. **22**(19): p. 8466-75.
309. Yalcin, A., et al., *Apoptosis in cerebellar granule neurons is associated with reduced interaction between CREB-binding protein and NF-kappaB*. *J Neurochem*, 2003. **84**(2): p. 397-408.
310. Wellmann, H., B. Kaltschmidt, and C. Kaltschmidt, *Retrograde transport of transcription factor NF-kappa B in living neurons*. *J Biol Chem*, 2001. **276**(15): p. 11821-9.
311. Meffert, M.K., et al., *NF-kappa B functions in synaptic signaling and behavior*. *Nat Neurosci*, 2003. **6**(10): p. 1072-8.
312. Mikenberg, I., et al., *Transcription factor NF-kappaB is transported to the nucleus via cytoplasmic dynein/dynactin motor complex in hippocampal neurons*. *PLoS ONE*, 2007. **2**(7): p. e589.
313. Merlo, E., et al., *Activation of the transcription factor NF-kappaB by retrieval is required for long-term memory reconsolidation*. *Learn Mem*, 2005. **12**(1): p. 23-9.
314. Kaltschmidt, B., et al., *NF-kappaB regulates spatial memory formation and synaptic plasticity through protein kinase A/CREB signaling*. *Mol Cell Biol*, 2006. **26**(8): p. 2936-46.
315. Bakalkin, G., T. Yakovleva, and L. Terenius, *NF-kappa B-like factors in the murine brain. Developmentally-regulated and tissue-specific expression*. *Brain Res Mol Brain Res*, 1993. **20**(1-2): p. 137-46.
316. Widera, D., et al., *Potential role of NF-kappaB in adult neural stem cells: the underrated steersman?* *Int J Dev Neurosci*, 2006. **24**(2-3): p. 91-102.
317. Lezoualc'h, F. and C. Behl, *Transcription factor NF-kappaB: friend or foe of neurons?* *Mol Psychiatry*, 1998. **3**(1): p. 15-20.
318. Maggirwar, S.B., et al., *Nerve growth factor-dependent activation of NF-kappaB contributes to survival of sympathetic neurons*. *J Neurosci*, 1998. **18**(24): p. 10356-65.

319. Middleton, G., et al., *Cytokine-induced nuclear factor kappa B activation promotes the survival of developing neurons*. J Cell Biol, 2000. **148**(2): p. 325-32.
320. Koulich, E., et al., *NF-kappaB is involved in the survival of cerebellar granule neurons: association of IkappaBbeta [correction of Ikappabeta] phosphorylation with cell survival*. J Neurochem, 2001. **76**(4): p. 1188-98.
321. Gutierrez, H., et al., *NF-kappaB signalling regulates the growth of neural processes in the developing PNS and CNS*. Development, 2005. **132**(7): p. 1713-26.
322. Taglialatela, G., R. Robinson, and J.R. Perez-Polo, *Inhibition of nuclear factor kappa B (NFkappaB) activity induces nerve growth factor-resistant apoptosis in PC12 cells*. J Neurosci Res, 1997. **47**(2): p. 155-62.
323. Chiarugi, A., *Characterization of the molecular events following impairment of NF-kappaB-driven transcription in neurons*. Brain Res Mol Brain Res, 2002. **109**(1-2): p. 179-88.
324. Schneider, A., et al., *NF-kappaB is activated and promotes cell death in focal cerebral ischemia*. Nat Med, 1999. **5**(5): p. 554-9.
325. Nurmi, A., et al., *Nuclear factor-kappaB contributes to infarction after permanent focal ischemia*. Stroke, 2004. **35**(4): p. 987-91.
326. Terai, K., A. Matsuo, and P.L. McGeer, *Enhancement of immunoreactivity for NF-kappa B in the hippocampal formation and cerebral cortex of Alzheimer's disease*. Brain Res, 1996. **735**(1): p. 159-68.
327. Kaltschmidt, B., et al., *Transcription factor NF-kappaB is activated in primary neurons by amyloid beta peptides and in neurons surrounding early plaques from patients with Alzheimer disease*. Proc Natl Acad Sci U S A, 1997. **94**(6): p. 2642-7.
328. Hunot, S., et al., *Nuclear translocation of NF-kappaB is increased in dopaminergic neurons of patients with parkinson disease*. Proc Natl Acad Sci U S A, 1997. **94**(14): p. 7531-6.
329. Grilli, M., et al., *Interleukin-1beta and glutamate activate the NF-kappaB/Rel binding site from the regulatory region of the amyloid precursor protein gene in primary neuronal cultures*. J Biol Chem, 1996. **271**(25): p. 15002-7.
330. Qin, Z.H., et al., *Nuclear factor kappaB nuclear translocation upregulates c-Myc and p53 expression during NMDA receptor-mediated apoptosis in rat striatum*. J Neurosci, 1999. **19**(10): p. 4023-33.
331. Luo, Y., et al., *Intrastriatal dopamine injection induces apoptosis through oxidation-involved activation of transcription factors AP-1 and NF-kappaB in rats*. Mol Pharmacol, 1999. **56**(2): p. 254-64.
332. Pizzi, M., et al., *Opposing roles for NF-kappa B/Rel factors p65 and c-Rel in the modulation of neuron survival elicited by glutamate and interleukin-1beta*. J Biol Chem, 2002. **277**(23): p. 20717-23.
333. Aleyasin, H., et al., *Nuclear factor-(kappa)B modulates the p53 response in neurons exposed to DNA damage*. J Neurosci, 2004. **24**(12): p. 2963-73.
334. Khoshnan, A., et al., *Activation of the IkappaB kinase complex and nuclear factor-kappaB contributes to mutant huntingtin neurotoxicity*. J Neurosci, 2004. **24**(37): p. 7999-8008.
335. Pannaccione, A., et al., *Nuclear factor-kappaB activation by reactive oxygen species mediates voltage-gated K⁺ current enhancement by neurotoxic beta-amyloid peptides in nerve growth factor-differentiated PC-12 cells and hippocampal neurones*. J Neurochem, 2005. **94**(3): p. 572-86.

336. Mattson, M.P. and S. Camandola, *NF-kappaB in neuronal plasticity and neurodegenerative disorders*. J Clin Invest, 2001. **107**(3): p. 247-54.
337. Siebenlist, U., G. Franzoso, and K. Brown, *Structure, regulation and function of NF-kappa B*. Annu Rev Cell Biol, 1994. **10**: p. 405-55.
338. Ghosh, S., M.J. May, and E.B. Kopp, *NF-kappa B and Rel proteins: evolutionarily conserved mediators of immune responses*. Annu Rev Immunol, 1998. **16**: p. 225-60.
339. Barger, S.W., et al., *Tumor necrosis factors alpha and beta protect neurons against amyloid beta-peptide toxicity: evidence for involvement of a kappa B-binding factor and attenuation of peroxide and Ca²⁺ accumulation*. Proc Natl Acad Sci U S A, 1995. **92**(20): p. 9328-32.
340. Guerrini, L., F. Blasi, and S. Denis-Donini, *Synaptic activation of NF-kappa B by glutamate in cerebellar granule neurons in vitro*. Proc Natl Acad Sci U S A, 1995. **92**(20): p. 9077-81.
341. Carter, B.D., et al., *Selective activation of NF-kappa B by nerve growth factor through the neurotrophin receptor p75*. Science, 1996. **272**(5261): p. 542-5.
342. Krushel, L.A., et al., *NF-kappaB activity is induced by neural cell adhesion molecule binding to neurons and astrocytes*. J Biol Chem, 1999. **274**(4): p. 2432-9.
343. Glazner, G.W., S. Camandola, and M.P. Mattson, *Nuclear factor-kappaB mediates the cell survival-promoting action of activity-dependent neurotrophic factor peptide-9*. J Neurochem, 2000. **75**(1): p. 101-8.
344. Rice, N.R., M.L. MacKichan, and A. Israel, *The precursor of NF-kappa B p50 has I kappa B-like functions*. Cell, 1992. **71**(2): p. 243-53.
345. Mercurio, F., et al., *p105 and p98 precursor proteins play an active role in NF-kappa B-mediated signal transduction*. Genes Dev, 1993. **7**(4): p. 705-18.
346. Dejardin, E., et al., *The lymphotoxin-beta receptor induces different patterns of gene expression via two NF-kappaB pathways*. Immunity, 2002. **17**(4): p. 525-35.
347. Xiao, W., *Advances in NF-kappaB signaling transduction and transcription*. Cell Mol Immunol, 2004. **1**(6): p. 425-35.
348. Xiao, G., et al., *Retroviral oncoprotein Tax induces processing of NF-kappaB2/p100 in T cells: evidence for the involvement of IKKalpha*. Embo J, 2001. **20**(23): p. 6805-15.
349. Xiao, G., et al., *Alternative pathways of NF-kappaB activation: a double-edged sword in health and disease*. Cytokine Growth Factor Rev, 2006. **17**(4): p. 281-93.
350. Takada, Y., et al., *Hydrogen peroxide activates NF-kappa B through tyrosine phosphorylation of I kappa B alpha and serine phosphorylation of p65: evidence for the involvement of I kappa B alpha kinase and Syk protein-tyrosine kinase*. J Biol Chem, 2003. **278**(26): p. 24233-41.
351. Canty, T.G., Jr., et al., *Oxidative stress induces NF-kappaB nuclear translocation without degradation of IkappaBalpha*. Circulation, 1999. **100**(19 Suppl): p. II361-4.
352. Natarajan, R., et al., *Atypical mechanism of NF-kappaB activation during reoxygenation stress in microvascular endothelium: a role for tyrosine kinases*. Free Radic Biol Med, 2002. **33**(7): p. 962.
353. Scheidereit, C., *IkappaB kinase complexes: gateways to NF-kappaB activation and transcription*. Oncogene, 2006. **25**(51): p. 6685-705.

354. Senftleben, U., et al., *Activation by IKK α of a second, evolutionary conserved, NF-kappa B signaling pathway*. *Science*, 2001. **293**(5534): p. 1495-9.
355. Ghosh, S. and M. Karin, *Missing pieces in the NF-kappaB puzzle*. *Cell*, 2002. **109 Suppl**: p. S81-96.
356. Pahl, H.L., *Activators and target genes of Rel/NF-kappaB transcription factors*. *Oncogene*, 1999. **18**(49): p. 6853-66.
357. Karin, M., *The beginning of the end: IkappaB kinase (IKK) and NF-kappaB activation*. *J Biol Chem*, 1999. **274**(39): p. 27339-42.
358. Schmitz, M.L., et al., *NF-kappaB: a multifaceted transcription factor regulated at several levels*. *Chembiochem*, 2004. **5**(10): p. 1348-58.
359. Yamamoto, Y. and R.B. Gaynor, *IkappaB kinases: key regulators of the NF-kappaB pathway*. *Trends Biochem Sci*, 2004. **29**(2): p. 72-9.
360. Memet, S., *NF-kappaB functions in the nervous system: from development to disease*. *Biochem Pharmacol*, 2006. **72**(9): p. 1180-95.
361. Black, I.B., I.A. Hendry, and L.L. Iversen, *Effects of surgical decentralization and nerve growth factor on the maturation of adrenergic neurons in a mouse sympathetic ganglion*. *J Neurochem*, 1972. **19**(5): p. 1367-77.
362. Kasting, J.F., *Earth's early atmosphere*. *Science*, 1993. **259**(5097): p. 920-6.
363. Canfield, D.E. and A. Teske, *Late Proterozoic rise in atmospheric oxygen concentration inferred from phylogenetic and sulphur-isotope studies*. *Nature*, 1996. **382**(6587): p. 127-32.
364. Goldblatt, C., T.M. Lenton, and A.J. Watson, *Bistability of atmospheric oxygen and the Great Oxidation*. *Nature*, 2006. **443**(7112): p. 683-6.
365. Webster, K.A., *Hypoxia: life on the edge*. *Antioxid Redox Signal*, 2007. **9**(9): p. 1303-7.
366. Fisher, S.A. and W.W. Burggren, *Role of hypoxia in the evolution and development of the cardiovascular system*. *Antioxid Redox Signal*, 2007. **9**(9): p. 1339-52.
367. Lahiri, S., et al., *Oxygen sensing in the body*. *Prog Biophys Mol Biol*, 2006. **91**(3): p. 249-86.
368. McGregor, K.H., J. Gil, and S. Lahiri, *A morphometric study of the carotid body in chronically hypoxic rats*. *J Appl Physiol*, 1984. **57**(5): p. 1430-8.
369. Cummins, E.P. and C.T. Taylor, *Hypoxia-responsive transcription factors*. *Pflugers Arch*, 2005. **450**(6): p. 363-71.
370. Semenza, G.L., *Targeting HIF-1 for cancer therapy*. *Nat Rev Cancer*, 2003. **3**(10): p. 721-32.
371. Manalo, D.J., et al., *Transcriptional regulation of vascular endothelial cell responses to hypoxia by HIF-1*. *Blood*, 2005. **105**(2): p. 659-69.
372. Lord, E.M., L. Harwell, and C.J. Koch, *Detection of hypoxic cells by monoclonal antibody recognizing 2-nitroimidazole adducts*. *Cancer Res*, 1993. **53**(23): p. 5721-6.
373. Chen, E.Y., M. Fujinaga, and A.J. Giaccia, *Hypoxic microenvironment within an embryo induces apoptosis and is essential for proper morphological development*. *Teratology*, 1999. **60**(4): p. 215-25.
374. Morrison, S.J., et al., *Culture in reduced levels of oxygen promotes clonogenic sympathoadrenal differentiation by isolated neural crest stem cells*. *J Neurosci*, 2000. **20**(19): p. 7370-6.

375. Studer, L., et al., *Enhanced proliferation, survival, and dopaminergic differentiation of CNS precursors in lowered oxygen*. J Neurosci, 2000. **20**(19): p. 7377-83.
376. Semenza, G.L. and G.L. Wang, *A nuclear factor induced by hypoxia via de novo protein synthesis binds to the human erythropoietin gene enhancer at a site required for transcriptional activation*. Mol Cell Biol, 1992. **12**(12): p. 5447-54.
377. Wang, G.L., et al., *Hypoxia-inducible factor 1 is a basic-helix-loop-helix-PAS heterodimer regulated by cellular O₂ tension*. Proc Natl Acad Sci U S A, 1995. **92**(12): p. 5510-4.
378. Maynard, M.A., et al., *Multiple splice variants of the human HIF-3 alpha locus are targets of the von Hippel-Lindau E3 ubiquitin ligase complex*. J Biol Chem, 2003. **278**(13): p. 11032-40.
379. Lee, J.W., et al., *Hypoxia-inducible factor (HIF-1)alpha: its protein stability and biological functions*. Exp Mol Med, 2004. **36**(1): p. 1-12.
380. Huang, L.E., et al., *Activation of hypoxia-inducible transcription factor depends primarily upon redox-sensitive stabilization of its alpha subunit*. J Biol Chem, 1996. **271**(50): p. 32253-9.
381. Talks, K.L., et al., *The expression and distribution of the hypoxia-inducible factors HIF-1alpha and HIF-2alpha in normal human tissues, cancers, and tumor-associated macrophages*. Am J Pathol, 2000. **157**(2): p. 411-21.
382. Makino, Y., et al., *Inhibitory PAS domain protein is a negative regulator of hypoxia-inducible gene expression*. Nature, 2001. **414**(6863): p. 550-4.
383. Makino, Y., et al., *Inhibitory PAS domain protein (IPAS) is a hypoxia-inducible splicing variant of the hypoxia-inducible factor-3alpha locus*. J Biol Chem, 2002. **277**(36): p. 32405-8.
384. Semenza, G.L., *Regulation of mammalian O₂ homeostasis by hypoxia-inducible factor 1*. Annu Rev Cell Dev Biol, 1999. **15**: p. 551-78.
385. Hu, C.J., et al., *Differential roles of hypoxia-inducible factor 1alpha (HIF-1alpha) and HIF-2alpha in hypoxic gene regulation*. Mol Cell Biol, 2003. **23**(24): p. 9361-74.
386. Wang, V., et al., *Differential gene up-regulation by hypoxia-inducible factor-1alpha and hypoxia-inducible factor-2alpha in HEK293T cells*. Cancer Res, 2005. **65**(8): p. 3299-306.
387. Raval, R.R., et al., *Contrasting properties of hypoxia-inducible factor 1 (HIF-1) and HIF-2 in von Hippel-Lindau-associated renal cell carcinoma*. Mol Cell Biol, 2005. **25**(13): p. 5675-86.
388. Maltepe, E., et al., *Abnormal angiogenesis and responses to glucose and oxygen deprivation in mice lacking the protein ARNT*. Nature, 1997. **386**(6623): p. 403-7.
389. Iyer, N.V., et al., *Cellular and developmental control of O₂ homeostasis by hypoxia-inducible factor 1 alpha*. Genes Dev, 1998. **12**(2): p. 149-62.
390. Ryan, H.E., J. Lo, and R.S. Johnson, *HIF-1 alpha is required for solid tumor formation and embryonic vascularization*. Embo J, 1998. **17**(11): p. 3005-15.
391. Carmeliet, P., et al., *Role of HIF-1alpha in hypoxia-mediated apoptosis, cell proliferation and tumour angiogenesis*. Nature, 1998. **394**(6692): p. 485-90.
392. Tian, H., et al., *The hypoxia-responsive transcription factor EPAS1 is essential for catecholamine homeostasis and protection against heart failure during embryonic development*. Genes Dev, 1998. **12**(21): p. 3320-4.

393. Peng, J., et al., *The transcription factor EPAS-1/hypoxia-inducible factor 2alpha plays an important role in vascular remodeling*. Proc Natl Acad Sci U S A, 2000. **97**(15): p. 8386-91.
394. Compernelle, V., et al., *Loss of HIF-2alpha and inhibition of VEGF impair fetal lung maturation, whereas treatment with VEGF prevents fatal respiratory distress in premature mice*. Nat Med, 2002. **8**(7): p. 702-10.
395. Kaelin, W.G., *The von Hippel-Lindau tumor suppressor protein: roles in cancer and oxygen sensing*. Cold Spring Harb Symp Quant Biol, 2005. **70**: p. 159-66.
396. Latif, F., et al., *Identification of the von Hippel-Lindau disease tumor suppressor gene*. Science, 1993. **260**(5112): p. 1317-20.
397. Brown, L.F., et al., *Increased expression of vascular permeability factor (vascular endothelial growth factor) and its receptors in kidney and bladder carcinomas*. Am J Pathol, 1993. **143**(5): p. 1255-62.
398. Iliopoulos, O., et al., *Tumour suppression by the human von Hippel-Lindau gene product*. Nat Med, 1995. **1**(8): p. 822-6.
399. Iliopoulos, O., et al., *Negative regulation of hypoxia-inducible genes by the von Hippel-Lindau protein*. Proc Natl Acad Sci U S A, 1996. **93**(20): p. 10595-9.
400. Maxwell, P.H., et al., *The tumour suppressor protein VHL targets hypoxia-inducible factors for oxygen-dependent proteolysis*. Nature, 1999. **399**(6733): p. 271-5.
401. Ohh, M., et al., *Ubiquitination of hypoxia-inducible factor requires direct binding to the beta-domain of the von Hippel-Lindau protein*. Nat Cell Biol, 2000. **2**(7): p. 423-7.
402. Tanimoto, K., et al., *Mechanism of regulation of the hypoxia-inducible factor-1 alpha by the von Hippel-Lindau tumor suppressor protein*. Embo J, 2000. **19**(16): p. 4298-309.
403. Jaakkola, P., et al., *Targeting of HIF-alpha to the von Hippel-Lindau ubiquitylation complex by O2-regulated prolyl hydroxylation*. Science, 2001. **292**(5516): p. 468-72.
404. Epstein, A.C., et al., *C. elegans EGL-9 and mammalian homologs define a family of dioxygenases that regulate HIF by prolyl hydroxylation*. Cell, 2001. **107**(1): p. 43-54.
405. Metzzen, E. and P.J. Ratcliffe, *HIF hydroxylation and cellular oxygen sensing*. Biol Chem, 2004. **385**(3-4): p. 223-30.
406. Hirsila, M., et al., *Characterization of the human prolyl 4-hydroxylases that modify the hypoxia-inducible factor*. J Biol Chem, 2003. **278**(33): p. 30772-80.
407. Bruick, R.K. and S.L. McKnight, *A conserved family of prolyl-4-hydroxylases that modify HIF*. Science, 2001. **294**(5545): p. 1337-40.
408. Huang, J., et al., *Sequence determinants in hypoxia-inducible factor-1alpha for hydroxylation by the prolyl hydroxylases PHD1, PHD2, and PHD3*. J Biol Chem, 2002. **277**(42): p. 39792-800.
409. D'Angelo, G., et al., *Hypoxia up-regulates prolyl hydroxylase activity: a feedback mechanism that limits HIF-1 responses during reoxygenation*. J Biol Chem, 2003. **278**(40): p. 38183-7.
410. Metzzen, E., et al., *Intracellular localisation of human HIF-1 alpha hydroxylases: implications for oxygen sensing*. J Cell Sci, 2003. **116**(Pt 7): p. 1319-26.

411. Oehme, F., et al., *Overexpression of PH-4, a novel putative proline 4-hydroxylase, modulates activity of hypoxia-inducible transcription factors.* Biochem Biophys Res Commun, 2002. **296**(2): p. 343-9.
412. Lieb, M.E., et al., *Mammalian EGLN genes have distinct patterns of mRNA expression and regulation.* Biochem Cell Biol, 2002. **80**(4): p. 421-6.
413. Appelhoff, R.J., et al., *Differential function of the prolyl hydroxylases PHD1, PHD2, and PHD3 in the regulation of hypoxia-inducible factor.* J Biol Chem, 2004. **279**(37): p. 38458-65.
414. Naranjo-Suarez, S., et al., *Down-regulation of hypoxia-inducible factor-2 in PC12 cells by nerve growth factor stimulation.* J Biol Chem, 2003. **278**(34): p. 31895-901.
415. Nilsson, G.E. and P.L. Lutz, *Anoxia tolerant brains.* J Cereb Blood Flow Metab, 2004. **24**(5): p. 475-86.
416. Li, D., et al., *Physiological hypoxia promotes survival of cultured cortical neurons.* Eur J Neurosci, 2005. **22**(6): p. 1319-26.
417. Lipscomb, E.A., et al., *Expression of the SM-20 gene promotes death in nerve growth factor-dependent sympathetic neurons.* J Neurochem, 1999. **73**(1): p. 429-32.
418. Lee, S., et al., *Neuronal apoptosis linked to EglN3 prolyl hydroxylase and familial pheochromocytoma genes: developmental culling and cancer.* Cancer Cell, 2005. **8**(2): p. 155-67.
419. Davies, in *Cranial Sensory Neurons. Neural cell culture a practical approach.* 1995, Oxford University Press. p. 153-176.
420. Sholl, D.A., *Dendritic organization in the neurons of the visual and motor cortices of the cat.* J Anat, 1953. **87**(4): p. 387-406.
421. West, M.J., *New stereological methods for counting neurons.* Neurobiol Aging, 1993. **14**(4): p. 275-85.
422. Cavalieri, B., *Geometria degli indivisibili.* 1966, Torino, Italy: Unione Tipografica Editrice.
423. Koong, A.C., E.Y. Chen, and A.J. Giaccia, *Hypoxia causes the activation of nuclear factor kappa B through the phosphorylation of I kappa B alpha on tyrosine residues.* Cancer Res, 1994. **54**(6): p. 1425-30.
424. Imbert, V., et al., *Tyrosine phosphorylation of I kappa B-alpha activates NF-kappa B without proteolytic degradation of I kappa B-alpha.* Cell, 1996. **86**(5): p. 787-98.
425. Singh, S., B.G. Darnay, and B.B. Aggarwal, *Site-specific tyrosine phosphorylation of IkappaBalpha negatively regulates its inducible phosphorylation and degradation.* J Biol Chem, 1996. **271**(49): p. 31049-54.
426. Liang, Y., Y. Zhou, and P. Shen, *NF-kappaB and its regulation on the immune system.* Cell Mol Immunol, 2004. **1**(5): p. 343-50.
427. Kaltschmidt, B., D. Widera, and C. Kaltschmidt, *Signaling via NF-kappaB in the nervous system.* Biochim Biophys Acta, 2005. **1745**(3): p. 287-99.
428. Albenisi, B.C. and M.P. Mattson, *Evidence for the involvement of TNF and NF-kappaB in hippocampal synaptic plasticity.* Synapse, 2000. **35**(2): p. 151-9.
429. Nickols, J.C., et al., *Activation of the transcription factor NF-kappaB in Schwann cells is required for peripheral myelin formation.* Nat Neurosci, 2003. **6**(2): p. 161-7.
430. Meffert, M.K. and D. Baltimore, *Physiological functions for brain NF-kappaB.* Trends Neurosci, 2005. **28**(1): p. 37-43.

431. Sole, C., et al., *The death receptor antagonist FAIM promotes neurite outgrowth by a mechanism that depends on ERK and NF-kappa B signaling*. J Cell Biol, 2004. **167**(3): p. 479-92.
432. Lin, Y.Z., et al., *Inhibition of nuclear translocation of transcription factor NF-kappa B by a synthetic peptide containing a cell membrane-permeable motif and nuclear localization sequence*. J Biol Chem, 1995. **270**(24): p. 14255-8.
433. Morishita, R., et al., *In vivo transfection of cis element "decoy" against nuclear factor-kappaB binding site prevents myocardial infarction*. Nat Med, 1997. **3**(8): p. 894-9.
434. Tomita, N., et al., *Transcription factor decoy for NFkappaB inhibits TNF-alpha-induced cytokine and adhesion molecule expression in vivo*. Gene Ther, 2000. **7**(15): p. 1326-32.
435. Rodriguez, M.S., et al., *Identification of lysine residues required for signal-induced ubiquitination and degradation of I kappa B-alpha in vivo*. Oncogene, 1996. **12**(11): p. 2425-35.
436. Roff, M., et al., *Role of IkappaBalpha ubiquitination in signal-induced activation of NFkappaB in vivo*. J Biol Chem, 1996. **271**(13): p. 7844-50.
437. Bui, N.T., et al., *Activation of nuclear factor kappaB and Bcl-x survival gene expression by nerve growth factor requires tyrosine phosphorylation of IkappaBalpha*. J Cell Biol, 2001. **152**(4): p. 753-64.
438. Azoitei, N., T. Wirth, and B. Baumann, *Activation of the IkappaB kinase complex is sufficient for neuronal differentiation of PC12 cells*. J Neurochem, 2005. **93**(6): p. 1487-501.
439. Oliver, J.M., et al., *Inhibition of mast cell Fc epsilon R1-mediated signaling and effector function by the Syk-selective inhibitor, piceatannol*. J Biol Chem, 1994. **269**(47): p. 29697-703.
440. Alonzi, T., et al., *Role of STAT3 and PI 3-kinase/Akt in mediating the survival actions of cytokines on sensory neurons*. Mol Cell Neurosci, 2001. **18**(3): p. 270-82.
441. Fukada, T., et al., *Two signals are necessary for cell proliferation induced by a cytokine receptor gp130: involvement of STAT3 in anti-apoptosis*. Immunity, 1996. **5**(5): p. 449-60.
442. Mattson, M.P., et al., *Activation of NF-kappaB protects hippocampal neurons against oxidative stress-induced apoptosis: evidence for induction of manganese superoxide dismutase and suppression of peroxynitrite production and protein tyrosine nitration*. J Neurosci Res, 1997. **49**(6): p. 681-97.
443. Daily, D., et al., *Glutaredoxin protects cerebellar granule neurons from dopamine-induced apoptosis by activating NF-kappa B via Ref-1*. J Biol Chem, 2001. **276**(2): p. 1335-44.
444. Digicaylioglu, M. and S.A. Lipton, *Erythropoietin-mediated neuroprotection involves cross-talk between Jak2 and NF-kappaB signalling cascades*. Nature, 2001. **412**(6847): p. 641-7.
445. Lipsky, R.H., et al., *Nuclear factor kappaB is a critical determinant in N-methyl-D-aspartate receptor-mediated neuroprotection*. J Neurochem, 2001. **78**(2): p. 254-64.
446. Piccioli, P., et al., *Inhibition of nuclear factor-kappaB activation induces apoptosis in cerebellar granule cells*. J Neurosci Res, 2001. **66**(6): p. 1064-73.
447. Fernyhough, P., et al., *Activation of nuclear factor-kappaB via endogenous tumor necrosis factor alpha regulates survival of axotomized adult sensory neurons*. J Neurosci, 2005. **25**(7): p. 1682-90.

448. Viatour, P., et al., *Phosphorylation of NF-kappaB and IkappaB proteins: implications in cancer and inflammation*. Trends Biochem Sci, 2005. **30**(1): p. 43-52.
449. Lipscomb, E.A., P.D. Sarmiere, and R.S. Freeman, *SM-20 is a novel mitochondrial protein that causes caspase-dependent cell death in nerve growth factor-dependent neurons*. J Biol Chem, 2001. **276**(7): p. 5085-92.
450. Straub, J.A., et al., *Induction of SM-20 in PC12 cells leads to increased cytochrome c levels, accumulation of cytochrome c in the cytosol, and caspase-dependent cell death*. J Neurochem, 2003. **85**(2): p. 318-28.
451. Xie, L., R.S. Johnson, and R.S. Freeman, *Inhibition of NGF deprivation-induced death by low oxygen involves suppression of BIMEL and activation of HIF-1*. J Cell Biol, 2005. **168**(6): p. 911-20.
452. Stoeckel, K., et al., *The significance of retrograde axonal transport for the accumulation of systemically administered nerve growth factor (NGF) in the rat superior cervical ganglion*. Brain Res, 1976. **109**(2): p. 271-84.
453. Hendry, I.A., *The effect of the retrograde axonal transport of nerve growth factor on the morphology of adrenergic neurones*. Brain Res, 1977. **134**(2): p. 213-23.
454. Johnson, E.M., Jr., et al., *Demonstration of the retrograde transport of nerve growth factor receptor in the peripheral and central nervous system*. J Neurosci, 1987. **7**(3): p. 923-9.
455. Grimes, M.L., et al., *Endocytosis of activated TrkA: evidence that nerve growth factor induces formation of signaling endosomes*. J Neurosci, 1996. **16**(24): p. 7950-64.
456. Molliver, D.C. and W.D. Snider, *Nerve growth factor receptor TrkA is down-regulated during postnatal development by a subset of dorsal root ganglion neurons*. J Comp Neurol, 1997. **381**(4): p. 428-38.
457. Zhuo, H. and C.J. Helke, *Presence and localization of neurotrophin receptor tyrosine kinase (TrkA, TrkB, TrkC) mRNAs in visceral afferent neurons of the nodose and petrosal ganglia*. Brain Res Mol Brain Res, 1996. **38**(1): p. 63-70.
458. Wright, L., *Cell survival in chick embryo ciliary ganglion is reduced by chronic ganglionic blockade*. Brain Res, 1981. **227**(2): p. 283-6.
459. Koike, T., D.P. Martin, and E.M. Johnson, Jr., *Role of Ca²⁺ channels in the ability of membrane depolarization to prevent neuronal death induced by trophic-factor deprivation: evidence that levels of internal Ca²⁺ determine nerve growth factor dependence of sympathetic ganglion cells*. Proc Natl Acad Sci U S A, 1989. **86**(16): p. 6421-5.
460. Mennerick, S. and C.F. Zorumski, *Neural activity and survival in the developing nervous system*. Mol Neurobiol, 2000. **22**(1-3): p. 41-54.
461. Collins, F. and J.D. Lile, *The role of dihydropyridine-sensitive voltage-gated calcium channels in potassium-mediated neuronal survival*. Brain Res, 1989. **502**(1): p. 99-108.
462. Burnstock, G., *P2X receptors in sensory neurones*. Br J Anaesth, 2000. **84**(4): p. 476-88.
463. Cockayne, D.A., et al., *P2X2 knockout mice and P2X2/P2X3 double knockout mice reveal a role for the P2X2 receptor subunit in mediating multiple sensory effects of ATP*. J Physiol, 2005. **567**(Pt 2): p. 621-39.
464. Xiang, Z., X. Bo, and G. Burnstock, *Localization of ATP-gated P2X receptor immunoreactivity in rat sensory and sympathetic ganglia*. Neurosci Lett, 1998. **256**(2): p. 105-8.

465. Mason, H.S., S. Bourke, and P.J. Kemp, *Selective modulation of ligand-gated P2X purinoceptor channels by acute hypoxia is mediated by reactive oxygen species*. Mol Pharmacol, 2004. **66**(6): p. 1525-35.
466. Davies, A.M. and R.M. Lindsay, *Neural crest-derived spinal and cranial sensory neurones are equally sensitive to NGF but differ in their response to tissue extracts*. Brain Res, 1984. **316**(1): p. 121-7.
467. Ernsberger, U. and H. Rohrer, *Neuronal precursor cells in chick dorsal root ganglia: differentiation and survival in vitro*. Dev Biol, 1988. **126**(2): p. 420-32.
468. Tong, J.X., M.E. Eichler, and K.M. Rich, *Intracellular calcium levels influence apoptosis in mature sensory neurons after trophic factor deprivation*. Exp Neurol, 1996. **138**(1): p. 45-52.
469. Cowen, T., et al., *Reduced age-related plasticity of neurotrophin receptor expression in selected sympathetic neurons of the rat*. Aging Cell, 2003. **2**(1): p. 59-69.
470. Orike, N., et al., *Differential regulation of survival and growth in adult sympathetic neurons: an in vitro study of neurotrophin responsiveness*. J Neurobiol, 2001. **47**(4): p. 295-305.
471. Bakal, R.S. and L.L. Wright, *Postnatal neuron death in the nodose ganglia of the rat*. Dev Neurosci, 1993. **15**(1): p. 22-6.
472. Linden, R., *The survival of developing neurons: a review of afferent control*. Neuroscience, 1994. **58**(4): p. 671-82.

Appendix

Poly-ornithine Solution

9.2g of boric acid (Sigma) was dissolved in 1L of dH₂O and adjusted to pH 8.4 using 5M NaOH. 500mg of poly-ornithine (sigma) was then dissolved in the borate solution and filter sterilised. The poly-ornithine solution was stored at 4°C for up to 2 weeks.

Trypsin

50mg Trypsin (Worthington) was dissolved in 5ml Ca²⁺/Mg²⁺ free PBS , filter sterilised and stored at -20°C.

PCR cycle conditions

PHD1:

1. 95 C for 1 min
 2. 95 C for 30 sec
 3. 63 C for 30 sec
 4. 72 C for 2 min
- 30 cycles of steps 2 to 4
5. 72 C for 10 mins
 6. 4 C

PHD2:

1. 94 C for 2 min
2. 94 C for 30 sec

3. 52 C for 30 sec

4. 72 C for 1 min 15 sec

32 cycles of steps 2 to 4

5. 72 C for 10 mins

6. 4 C

PHD3:

1. 95 C for 1 min

2. 95 C for 30 sec

3. 63 C for 30 sec

4. 72 C for 2 min

30 cycles of steps 2 to 4

5. 72 C for 10 mins

6. 4 C

Nuclear Factor- κ B Activation via Tyrosine Phosphorylation of Inhibitor κ B- α Is Crucial for Ciliary Neurotrophic Factor-Promoted Neurite Growth from Developing Neurons

Denis Gallagher,¹ Humberto Gutierrez,¹ Nuria Gavalda,¹ Gerard O'Keeffe,¹ Ron Hay,² and Alun M. Davies¹

¹School of Biosciences, Cardiff CF10 3US, United Kingdom, and ²School of Life Sciences, University of Dundee, Dundee DD1 5EH, United Kingdom

The cytokine ciliary neurotrophic factor (CNTF) promotes the growth of neural processes from many kinds of neurons in the developing and regenerating adult nervous system, but the intracellular signaling mechanisms mediating this important function of CNTF are poorly understood. Here, we show that CNTF activates the nuclear factor- κ B (NF- κ B) transcriptional system in neonatal sensory neurons and that blocking NF- κ B-dependent transcription inhibits CNTF-promoted neurite growth. Selectively blocking NF- κ B activation by the noncanonical pathway that requires tyrosine phosphorylation of inhibitor κ B- α (I κ B- α), but not by the canonical pathway that requires serine phosphorylation of I κ B- α , also effectively inhibits CNTF-promoted neurite growth. CNTF treatment activates spleen tyrosine kinase (SYK) whose substrates include I κ B- α . CNTF-induced SYK phosphorylation is rapidly followed by increased tyrosine phosphorylation of I κ B- α , and blocking SYK activation or tyrosine phosphorylation of I κ B- α prevents CNTF-induced NF- κ B activation and CNTF-promoted neurite growth. These findings demonstrate that NF- κ B signaling by an unusual activation mechanism is essential for the ability of CNTF to promote the growth of neural processes in the developing nervous system.

Key words: NF- κ B; neurite; CNTF; SYK; development; sensory neuron

Introduction

Nuclear factor- κ B (NF- κ B) is a ubiquitously expressed transcription factor system that consists of homodimers or heterodimers of five structurally related proteins: p65, RelB, c-Rel, p50, and p52, of which the p50/p65 heterodimer is the most abundant and widely expressed (Hayden and Ghosh, 2004). NF- κ B is held in an inactive form in the cytosol by interaction with a member of the I κ B family of inhibitory proteins, I κ B α , I κ B β , I κ B ϵ , I κ B γ , Bcl-3, p100 and p105, of which I κ B α is the predominantly expressed inhibitor. In the canonical NF- κ B signaling pathway, NF- κ B is activated by phosphorylation of I κ B α on serine residues 32 and 36 by an I κ B kinase complex. This leads to ubiquitination and proteasome-mediated degradation of I κ B α and translocation of the liberated NF- κ B to the nucleus where it binds to consensus κ B sequences in the promoter and enhancer regions of responsive genes (Hayden and Ghosh, 2004). NF- κ B can also be activated by several alternative mechanisms including one in which I κ B α is phosphorylated on tyrosine 42, which results in its dissociation from NF- κ B without proteasome-mediated degradation (Koong et al., 1994; Imbert et al., 1996; Bui et al., 2001; Takada et al., 2003).

Classically, NF- κ B has been shown to regulate the expression of genes involved in innate and adaptive immune responses,

stress responses, cell survival, and cell proliferation (Liang et al., 2004). In the nervous system, NF- κ B is activated by a variety of neurotrophic factors, cytokines, and neurotransmitters, and can promote neuronal survival or bring about neuronal death. NF- κ B signaling also regulates synaptic function, plays a role learning and memory and participates in peripheral nerve myelination (Kaltschmidt et al., 2005).

CNTF promotes the survival of a variety of neurons (Horton et al., 1998; Nishimune et al., 2000) and stimulates neurite growth and axon regeneration in several *in vitro* and *in vivo* experimental paradigms in the developing and mature nervous system (Hartnick et al., 1996; Cui and Harvey, 2000; Siegel et al., 2000). Binding of CNTF to a receptor complex consisting of gp130, leukemia inhibitory factor receptor β , and CNTF receptor α (Stahl and Yancopoulos, 1994) leads to the activation of several signal transduction pathways including JAK (Janus kinase)/STAT (signal transducer and activator of transcription), MEK [extracellular signal-regulated kinase (ERK) kinase]/MAPK (mitogen-activated protein kinase), phosphoinositide 3-kinase (PI3-K)/Akt, and NF- κ B (Nishimune et al., 2000; Rane and Reddy, 2000). Because NF- κ B signaling via the canonical activation pathway partially contributes to the neurite growth-promoting effects of the neurotrophins NGF and BDNF (Sole et al., 2004; Gutierrez et al., 2005), we investigated whether NF- κ B signaling plays any role in the neurite growth-promoting effects of CNTF. Using neonatal mouse nodose ganglion sensory neurons, which are supported by CNTF (Horton et al., 1998), we show by a variety of complementary experimental approaches that NF- κ B signaling is essential for CNTF-promoted neurite growth and that the NF- κ B ac-

Received Feb. 12, 2007; revised June 18, 2007; accepted July 14, 2007.

This work was supported by The Wellcome Trust. N.G. was supported by the Beatriu de Pinós Fellowship (Generalitat de Catalunya, Spain). We thank Yumi Tohyama for the dominant-negative SYK construct.

Correspondence should be addressed to Alun M. Davies at the above address. E-mail: daviesalun@cf.ac.uk.

DOI:10.1523/JNEUROSCI.0608-07.2007

Copyright © 2007 Society for Neuroscience 0270-6474/07/279664-06\$15.00/0

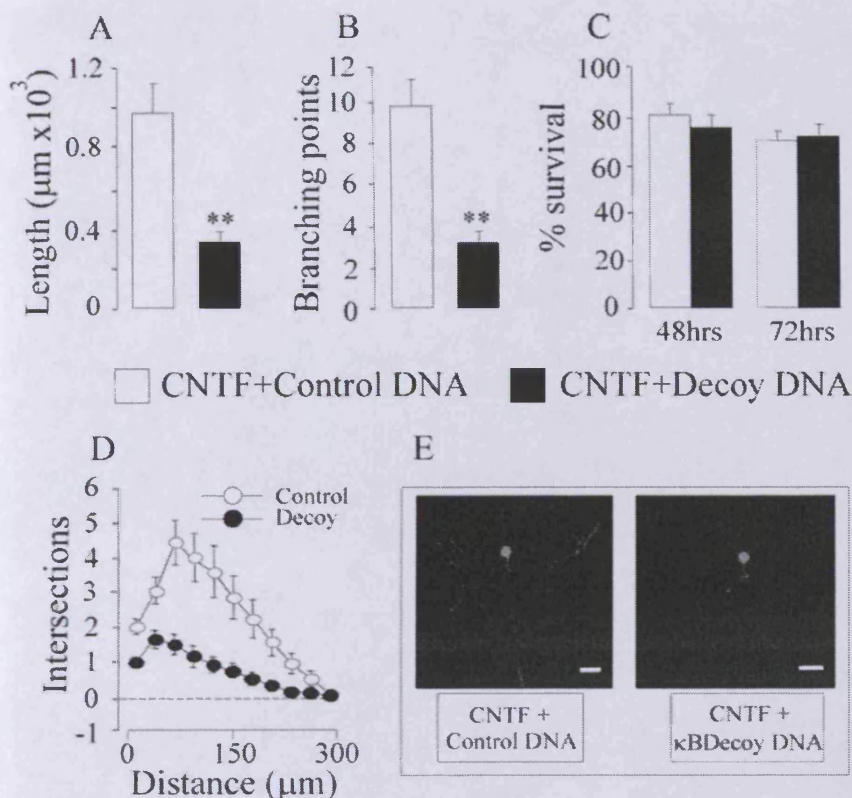


Figure 1. Effect of κ B decoy DNA on CNTF-promoted neurite growth. Three hours after plating, P0 nodose neurons were transfected with a YFP expression plasmid together with either κ B decoy DNA or a scrambled control DNA. **A–D**, After 24 h incubation with 50 ng/ml CNTF, neurite arbor length (**A**), branch point number (**B**), Sholl analysis (**D**), and neuronal survival (**C**) were ascertained. Means \pm SEs of a typical experiment are shown (50–90 neurons per condition). Very similar data were obtained in three independent experiments. ** $p < 0.001$. **E**, Photomicrographs show typical control transfected and κ B decoy DNA-transfected neurons. Scale bars, 30 μm .

tivation mechanism used by CNTF for promoting growth is distinct from that used by the neurotrophins.

Materials and Methods

Neuron culture and transfection. Dissociated cultures of nodose ganglion neurons from newborn mice were grown in polyornithine/laminin-coated 35 mm dishes in defined medium and were transfected 3 h after plating with plasmid-coated or oligonucleotide-coated (κ B decoy dsDNA, 5'-GAGGGGACTTTCCT-3'; scrambled control dsDNA, 5'-GATGCGTCTGTCGCA-3') gold microcarriers using the Bio-Rad (Hercules, CA) Gene-gun (Gutierrez et al., 2005). Immunocytochemistry was used to confirm that nodose neurons transfected with expression plasmids for Tyr I κ B α , Ser I κ B α , and Syk dominant-negative mutants have increased expression of the corresponding protein (data not shown). The survival of transfected neurons was quantified by counting the numbers of yellow fluorescent protein (YFP)-labeled neurons 12 h after plating and at later time points and expressing the latter as a percentage of the former. Survival in nontransfected cultures was estimated by counting the number of neurons in a grid 3 and 24 h after plating and expressing the latter as a percentage of the former.

Quantification of fluorescence. To estimate the relative level of NF- κ B activation, neurons were transfected with a plasmid expressing green fluorescent protein (GFP) under the control of an NF- κ B promoter. Neurons were imaged with a Zeiss (Oberkochen, Germany) Axioplan confocal microscope and mean soma fluorescence intensity was obtained using LSM510 software.

Analysis of neuritic arbors. YFP-labeled neurons were visualized and digitally acquired using an Axioplan Zeiss confocal microscope. In non-

transfection experiments, neurons were fluorescently labeled with the vital dye calcein-AM (Invitrogen, Eugene, OR). Neuritic arbors were traced using LSM510 software from which total neurite length and number of branch points was calculated and Sholl analysis was performed (Gutierrez et al., 2005).

Western blots. Neurons were plated at high density in polyornithine/laminin-coated 96-well plates (5000 neurons per well). Four hours after plating, 50 ng/ml CNTF was added for the indicated times. The cells were lysed in radioimmunoprecipitation assay buffer and insoluble debris was removed by centrifugation. Samples were transferred to polyvinylidene difluoride membranes using the Bio-Rad TransBlot. Membranes were blocked with 5% dried milk in PBS with 0.1% Tween 20. Membranes were then incubated with anti-phospho-Tyr I κ B- α antibody (1:200; Abcam, Cambridge, UK), anti-phospho-Syk antibody (1:1000; Cell Signaling Technology, Beverly, MA), anti-I κ B- α antibody (1:1000; Cell Signaling Technology), or anti- β -III tubulin antibody (1:10000; Promega, Hawthorne, Australia), which were detected with peroxidase-linked secondary antibody (GE Healthcare Bio-Sciences, Piscataway, NJ) and ECL-plus (GE Healthcare Bio-Sciences). Densitometry was performed using Adobe (San Jose, CA) Photoshop.

Results

Blocking NF- κ B-dependent transcription inhibits CNTF-promoted neurite growth

To investigate the importance of NF- κ B in mediating the response of neurons to CNTF, we studied the consequences of specifically inhibiting a key step in NF- κ B signaling, the binding of activated NF- κ B

to regulatory elements in target genes. This was blocked by transfecting neurons with double stranded DNA oligonucleotides containing the κ B consensus binding sequence. This κ B decoy DNA has been successfully used *in vitro* and *in vivo* to inhibit NF- κ B transcriptional activity by sequestering transcriptionally active NF- κ B complexes (Morishita et al., 1997; Tomita et al., 2000; Gutierrez et al., 2005). Postnatal day 0 (P0) nodose ganglion neurons were transfected with gold particles coated with either the κ B decoy DNA or a control oligonucleotide of scrambled sequence 3 h after plating. The cultures received CNTF after transfection and neuronal survival and neurite arbor size and complexity were quantified 24 h after plating.

The κ B decoy DNA, but not the control oligonucleotide caused a marked threefold reduction in neurite length and branching and a substantial reduction in neurite growth as quantified by Sholl analysis (Fig. 1). Despite the dramatic effect on neurite growth, the cell bodies of neurons transfected with κ B decoy DNA retained a normal appearance (Fig. 1E) and continued to survive just as well as control-transfected neurons in the presence of CNTF, with \sim 70% of the neurons surviving up to 72 h after plating (Fig. 1C). Accordingly, NF κ B reporter activity was significantly reduced in neurons transfected with κ B decoy DNA and not in neurons transfected with control DNA (see Fig. 4D). These results suggest that NF- κ B-dependent transcription is required for CNTF-promoted neurite growth from newborn

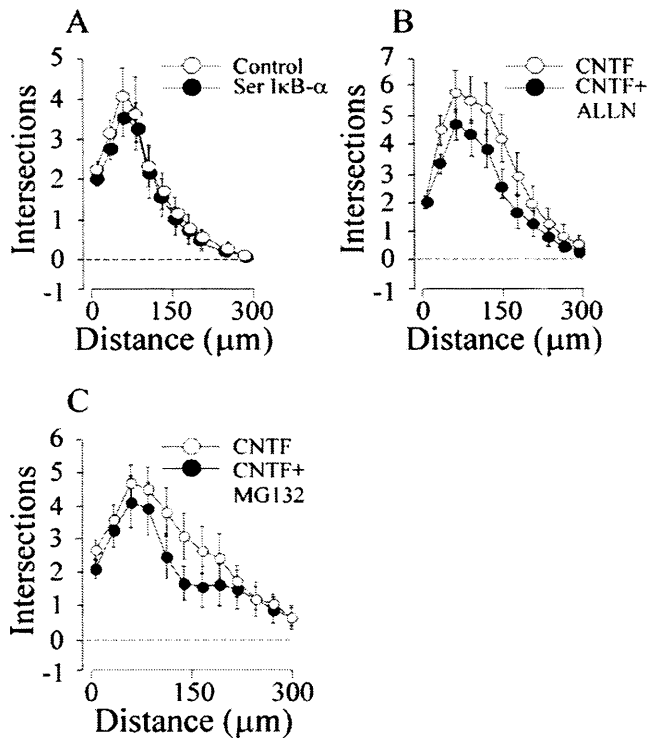


Figure 2. CNTF does not promote neurite growth by canonical NF- κ B signaling. *A–C*, Three hours after plating, P0 nodose neurons were transfected with a YFP expression plasmid together with either a plasmid expressing the 32/36-SS/AA I κ B- α mutant (Ser I κ B- α) or an empty control plasmid (*A*) were treated with either 4 μ M ALLN or vehicle control (*B*) or were treated with 20 nM MG132 or vehicle control (*C*). After 24 h incubation with 50 ng/ml CNTF, Sholl analysis was performed. Means \pm SEs of a typical experiment are shown (50–90 neurons per condition). Very similar data were obtained in three independent experiments. Statistical comparisons are with respect to the empty plasmid-transfected neurons or vehicle-treated neurons.

mouse nodose ganglion neurons, but is not needed for the survival of these neurons with CNTF. Similar decreases in the size and complexity of neurite arbors without any neuronal loss were observed in CNTF-supported nodose neurons treated with SN50, a cell-permeable inhibitor of NF- κ B nuclear translocation (data not shown). Conversely, combined overexpression of p65/p50 in CNTF-supported neurons resulted in a significant increase in neurite length and branching (data not shown).

CNTF does not promote neurite growth via the canonical NF- κ B signaling pathway

The canonical NF- κ B signaling pathway can be selectively inhibited by an I κ B- α protein possessing serine to alanine substitutions at residues 32 and 36 that prevent its phosphorylation by the I κ B kinase complex, but do not affect its association with NF- κ B dimers (Roff et al., 1996). We showed previously that expression of this 32/36-SS/AA I κ B- α mutant in nodose neurons grown with BDNF causes a 30% reduction in neurite arbor size (Gutierrez et al., 2005). In marked contrast to nodose neurons grown with BDNF, this 32/36-SS/AA I κ B- α had no effect whatsoever on the neurite arbors of nodose neurons grown with CNTF, as shown by Sholl analysis (Fig. 2*A*), suggesting that CNTF does not mediate its effects on neurite growth via the canonical NF- κ B pathway.

Additional confirmation of the lack of involvement of canonical NF- κ B signaling in CNTF-promoted neurite growth was obtained by inhibiting another key step in this pathway,

proteasome-mediated degradation of ubiquitinated phosphoserine I κ B- α (Hayden and Ghosh, 2004). We showed previously that the proteasome inhibitor *N*-acetyl-Leu-Leu-norleucinal (ALLN) reduces the size of the neurite arbors of nodose neurons grown with BDNF (Gutierrez et al., 2005). Neither ALLN (Fig. 2*B*) nor another proteasome inhibitor MG132 (Fig. 2*C*) affected neurite arbor size in CNTF-supplemented cultures, suggesting that proteasome function is not required for CNTF-promoted growth. In contrast, we confirmed that both MG132 and ALLN significantly reduced BDNF-promoted neurite growth (data not shown). Western blot analysis of the level I κ B- α protein in nodose neurons at intervals after CNTF treatment also failed to show any evidence of I κ B- α degradation (see Fig. 4*C*).

Tyrosine phosphorylation of I κ B- α is required for CNTF-promoted growth

The noncanonical NF- κ B activation mechanism that involves tyrosine phosphorylation of I κ B α can be effectively and specifically blocked with an I κ B- α protein that has a tyrosine to phenylalanine substitution at residue 42 (Imbert et al., 1996). Nodose neurons transfected with a plasmid expressing this Y42F I κ B- α mutant had markedly smaller and less branched neurite arbors than control-transfected neurons when grown with CNTF (Fig. 3*A–C*). The survival of newborn nodose neurons grown with CNTF was not effected by expression of the Y42F I κ B- α mutant with 70–80% of neurons surviving after 24 h, confirming the above data that NF- κ B signaling does not mediate the survival response of these neurons to CNTF. Although expression of the Y42F I κ B- α mutant markedly inhibited CNTF-promoted neurite growth, its expression had no significant effect on the size and complexity of neurite arbors of nodose neurons grown with BDNF (data not shown). These results suggest that phosphotyrosine I κ B- α -dependent activation of NF- κ B is essential for CNTF-promoted neurite-growth but not for BDNF-promoted growth.

SYK is required for CNTF-promoted neurite growth

We investigated the potential involvement of the spleen tyrosine kinase (SYK) in CNTF-promoted neurite growth because this protein-tyrosine kinase has been shown previously to phosphorylate I κ B- α on tyrosine 42 in myeloid cells (Takada et al., 2003). Because the enzymatic activity of SYK is regulated by tyrosine phosphorylation (Berton et al., 2005), we quantified the level of phospho-SYK in nodose neurons at intervals after CNTF treatment to see whether CNTF is capable of activating SYK. Western blotting using an anti-phospho-SYK antibody failed to detect phospho-SYK in untreated neurons, but within 5 min of CNTF treatment, a very strong signal was evident which decreased markedly by 30 min (Fig. 4*A*). In contrast, BDNF treatment did not induce SYK phosphorylation (data not shown). Western blot analysis using a specific anti-phosphotyrosine I κ B α antibody revealed that the rapid rise and peak in phospho-SYK 5 min after CNTF treatment was followed by a rise in phosphotyrosine I κ B- α that was first evident after 15 min treatment with CNTF and was further elevated after 30 min (Fig. 4*B*).

To determine whether the sequential tyrosine phosphorylation of SYK and I κ B α in response to CNTF is necessary for CNTF-promoted NF- κ B activation, we transfected nodose neurons with a reporter construct in which GFP is under the control of an NF- κ B promoter and studied the effects of inhibiting SYK activation and blocking tyrosine phosphorylation of I κ B α on reporter signal intensity (Fig. 4*D*). Whereas CNTF treatment promoted a twofold increase in reporter signal compared with

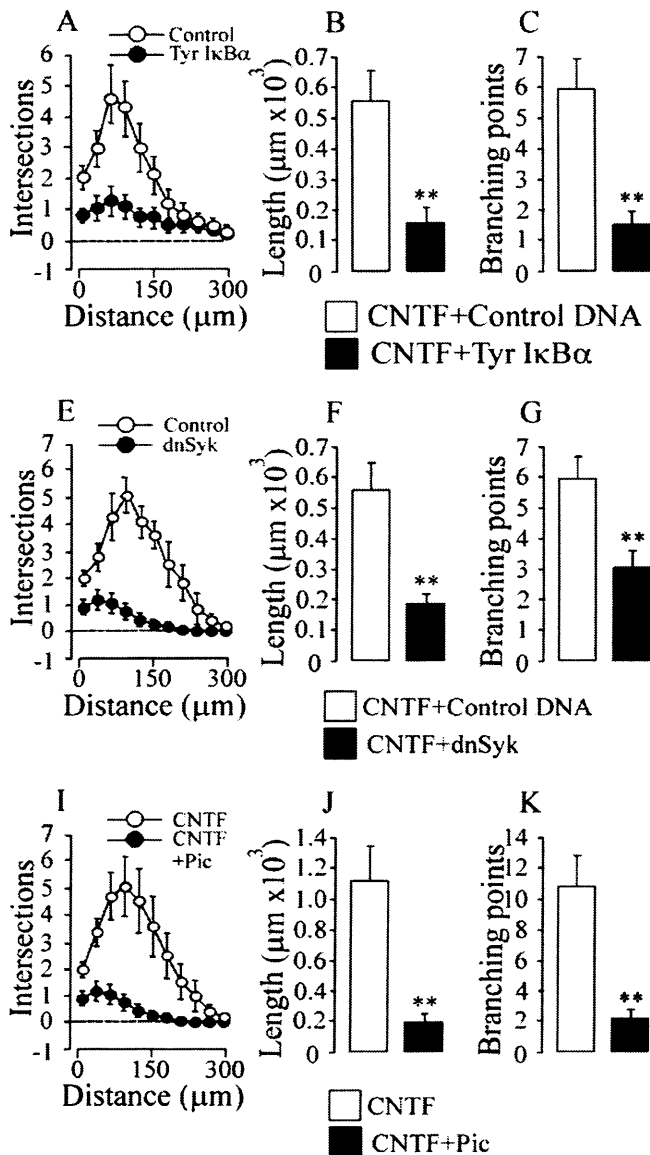


Figure 3. Tyrosine phosphorylation of I κ B α and activation of SYK kinase are required for CNTF-promoted neurite growth. *A–K*, Three hours after plating, P0 nodose neurons were transfected with a YFP expression plasmid together with either a plasmid expressing the Y42F I κ B α mutant (Tyr I κ B α) or an empty control plasmid (*A–C*), or were transfected with a YFP expression plasmid together with either a plasmid expressing a dominant-negative SYK protein (dnSyk) or an empty control plasmid (*E–G*), or treated with either 10 μ M piceatannol (Pic) or vehicle control (*I–K*). After 24 h incubation with 50 ng/ml CNTF, Sholl analysis (*A*, *E*, *I*), neurite arbor length (*B*, *F*, *J*), and branch point number (*C*, *G*, *K*) were ascertained. Means \pm SEs of a typical experiment are shown (50–90 neurons per condition). Very similar data were obtained in three independent experiments. Statistical comparisons are with respect to either control-transfected neurons or vehicle-treated neurons. ** $p < 0.001$.

untreated controls, this rise was completely blocked in neurons treated with the potent selective SYK inhibitor piceatannol (Oliver et al., 1994) and in neurons transfected with the Y42F I κ B α plasmid.

To test the role of SYK in mediating the neurite growth-promoting effects of CNTF, we studied the neurite arbors of CNTF-supported nodose neurons that were either treated with piceatannol or transfected with a plasmid expressing dominant-negative SYK. Both approaches caused a substantial reduction in

CNTF-promoted neurite growth (Fig. 3*E–K*) and NF- κ B activation, but not BDNF-promoted neurite growth (data not shown), and had no effect on survival with either factor (data not shown). These findings indicate that CNTF-dependent activation of SYK and the subsequent activation of NF- κ B by tyrosine phosphorylation of I κ B α are essential steps in the neurite growth response of neurons to CNTF, but not BDNF.

Discussion

Using a variety of complementary experimental approaches, we have demonstrated that NF- κ B signaling by an uncommon non-canonical activation mechanism is essential for the ability of CNTF to promote neurite growth. Inhibiting NF- κ B-dependent transcription, blocking tyrosine phosphorylation of I κ B α and inhibiting SYK activation each caused very substantial reductions in the size and complexity of the neurite arbors of CNTF-stimulated neurons. Although NF- κ B signaling makes a small contribution to the neurite growth-promoting effects of the neurotrophins NGF and BDNF (Sole et al., 2004; Gutierrez et al., 2005), the essential role of NF- κ B signaling in CNTF-promoted growth is a striking, novel finding. Although CNTF is known to activate signaling pathways implicated in regulating neurite growth such as MEK/ERK and PI3-K/Akt (Alonzi et al., 2001), there have been no direct studies of the involvement of these or other signaling pathways in mediating the neurite growth promoting effects of CNTF and related neurotrophic cytokines in primary neurons. Our results therefore provide an important insight into the intracellular signaling mechanisms that are crucial for the neurite growth-promoting actions of cytokines like CNTF.

A striking finding of our study is that CNTF uses a distinctive noncanonical NF- κ B activation mechanism involving tyrosine phosphorylation of I κ B α to promote neurite growth. Previous work has shown that the contribution of NF- κ B signaling to neurotrophin-promoted neurite growth occurs via the canonical pathway that involves serine phosphorylation of I κ B α and proteasome mediated degradation of I κ B α (Sole et al., 2004; Gutierrez et al., 2005). Our demonstration that neither the 32/36-SS/AA I κ B α mutant nor proteasome inhibition affect CNTF-promoted neurite growth indicate that the canonical NF- κ B activation mechanism plays no part in the neurite growth-promoting actions of CNTF. Rather, we show that CNTF promotes tyrosine phosphorylation of I κ B α and selectively blocking this with a Y42F I κ B α mutant completely inhibits CNTF-enhanced NF- κ B transcriptional activity and blocks CNTF-promoted neurite growth. Because the Y42F I κ B α mutant does not affect BDNF-promoted neurite growth, our findings imply that different NF- κ B activation mechanisms are exclusively required for the neurite growth-promoting effects of CNTF and neurotrophins.

Our work has implicated the SYK protein-tyrosine kinase in CNTF-promoted NF- κ B activation and neurite growth. We have shown that CNTF promotes rapid sequential tyrosine phosphorylation of SYK and I κ B α . Pharmacological blockade of SYK and expression of a dominant-negative SYK protein inhibit CNTF-promoted neurite growth. SYK is a widely expressed protein-tyrosine kinase (Yanagi et al., 2001) that has been extensively studied from the standpoint of its role in immunoreceptor signaling in leukocytes (Berton et al., 2005). Although overexpression of SYK has been reported to promote the differentiation of embryonal carcinoma P19 cells into neuron-like cells (Tsujimura et al., 2001), we provide the first clear evidence in primary neurons that SYK plays a crucial role in regulating the growth of neural processes. In future work it will be interesting to ascertain

the link between the CNTF receptor complex and SYK and to establish whether other signaling pathways activated by CNTF cooperate with NF- κ B in mediating the effects of this cytokine on neurite growth.

Investigation of the key role of NF- κ B signaling in CNTF-promoted neurite growth has been facilitated in newborn nodose neurons because CNTF supports the survival of the majority of these neurons in culture and NF- κ B inhibition has no detectable effect on their survival. Previous work has established a neuroprotective role for NF- κ B for a variety of CNS neurons (Kaltschmidt et al., 2005) and NF- κ B signaling has been shown to contribute to the survival response of embryonic sympathetic and sensory to NGF (Maggirwar et al., 1998; Hamanoue et al., 1999) and adult DRG neurons to tumor necrosis factor- α (Feryhough et al., 2005). Although it has been reported that NF- κ B plays a role in mediating the survival response of cultured fetal nodose neurons to CNTF (Middleton et al., 2000), our more extensive investigation in which NF- κ B activation has been blocked by variety of complementary approaches contradicts this general conclusion. Whereas inhibiting NF- κ B signaling leaves the cell bodies of newborn nodose neurons without processes, these cell bodies retained a normal appearance and were stained with the vital dye calcein-AM with no significant loss in number up to 48 h *in vitro*. Likewise, inhibiting NF- κ B activation in fetal nodose neurons by the same diverse approaches virtually eliminated neurite growth while leaving cell bodies intact and viable (data not shown). Our findings therefore clearly demonstrate that NF- κ B signaling is crucial for the growth of neurites from developing nodose neurons stimulated with CNTF, but is not required for the survival response of these neurons to CNTF.

Studying primary neurons is a very powerful approach for elucidating growth factor physiology and signaling in the appropriate cellular and developmental context. Our studies of newborn nodose neurons have demonstrated a striking, essential role for NF- κ B signaling in CNTF-promoted neurite growth and revealed that the NF- κ B activation mechanism mediating this response of neurons to CNTF is distinct from the NF- κ B activation mechanism mediating the much smaller contribution of NF- κ B signaling to neurotrophin-promoted neurite growth. Although the very limited availability of primary neurons presents considerable technical challenges for biochemical studies of signaling networks, future progress on unraveling how cytokines and neuro-

trophins influence NF- κ B signaling in distinctive ways and how this in turn has such marked effects on neurite growth will be important in understanding the emerging role of NF- κ B signaling in regulating neuronal morphology in development.

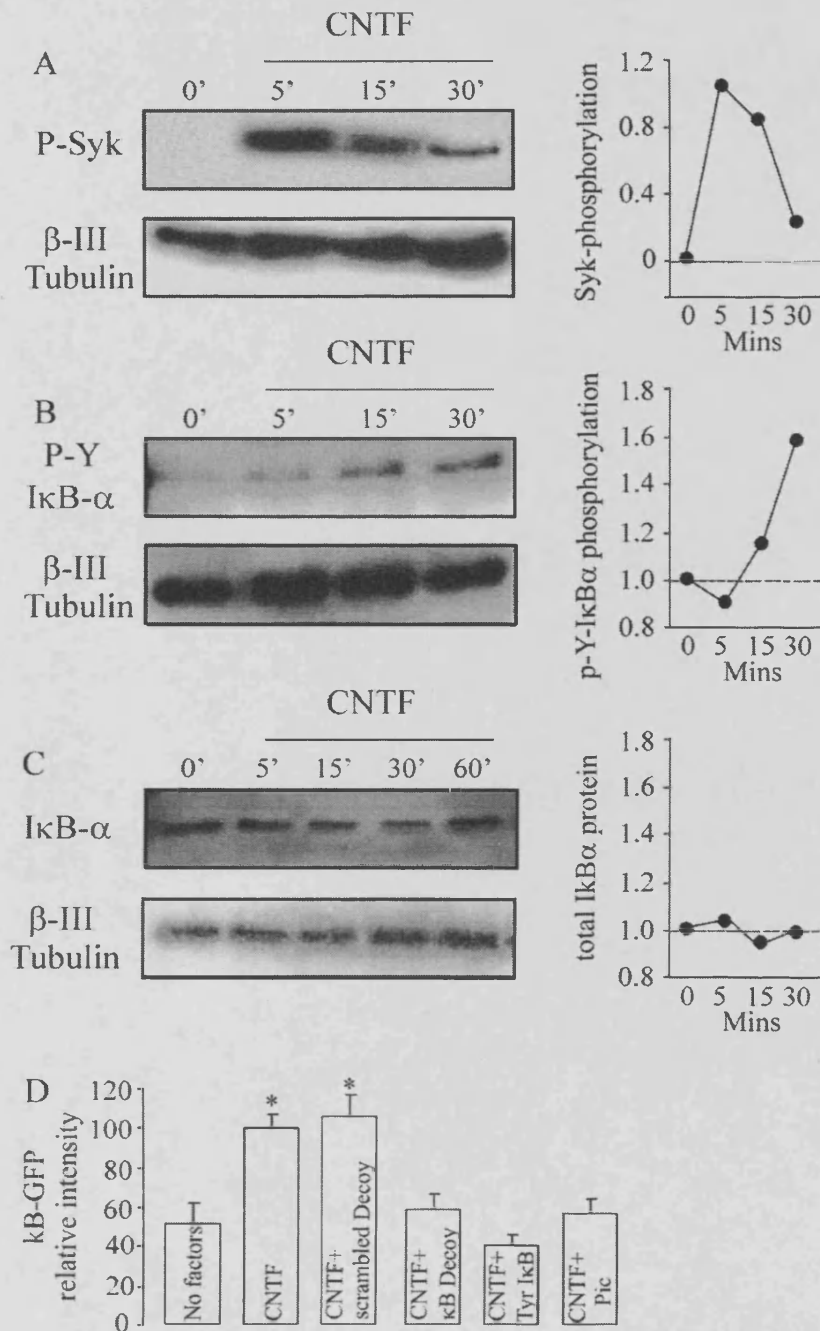


Figure 4. CNTF promotes tyrosine phosphorylation of SYK and I κ B- α and enhances NF- κ B transcriptional activity without I κ B- α degradation. **A–C**, Representative Western blots showing phosphotyrosine-SYK (**A**), phosphotyrosine-I κ B- α (**B**), and total I κ B- α protein (**C**) relative to β -III tubulin protein in cultured PO nodose neurons exposed to 50 ng/ml CNTF for the times indicated. Graphs of densitometric estimates of the relative phosphotyrosine-SYK and phosphotyrosine-I κ B- α levels in blots **A–C** are shown (similar data were obtained in three independent experiments). **D**, Relative level of NF- κ B-driven GFP fluorescence in PO nodose neurons 24 h after transfection with the NF- κ B reporter plasmid together with either the Y42F I κ B- α plasmid, an empty control plasmid, κ B decoy DNA, scrambled control oligonucleotide, or treatment with 10 μ M piceatannol (Syk inhibitor). Means \pm SEs of fluorescence measurements on 40–60 neurons per experiment are shown. Statistical comparisons are with respect to controls; * p < 0.05.

References

- Alonzi T, Middleton G, Wyatt S, Buchman V, Betz UA, Muller W, Musiani P, Poli V, Davies AM (2001) Role of STAT3 and PI 3-kinase/Akt in mediating the survival actions of cytokines on sensory neurons. *Mol Cell Neurosci* 18:270–282.
- Berton G, Mocsaï A, Lowell CA (2005) Src and Syk kinases: key regulators of phagocytic cell activation. *Trends Immunol* 26:208–214.
- Bui NT, Livolsi A, Peyron JF, Prehn JH (2001) Activation of nuclear factor κ B and Bcl-x survival gene expression by nerve growth factor requires tyrosine phosphorylation of I κ B α . *J Cell Biol* 152:753–764.
- Cui Q, Harvey AR (2000) CNTF promotes the regrowth of retinal ganglion cell axons into murine peripheral nerve grafts. *NeuroReport* 11:3999–4002.
- Fernyhough P, Smith DR, Schapansky J, Van Der Ploeg R, Gardiner NJ, Tweed CW, Kontos A, Freeman L, Purves-Tyson TD, Glazner GW (2005) Activation of nuclear factor- κ B via endogenous tumor necrosis factor α regulates survival of axotomized adult sensory neurons. *J Neurosci* 25:1682–1690.
- Gutierrez H, Hale V, Dolcet X, Davies A (2005) NF- κ B signalling regulates the growth of neural processes in the developing peripheral and central nervous systems. *Development* 132:1713–1726.
- Hamanoue M, Middleton G, Wyatt S, Jaffray E, Hay RT, Davies AM (1999) p75-mediated NF- κ B activation enhances the survival response of developing sensory neurons to nerve growth factor. *Mol Cell Neurosci* 14:28–40.
- Hartnick CJ, Staecker H, Malgrange B, Lefebvre PP, Liu W, Moonen G, Van de Water TR (1996) Neurotrophic effects of BDNF and CNTF, alone and in combination, on postnatal day 5 rat acoustic ganglion neurons. *J Neurobiol* 30:246–254.
- Hayden MS, Ghosh S (2004) Signaling to NF- κ B. *Genes Dev* 18:2195–2224.
- Horton AR, Barlett PF, Pennica D, Davies AM (1998) Cytokines promote the survival of mouse cranial sensory neurones at different developmental stages. *Eur J Neurosci* 10:673–679.
- Imbert V, Rupec RA, Livolsi A, Pahl HL, Traenckner EB, Mueller-Dieckmann C, Farahifar D, Rossi B, Aubergier P, Baeuerle PA, Peyron JF (1996) Tyrosine phosphorylation of I κ B- α activates NF- κ B without proteolytic degradation of I κ B- α . *Cell* 86:787–798.
- Kaltschmidt B, Widera D, Kaltschmidt C (2005) Signaling via NF- κ B in the nervous system. *Biochim Biophys Acta* 1745:287–299.
- Koong AC, Chen EY, Giaccia AJ (1994) Hypoxia causes the activation of nuclear factor kappa B through the phosphorylation of I κ B α on tyrosine residues. *Cancer Res* 54:1425–1430.
- Liang Y, Zhou Y, Shen P (2004) NF- κ B and its regulation on the immune system. *Cell Mol Immunol* 1:343–350.
- Maggirwar SB, Sarmiere PD, Dewhurst S, Freeman RS (1998) Nerve growth factor-dependent activation of NF- κ B contributes to survival of sympathetic neurons. *J Neurosci* 18:10356–10365.
- Middleton G, Hamanoue M, Enokido Y, Wyatt S, Pennica D, Jaffray E, Hay RT, Davies AM (2000) Cytokine-induced nuclear factor kappa B activation promotes the survival of developing neurons. *J Cell Biol* 148:325–332.
- Morishita R, Sugimoto T, Aoki M, Kida I, Tomita N, Moriguchi A, Maeda K, Sawa Y, Kaneda Y, Higaki J, Ogihara T (1997) *In vivo* transfection of cis element “decoy” against nuclear factor- κ B binding site prevents myocardial infarction. *Nat Med* 3:894–899.
- Nishimune H, Vasseur S, Wiese S, Birling MC, Holtmann B, Sendtner M, Iovanna JL, Henderson CE (2000) Reg-2 is a motoneuron neurotrophic factor and a signalling intermediate in the CNTF survival pathway. *Nature Cell Biol* 2:906–914.
- Oliver JM, Burg DL, Wilson BS, McLaughlin JL, Geahlen RL (1994) Inhibition of mast cell Fc epsilon R1-mediated signaling and effector function by the Syk-selective inhibitor, piceatannol. *J Biol Chem* 269:29697–29703.
- Rane SG, Reddy EP (2000) Janus kinases: components of multiple signaling pathways. *Oncogene* 19:5662–5679.
- Roff M, Thompson J, Rodriguez MS, Jacque JM, Baleux F, Arenzana-Seisdedos F, Hay RT (1996) Role of I κ B α ubiquitination in signal-induced activation of NF κ B *in vivo*. *J Biol Chem* 271:7844–7850.
- Siegel SG, Patton B, English AW (2000) Ciliary neurotrophic factor is required for motoneuron sprouting. *Exp Neurol* 166:205–212.
- Sole C, Dolcet X, Segura MF, Gutierrez H, Diaz-Meco MT, Gozzelino R, Sanchis D, Bayascas JR, Gallego C, Moscat J, Davies AM, Comella JX (2004) The death receptor antagonist FAIM promotes neurite outgrowth by a mechanism that depends on ERK and NF- κ B signaling. *J Cell Biol* 167:479–492.
- Stahl N, Yancopoulos GD (1994) The tripartite CNTF receptor complex: activation and signalling involves components shared with other cytokines. *J Neurobiol* 25:1454–1466.
- Takada Y, Mukhopadhyay A, Kundu GC, Mahabeshwar GH, Singh S, Aggarwal BB (2003) Hydrogen peroxide activates NF- κ B through tyrosine phosphorylation of I κ B α and serine phosphorylation of p65: evidence for the involvement of I κ B α kinase and Syk protein-tyrosine kinase. *J Biol Chem* 278:24233–24241.
- Tomita N, Morishita R, Tomita S, Gibbons GH, Zhang L, Horiuchi M, Kaneda Y, Higaki J, Ogihara T, Dzau VJ (2000) Transcription factor decoy for NF κ B inhibits TNF- α -induced cytokine and adhesion molecule expression *in vivo*. *Gene Ther* 7:1326–1332.
- Tsujimura T, Yanagi S, Inatome R, Takano T, Ishihara I, Mitsui N, Takahashi S, Yamamura H (2001) Syk protein-tyrosine kinase is involved in neuron-like differentiation of embryonal carcinoma P19 cells. *FEBS Lett* 489:129–133.
- Yanagi S, Inatome R, Takano T, Yamamura H (2001) Syk expression and novel function in a wide variety of tissues. *Biochem Biophys Res Commun* 288:495–498.

Abnormal Sympathoadrenal Development and Systemic Hypotension in *PHD3*^{-/-} Mice[∇]

Tammie Bishop,^{1†} Denis Gallagher,^{2†} Alberto Pascual,³ Craig A. Lygate,⁴ Joseph P. de Bono,⁴
Lynn G. Nicholls,¹ Patricia Ortega-Saenz,³ Henrik Oster,⁴ Bhatiya Wijeyekoon,¹ Andrew I. Sutherland,¹
Alexandra Grosfeld,¹ Julian Aragones,^{5,6} Martin Schneider,^{5,6} Katie van Geyte,^{5,6} Dania Teixeira,²
Antonio Diez-Juan,^{5,6} Jose Lopez-Barneo,³ Keith M. Channon,⁴ Patrick H. Maxwell,⁷
Christopher W. Pugh,¹ Alun M. Davies,² Peter Carmeliet,^{5,6} and Peter J. Ratcliffe^{1*}

The Henry Wellcome Building for Molecular Physiology, University of Oxford, Headington Campus, Roosevelt Drive, Oxford OX3 7BN, United Kingdom¹; School of Biosciences, Cardiff University, Museum Avenue, P.O. Box 911, Cardiff CF10 3US, United Kingdom²; Laboratorio de Investigaciones Biomédicas, Hospital Universitario Virgen del Rocío, Universidad de Sevilla, Sevilla, Spain³; The Henry Wellcome Building for Genomic Medicine, University of Oxford, Headington Campus, Roosevelt Drive, Oxford OX3 7BN, United Kingdom⁴; Department for Transgene Technology and Gene Therapy, VIB, 3000 Leuven, Belgium⁵; The Center for Transgene Technology and Gene Therapy, K. U. Leuven, 3000 Leuven, Belgium⁶; and Renal Laboratory, Hammersmith Campus, Imperial College London, Du Cane Road, London W12 0NN, United Kingdom⁷

Received 13 November 2007/Returned for modification 19 December 2007/Accepted 25 February 2008

Cell culture studies have implicated the oxygen-sensitive hypoxia-inducible factor (HIF) prolyl hydroxylase *PHD3* in the regulation of neuronal apoptosis. To better understand this function *in vivo*, we have created *PHD3*^{-/-} mice and analyzed the neuronal phenotype. Reduced apoptosis in superior cervical ganglion (SCG) neurons cultured from *PHD3*^{-/-} mice is associated with an increase in the number of cells in the SCG, as well as in the adrenal medulla and carotid body. Genetic analysis by intercrossing *PHD3*^{-/-} mice with *HIF-1α*^{+/-} and *HIF-2α*^{+/-} mice demonstrated an interaction with *HIF-2α* but not *HIF-1α*, supporting the nonredundant involvement of a *PHD3*–*HIF-2α* pathway in the regulation of sympathoadrenal development. Despite the increased number of cells, the sympathoadrenal system appeared hypofunctional in *PHD3*^{-/-} mice, with reduced target tissue innervation, adrenal medullary secretory capacity, sympathoadrenal responses, and systemic blood pressure. These observations suggest that the role of *PHD3* in sympathoadrenal development extends beyond simple control of cell survival and organ mass, with functional *PHD3* being required for proper anatomical and physiological integrity of the system. Perturbation of this interface between developmental and adaptive signaling by hypoxic, metabolic, or other stresses could have important effects on key sympathoadrenal functions, such as blood pressure regulation.

In response to low oxygen tensions, organisms mount a wide-ranging adaptive response involving many cellular and systemic processes. Activation of hypoxia-inducible factor (HIF) plays a central role in this process, inducing transcriptional targets that enhance oxygen delivery, better adapt cells to hypoxia, or modulate cell proliferation or survival pathways (reviewed in references 16 and 37). Hypoxia may, under different circumstances, either promote or protect cells from apoptosis, and HIF itself contributes to these processes both indirectly, through the defense of cellular energy supplies, and directly, via transcriptional changes in proapoptotic or prosurvival genes. However, to generate the anatomical and physiological integrity required for oxygen homeostasis in the intact organism, these adaptive responses to hypoxia must also be accurately interfaced with the developmental control of growth.

Though the nature of these adaptive-developmental connec-

tions remains poorly understood, it is of interest that the cellular oxygen sensor *PHD3* (otherwise termed *EGLN3* or *HPH1*), one of three Fe(II)-dependent dioxygenases now known to negatively regulate HIF by prolyl hydroxylation of HIF- α subunits (*HIF-1 α* and *HIF-2 α*) (6, 13), had been previously identified as a gene involved in developmental apoptosis of neurons (23–25, 40). Over 50% of neurons produced during development die through apoptosis before adulthood (reviewed in references 10 and 31). This process is largely regulated by neurotrophic factors that are secreted in limited amounts by target tissues such that only those neurons making appropriate connections survive. During the investigation of these phenomena, *PHD3* mRNA was identified as a neuronal transcript that is induced by withdrawal of the neurotrophin nerve growth factor (NGF) (24). Further studies have demonstrated that overexpression of *PHD3* in primary sympathetic neurons cultured from the developing superior cervical ganglion and in the adrenal medullary tumor cell line PC12 results in apoptosis even in the presence of saturating quantities of NGF (23, 24). This effect was not reproduced by a catalytically inactive *PHD3* mutant (23), whereas hypoxia was able to suppress apoptosis in sympathetic neurons (44). Furthermore, knock-down of *PHD3* by small interfering RNA in PC12 cells prevented apoptosis even in the absence of NGF (23). Taken

* Corresponding author. Mailing address: The Henry Wellcome Building for Molecular Physiology, University of Oxford, Headington Campus, Roosevelt Drive, Oxford OX3 7BN, United Kingdom. Phone: (44) 1865 287 990. Fax: (44) 1865 287 992. E-mail: pjr@well.ox.ac.uk.

† T.B. and D.G. contributed equally to this work.

[∇] Published ahead of print on 10 March 2008.

together, these observations in cultured cells indicate that the oxygen-sensitive catalytic activity of PHD3 has a role in the regulation of neuronal apoptosis, raising important questions about the extent of PHD3-dependent neuronal apoptosis in vivo and its role in the intact animal.

To address this, we have inactivated PHD3 (by homologous recombination in the mouse) and have analyzed the developmental and physiological effects on neuronal apoptosis. We show that PHD3-dependent modulation of NGF-dependent survival is a lineage-specific property affecting the sympathetic nervous system and that sympathetic neurons from *PHD3*^{-/-}, but not *PHD2*^{+/-} or *PHD1*^{+/-}, mice manifest increased NGF-promoted neurite growth as well as enhanced survival. Increased numbers of sympathetic neurons survive to adulthood, and *PHD3*^{-/-} mice have increased numbers of neurons in the superior cervical ganglia (SCG) and increased numbers of chromaffin and glomus cells in the adrenal medulla and carotid body. However, despite this increase in cell number, the sympathoadrenal system was dysfunctional in *PHD3*^{-/-} mice, with reduced innervation of target organs and dysregulated responses, including reduced catecholamine secretion and reduced systemic blood pressure. The findings demonstrate a key role for PHD3 in regulating the anatomical and physiological integrity of the sympathoadrenal system.

MATERIALS AND METHODS

Targeting vector and PHD3 inactivation. For construction of the PHD3 targeting vector, the following fragments were cloned in a pPNTLox2 vector (from 5' to 3'): a 3.4-kb BamHI fragment located 3.1 kb upstream of exon 1 (5' flank) and a neomycin resistance cassette in the opposite orientation, a 3.9-kb EcoRI fragment located 1.4 kb downstream of exon 1 (3' flank), and a thymidine kinase selection cassette (Fig. 1A). Embryonic stem (ES) cells (129 SvEv background) were electroporated with the linearized targeting vector for PHD3 as described elsewhere (39). Resistant clones were screened for homologous recombination by Southern blotting (Fig. 1B) and PCR (not shown). Correctly recombined ES cells were then aggregated with morula-stage embryos. To obtain *PHD3*^{+/-} germ line offspring in a 50% Swiss/50% 129 SvEv background, chimeric male mice were intercrossed with wild-type Swiss female mice. PHD3 mRNA transcripts were quantified by RNase protection assay in embryos (Fig. 1C), using a riboprobe protecting bp 217 to 383, 5' to 3', of PHD3 mRNA, and real-time reverse transcription-PCR (RT-PCR) in mouse embryonic fibroblasts (Fig. 1D), using the following forward and reverse primers: 5'-TCCCCTCTCCACCTTC-3' and 5'-CTGTAGCCGTATTCATTGTC-3' for glyceraldehyde-3-phosphate dehydrogenase (GAPDH); 5'-CTATGGGAAGAGCAAAGC-3' and 5'-AGAGCAGATGATGTGGAA-3' for PHD3, which amplify bp 1779 to 2008, a sequence distal to the deleted region, in response to normoxia or hypoxia (1% oxygen for 16 h). PHD3 protein levels were also measured by Western blotting in mouse embryonic fibroblasts with a monoclonal mouse anti-PHD3 antibody, P3-188c (1), to confirm their absence in *PHD3*^{-/-} tissues.

Animals. Wild-type, *PHD3*^{-/-}, *PHD1*^{+/-}, *PHD2*^{+/-}, *PHD3*^{+/-}; *HIF-1α*^{+/-}, and *PHD3*^{-/-}; *HIF-2α*^{+/-} and *HIF-2α*^{+/-} mice on a mixed Swiss/129SvEv genetic background were used in the experiments. Mice from the same litter were used for all comparisons, except for *HIF-2α*^{+/-} versus *PHD3*^{-/-}; *HIF-2α*^{+/-} (see Fig. 5D, below) where appropriate crosses were unlikely, by Mendelian inheritance, to produce the required genotypes within littermates. For adult mice, males of between 3 and 6 months of age were used.

Neuronal culture. SCG, dorsal root ganglia (DRG), and trigeminal ganglia (TG) were dissected from postnatal day 0 (P0) mouse pups, trypsinized in 0.05% trypsin in Hanks' balanced salt solution (Gibco) for 20 min at 37°C, and dissociated by trituration. Dissociated cultures of SCG, DRG, and TG neurons were then plated at low density (150 to 300 cells/dish) on a poly-ornithine/laminin substrate in 35-mm tissue culture dishes in defined, serum-free medium, as described previously (11). A range of concentrations (0 to 250 ng/ml) of NGF or neurotrophin 3 (NT-3; both were from R&D Systems, Minneapolis, MN) was added to support the survival of cultured neurons.

Neuronal survival was measured by counting the number of neurons in a 12-by-12-mm grid in the center of the dish both 3 and 24 h after plating (as described

in reference 11). The number of neurons surviving after 24 h was expressed as a percentage of the initial number of neurons.

Total viable neuronal counts were measured by counting the number of phase-bright neurons using a Neubauer hemocytometer immediately following dissociation of neurons.

Neuritic morphology was measured by culturing neonatal SCG neurons for 24 h with 10, 0.4, or 0.08 ng/ml NGF, as described above. Caspase inhibitors (100 μM; Calbiochem) were added to cultures containing limiting levels of NGF (0.4 and 0.08 ng/ml) in order to avoid biased sampling of differentially surviving neurons. Neurons were then fluorescently labeled with the vital dye calcein-AM (Invitrogen), and images were acquired using an Axioplan Zeiss laser scanning confocal microscope. Neuritic arbors were traced using LSM510 software in order to calculate the total neurite length and the extent of arborization by Sholl analysis. For the latter, concentric, digitally generated rings, 30 μm apart, were centered on the cell soma, and the number of neurites intersecting each ring was counted (38).

Quantitative RT-PCR. Dissociated SCG, DRG, and TG neurons from wild-type P0 mouse pups were cultured overnight in 10 ng/ml NGF as described above. Neurons were then washed with defined culture medium and grown in either the presence or absence of NGF for 10 h (the time point at which PHD3 mRNA induction is maximal in the SCG [24]) before harvesting the cells for RNA. Total RNA was isolated with the RNeasy Mini extraction kit (Qiagen, Hilden, Germany) and then reverse transcribed for 1 h at 37°C with StrataScript reverse transcriptase (Stratagene). Reverse transcription reactions were amplified using the Brilliant QPCR core reagent kit (Stratagene) according to the manufacturer's protocol. The PCR was performed with the Mx3000P apparatus (Stratagene) for 45 cycles of 95°C for 30 s, 52°C (for PHD3) or 51°C (for GAPDH) for 1 min, and 72°C for 30 s. A melting curve was obtained to confirm that the Sybr green (Molecular Probes) signal corresponded to a unique and specific amplicon. Standard curves were generated for every real-time PCR run by using serial fourfold dilutions of a reverse-transcribed RNA extract from adult heart. Primers for PHD3 and GAPDH were as described above.

Histological and stereological analyses. To estimate the total tyrosine hydroxylase (TH)-positive cell number, the SCG, adrenal medulla, and carotid body from adult mice were fixed in formalin overnight and then transferred into phosphate-buffered saline (PBS) containing 30% sucrose. Twenty-μm sections were blocked for 1 h at room temperature with 10% fetal calf serum and 1 mg/ml bovine serum albumin containing 0.1% Triton X-100 in PBS and then incubated for 16 h at 4°C with a rabbit anti-TH polyclonal antibody (Pel-Freez; diluted 1:1,000 in blocking solution). The sections were washed four times in PBS-Triton before being incubated with goat anti-rabbit secondary antibody (Envision+; Dako). Stereological estimation of the number of TH-positive cells was performed on sections spaced 80 μm (SCG and adrenal medulla) or 40 μm (carotid body) throughout the organ. The number of cells was estimated by systematic random sampling using a 106,954-μm³ optical disector (43), excluding cells in the superficial planes of sections. The volume of each organ was estimated according to Cavalieri's principle (8). The adrenal medulla cell volume was calculated using a rotator vertical probe. Seven randomly selected TH-positive cells were measured in different sections per individual adrenal gland. Stereological measurements were performed using the CAST grid system (Olympus) with a coefficient of error of <0.09.

To detect apoptosis in the SCG from P0 mice, tissues were fixed in formalin overnight and then transferred to 70% ethanol and paraffin embedded. The terminal deoxynucleotidyltransferase-mediated dUTP-biotin nick end labeling (TUNEL) method was performed on 7-μm sections of the SCG using the ApopTag peroxidase in situ apoptosis detection kit (Chemicon International) according to the manufacturer's directions.

To assess the density of sympathetic innervation, the eyes and submandibular and pineal glands from adult mice (or P5 mice for the pineal glands) were fixed and cryoprotected as above. Fifteen-μm serial sections were blocked for 1 h at room temperature with 10% normal goat serum containing 0.1% Triton X-100 in 10 mM PBS and then incubated for 18 h at 4°C with a rabbit anti-TH polyclonal antibody (diluted 1:200 in PBS with 1% normal goat serum; Chemicon). The sections were washed three times in PBS before being incubated with goat anti-rabbit secondary antibody (Alexa-Fluor, diluted 1:500 in PBS with 1% normal goat serum; Invitrogen). The outlines of the iris and submandibular and pineal glands were traced using Adobe Photoshop 7. The total and TH-positive areas were measured using automated pixel counts, and the ratio of TH-positive area to total area was used to calculate the TH-positive density.

Pupillometry. Adult wild-type and *PHD3*^{-/-} mice were dark adapted for 1 h. Subsequently, animals were removed from their home cage, immobilized by scruffing, and pupil reactions were monitored (at 0 lx followed by 150 lx of bright white light) using a commercial charge-coupled-device camcorder (DCR-

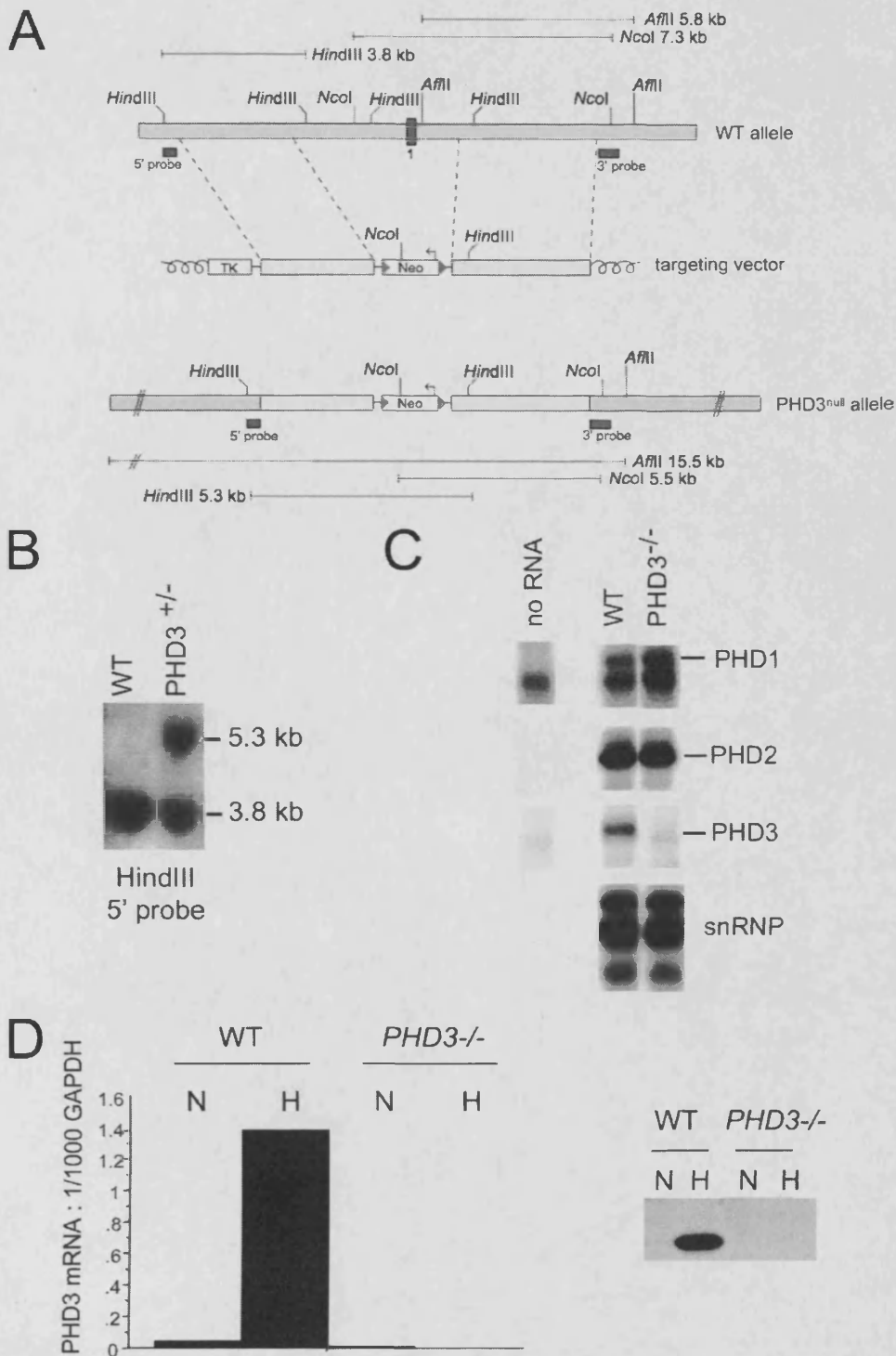


FIG. 1. PHD3 targeting strategy. (A) Targeting strategy for PHD3 inactivation. Top: wild-type PHD3 allele diagram, indicating the position of exon 1 (dark box in the genomic structure). Middle: outline of the targeting vector, specifying the genomic sequences used as 5' and 3' homology flanks, inserted on each side of a neomycin resistance (Neo) cassette. A thymidine kinase (TK) gene outside the flanking homologies allowed for negative selection against random integration events. Bottom: replacement of exon 1 by the Neo cassette after homologous recombination. Diagnostic restriction fragments are indicated with their relative sizes by the thin lines under or above the alleles. Dark bars under the genes represent the probes used for Southern blot analysis. (B) Southern blot analysis of genomic DNA from recombinant ES cells, digested with HindIII and hybridized with the 5' external probe. The 3.8-kb and 5.3-kb genomic fragments correspond to PHD3 wild-type (WT) and PHD3^{muti} alleles, respectively. (C) RNase protection assay demonstrating PHD1, -2, and -3 mRNA levels in total RNA extracted from wild-type and PHD3^{-/-} embryos. U6 small nuclear RNA (snRNP) was used as an internal control. (D) Quantitative RT-PCR (left panel) and Western blot assay (right panel) showing induction of PHD3 mRNA and protein in wild-type, but not PHD3^{-/-}, mouse embryonic fibroblasts in response to hypoxia. N, normoxia; H, hypoxia (1% oxygen for 16 h).

HC17E; Sony, Tokyo, Japan) attached to a dissecting microscope (Olympus, Tokyo, Japan) under infrared light-emitting diode illumination (λ_{max} of 850 nm). Pupil areas were estimated by manually fitting an ellipse to digitalized video still images using Windows Movie Maker (Microsoft, Redmond, WA) and Adobe Photoshop (San Jose, CA) software.

In vivo hemodynamics. Adult mice were anesthetized with 2% isoflurane in 100% oxygen via a nose cone. Mice were placed supine with body temperature regulated at 37°C and allowed to breathe spontaneously. The right carotid artery was cannulated with a 1.4 French microtipped cannula (SPR-839; Millar Instruments, Houston, TX) advanced retrograde into the left ventricular (LV) cavity under ultrasound guidance. The right jugular vein was cannulated with polyethylene tubing for intravenous drug administration. Isoflurane was reduced to 1.5%, followed by a period of equilibration until hemodynamic indices were stable for >15 min. Pressure measurements were recorded using a Powerlab 4SP data recorder (ADInstruments, Chalgrove, United Kingdom) at baseline in both the LV and aorta and in the LV during infusion of β_1 -adrenoreceptor stimulation with dobutamine hydrochloride (16 ng/g of body wt/min).

A subset of these mice were used to test baroreceptor reflex function by intravenous bolus administration of the α_1 -adrenoreceptor agonist phenylephrine hydrochloride (at 50 $\mu\text{g}/\text{kg}$) to induce brief periods of elevated blood pressure (30). Baroreceptor reflex gain was calculated as the maximal change in heart rate over the maximal change in blood pressure. Drug solutions for bolus injection were made up in 0.9% saline and a volume of 5 μl . Mice were killed by cervical dislocation or removal of the heart, and the cardiac chambers blotted and weighed.

Radiotelemetry. PAC10 radiotelemeters (Data Sciences International, MN) were implanted in the left carotid artery of adult mice under isoflurane anesthesia as previously described (7, 29). Mice were allowed to recover for 10 days following the operation, and then continuous measurements of blood pressure and activity state were recorded, at 500 Hz, for three consecutive days using standard acquisition software (Data Sciences International, MN). Blood pressure was analyzed on a beat-per-beat basis according to the activity state of the mouse at the time of recording (Spike 2, version 6.1; Cambridge Electronic Design, Cambridge, United Kingdom). Two activity states were defined: rest, no movement of the animal as detected by the telemeter within 30 s of measurement; activity, movement of the mouse within its cage at the time of recording.

Amperometric recording of single-cell catecholamine secretion in isolated slices. Adult mouse suprarenal gland dissection, slicing, and culture, as well as the measurement of catecholamine secretion, were performed following previously described procedures (14). Slices were transferred to a recording chamber and continuously perfused with a solution containing 117 mM NaCl, 4.5 mM KCl, 23 mM NaHCO_3 , 1 mM MgCl_2 , 2.5 mM CaCl_2 , 5 mM glucose, and 5 mM sucrose. When 40 mM or 20 mM potassium solutions were used, equimolar quantities of sodium were used to replace potassium. The solution was bubbled with a gas mixture of 5% CO_2 to adjust the pH to 7.2. All the experiments were performed in a chamber at 36°C. Secretion rate (femtocoulombs/min) was calculated as the amount of charge transferred to the recording electrode during a given time period (32).

Plasma catecholamines. Blood from adult mice (anesthetized with Nembutal; 600 $\mu\text{g}/\text{kg}$ of body weight) was collected into heparinized tubes on ice that were then centrifuged at $6,000 \times g$ for 5 min at 4°C to separate plasma. Plasma catecholamine levels were quantified by immunoassay according to the manufacturer's instructions (IBL-Hamburg).

Statistical analyses. Data are expressed as means \pm standard errors of the means (SEM), with the number of experiments indicated. Statistical analyses were performed using Student's *t* test. *P* values of <0.05 were considered statistically significant.

RESULTS

Generation of PHD3-deficient mice. Mice deficient in PHD3 were generated by standard homologous recombination procedures in ES cells. The PHD3 targeting strategy involved removing a genomic region encompassing the promoter and first exon, including the translational initiation site (Fig. 1A and B), and cells from *PHD3*^{-/-} homozygous animals expressed no PHD3 transcript (Fig. 1C and D, left panel) or protein (Fig. 1D, right panel). A small reduction in the expected number of *PHD3*^{-/-} live births was noted among the

offspring of heterozygous matings (*PHD3*^{+/+}, 77 [29%], *PHD3*^{+/-}, 145 [54%], *PHD3*^{-/-}, 47 [17%]), but otherwise *PHD3*^{-/-} mice appeared healthy and reached adult life without obvious abnormality.

Enhanced survival of sympathetic neurons from PHD3^{-/-} mice in vitro. Because experimental manipulation of PHD3 expression in cultured sympathetic neurons and PC12 cells has been reported to affect cell survival (23–25, 40), we directly compared the survival of sympathetic neurons obtained from the SCG of wild-type and *PHD3*^{-/-} mice. Heterozygous mice were mated to obtain offspring of all three genotypes, and dissociated low-density cultures of SCG neurons were established from newborn littermates. To minimize variability arising from technical considerations, in this and all subsequent experiments, comparisons of ganglia explanted from mice of different genotypes were performed in a pair-wise fashion at the same experimental session. The neurons were cultured with a range of NGF concentrations, and neuronal survival was estimated 24 h after plating. At nonsaturating concentrations of NGF, the survival of neurons from *PHD3*^{-/-} mice was consistently enhanced compared to that of neurons from wild-type mice (Fig. 2A, left panel). Interestingly, loss of PHD3 did not confer a survival advantage at very low NGF concentrations, suggesting that, although PHD3 reduces the capacity of neurons to survive in the presence of NGF, it is not required for the death of NGF-deprived neurons.

To test whether other prolyl hydroxylases that regulate HIF also affect the NGF survival response, similar cultures of SCG neurons were established from *PHD1*^{-/-} and *PHD2*^{+/-} mice (2) and compared with those from their littermate controls (*PHD2*^{-/-} mice could not be used because they die in utero between embryonic day 12.5 [E12.5] and E14.5 [2, 41]). In contrast with neurons from *PHD3*^{-/-} mice, no differences in NGF dose responses were observed (Fig. 2A, middle and right panels).

NGF promotes neuronal survival by binding to and activating the receptor tyrosine kinase TrkA (10). Because NT-3 is also capable of promoting the survival of neonatal SCG neurons in culture by a TrkA-dependent mechanism (12), we investigated whether inactivation of PHD3 affects the survival response of SCG neurons to this neurotrophin. As with NGF, SCG neurons from *PHD3*^{-/-} mice survived more effectively with NT-3 than neurons from wild-type littermates (Fig. 2B).

In addition to sympathetic neurons, large numbers of sensory neurons in the developing peripheral nervous system are also dependent on NGF for survival. To ascertain whether the absence of PHD3 also affects the NGF survival response of these neurons, we established low-density dissociated cultures from two populations of sensory neurons that are mostly comprised of NGF-dependent neurons: those of the DRG and TG. In contrast to SCG neurons, the NGF dose responses of DRG and TG neurons from wild-type and *PHD3*^{-/-} mice were completely overlapping (Fig. 2C). Since NGF withdrawal has been reported to induce PHD3 mRNA expression in sympathetic neurons (24), we considered whether this property might underlie the specificity of PHD3-dependent survival effects. To investigate this, we cultured SCG, DRG, and TG neurons with NGF and deprived them of this neurotrophin by extensive washing 12 h after plating. Measurement of PHD3 mRNA by

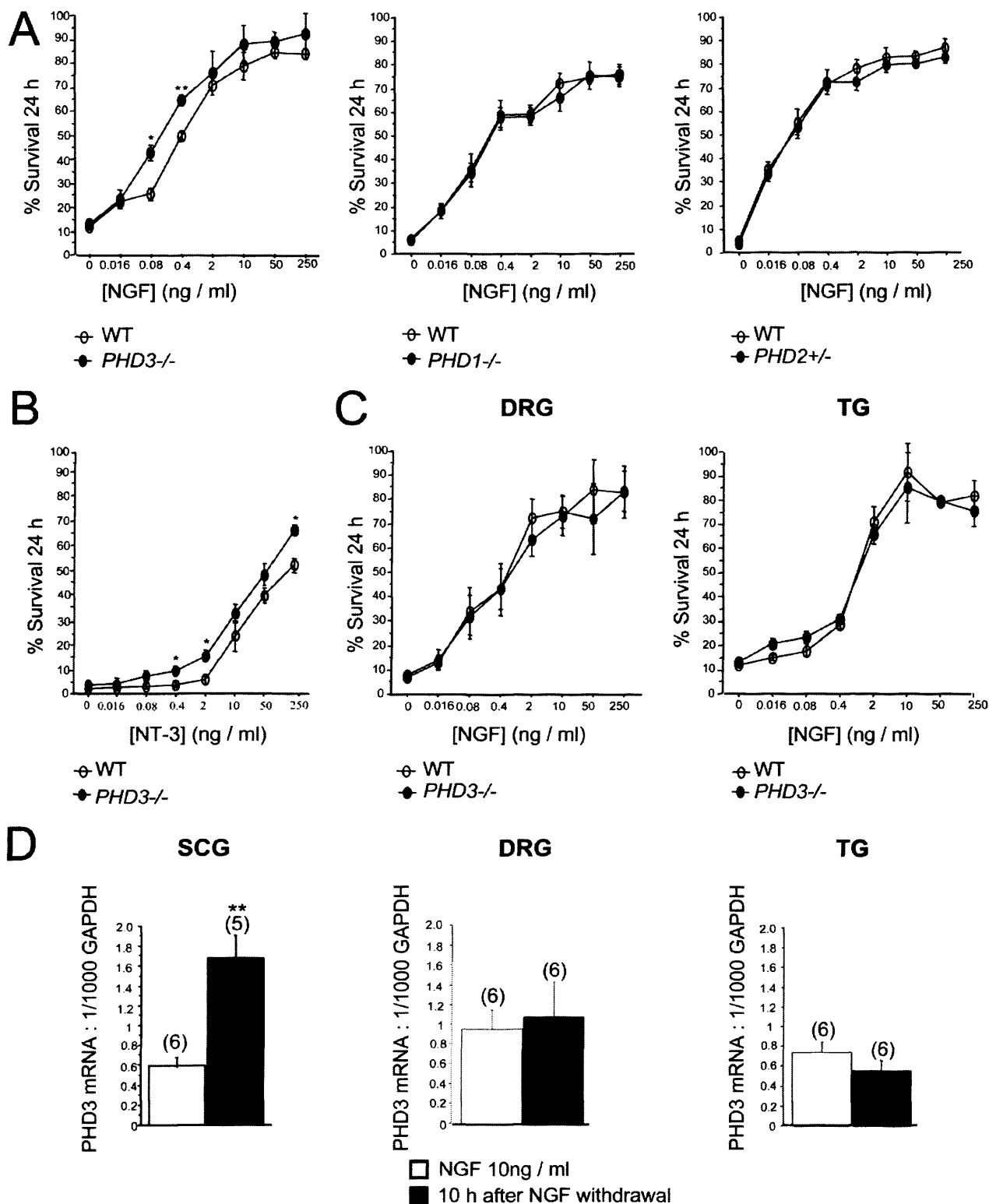


FIG. 2. Survival of neurons cultured from *PHD3*^{-/-} mice. (A) NGF dose-response curves, demonstrating increased neuronal survival in neurons cultured from the SCG of P0 *PHD3*^{-/-} mice but not *PHD1*^{-/-} or *PHD2*^{+/-} mice. Neuronal survival was estimated by expressing the number of surviving neurons after 24 h in culture as a percentage of the initial number of neurons at 3 h postplating. (B) NT-3 dose-response curve, showing increased survival in neurons cultured from the SCG of P0 *PHD3*^{-/-} mice. (C) NGF dose-response curves, showing no change in survival in neurons cultured from the DRG and TG of P0 *PHD3*^{-/-} mice. (D) Quantitative RT-PCR showing induction of PHD3 mRNA after NGF withdrawal in the SCG, but not the DRG or TG, from P0 wild-type mice. Values for this and all subsequent figures are presented as means \pm SEM ($n = 3$) for dose-response curves, or n as indicated in parentheses. *, $P < 0.05$ versus control; **, $P < 0.01$ versus control.

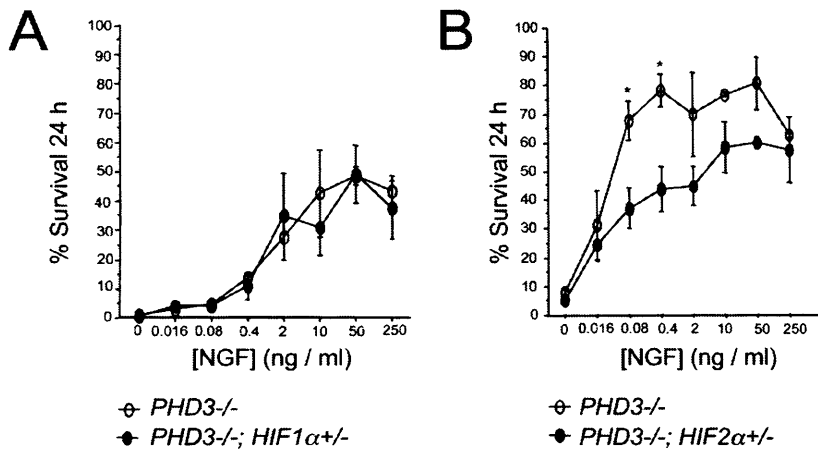


FIG. 3. HIF dependence of the PHD3 survival effect. NGF dose-response curves for neonatal SCG neurons showing no difference in survival of neurons derived from $PHD3^{-/-}$; $HIF-1\alpha^{+/-}$ versus $PHD3^{-/-}$ mice (A) and reduced survival of neurons derived from $PHD3^{-/-}$; $HIF-2\alpha^{+/-}$ versus $PHD3^{-/-}$ mice (B).

RT-PCR 10 h after deprivation revealed a greater-than-twofold increase in PHD3 mRNA relative to GAPDH mRNA in sympathetic neurons but no significant change in sensory neurons (Fig. 2D). Thus, both PHD3-dependent neuronal survival and responsiveness of PHD3 mRNA to NGF withdrawal appear to be specific to sympathetic neurons rather than a general property of NGF-sensitive neurons.

HIF-2-dependent survival in sympathetic neurons from $PHD3^{-/-}$ mice in vitro. Because of the known function of PHD3 as a HIF hydroxylase regulating the abundance of HIF-1 α and HIF-2 α , we investigated whether the influence of PHD3 on the NGF dose response of SCG neurons depends on either HIF-1 α or HIF-2 α . Since homozygous inactivation of HIF-1 α or HIF-2 α results in embryonic lethality (20, 33, 34, 42), we analyzed the effects of heterozygous inactivation by generating appropriate crosses with $PHD3^{-/-}$ animals to allow for littermate comparisons. Although we observed some variation in the overall survival of explanted neurons from $PHD3^{-/-}$ mice at different experimental sessions, clear differences were observed in pair-wise comparisons of $PHD3^{-/-}$ animals with and without heterozygous inactivation of different HIF- α isoforms. Heterozygous HIF-1 α inactivation did not significantly affect the NGF dose response of cultured PHD3-deficient SCG neurons ($PHD3^{-/-}$ versus $PHD3^{-/-}$; $HIF-1\alpha^{+/-}$ littermate neonates) (Fig. 3A). In contrast, inactivating one allele of HIF-2 α caused a significant shift in the NGF dose response of PHD3-deficient SCG neurons to higher NGF concentrations ($PHD3^{-/-}$ versus $PHD3^{-/-}$; $HIF-2\alpha^{+/-}$ littermate neonates) (Fig. 3B), suggesting that appropriate expression of HIF-2 α , but not HIF-1 α , is required for the influence of PHD3 on the NGF survival dose response in culture.

Enhanced NGF-promoted neurite growth of sympathetic neurons from $PHD3^{-/-}$ mice in vitro. In addition to supporting the survival of developing sympathetic neurons, NGF also promotes the growth of neurites from these neurons in culture (15). For this reason, we investigated neurite arbor size and complexity in sympathetic neurons from $PHD3^{-/-}$ mice. Low-density cultures of SCG neurons from P0 $PHD3^{-/-}$ and wild-

type mice were grown with different concentrations of NGF, and neurite arbor size and complexity were quantified 24 h after plating. At subsaturating concentrations of NGF (Fig. 4B and C), but not at saturating levels (Fig. 4A), the neurite arbors of PHD3-deficient neurons were significantly longer than those of wild-type neurons. Sholl analysis, which provides a graphic representation of neurite branching with distance from the cell body, revealed that the neurite arbors of PHD3-deficient neurons were larger and more branched than those of wild-type mice in the presence of subsaturating levels of NGF (Fig. 4B and C). The typical appearance of the neurite arbors of PHD3-deficient and wild-type SCG neurons grown with subsaturating NGF are illustrated in Fig. 4D. Because the neurites in short-term SCG cultures, such as those used in our study, are exclusively axons rather than dendrites, we conclude that PHD3 also modulates axonal growth and branching in culture.

PHD3-deficient mice have increased numbers of SCG neurons. To ascertain the developmental and physiological relevance of our in vitro observations, we compared the number of neurons in the SCG of wild-type and $PHD3^{-/-}$ mice. The neuronal complement of the SCG of newborn animals was estimated by counting the number of neurons in trypsin-dissociated cell suspensions obtained from carefully dissected ganglia. In order to minimize variability assignable to genetic background, absolute age of neurons, and dissociation technique, these comparisons were made between ganglia explanted at the same experimental session from mice within the same litter. Neurons were recognized and distinguished from nonneuronal cells by their characteristic large, phase-bright, spherical cell bodies under phase-contrast optics. SCG dissected from $PHD3^{-/-}$ newborn mice appeared larger than those of wild-type littermates (Fig. 5A) and contained significantly more neurons (Fig. 5B). Likewise, stereological measurements carried out on serially sectioned SCG in 3- to 6-month-old mice revealed that the SCG was larger and contained significantly more neurons in $PHD3^{-/-}$ mice compared with age-matched wild-type animals (Fig. 5C). As expected, the number of neurons in the SCG of

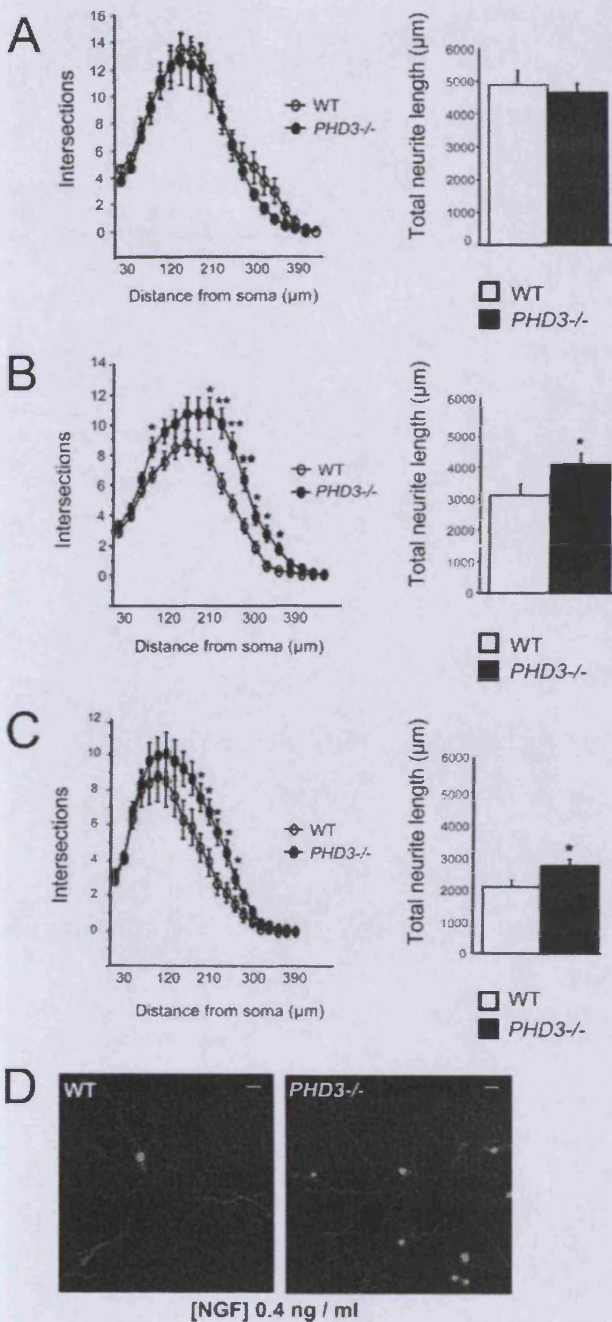


FIG. 4. Neurite length and arborization of sympathetic neurons cultured from *PHD3*^{-/-} mice. Increased neurite length and arborization in P0 *PHD3*^{-/-} mice at 0.4 (B) and 0.08 ng/ml NGF (C), but not at 10 ng/ml NGF (A). Neurite length is presented as the mean \pm SEM on 40 to 70 neurons per genotype (similar results were obtained in three independent experiments). (D) Representative images of neurons cultured in 0.4 ng/ml NGF and fluorescently labeled with the vital dye calcein-AM. Bar, 50 μ m.

wild-type adults was lower than that in newborns as a result of ongoing programmed cell death in the immediate postnatal period. However, the number of neurons in the SCG of *PHD3*^{-/-} mice remained substantially unchanged be-

tween birth and adulthood, suggesting that programmed cell death during at least the postnatal period was largely curtailed in these mice. In keeping with this, we observed a modest reduction in the number of apoptotic or TUNEL-positive cells in the SCG from P0 *PHD3*^{-/-} mice (\sim 30% decrease, $n = 7$, $P < 0.05$, from 6.7×10^{-5} to 4.9×10^{-5} TUNEL-positive cells/ μ m² SCG area).

In contrast to the effect of *PHD3* deletion on SCG neuron number, there were no significant differences between the numbers of neurons in the SCG of either *PHD1*^{-/-} or *PHD2*^{+/-} neonates compared with wild-type littermates (data not shown).

To investigate the in vivo significance of HIF- α gene dosage on the survival of cultured neurons from *PHD3*^{-/-} mice, we compared the number of neurons in the SCG of *PHD3*^{-/-} versus *PHD3*^{+/-}; *HIF-1 α* ^{+/-} littermate neonates and *PHD3*^{-/-} versus *PHD3*^{+/-}; *HIF-2 α* ^{+/-} littermate neonates. Consistent with the studies of survival in culture, these studies revealed that heterozygous inactivation of HIF-2 α , but not HIF-1 α , reduced the SCG neuronal population in *PHD3*^{-/-} animals (Fig. 5D). Interestingly, this effect was not observed in the *PHD3*-positive background (comparison of wild-type versus *HIF-2 α* ^{+/-} mice) (Fig. 5D). Further experiments designed to test the effect of *PHD3* inactivation in the context of HIF-2 α heterozygosity (comparison of *PHD3*^{-/-}; *HIF-2 α* ^{+/-} versus *HIF-2 α* ^{+/-} mice) revealed no significant differences in SCG cell numbers (Fig. 5D), suggesting that *PHD3* dependent effects on cell number were affected by integrity of the HIF-2 α pathway and vice versa. Taken together with our in vitro survival data, these in vivo observations suggest that the selective increase in SCG neurons in *PHD3*^{-/-} mice results from reduced cell loss during the phase of programmed cell death in the perinatal period as a consequence of the enhanced sensitivity of *PHD3*-deficient neurons to NGF and that this effect is at least partially dependent on HIF-2 α .

***PHD3*-deficient mice have increased numbers of cells in the adrenal medulla and carotid body.** NGF-dependent cells of the sympathoadrenal axis extend to the neural crest-derived chromaffin and glomus cells of the adrenal medulla and carotid body. Our findings that *PHD3*^{-/-} mice have significantly more sympathetic neurons than wild-type mice prompted us to examine cell number elsewhere in the sympathoadrenal system. Stereological analysis of adult mice (3 to 6 months old) revealed significantly more TH-positive cells in both the adrenal medulla and the carotid body (Fig. 6). Interestingly, though total numbers of cells were increased in both organs in *PHD3*^{-/-} mice, overall organ volume was increased for the carotid body, but decreased for the adrenal medulla, in *PHD3*^{-/-} mice (Fig. 6). The latter phenomenon may be explained by a reduction in chromaffin cell volume (from 1,743 μ m³ in wild-type to 1,195 μ m³ in *PHD3*^{-/-} mice; $P < 0.05$; $n = 7$), consistent with the significant increase in TH-positive cell density in the adrenal medulla (Fig. 6A).

Sympathetic innervation of target tissues. Given that inactivation of *PHD3* in vivo results in increased numbers of SCG neurons surviving to adulthood and that NGF is more effective in promoting neurite growth from cultured *PHD3*-deficient SCG neurons, we asked whether sympathetic innervation density is increased in *PHD3*^{-/-} mice. The SCG innervates several anatomically discrete structures, including the iris, submandib-

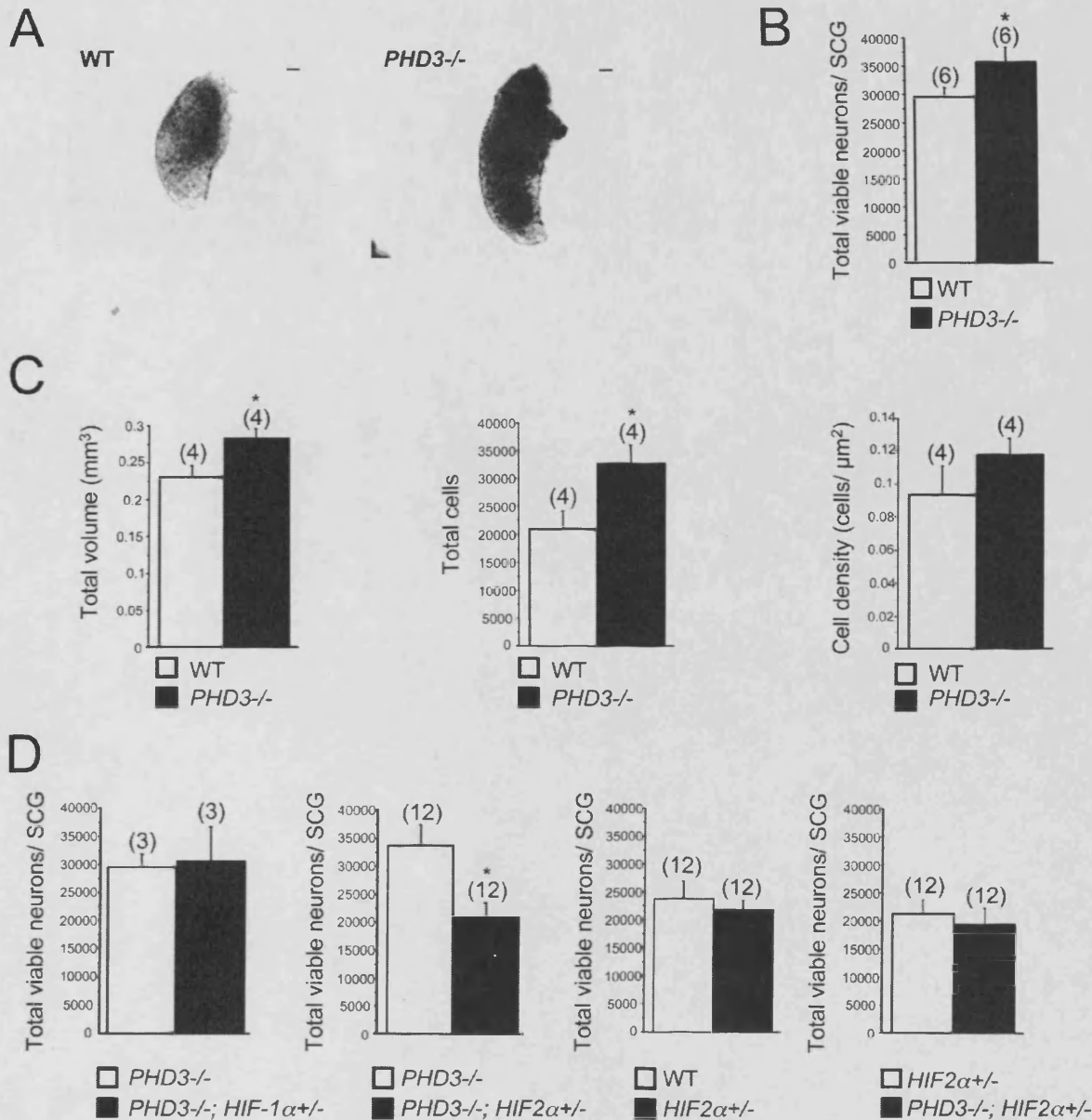


FIG. 5. Effect of genetic inactivation of PHD3 on anatomy of SCG. (A) Bright-field images of wild-type and *PHD3*^{-/-} neonatal SCG. Bar, 100 μm. (B) Neuronal complement of neonatal SCG in wild-type and *PHD3*^{-/-} mice; counts are of viable trypsin-dissociated neurons. (C) Stereological analysis of TH-positive neurons showing increased cell numbers in the SCG from adult *PHD3*^{-/-} mice. (D) Comparison of neuronal complement of neonatal SCG in mice of the indicated genotypes. Counts are as for panel B. HIF-2α heterozygosity, but not HIF-1α heterozygosity, is associated with reduced neuronal complement.

ular gland, and pineal gland, whose innervation density can be relatively easily estimated by quantifying the area occupied by TH-positive nerve fibers in tissue sections. Surprisingly, this analysis revealed significantly fewer TH-positive fibers in the iris, submandibular gland, and pineal gland of *PHD3*^{-/-} mice compared with wild-type animals (Fig. 7A, B, and C).

Physiological effects on the sympathetic nervous system. We next sought to assess the integrity of physiological responses that are dependent on the sympathetic nervous system. Be-

cause of the reduced sympathetic innervation of the iris in *PHD3*^{-/-} mice (Fig. 7A), we tested light-to-dark pupillary responses. While no differences in pupil diameter were seen under normal lighting conditions (150 lx) (Fig. 7D), pupil diameter was significantly decreased in the dark-adapted eye from *PHD3*^{-/-} mice (0 lx) (Fig. 7D). This implies decreased tone in the sympathetically innervated dilator pupillae muscle fibers of *PHD3*^{-/-} mice.

Since one of the most important roles of sympathoadrenal

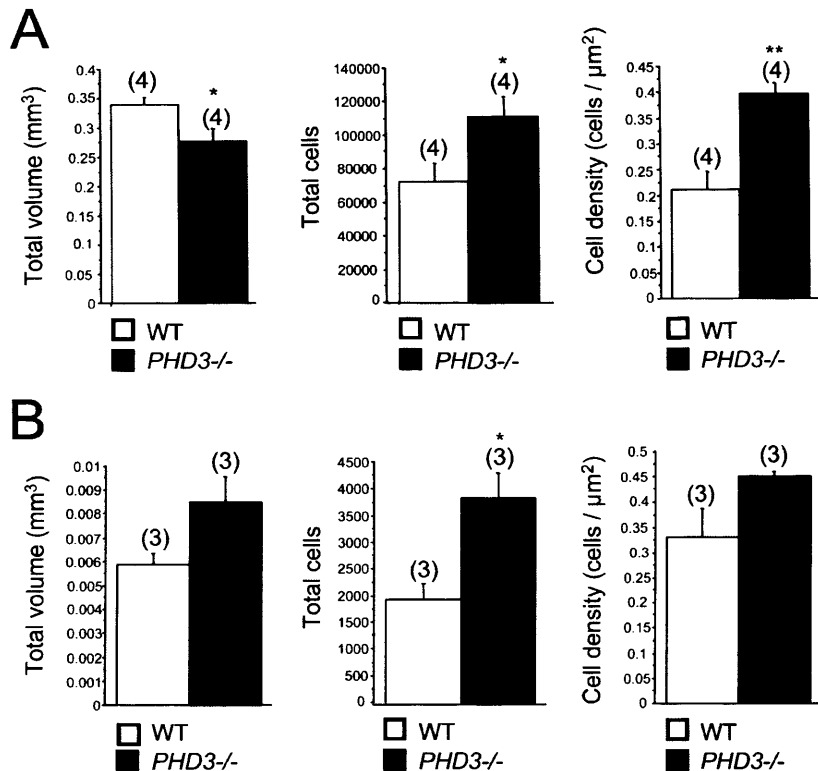


FIG. 6. Effect of genetic inactivation of PHD3 on the anatomy of other sympathoadrenal tissues, the adrenal medulla (A) and carotid body (B). Stereological analysis of TH-positive neurosecretory cells demonstrating increased cell numbers in the adrenal medulla (A) and carotid body (B) of adult *PHD3*^{-/-} mice.

function is in the control of blood pressure, we went on to perform a series of measurements of systemic blood pressure regulation. First, a series of resting measurements were performed under anesthesia. These revealed a modest but significant reduction in blood pressure in *PHD3*^{-/-} mice versus wild-type littermates (Table 1) but no significant differences in heart rate (Table 1). Consistent with reduced arterial pressure, we found that left ventricular weights were significantly reduced in *PHD3*^{-/-} mice versus wild-type mice (Table 1).

To pursue the differences in blood pressure further, measurements of aortic blood pressure were repeated in conscious mice using radiotelemetry. These confirmed that, at rest, *PHD3*^{-/-} mice were hypotensive compared to wild-type mice, with reduced systolic blood pressures (Fig. 8). Furthermore, the difference in systolic blood pressure was enhanced when the mice became active, with as much as 20 mm Hg difference in systolic pressure between *PHD3*^{-/-} mice and littermate controls (Fig. 8).

If reduced blood pressure were due to sympathoadrenal dysfunction rather than a primary cardiac or vascular defect, we argued that responses to exogenous adrenoceptor agonists should be preserved or even exaggerated. Under anesthesia, we measured responses to infusions of the α_1 -agonist phenylephrine and the β_1 -agonist dobutamine. Results are shown in Table 1. In response to the exogenous α_1 -adrenoceptor agonist phenylephrine, the maximal rise in blood pressure was exaggerated in *PHD3*^{-/-} mice versus wild-type littermates. Interestingly, reflex bradycardia was blunted in *PHD3*^{-/-} animals, suggesting that

baroreceptor reflex sensitivity, a measure of endogenous autonomic function, was reduced. In response to the exogenous β_1 -adrenoceptor agonist dobutamine, *PHD3*^{-/-} mice also showed an exaggerated increase in heart rate and contractility, consistent with reduced intrinsic sympathetic function rather than a primary cardiac or vascular cause of hypotension.

Finally, we tested adrenal medullary function both by measuring individual chromaffin cell catecholamine secretion rates by amperometry in explanted adrenal slices and by measuring total circulating catecholamine levels in intact animals. Amperometrically measured basal secretion of catecholamines was reduced by approximately 50% in chromaffin cells from *PHD3*^{-/-} mice (Fig. 9A). Secretion in response to potassium-induced depolarization was similarly reduced (20 mM potassium) or reduced to a smaller extent (40 mM potassium) in *PHD3*^{-/-} mice (Fig. 9A), consistent with reduced secretory capacity. Plasma catecholamine levels were also lower in *PHD3*^{-/-} mice (Fig. 9B), suggesting that the observed increase in chromaffin cell number was not sufficient to compensate for the decrease in chromaffin cell functionality under physiological conditions.

DISCUSSION

Our findings show that the HIF prolyl hydroxylase PHD3 has an important role in regulating the development of the sympathoadrenal system and that its ablation has substantial physiological consequences that extend into adult life.

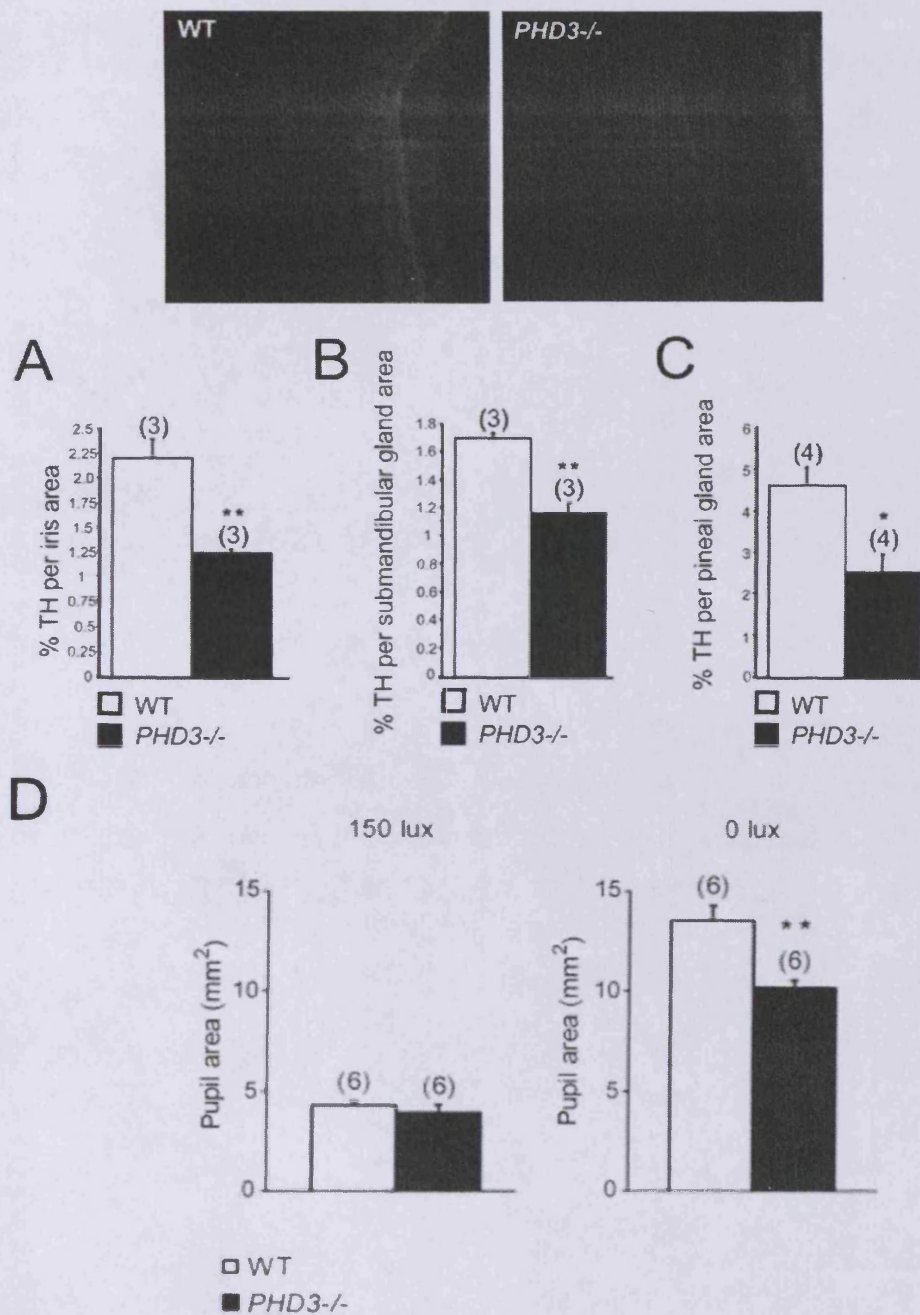


FIG. 7. Sympathetic innervation of SCG target tissues from *PHD3*^{-/-} mice: immunohistochemistry demonstrating TH-positive neurons in SCG target tissues. Shown are representative images of TH-stained (bright red) neurons in the iris. Measured as the ratio of the TH-positively stained area over the total area of the SCG target tissue, there was decreased sympathetic innervation density of the iris (A), submandibular gland (B), and pineal gland (C). (D) Average pupil sizes in conscious, adult *PHD3*^{-/-} mice and wild-type controls under normal illumination (150 lx of bright white light) and after 1 h of dark adaptation (0 lx).

We observed significantly more neurons in the SCG of newborn *PHD3*^{-/-} mice compared with wild-type littermates, and this elevated number of SCG neurons was maintained to adulthood. The apparent failure of the neuronal complement of the SCG to decrease in *PHD3*^{-/-} mice postnatally, when naturally

occurring programmed cell death ordinarily matches the number of sympathetic neurons to the requirements of their targets, suggests that the elevated number of neurons in the SCG of *PHD3*-deficient mice is due to reduced cell death, in keeping with the observed shift in the NGF survival dose response

TABLE 1. Cardiovascular function in anesthetized mice^a

| Parameter (no. of animals in exptl groups) | Result for group | | P value |
|--|------------------|----------------------------|---------|
| | Wild type | <i>PHD3</i> ^{-/-} | |
| Postmortem ventricular wt (10 WT, 7 <i>PHD3</i> ^{-/-}) | | | |
| LV/body wt (mg/g) | 3.19 ± 0.10 | 2.72 ± 0.06 | 0.001 |
| RV/body wt (mg/g) | 0.98 ± 0.04 | 0.99 ± 0.03 | 0.85 |
| Arterial pressure (10 WT, 8 <i>PHD3</i> ^{-/-}) | | | |
| Systolic (mmHg) | 105 ± 3 | 94 ± 5 | 0.009 |
| Diastolic (mmHg) | 75 ± 2 | 69 ± 2 | 0.06 |
| MAP (mm Hg) | 89 ± 2 | 79 ± 1 | 0.005 |
| LV hemodynamics: baseline (10 WT, 7 <i>PHD3</i> ^{-/-}) | | | |
| <i>dP/dt</i> _{max} (mm Hg/s) | 7,858 ± 474 | 7,363 ± 623 | 0.53 |
| Heart rate (bpm) | 437 ± 11 | 446 ± 17 | 0.66 |
| LV hemodynamics: dobutamine (9 WT, 7 <i>PHD3</i> ^{-/-}) | | | |
| <i>dP/dt</i> _{max} (% of baseline) | 126 ± 4 | 152 ± 13 | 0.04 |
| Heart rate (% of baseline) | 117 ± 2 | 129 ± 3 | 0.006 |
| LV hemodynamics: phenylephrine (5 WT, 4 <i>PHD3</i> ^{-/-}) | | | |
| MAP (% of baseline) | 135 ± 5 | 159 ± 22 | 0.07 |
| Heart rate (% of baseline) | -31 ± 5 | -21 ± 15 | 0.28 |
| Baroreceptor gain (bpm/mm Hg) | -6.6 ± 1.3 | -2.5 ± 0.9 | 0.04 |

^a All values are means ± SEM. WT, wild type; MAP, mean arterial pressure; bpm, beats per minute.

of *PHD3*-deficient SCG neurons in culture to lower NGF concentrations. Interestingly, the effect of *PHD3* inactivation on NGF responsiveness in the peripheral nervous system appears to be restricted to neurons of the sympathetic lineage, as neural crest-derived, NGF-dependent sensory neurons from *PHD3*^{-/-} mice responded normally to NGF. It is unclear whether dysregulated apoptosis might occur in regions within the central nervous system in *PHD3*^{-/-} mice. However, these mice are viable as adults, without obvious neurological abnormalities. In addition, brains from *PHD3*^{-/-} mice were not obviously abnormal and were not significantly different in weight (0.43 ± 0.01 g versus 0.43 ± 0.00 g in *PHD3*^{-/-} and wild-type males; 0.42 ± 0.01 g versus 0.44 ± 0.01 g in *PHD3*^{-/-} and wild-type females). Nevertheless, these observations do not preclude dysregulation of apoptosis that is compensated for or might be revealed in pathological situations.

As well as enhancing the sensitivity of SCG neurons to the survival-promoting effects of NGF, deletion of *PHD3* also makes these neurons more responsive to the neurite growth-promoting effects of NGF in culture. Because target-derived NGF is not only required for sympathetic neuron survival during development in vivo but is also responsible for the terminal growth and branching of sympathetic axons in their targets, we expected to find increased sympathetic innervation density in *PHD3*^{-/-} mice. Surprisingly, we observed the opposite in several SCG target tissues in these animals. One possible explanation for this apparent paradox is that the increased number of sympathetic neurons innervating target tissues results in elevated uptake and removal of NGF from these tissues by retrograde axonal transport, resulting in lower ambient levels of NGF in the targets. Whereas retrograde transport of NGF in signaling endosomes to the cell bodies of sympathetic neurons is required for survival, the extent of axonal growth and branching in target tissues is governed by the ambient level of NGF in these tissues (15).

In addition to possessing elevated numbers of sympathetic neurons, *PHD3*^{-/-} mice have increased numbers of chromaffin and glomus cells in the adrenal medulla and carotid body. Together with sympathetic neurons, these cells are derived from the sympathoadrenal neural crest lineage (22). Whether the increase in chromaffin or glomus cell number in *PHD3*^{-/-} mice results from enhanced survival or from enhanced proliferation and/or differentiation of their precursors is not known.

Despite the increased number of cells in parts of the sympathoadrenal system of *PHD3*^{-/-} mice, we observed impaired homeostatic and physiological responses regulated by this system, including reduced blood pressure, impaired light-to-dark pupillary dilation, and reduced catecholamine secretion from adrenal chromaffin cells, with lower plasma catecholamine levels in *PHD3*^{-/-} mice. Sympathetic function is a key determinant of systemic blood pressure regulation (reviewed in reference 17), and elevated sympathetic activity is present in many forms of human hypertension. Apart from the findings reported here, we have not so far observed other basal abnormalities in *PHD3*^{-/-} mice. Thus, though *PHD3* could have other, as-yet-unknown effects on blood pressure regulation, the evidence for sympathetic hypofunction, reduced catecholamine secretion, reduced responses to activity, and preserved responses to exogenous adreno-agonists all support a causal link between sympathoadrenal dysregulation and blood pressure dysregulation in *PHD3*^{-/-} animals.

Though previous cellular studies have implicated oxygen-dependent catalytic activity of *PHD3* in the regulation of neuronal survival, these studies have given conflicting data on the role played by the known substrates HIF-1 α and HIF-2 α (23, 44). In the current work we found that heterozygous inactivation of HIF-2 α , but not HIF-1 α , had major effects on sympathetic neuronal survival and the neuronal complement of the SCG.

Interestingly, neonatal sympathetic failure has been ob-

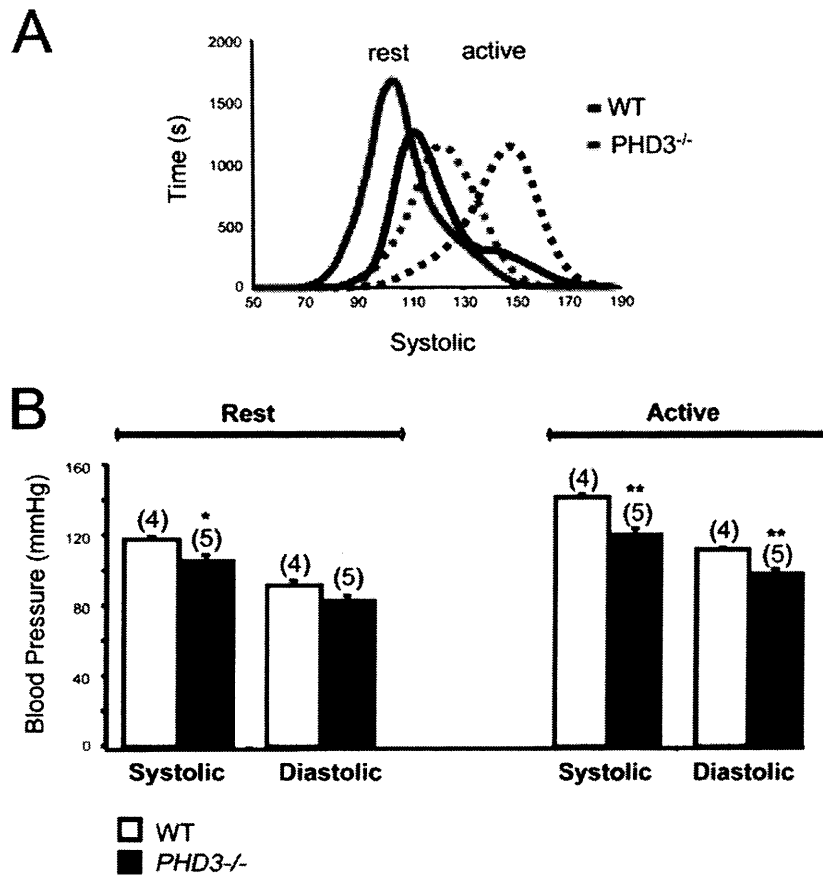


FIG. 8. Aortic blood pressures in conscious, adult *PHD3*^{-/-} mice, as measured by radiotelemetry. (A) Pooled frequency histogram of systolic blood pressure over the 3-day recording period (using 1 mm Hg bins) from four (wild-type) or five (*PHD3*^{-/-}) resting (solid lines) and active (dotted lines) mice. (B) Average blood pressure recordings over a 3-day recording period. Decreased systolic and diastolic blood pressures were observed in *PHD3*^{-/-} mice. These differences were enhanced when the mice were active.

served in *HIF-2α*^{-/-} mice, and *HIF-2α* mRNA has been reported to be strongly expressed in sympathoadrenal tissues of the mouse (42). Though difficulties in obtaining background-free immunohistochemical signals precluded assessment in the mouse, we have also found that *PHD3* is strongly expressed in the rat sympathoadrenal system, suggesting that the two proteins are coexpressed in this lineage (B. Wijeyekoon and C. W. Pugh, unpublished data). Interestingly, studies of small interfering RNA-mediated suppression of PHDs in tissue culture have indicated that *PHD3* appears to exert greater regulatory effects on *HIF-2α* than *HIF-1α* (1). Taken together, the simplest synthesis of these findings is that *PHD3* inactivation promotes sympathoadrenal neuronal survival, at least in part, through upregulation of *HIF-2α*. Nevertheless, consistent with a recent report of pharmacological *PHD* inhibition in sympathetic neurons (26), *HIF-2α* protein levels in the SCG of these normoxic animals were below the detection threshold for immunohistochemistry, so this could not be confirmed. It should also be noted that this explanation does not preclude the existence of other *PHD3* substrates that may contribute to the observed effect. Indeed, the lack of effect of *HIF-2α* heterozygosity on a *PHD3*-positive background suggests that the relationship between *HIF-2α* and neuronal survival is not simple

and depends on *PHD3* status, perhaps implying the existence of other substrates in addition to *HIF-2α*. Thus, the importance of *PHD3*, as opposed to *PHD1* or *PHD2*, in neuronal apoptosis might reflect the existence of a discrete, non-*HIF*, *PHD3* substrate in this process, or the relative abundance of *PHD3* in these cells coupled to the preferred targeting of *HIF-2α* by *PHD3*, or both.

Whether and how adult sympathetic hypofunction in *PHD3*^{-/-} mice relates to dysregulation of *HIF-2α* is also unclear. Together with the finding of sympathetic failure in association with complete inactivation of *HIF-2α* in some but not all studies (33, 42), our findings suggest that although an intact *PHD3*/*HIF-2α* system is necessary for proper sympathoadrenal development, there is no simple relationship of hyper- or hypofunctionality to predicted effects of these genotypes on *HIF-2α* levels.

While we have demonstrated physiological deficits in adult *PHD3*^{-/-} mice, it is not clear whether deficits arise purely as a consequence of *PHD3* deficiency during development or whether there is an ongoing *PHD3* requirement for sympathetic function in the adult. A great deal of interest has been generated by the possibility that environmental effects on development might influence medically important aspects of

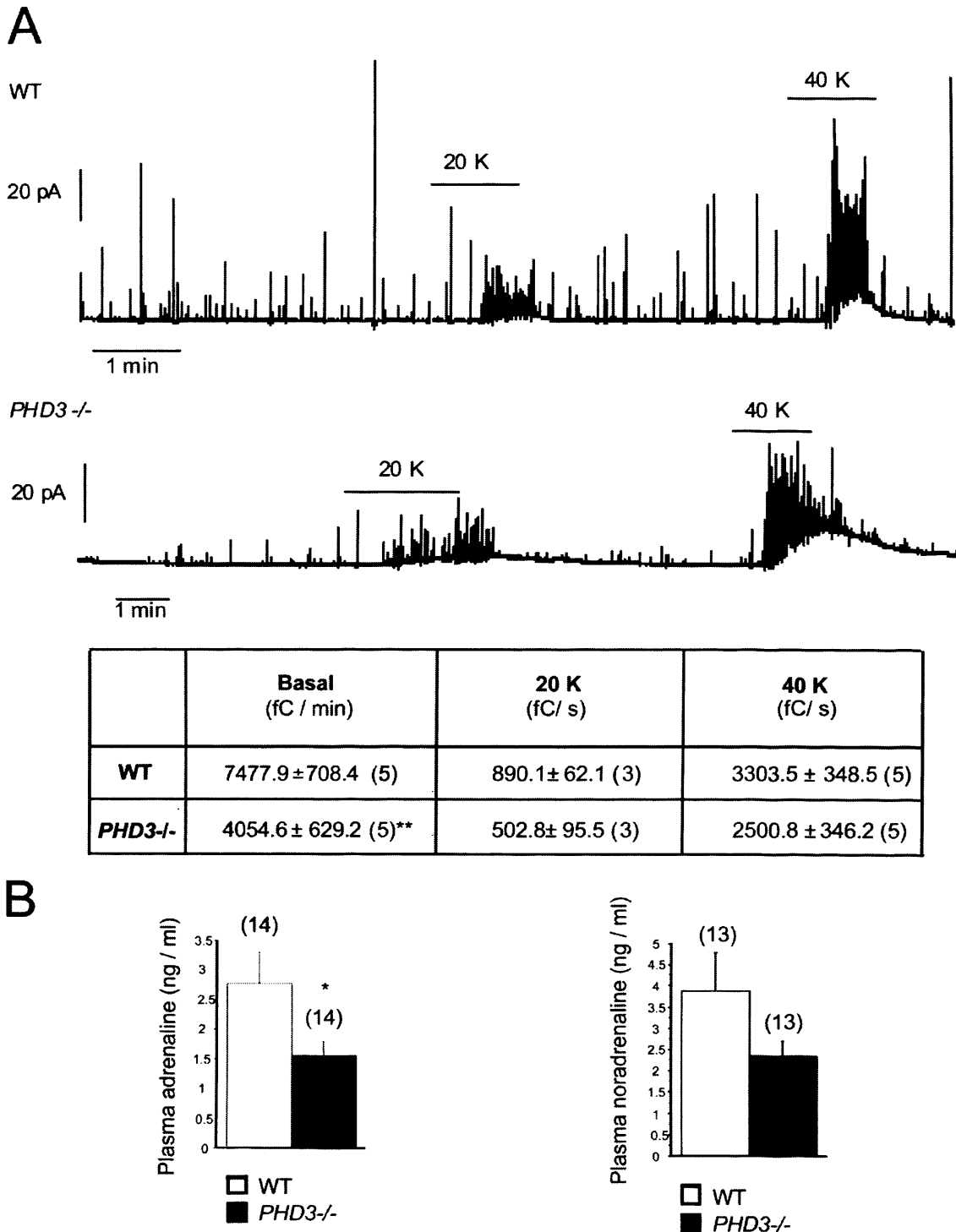


FIG. 9. Catecholamine secretion in *PHD3*^{-/-} mice. (A) Representative amperometric recordings of basal catecholamine release, as well as responsiveness to induction by 20 mM and 40 mM potassium (20K and 40K), of adrenal slices isolated from adult mice. The table shows the secretion rate (in fC/min) under basal conditions, as well as with 20 mM and 40 mM potassium (20 and 40 K). (B) Circulating catecholamines (adrenaline and noradrenaline) from anesthetized, adult mice. Both adrenal slice and circulating catecholamines are reduced in *PHD3*^{-/-} mice.

adult physiology, such as blood pressure regulation (reviewed in references 3 to 5 and 28). However, there are as yet few mechanistic clues as to how such processes might operate. The dependence of PHD activity on oxygen and cofactors, such as the Krebs cycle intermediate 2-oxoglutarate, Fe(II), and ascorbate (35), and inhibition of PHDs by metabolic intermediates, such as succinate, fumarate, pyruvate, and oxaloacetate (9, 18, 19, 21, 27, 36), raises the interesting possibility that environmental influences on PHD3 activity could perturb sympathetic development in a manner that might have important effects on cardiovascular control.

In conclusion, our findings reveal an important role for PHD3 in the developing sympathoadrenal system. It is an intriguing possibility that this connection between hypoxia pathways and the developing sympathoadrenal system might be a means by which changes in oxygen tension could influence key aspects of anatomical and physiological maturation of this system. Whether this provides a paradigm for environmental influences affecting development will be of interest in the future.

ACKNOWLEDGMENTS

This work was supported by the British Heart Foundation, the Wellcome Trust, and the EU Framework 6 Pulmotension Consortium.

We thank P. van Wesemael, M. Dewerchin, S. Wyls, E. Gils, B. Hermans, L. Kieckens, and L. Notebaert (Katholieke Universiteit Leuven, Belgium), as well as D. Adlam, S. Neubauer, R. Foster, and K. Buckler (University of Oxford, United Kingdom), for their contribution.

We have declared that no conflict of interest exists.

REFERENCES

- Appelhoff, R. J., Y. M. Tian, R. R. Raval, H. Turley, A. L. Harris, C. W. Pugh, P. J. Ratcliffe, and J. M. Gleadle. 2004. Differential function of the prolyl hydroxylases PHD1, PHD2, and PHD3 in the regulation of hypoxia-inducible factor. *J. Biol. Chem.* **279**:38458–38465.
- Aragones, J., M. Schneider, K. Van Geyte, P. Fraisl, T. Dresselaers, M. Mazzone, R. Dirks, S. Zacchigna, H. Lemieux, N. H. Jeoung, D. Lambrechts, T. Bishop, P. Lafuste, A. Diez-Juan, S. K. Harten, P. Van Noten, K. De Bock, C. Willam, M. Tjwa, A. Grosfeld, R. Navet, L. Moons, T. Vandendriessche, C. Derouse, B. Wijeyekoon, J. Nuyts, B. Jordan, R. Silasi-Mansat, F. Lupu, M. Dewerchin, C. Pugh, P. Salmon, L. Mortelmans, B. Gallez, F. Gorus, J. Buyse, F. Sluse, R. A. Harris, E. Gnaiger, P. Hespel, P. Van Hecke, F. Schuit, P. Van Veldhoven, P. Ratcliffe, M. Baes, P. Maxwell, and P. Carmeliet. 2008. Deficiency or inhibition of oxygen sensor Phd1 induces hypoxia tolerance by reprogramming basal metabolism. *Nat. Genet.* **40**:170–180.
- Barker, D. J. 1995. Fetal origins of coronary heart disease. *BMJ* **311**:171–174.
- Barker, D. J. 2002. Fetal programming of coronary heart disease. *Trends Endocrinol. Metab.* **13**:364–368.
- Barker, D. J., S. P. Bagby, and M. A. Hanson. 2006. Mechanisms of disease: in utero programming in the pathogenesis of hypertension. *Nat. Clin. Pract. Nephrol.* **2**:700–707.
- Bruick, R. K., and S. L. McKnight. 2001. A conserved family of prolyl-4-hydroxylases that modify HIF. *Science* **294**:1337–1340.
- Butz, G. M., and R. L. Davisson. 2001. Long-term telemetric measurement of cardiovascular parameters in awake mice: a physiological genomics tool. *Physiol. Genomics* **5**:89–97.
- Cavalieri, B. 1966. *Geometria degli indivisibili*. Unione Tipografica Editrice, Torino, Italy.
- Dalgard, C. L., H. Lu, A. Mohyeldin, and A. Verma. 2004. Endogenous 2-oxoacids differentially regulate expression of oxygen sensors. *Biochem. J.* **380**:419–424.
- Davies, A. M. 2003. Regulation of neuronal survival and death by extracellular signals during development. *EMBO J.* **22**:2537–2545.
- Davies, A. M., K. F. Lee, and R. Jaenisch. 1993. p75-deficient trigeminal sensory neurons have an altered response to NGF but not to other neurotrophins. *Neuron* **11**:565–574.
- Davies, A. M., L. Minichiello, and R. Klein. 1995. Developmental changes in NT3 signalling via TrkA and TrkB in embryonic neurons. *EMBO J.* **14**:4482–4489.
- Epstein, A. C., J. M. Gleadle, L. A. McNeill, K. S. Hewitson, J. O'Rourke, D. R. Mole, M. Mukherji, E. Metzzen, M. I. Wilson, A. Dhanda, Y. M. Tian, N. Masson, D. L. Hamilton, P. Jaakkola, R. Barstead, J. Hodgkin, P. H. Maxwell, C. W. Pugh, C. J. Schofield, and P. J. Ratcliffe. 2001. C. elegans EGL-9 and mammalian homologs define a family of dioxygenases that regulate HIF by prolyl hydroxylation. *Cell* **107**:43–54.
- Garcia-Fernandez, M., R. Mejias, and J. Lopez-Barneo. 2007. Developmental changes of chromaffin cell secretory response to hypoxia studied in thin adrenal slices. *Pflugers Arch.* **454**:93–100.
- Glebova, N. O., and D. D. Ginty. 2005. Growth and survival signals controlling sympathetic nervous system development. *Annu. Rev. Neurosci.* **28**:191–222.
- Gordan, J. D., and M. C. Simon. 2007. Hypoxia-inducible factors: central regulators of the tumor phenotype. *Curr. Opin. Genet. Dev.* **17**:71–77.
- Guyenet, P. G. 2006. The sympathetic control of blood pressure. *Nat. Rev. Neurosci.* **7**:335–346.
- Hewitson, K. S., B. M. Lienard, M. A. McDonough, I. J. Clifton, D. Butler, A. S. Soares, N. J. Oldham, L. A. McNeill, and C. J. Schofield. 2007. Structural and mechanistic studies on the inhibition of the hypoxia-inducible transcription factor hydroxylases by tricarboxylic acid cycle intermediates. *J. Biol. Chem.* **282**:3293–3301.
- Isaacs, J. S., Y. J. Jung, D. R. Mole, S. Lee, C. Torres-Cabala, Y. L. Chung, M. Merino, J. Trepel, B. Zbar, J. Toro, P. J. Ratcliffe, W. M. Linehan, and L. Neckers. 2005. HIF overexpression correlates with biallelic loss of fumarate hydratase in renal cancer: novel role of fumarate in regulation of HIF stability. *Cancer Cell* **8**:143–153.
- Iyer, N. V., L. E. Kotch, F. Agani, S. W. Leung, E. Laughner, R. H. Wenger, M. Gassmann, J. D. Gearhart, A. M. Lawler, A. Y. Yu, and G. L. Semenza. 1998. Cellular and developmental control of O₂ homeostasis by hypoxia-inducible factor 1 alpha. *Genes Dev.* **12**:149–162.
- Koivunen, P., M. Hirsila, A. M. Remes, I. E. Hassinen, K. I. Kivirikko, and J. Myllyharju. 2007. Inhibition of hypoxia-inducible factor (HIF) hydroxylases by citric acid cycle intermediates: possible links between cell metabolism and stabilization of HIF. *J. Biol. Chem.* **282**:4524–4532.
- Le Douarin, N. M. 1986. Cell line segregation during peripheral nervous system ontogeny. *Science* **231**:1515–1522.
- Lee, S., E. Nakamura, H. Yang, W. Wei, M. S. Linggi, M. P. Sajan, R. V. Farese, R. S. Freeman, B. D. Carter, W. G. Kaelin, Jr., and S. Schlisio. 2005. Neuronal apoptosis linked to EglN3 prolyl hydroxylase and familial pheochromocytoma genes: developmental culling and cancer. *Cancer Cell* **8**:155–167.
- Lipscomb, E. A., P. D. Sarmiere, R. J. Crowder, and R. S. Freeman. 1999. Expression of the SM-20 gene promotes death in nerve growth factor-dependent sympathetic neurons. *J. Neurochem.* **73**:429–432.
- Lipscomb, E. A., P. D. Sarmiere, and R. S. Freeman. 2001. SM-20 is a novel mitochondrial protein that causes caspase-dependent cell death in nerve growth factor-dependent neurons. *J. Biol. Chem.* **276**:5085–5092.
- Lomb, D. J., J. A. Straub, and R. S. Freeman. 2007. Prolyl hydroxylase inhibitors delay neuronal cell death caused by trophic factor deprivation. *J. Neurochem.* **103**:1897–1906.
- Lu, H., C. L. Dalgard, A. Mohyeldin, T. McFate, A. S. Tait, and A. Verma. 2005. Reversible inactivation of HIF-1 prolyl hydroxylases allows cell metabolism to control basal HIF-1. *J. Biol. Chem.* **280**:41928–41939.
- McMillen, I. C., and J. S. Robinson. 2005. Developmental origins of the metabolic syndrome: prediction, plasticity, and programming. *Physiol. Rev.* **85**:571–633.
- Mills, P. A., D. A. Huetteman, B. P. Brockway, L. M. Zwiers, A. J. Gelsema, R. S. Schwartz, and K. Kramer. 2000. A new method for measurement of blood pressure, heart rate, and activity in the mouse by radiotelemetry. *J. Appl. Physiol.* **88**:1537–1544.
- Niederhoffer, N., L. Hein, and K. Starke. 2004. Modulation of the baroreceptor reflex by alpha 2A-adrenoceptors: a study in alpha 2A knockout mice. *Br. J. Pharmacol.* **141**:851–859.
- Oppenheim, R. W. 1991. Cell death during development of the nervous system. *Annu. Rev. Neurosci.* **14**:453–501.
- Pardal, R., and J. Lopez-Barneo. 2002. Carotid body thin slices: responses of glomus cells to hypoxia and K⁺-channel blockers. *Respir. Physiol. Neurobiol.* **132**:69–79.
- Peng, J., L. Zhang, L. Drysdale, and G. H. Fong. 2000. The transcription factor EPAS-1/hypoxia-inducible factor 2 α plays an important role in vascular remodeling. *Proc. Natl. Acad. Sci. USA* **97**:8386–8391.
- Ryan, H. E., J. Lo, and R. S. Johnson. 1998. HIF-1 alpha is required for solid tumor formation and embryonic vascularization. *EMBO J.* **17**:3005–3015.
- Schofield, C. J., and Z. Zhang. 1999. Structural and mechanistic studies on 2-oxoglutarate-dependent oxygenases and related enzymes. *Curr. Opin. Struct. Biol.* **9**:722–731.
- Selak, M. A., S. M. Armour, E. D. MacKenzie, H. Boulahbel, D. G. Watson, K. D. Mansfield, Y. Pan, M. C. Simon, C. B. Thompson, and E. Gottlieb. 2005. Succinate links TCA cycle dysfunction to oncogenesis by inhibiting HIF-1 α prolyl hydroxylase. *Cancer Cell* **7**:77–85.
- Semenza, G. L. 2003. Targeting HIF-1 for cancer therapy. *Nat. Rev. Cancer* **3**:721–732.

38. **Sholl, D. A.** 1953. Dendritic organization in the neurons of the visual and motor cortices of the cat. *J. Anat.* **87**:387–406.
39. **Stalmans, I., Y. S. Ng, R. Rohan, M. Fruttiger, A. Bouche, A. Yuce, H. Fujisawa, B. Hermans, M. Shani, S. Jansen, D. Hicklin, D. J. Anderson, T. Gardiner, H. P. Hammes, L. Moons, M. Dewerchin, D. Collen, P. Carmeliet, and P. A. D'Amore.** 2002. Arteriolar and venular patterning in retinas of mice selectively expressing VEGF isoforms. *J. Clin. Investig.* **109**:327–336.
40. **Straub, J. A., E. A. Lipscomb, E. S. Yoshida, and R. S. Freeman.** 2003. Induction of SM-20 in PC12 cells leads to increased cytochrome *c* levels, accumulation of cytochrome *c* in the cytosol, and caspase-dependent cell death. *J. Neurochem.* **85**:318–328.
41. **Takeda, K., V. C. Ho, H. Takeda, L. J. Duan, A. Nagy, and G. H. Fong.** 2006. Placental but not heart defects are associated with elevated hypoxia-inducible factor alpha levels in mice lacking prolyl hydroxylase domain protein 2. *Mol. Cell. Biol.* **26**:8336–8346.
42. **Tian, H., R. E. Hammer, A. M. Matsumoto, D. W. Russell, and S. L. McKnight.** 1998. The hypoxia-responsive transcription factor EPAS1 is essential for catecholamine homeostasis and protection against heart failure during embryonic development. *Genes Dev.* **12**:3320–3324.
43. **West, M. J.** 1993. New stereological methods for counting neurons. *Neurobiol. Aging* **14**:275–285.
44. **Xie, L., R. S. Johnson, and R. S. Freeman.** 2005. Inhibition of NGF deprivation-induced death by low oxygen involves suppression of BIMEL and activation of HIF-1. *J. Cell Biol.* **168**:911–920.

